

# **Nano-Engineered Titanium Implants for Complex Bone Therapies**

A thesis submitted in fulfilment of the requirement for the degree of

## **Doctor of Philosophy**

Engineering (Nanotechnology)

By **Karan Gulati**

**August 2015**



THE UNIVERSITY  
*of* ADELAIDE

**School of Chemical Engineering**

**Faculty of Engineering, Computer, and Mathematical Sciences**

**The University of Adelaide**

# CONTENTS

<b>ABSTRACT</b>	<b>iv</b>
<b>PREFACE</b>	<b>vii</b>
<b>LIST OF PUBLICATIONS</b>	<b>viii</b>
<b>Book Chapter</b>	<b>viii</b>
<b>Published/Accepted Articles</b>	<b>viii</b>
<b>Submitted Articles</b>	<b>ix</b>
<b>Articles in Final Preparation</b>	<b>x</b>
<b>Peer-Reviewed Conference Publications</b>	<b>x</b>
<b>Conference Presentations</b>	<b>xi</b>
<b>DECLARATION</b>	<b>xv</b>
<b>ACKNOWLEDGEMENTS</b>	<b>xvi</b>
<b>CHAPTER 1: Introduction</b>	<b>1</b>
1.1 Bone Implants and Challenges	2
1.2 Complex Bone Conditions Demanding Effective Therapies	4
1.2.1 Osteomyelitis	4
1.2.2 Osteoporotic Fractures	5
1.3 Local Drug Delivery in Bone	6
1.3.1 Surface Modification of Bone Implants	6
1.3.2 Research Gap	10
1.3.3 Nano-engineering Bone Implants: Titania Nanotubes	11
1.4 Fabrication of TNTs	12
1.4.1 Electrochemical Anodization	14
1.4.2 Progress in Ti Anodization	16
1.4.3 TNTs on Complex Substrate Geometries	19
1.4.4 TNTs on Ti Alloys	20
1.5 Therapeutic Functions of TNTs/Ti Implants	20

1.5.1	Modulation of Immune Responses	21
1.5.2	Antibacterial Effects	24
1.5.3	Augmenting Osseointegration of Implants	28
1.5.4	TNTs for Complex Therapies	32
1.6	Advancing Therapeutic Releasing Functions of TNTs	33
1.6.1	Controlled Therapeutic Release from TNT/Ti Implants	34
1.6.2	TNTs for Triggered Therapeutic Release	39
1.6.3	TNTs for Multi-Therapy and Bio-Sensing	41
1.6.4	Challenges for TNTs/Ti Bone Implants for Improved Therapeutics	42
1.7	Objectives	43
1.8	Thesis Structure	45
1.9	References	47
<b>CHAPTER 2</b>		<b>69</b>
2.1	Introduction and Objectives	70
2.2	Fabrication of TNTs on Various Substrates	70
2.2.1	Ti Flat Foil Substrate	70
2.2.2	Ti Wires and 3D Printed Ti alloys	73
2.3	Therapeutic Loading inside TNTs	74
2.3	Release of Therapeutics from TNTs <i>in-vitro</i>	75
2.4	Strategies to Control Therapeutic Release	76
2.5	Experimental Setup to Confirm Bone Therapeutic Effects	77
2.6	Structural Characterization of TNT implants	78
2.7	References	79
<b>CHAPTER 3: Periodically Tailored Titania Nanotubes for Enhanced Drug Loading and Releasing Performances</b>		<b>80</b>
<b>CHAPTER 4: Optimizing Anodization Conditions for the Growth of Titania Nanotubes on Curved Surfaces</b>		<b>90</b>
<b>CHAPTER 5: Titania Nanotube (TNT) Implants Loaded with Parathyroid Hormone (PTH) for Potential Localized Therapy of Osteoporotic Fractures</b>		<b>110</b>

<b>CHAPTER 6:</b> <i>In-Situ</i> Transformation of Chitosan Films into Microtubular Structures: A New Bio-Interface for Bone Implants	<b>126</b>
<b>CHAPTER 7:</b> Chemical Reduction of Titania (TiO <sub>2</sub> ) into Conductive Titanium (Ti) Nanotubes Arrays for Combined Drug-Delivery and Electrical Stimulation Therapy	<b>164</b>
<b>CHAPTER 8:</b> 3D Printed Titanium Implants with Combined Micro Particles and Nanotube Topography Promote Interaction with Human Osteoblasts and Osteocyte-Like Cells	<b>171</b>
<b>CHAPTER 9</b>	<b>217</b>
9.1 Conclusions	218
9.1.1 Periodically Tailored Titania Nanotubes for Enhanced Drug Loading and Releasing Performances	219
9.1.2. Optimizing Anodization Conditions for the Growth of Titania Nanotubes on Curved Surfaces	220
9.1.3. Titania Nanotube (TNT) Implants Loaded with Parathyroid Hormone (PTH) for Potential Localized Therapy of Osteoporotic Fractures	221
9.1.4. <i>In-Situ</i> Transformation of Chitosan Films into Microtubular Structures: A New Bio-Interface for Bone Implants	222
9.1.5. Chemical Reduction of Titania (TiO <sub>2</sub> ) into Conductive Titanium (Ti) Nanotubes Arrays for Combined Drug-Delivery and Electrical Stimulation Therapy	223
9.1.6. 3D Printed Titanium Implants with Combined Micro Particles and Nanotube Topography Promote Interaction with Human Osteoblasts and Osteocyte-Like Cells	224
9.2. Recommendations for Future work	225
<b>APPENDIX A:</b> <i>Ex-Vivo</i> Implantation of Nano-Engineered Implants: Investigating Drug Diffusion and Integration inside the Bone Microenvironment	<b>227</b>
<b>APPENDIX B:</b> Nano-Engineered Titanium for Enhanced Bone Therapy	<b>258</b>
<b>APPENDIX C:</b> Local Drug Delivery in Bone by Drug Releasing Implants: Perspectives of Nano-Engineered Titania Nanotubes	<b>265</b>
<b>APPENDIX D:</b> Titania Nanotubes for Local Drug Delivery from Implant Surfaces	<b>283</b>



# ABSTRACT

A number of bone pathologies, such as fracture, infection or cancer, require drug therapy. However, conventional systemic drug administration is inefficient, wasteful, may not reach the target bone tissue in effective concentrations, and may cause unwanted side effects in other tissues. Ideally, drug should be delivered locally at the specific site, and in an optimal therapeutic concentration. Surface modification of the titanium implants can meet these challenges effectively by enabling effective delivery of therapeutics directly at the bone site for an extended period. Among the various suggested implant modifications, titania (TiO<sub>2</sub>) nanotubes (TNTs), which can easily be fabricated on Ti surfaces *via* cost-effective electrochemical anodization, is emerging as a possible strategy for local drug delivery.

This thesis describes advances in TNT/Ti implant technology towards achieving effective therapeutic and cellular modulating action from the surface of Ti wire implants, which have been nano-engineered to fabricate TNTs. The concept was to design and optimize novel therapeutic features of TNTs, using simple and scalable technologies that can ensure easy integration into implants currently on the market. Specifically, in order to address complex bone conditions such as infection, inflammation, and cancers of bone, TNTs were fabricated on Ti wires that could be inserted into bone for 3D in-bone therapeutic release.

The main points of the thesis can be summarized as:

1. *Structural engineering of TNTs*: Periodic tailoring of the TNT structures using a modulated electrochemical anodization process in an attempt to enhance drug loading and releasing abilities of the TNTs.
2. *Fabrication optimization of TNTs on curved surfaces*: Optimization of anodization conditions was undertaken, with a special focus on defining the role of electrolyte ageing,

in order to fabricate a mechanically robust anodic layer (TNTs) on complex curved surfaces such as Ti wires. The purpose of this was to enable easy integration of TNT technology into the current implant market, which includes widely varied geometries (pins, screws, plates, meshes, etc.).

3. *Therapies for complex bone conditions*: Demonstration of TNTs/Ti wire abilities to meet a range of therapeutic needs was modelled, by determining the effect of local release of osteoporotic drugs from TNTs, when inserted into collagen gels containing human osteoblasts. This was followed by analysis of the therapeutic effect on cells, and cell spread/migration morphology on the TNT surfaces.
4. *Formation of chitosan-microtubes on TNTs in-situ*: Investigation of the fate of chitosan-modified TNT/Ti implants in phosphate buffer (isotonic to human blood). Chitosan degradation into micro-tubes on the surface of TNTs was investigated to elucidate the mechanism underlying the *in-situ* formation of these novel structures.
5. *Titanium (Ti) nanotubes vs titania (TiO<sub>2</sub>) nanotubes*: Conventional titania (TiO<sub>2</sub>) nanotubes were chemically reduced into titanium while preserving the nano-topography. The converted conducting titanium nanotube implants were proposed for electrical stimulation therapy and local drug delivery.
6. *TNTs on 3D printed Ti alloys*: Fabrication optimization of TNTs on a unique micro-rough 3D printed Ti alloy, to enable varied surface features, including irregular micro-roughness combined with nano-topography of TNTs. Comparison was then made of cell adhesion, attachment and modulation of osteoblast function by TNTs/Ti 3D implants with conventional smooth, micro-rough and TNTs/Ti flat foil surfaces.

The investigations presented in the thesis are expected to open doors towards the development of advanced in-bone therapeutic implants, in the form of easy-to-tailor nano-engineered Ti

wires, with superior 3D drug releasing abilities and enhanced bone healing functionalities. The emphasis has been on designing the simplest and most cost-effective methodologies to permit easy integration into the current implant market. Applications for these implants could be in the treatment of fractures, bone infections/cancers and ‘local’ osteoporosis in bones.

# **PREFACE**

This thesis is submitted as a ‘thesis by publication’ in accordance with “Specifications for Thesis 2013” of The University of Adelaide. The PhD research spanning 3.5 years generated 1 book chapter, 15 peer-reviewed journal articles [9 published, 3 submitted, and 3 in final preparation for submission in August 2015], and 2 peer-reviewed conference publications. Furthermore the PhD research was also presented at 19 national and international conferences. Six research chapters included in this thesis were published (or submitted or in final preparation for submission) as research articles in highly ranked journals in the field. A complete list of publications is provided in the following pages.

# LIST OF PUBLICATIONS

## Published Book Chapter

**K. Gulati**, M. Kogawa, S. Maher, G. Atkins, D. Findlay, D. Losic “Titania Nanotubes for Local Drug Delivery from Implant Surfaces” in book *Electrochemically Engineered Nanoporous Materials: Methods, Properties and Applications* 2015, ed. by D. Losic and A. Santos (Springer International Publishing AG - Germany). Springer Series in Materials Science 220, DOI: 10.1007/978-3-319-20346-1\_10

## Peer-reviewed Journal Articles

### Published/Accepted Articles

1. **K. Gulati**, A. Santos, D. Findlay, D. Losic “Optimizing Anodization Conditions for Fabricating Well-Adherent and Robust Titania Nanotubes on Curved Surfaces” *Journal of Physical Chemistry C*, 2015, **119**, 16033–16045. DOI: 10.1021/acs.jpcc.5b03383
2. **K. Gulati**, K. Kant, D. Losic “Periodically Tailored Titania Nanotubes for Enhanced Drug Loading and Releasing Performances” *Journal of Materials Chemistry B*, 2015, **3**, 2553-2559.
3. **K. Gulati**, M. S. Aw, D. Findlay, D. Losic “Local Drug Delivery in Bone by Drug Releasing Implants: Perspectives of Nano-Engineered Titania Nanotubes” *Therapeutic Delivery*, 2012, **3**, 857-873.
4. **K. Gulati**, M. S. Aw, D. Losic “Nano-Engineered Ti Wires for Local Delivery of Chemotherapeutics in Brain” *International Journal of Nanomedicine* 2012, **7**, 2069-2076.

5. V. S. Saji, T. Kumeria, **K. Gulati**, M. Prideaux, S. Rahman, M. Alsawat, A. Santos, G. J. Atkins, D. Losic. “Localized Drug Delivery of Selenium (Se) using Nanoporous Anodic Aluminium Oxide for Bone Implants” *Journal of Materials Chemistry B*, 2015 (accepted).
6. T. Kumeria, H. T. Mon, M. S. Aw, **K. Gulati**, A. Santos, H. J. Griesser, D. Losic “Advanced Biopolymer-Coated Drug-Releasing Titania Nanotubes (TNTs) Implants with Simultaneously Enhanced Osteogenic and Antibacterial Properties” *Colloids and Surfaces B: Biointerfaces*, 2015, **130**, 255–263.
7. D. Losic, M. S. Aw, A. Santos, **K. Gulati**, M. Bariana “Titania Nanotube Arrays for Local Drug Delivery: Recent Advances and Perspectives” *Expert Opinion on Drug Delivery*, 2015, **12**, 103-127.
8. T. Kumeria, **K. Gulati**, A. Santos, D. Losic “Real-Time and In Situ Drug Release Monitoring from Nanoporous Implants under Dynamic Flow Conditions by Reflectometric Interference Spectroscopy” *ACS Applied Material & Interfaces*, 2013, **5**, 5436–5442.
9. M. S. Aw, K. A. Khalid, **K. Gulati**, G. J. Atkins, P. Pivonka, D. M. Findlay, D. Losic “Characterization of Drug Release Kinetics in Trabecular Bone from Titania Nanotube Implants” *International Journal of Nanomedicine*, 2012, **7**, 4883-4892.

### **Submitted Articles**

10. **K. Gulati**, M. Prideaux, M. Kogawa, L. Lima-Marques, G. J. Atkins, D. M. Findlay, D. Losic “3D Printed Titanium Implants with Combined Micro Particles and Nanotube Topography Promote Interaction with Human Osteoblasts and Osteocyte-Like Cells” *Biomaterials*, 2015. (Under Review)

11. **K. Gulati**, L. Johnson, R. Karunagaran, D. Findlay, D. Losic “*In-Situ* Transformation of Chitosan Films into Microtubular Structures: A New Bio-Interface for Bone Implants” *Biomacromolecules*, 2015. (Submitted)
12. **K. Gulati**, M. Kogawa, M. Prideaux, D. M. Findlay, G. J. Atkins, D. Losic “Titania Nanotube (TNT) Implants Loaded with Parathyroid Hormone (PTH) for Potential Localized Therapy of Osteoporotic Fractures” *Journal of Materials Chemistry B*, 2015. (Submitted)

### **Articles in Final Preparation** (for submission in August 2015)

13. **K. Gulati**, S. Chandrasekaran, N. H. Voelcker, D. M. Findlay, D. Losic “Chemical Reduction of Titania (TiO<sub>2</sub>) into Conductive Titanium (Ti) Nanotubes Arrays for Combined Drug-Delivery and Electrical Stimulation Therapy” *Chemical Communications*, 2015.
14. S. Rahman\*, **K. Gulati\***, M. Kogawa, G. J. Atkins, P. Pivonka, D. M. Findlay, D. Losic “*Ex-Vivo* Implantation of Nano-Engineered Implants: Investigating Drug Diffusion and Integration inside the Bone Microenvironment” *Journal of Biomedical Materials Research Part A*, 2015 (**Equal Contribution**).
15. G. Kaur, **K. Gulati**, T. Willsmore, I. Zinonos, S. Hay, D. Losic, A. Evdokiou. Nano-engineered Titanium Wire Implants towards Localized Anticancer Efficacy. *Biomaterials*, 2015.

### **Peer-Reviewed Conference Publications**

1. H. Mokhtarzadeh, M. S. Aw, K. A. Khalid, **K. Gulati**, G. J. Atkins, D. Findlay, D. Losic, P. Pivonka “Computational and Experimental Model of Nanoengineered Drug Delivery System for Trabecular Bone”. 11th World Congress on Computational Mechanics

(WCCM XI). July 2014 Barcelona, Spain. [5th European Conference on Computational Mechanics (ECCM V). 6th European Conference on Computational Fluid Dynamics (ECFD VI)]. E. Oñate, J. Oliver and A. Huerta (Eds).

2. **K. Gulati**, G. J. Atkins, D. M. Findlay, D. Losic “Nano-Engineered Titanium for Enhanced Bone Therapy”. Proc SPIE Biosensing and Nanomedicine VI 2013: published online 11 September 2013, doi:10.1117/12.2027151

## **Conference Presentations:**

1. **K. Gulati**, M. Prideaux, M. Kogawa, G. Atkins, D. Findlay, D. Losic “Nano-engineered titanium wires for enhanced in-bone therapeutic action” International Nanomedicine Conference. Sydney, Australia, July 2015 (**Oral Presentation**).
2. D. Losic, **K. Gulati**, G. Kaur, S. Maher, S. Rahman, G. J. Atkins, D. M. Findlay, A. Evdokiou "Drug Releasing Implants Based on Nanoengineered Titania Nanotubes for Localized Bone and Cancer Therapy" The 3rd International Translational Nanomedicine (ITNANO) Conference, Milocer, Montenegro, June 2015 (**Oral Presentation**).
3. **K Gulati**, D. Findlay, D. Losic “Healing injured bones: nano-engineered drug releasing bone implants” Go8-C9 PhD Forum 2014 Global challenges of ageing populations: graduate perspectives from China and Australia, Sydney, Australia, Dec 2014 (**Oral Presentation**).
4. D. Losic, M. S. Aw, **K. Gulati**, Y. Wang, M. Bariana, G. Kaur, S. Rahman, A. Santos, D. Findlay, A. Evdokiou “Electrochemically nanoengineered drug-releasing implants for localized drug delivery and advanced bone and cancer therapies” Taishan Academic Forum, TAF-GNB 2014, Qingdao, China, October 2014 (**Oral Presentation**).
5. H. Mokhtarzadeh, M. S. Aw, K. A. Khalid, **K. Gulati**, G. J. Atkins, D. Findlay, D. Losic, P. Pivonka “Computational and experimental model of nanoengineered drug delivery



- system for trabecular bone” 11th World Congress on Computational Mechanics (WCCM XI) Barcelona, Spain, July 2014 (**Oral Presentation, Publication**).
6. **K. Gulati**, S. Rahman, M. Kogawa, H. Mokhtarzadeh, P. Pivonka, G. J. Atkins, D. M. Findlay, D. Losic “Optimisation of nano-engineered drug-eluting bone implants” Australian Nanotechnology Network (ANN) Early Career Workshop, Sydney, Australia, July 2014 (**Poster Presentation, Travel Support**).
  7. **K. Gulati**, S. Rahman, M. Kogawa, H. Mokhtarzadeh, P. Pivonka, G. J. Atkins, D. M. Findlay, D. Losic “In-bone therapeutic implants: concept, fabrication and drug release” NanoBio 2014, Brisbane, Australia, July 2014 (**Oral Presentation, Travel Support**).
  8. H. Mokhtarzadeh, M. S. Aw, K. A. Khalid, **K. Gulati**, G. J. Atkins, D. Findlay, D. Losic, P. Pivonka “Experimental and finite element models of nano-engineered drug delivery system for trabecular bone” The eighth Clare Valley Bone Meeting, South Australia, Australia, March 2014 (**Poster Presentation**).
  9. **K. Gulati**, G. J. Atkins, D. M. Findlay, D. Losic “Optimising the fabrication of titania nanotubes for enhanced bone implant therapy” ICONN 2014, Adelaide, Australia, Feb 2014. (**Poster Presentation**).
  10. **K. Gulati**, G. J. Atkins, D. M. Findlay, D. Losic “Nano-engineered titanium for enhanced bone therapy” SPIE International Symposium on NanoScience + Engineering, part of Optics and Photonics 2013 event., California, USA, August 2013 (**Oral Presentation, Travel Support, Publication**).
  11. **K. Gulati**, D. Findlay, D. Losic “Healing traumatised bones: perspectives of nano-engineered drug-releasing implants” Australian Nanotechnology Network (ANN) Early Career Workshop, 25-26 July 2013, Flinders University, SA, Australia. (**Oral Presentation, Best Presentation Award**).
  12. T. Kumeria, A. Santos, **K. Gulati**, D. Losic “Drug release Kinetics from nanoporous anodic alumina implant under dynamic flow conditions” 4th Australia and New Zealand

- Micro/Nanofluidics Symposium (ANZMNF), Adelaide, Australia, April 2013 (**Poster Presentation**).
13. M. Kurian, **K. Gulati**, M. S. Aw, S. Hay, A. Evdokiou, D. Losic “Implants with titania nanotubes for human breast cancer therapy” 22nd Meeting of the Australasian Society for Biomaterials and Tissue Engineering, South Australia, Australia, April 2013. (**Poster Presentation**).
  14. J. Kaiser, P. R. Buenzli, M. S. Aw, K. A. Khalid, **K. Gulati**, G. J. Atkins, P. Pivonka, D. M. Findlay, D. Losic “Computational and experimental characterization of drug release kinetics in trabecular bone from titania nanotube implants” Australian and New Zealand Bone and Mineral Society (ANZBMS) Meeting, Perth, Western Australia, September 2012. (**Poster Presentation**).
  15. **K Gulati**, T. Altalhi, D. Findlay, D. Losic “Advanced drug-releasing implants for bone therapies composed of carbon nanotubes and titania nanotube arrays” Oz Carbon 2012, Adelaide, Australia, July 2012 (**Poster Presentation**).
  16. D. Losic, M. S. Aw, **K. Gulati**, T. Kumeria “Self-organized nanopore and nanotube arrays for biomedical applications” International Nanomedicine conference, Sydney, Australia, July 2012 (**Invited Key Lecture**).
  17. **K. Gulati**, M. S. Aw, G. J. Atkins, D. M. Findlay, D. Losic “Nano-engineered titania nanotube arrays as drug-releasing implants for advanced bone therapeutics” NT 12 Thirteenth International Conference on the Science and Application of Nanotubes, Brisbane, Australia. June 2012 (**Oral Presentation**).
  18. **K. Gulati**, K. Kant, D. Losic “Titania nanotube arrays: improved drug loading and releasing characteristics by tailoring nanotube structures” NT 12, Brisbane, Australia, June 2012 (**Poster Presentation**).

19. **K. Gulati**, T. Altalhi, D. Losic “Characterization of titania nanotube arrays with carbon nanotubes for drug delivery applications” NT 12, Brisbane, Australia, June 2012 (**Poster Presentation**).

# DECLARATION

I certify that this work contains no material which has been accepted for the award of any other degree or diploma in my name in any university or other tertiary institution and, to the best of my knowledge and belief, contains no material previously published or written by another person, except where due reference has been made in the text. In addition, I certify that no part of this work will, in the future, be used in a submission in my name for any other degree or diploma in any university or other tertiary institution without the prior approval of the University of Adelaide and where applicable, any partner institution responsible for the joint-award of this degree.

I give consent to this copy of my thesis when deposited in the University Library, being made available for loan and photocopying, subject to the provisions of the Copyright Act 1968. The author acknowledges that copyright of published works contained within this thesis resides with the copyright holder(s) of those works. I also give permission for the digital version of my thesis to be made available on the web, *via* the University's digital research repository, the Library search and also through web search engines, unless permission has been granted by the University to restrict access for a period of time.

KARAN GULATI

24/09/2015

# ACKNOWLEDGEMENTS

This journey has been amazing, from ‘nowhere to go’ to ‘yes I always wanted to be a scientist’. It would have been very difficult, if there wasn’t continuous support and ‘push’ from Prof Dusan Losic. For all the crazy ideas I had, he gave me the freedom to explore them. He always says ‘this is just the beginning’, and yes indeed this is the beginning. He believed in me and taught me so many things, that now I stand confident as a young researcher. I consider myself to be very lucky to have had a mentor like Prof Losic. Prof David Findlay, a true bone expert and one of those researchers who are always smiling, assisted me throughout the journey. He always edited all the abstracts and manuscripts so very quickly, and the more red marks I saw, the more confident I was with the final document. I would also like to thank The University of Adelaide for providing me the wonderful platform and the scholarship.

Prof Gerald Atkins allowed a material science person like me into his bone biology lab and always helped in designing the experiments and improving the manuscripts. If Masakazu Kogawa would have refused to train me in times when he was so much occupied, this thesis would have been really difficult to compile. He is a true genius and has helped me in times when I had nowhere to go. On the other hand, Matthew Prideaux always agreed to my not-so-crazy implant ideas, and did the cell studies when I was so very occupied (and also untrained). I have learnt many things while working in the Ortho Lab at IMVS, under the supervision of Prof Gerald, Masa and Matt, true hard-working professionals. Another person who was always available to assist me is Abel Santos. I see him as a true scientist, very professional and helpful. Tushar Kumeria, Ramesh Karunagaran and Lucas Johnson deserve special thanks for being there whenever I was confused and stuck. I would also like to appreciate the contribution from Luis Lima-Marques at IPAS for the 3D printing, which changed everything.

The support from the characterization facility at Adelaide Microscopy, particularly Ken Neubauer, Lyn Waterhouse, Aoife McFadden and Agatha Labrinidis, is very much appreciated. They as a team were always there to help, even after hours and on the weekends. I would also like to thank the Losic research group and School of Chemical Engineering for providing a friendly and nurturing environment. I would also like to thank Manpreet, Gagan and Saji, for making the lab an interesting place to work in. These 3.5 years were awesome, and mostly less-stressful, thanks to fun times with Bhai, Bandu, Yogesh, Shaurya, Krishna, Vikram, Yatin and others. Not to forget overseas support from Jammy, Guptaji, Harish, Gaurav and Sanchit.

Nothing would have been possible, if it wasn't for Maneet, the person who was the driving force for every motivation and energy. Being a family away from home, she was always there for me, through thick and thin times. For her support and endless love, I consider myself very lucky. I wish and pray for her to complete her PhD smoothly and timely, so that we can go on the much awaited vacation, which I imagined every time I got bored of writing.

Thanks to my parents, who believed in me and blessed me throughout this journey. It's all their prayers and blessings, and nothing else. Simran, Piyush and Subhash Uncle, were the other pillars, always motivating me and praising me. Special thanks to little Harnoor, her photos and videos uplifted my mood in times full of tension and sleeplessness.

# CHAPTER 1

---

## INTRODUCTION

**Karan Gulati**

School of Chemical Engineering, The University of Adelaide,  
South Australia 5005, Australia

**This chapter is based on the following published book chapter and review articles:**

1. **K. Gulati**, M. Kogawa, S. Maher, G. Atkins, D. Findlay, D. Losic “Titania Nanotubes for Local Drug Delivery from Implant Surfaces” in book *Electrochemically Engineered Nanoporous Materials: Methods, Properties and Applications* 2015, ed. by D. Losic and A. Santos (Springer International Publishing AG - Germany). Springer Series in Materials Science 220, **DOI**: 10.1007/978-3-319-20346-1\_10
2. D. Losic, M. S. Aw, A. Santos, **K. Gulati**, M. Bariana “Titania Nanotube Arrays for Local Drug Delivery: Recent Advances and Perspectives” *Expert Opinion on Drug Delivery*, 2015, **12**, 103-127.
3. **K. Gulati**, M. S. Aw, D. Findlay, D. Losic “Local Drug Delivery in Bone by Drug Releasing Implants: Perspectives of Nano-Engineered Titania Nanotubes” *Therapeutic Delivery*, 2012, **3**, 857-873.

# CHAPTER 1: INTRODUCTION

## 1.1. Bone Implants and Challenges

Metal implants, frequently composed of titanium and its alloys, are commonly used for long-bone fracture/non-union fixation, correcting spinal fractures, total joint replacements for arthritic/osteoporotic joints, and maxillofacial applications <sup>1</sup>. These implants, mostly in the shape of screws, plates, meshes, pins etc., mechanically stabilize the traumatized/fractured bones so as to reduce pain, enable optimal alignment and healing. The mechanical properties of these various implants are paramount for their optimal performance <sup>2-3</sup>. Furthermore, the mechanics and biology at the bone-implant interface can determine the fate of the implant and success of bone healing. Conventional bone implants are more focused on ‘mechanical fixation’ and rely on the ‘self-healing’ property of the traumatized bone. Many factors contribute towards failure of fracture healing, including patient condition (disease, medications, smoking/alcohol, and diabetes), local factors (severe fractures, infection, and poor vasculature) and surgery/implant characteristics (inappropriate implant functioning, low bone stock etc.) <sup>1,4</sup>.

Factors that compromise the short- and long-term success of joint replacements/fracture fixation implants are loosening/rejection, inadequate bone integration and deep bone infections, which can cause amputation or even death <sup>5</sup>. Reports have suggested that each year several million dollars are spent in correcting/replacing failed implants/joint replacements, with considerable morbidity and mortality <sup>6</sup>. Moreover complications due to implant failures have resulted in class action law suits. Aside from implant-induced inflammation and infection, mechanical failure/implant fracture and toxic release of particles and/or metal ions from implants have also caused serious problems <sup>7</sup>.



Infection due to implant placement in bone is relatively rare, but a devastating side effect of orthopaedic surgery. The current way to treat bone for infection or other disease states is systemic drug administration. Bacterial infection, in particular, can be very difficult to treat and eradicate in bone, because of the difficulty of achieving effective drug concentrations at the affected site and development of bacterial biofilms, which are highly resistant to treatment<sup>8-9</sup>. Such problems mean that systemic therapy can be ineffective, as well as exposing all tissues of the body with high levels of drug, potentially wasting expensive drug and risking adverse events. **Figure 1.1** summarizes the common challenges associated with bone implant placement and the sub-optimal conventional therapeutic approaches.

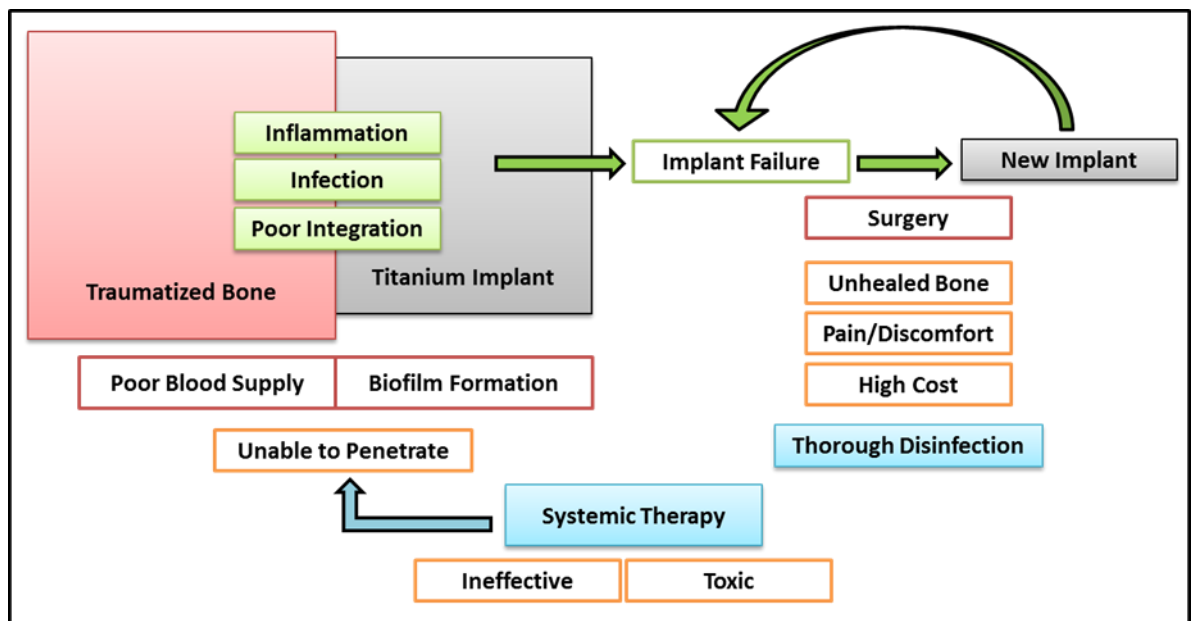


**Figure 1.1.** Challenges faced by conventional bone implants and the sub-optimal efficacy of systemic drug administration.

## 1.2. Complex Bone Conditions Demanding Effective Therapies

### 1.2.1. Osteomyelitis

Osteomyelitis (OM) is the infectious inflammation of bone, and its incidence in the USA is 1-2 %, with higher prevalence in developing nations <sup>10-11</sup>. The increase in the number of hip/knee replacements surgeries in the past decade has also led to an increase in OM cases. Furthermore, in spite of following strict aseptic procedures and antibiotic prophylaxis, OM occurrence is as high as 22-66% post orthopaedic surgeries, and the associated mortality rate is around 2% <sup>12</sup>. These infections are mostly caused by flora that commonly reside on the skin and in the mouth, mainly *Staphylococcus aureus* and *Staphylococcus epidermidis* <sup>13-14</sup>. Urgent treatment is required after the onset of bone infections so as to avoid the spread to new sites in the patient's body. Conventional treatment involves 2-6 weeks of intravenous antibiotic administration and a 6-month oral antibiotic course (for chronic infection), together with surgical removal of infected bone <sup>15-16</sup>. This approach has several limitations: side effects, ineffective drug concentration at the trauma site, and bone loss/damage and the need for complex surgery to address this.

To address these challenges, local drug delivery or LDD has been suggested, and the first attempts towards treating OM involved potent hydrophilic antibiotics incorporated into poly(methyl methacrylate) or PMMA beads <sup>17</sup>. However, this FDA-approved polymeric LDD strategy has its own challenges, including: non bio-degradability of PMMA and the need to remove *via* surgery, toxicity, fast burst and poorly controllable release, and the possibility of promoting antibiotic resistance <sup>18-19</sup>. As a result, alternative LDD strategies were devised, mainly using bioresorbable alternatives such as calcium sulphate cements <sup>20</sup>. Although these are relatively non-toxic and biodegradable, they do not always enable bone formation, leaving a fibrous gap instead <sup>21-22</sup>. Hence there is an urgent need to develop alternative LDD strategies

that can deliver potent antibiotics locally for a prolonged duration and in a controlled and sustained manner, while not inhibiting osteogenesis.

### 1.2.2. Osteoporotic Fractures

Millions of people worldwide are diagnosed each year with osteoporosis (OP) and low bone density<sup>23</sup>. OP represents a pathological condition characterised by loss of bone mineral at a rate that exceeds the new bone formation, whereby the bones become fragile and fracture prone. With the increase in the ageing population and negative lifestyle factors, the number of OP patients is predicted to increase. Furthermore, OP fractures can result in high morbidity or mortality rates<sup>24</sup>. Reports have claimed that one in three women and one in five men with age > 50 years will suffer OP fracture<sup>25</sup>. With below average healing capacity and low bone stock, OP fractures can be very hard to heal, and often require long-term hospitalization and invasive surgeries<sup>26</sup>.

To reduce OP fracture healing times, several therapeutics have been suggested, although only parathyroid hormone (PTH) and bone morphogenetic proteins (BMPs) are currently approved<sup>27-29</sup>. Systemic administration of such potent therapeutics is, in the case of BMP not possible. As a result, LDD of such therapeutics have been investigated<sup>30-33</sup>. Various strategies, including polymeric beads, co-polymer matrices and calcium-phosphate modifications on Ti implants have been investigated, in an attempt to augment bone formation directly at the fracture site<sup>30-33</sup>. However, limitations associated with polymeric and ceramic implant systems, as mentioned earlier, have again driven the research towards finding more suitable alternatives.

## 1.3. Local Drug Delivery in Bone

Ineffectiveness of conventional treatments to target bone conditions has driven the need for local drug delivery or LDD. The concept of drug delivery locally from implants at the bone site was introduced by Buchholz *et al.*, whereby the need to locally administer potent antibiotics to combat bacterial infection was suggested<sup>34-35</sup>. This means releasing therapeutics locally at the site desired, from the surface of the implant, bypassing the need for systemic drug delivery. The idea is to have sufficient local concentration of the drug so as to address the disease/fracture, while minimising any unnecessary toxicity throughout the body. In LDD, the implant is modified to contain therapeutics, which upon surgical placement, will be released locally by simple diffusion. To achieve this, the surface of the implant needs to be engineered so as to contain substantial drug amounts.

Besides improving implant acceptance and prevent implant-related complications, LDD has opened the way for effective treatment of conditions, such as osteoporosis, bone cancers, and bone infections. Moreover, the target tissue/condition determines the choice of implant material, which to date include biopolymers, ceramics, and metals/alloys. However, for load-bearing situations, such as fracture-fixation or total joint replacements, titanium and its alloys are most preferred due to their properties of corrosion-resistance, biomechanics and ease of functionalization<sup>36</sup>. The simplest of the LDD examples include coating the surface of implants with potent therapeutic formulations, such as antibiotics or growth factors.

### 1.3.1. Surface Modification of Bone Implants

The surface characteristics of bone implants or biomaterials, for example topography, chemistry or surface energy, play an important role in determining cellular functions and hence successful tissue integration<sup>37</sup>. The first steps of cell-to-material interaction include cell attachment, adhesion and spreading, which must be modulated by the implant surface to

encourage implant acceptance and tissue healing. For bone implants, appropriate surface roughness can enhance osseointegration (OI), but also rough surfaces can allow substantial quantities of active therapeutics (antibiotics or bone forming proteins) to be loaded and hence released locally. In order to achieve this, various surface modification strategies for titanium bone implants have been proposed <sup>38</sup>.

### ***1.3.1.1. Micro-Scale Roughening***

Numerous investigations have been conducted to tailor surface roughness to achieve enhanced cellular activity and hence therapeutic effects <sup>39</sup>. Furthermore, various *in-vitro/in-vivo* studies, along with mathematical modelling have indicated that roughness in the scale of micro-meter (especially hemispherical pits ~ 1.5  $\mu\text{m}$  deep and ~ 4  $\mu\text{m}$  wide), provides the most suitable bioactivity <sup>40-41</sup>. The most common techniques to engender micro-scale roughness include sand-blasting, acid-etching, plasma treatment and electrochemical anodization. In sand-blasting, the implant surface is bombarded with abrasive particles (alumina, titania and hydroxyapatite/HAP) under high-pressure. Among the various choices, HAP has been recognised as the best particle, which promises increased bone cell adhesion as compared to others <sup>42-45</sup>. A similar effect can also be achieved by chemical etching of Ti with strong acids such as:  $\text{HNO}_3$ ,  $\text{HCl}$ ,  $\text{H}_2\text{SO}_4$  and  $\text{HF}$  <sup>46</sup>. The typical procedure involves immersion of Ti implants into these etching acids for prolonged durations. HF etching further enables incorporation of active fluoride ions inside the micro-rough Ti, which has been shown to positively influence bone cell functions <sup>47</sup>. Plasma-assisted spraying of Ti, Zr or  $\text{Al}_2\text{O}_3$  also induces micro-scale roughness to the implant surface. This technique has been demonstrated to improve wear resistance of the resulting surface (as compared to sand-blasting and acid-etching). However, with the use of Zr/ $\text{Al}_2\text{O}_3$ , compromised osseointegration of the implant has been reported <sup>48</sup>. Furthermore, the plasma process is complicated and expensive, thereby limiting its use.

Electrochemical anodization (EA) has been used for many decades to grow a thick oxide layer on the surface of metals to achieve anti-corrosion and colouring effects <sup>49</sup>. In general, EA represents a very cost-effective and scalable technology, whereby oxide forms on metal surfaces when metal is exposed to suitable electrolytes (sulphuric, phosphoric, acetic acid etc.), under the influence of voltage. Furthermore, this technique allows easy control over the thickness and properties (mechanical and chemical) of the resultant oxide, by varying anodization conditions such as electrolyte concentration, voltage, time and temperature <sup>49-50</sup>. When the same process is continued for extended periods of time at high voltages (> 100 V), a metal oxide film with irregular micro-porosity and enhanced mechanical properties is obtained (spark anodization or micro-arc oxidation) <sup>51</sup>. Furthermore, upon immersion in simulated body fluid (SBF), such micro-porous oxides enable HAP growth, which significantly improved implant bioactivity <sup>52</sup>.

### ***1.3.1.2. Promoting Bioactivity and Biosafety of Implants***

It is well known that the protein adsorption and conformation on the implant surface is the first event upon implant placement inside the traumatized tissue, which to a great extent decides the fate of the implant <sup>53-54</sup>. If the surface of the implant is modified such that these protein/cellular interactions can be modulated, then the implant acceptance and survival chances can be significantly increased. This can be achieved by incorporation of various bioactive species in/on the implant surface, in particular Ca, P, HAP (hydroxyapatite) or growth factors. For instance, CaP coatings on Ti implants have shown promising results for enhancing bone cell functions, which can be improved further by immobilizing growth factors <sup>55</sup>. Furthermore several biopolymers and ceramics have also been applied to promote bioactivity of the implant by modulating protein interactions and promoting cell functions <sup>56</sup>. These studies utilised bioactive species (biomolecules/growth factors) incorporated inside porous ceramics and biodegradable/bioactive polymers. The dual effect of bioactive

polymers/ceramics and active species such as BMPs (bone morphogenetic proteins), can significantly increase implant biomechanics and bone-remodelling abilities<sup>57</sup>. These strategies have shown promising results in improving bioactivity of the implant and healing rates of the traumatized bones, however, inadequate release kinetics due to unpredictable polymeric degradation has driven more research towards finding more reliable bioactive solutions to ensure long-term success of bone implants.

Protein reactions on the implant surface are electrochemical in nature, which often leads to oxidation of the implant surfaces, often leading to thicker oxides with time<sup>54,58</sup>. These reactions can also cause metal corrosion and studies have reported the release of by-products of such reactions from the implant surface, which have been detected in the body of the patient<sup>59-60</sup>. Furthermore, leaching of metal ions in particular can adversely affect bone healing rates<sup>61</sup>. As a result, and to ensure biosafety and biocompatibility of the implant and its modifications, it is important to avoid toxicity by utilising only stable, well-adherent and biocompatible/biodegradable strategies to modify implant surfaces.

### ***1.3.1.3. Releasing Therapeutics from Implant Surfaces***

The need for systemic drug administration can be bypassed by local release of therapeutics, for example from the surface of the implant, directly at the site of implantation/trauma (**Figure 1.2**). The simplest of such strategies include coating or adsorption of active therapeutics such as antibiotics or proteins, into the titanium implant surfaces or its modifications (micro-rough surface or biopolymer coatings)<sup>62-63</sup>. Such investigations have demonstrated improved implant performances including prevention of bacterial infection and promotion of bone cell functions<sup>64-66</sup>. However, these therapeutic coatings often fail, mainly due to poor mechanical stability, quick consumption and fast release kinetics, and re-triggered bacterial invasion<sup>65-66</sup>.

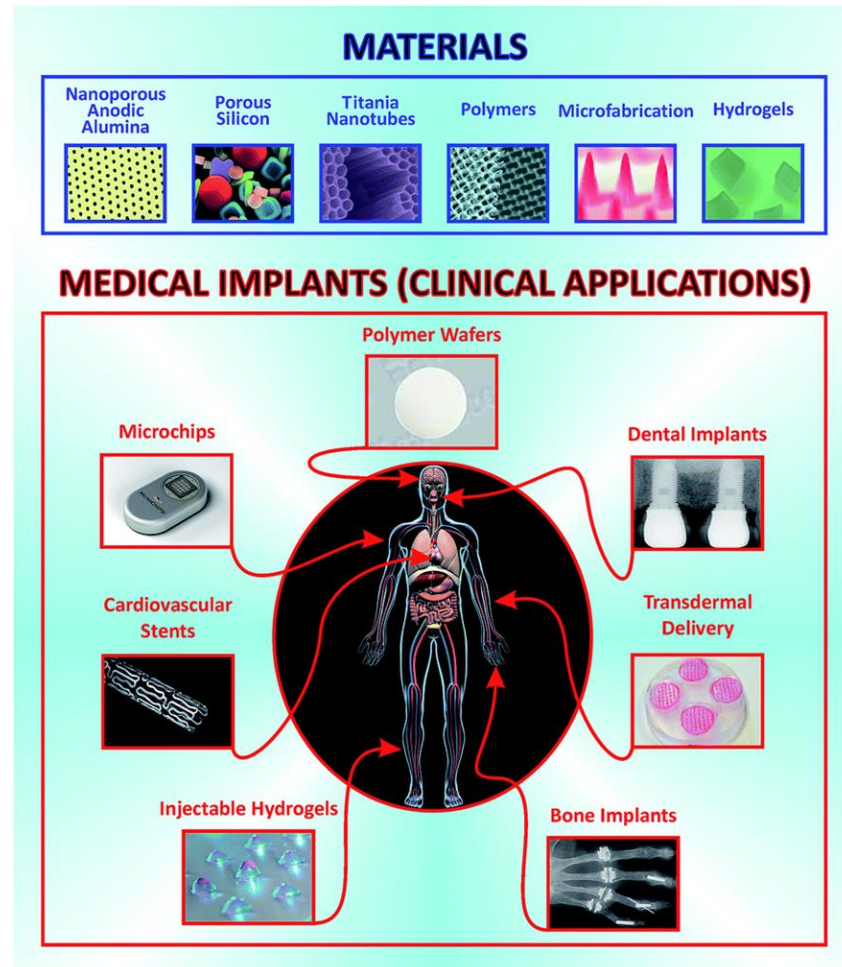


**Figure 1.2.** Various micro-/nano-engineering strategies for fabricating drug-eluting implants catering to wide range of therapeutic needs (with permission from [68]).

### 1.3.2. Research Gap

Multiple strategies have been suggested to improve bone implant acceptance/survival and enable quicker healing rates; however each strategy has some challenges that must be addressed before proceeding to clinical trials. Improper therapeutic release, compromised biocompatibility, inadequate modulation of cellular functions, poor mechanical stability and release of toxic metal ions, limit one or the other implant structural modification strategy. Furthermore, for load bearing conditions such as fracture fixation or total joint replacements, only polymeric/ceramic implants can cause poor mechanics with the healing bone, for instance failure under pressure, and implant loosening due to early degradation/corrosion.



Metallic implants, particularly Ti and its alloys, which have been established for their corrosion resistance, biocompatibility and appropriate biomechanics with human bone, stand out as the most suitable implant material choices. While combining multiple strategies into one implant modification (like therapeutic loaded polymers/ceramics on micro-rough Ti) did improve bone implant function, for long-term osseointegration after consumption of polymers, these approaches demand improvements. Also, mere coating of therapeutics on roughened Ti implants does not provide optimum release kinetics for prolonged durations, and in fact very high release concentrations can adversely affect the osseointegration of the implant.

The following properties of a metal implant modification are desired to fabricate the next generation of bone implants with drug-releasing function that can also cater to complex bone conditions such as deep bone infections, osteoporotic fractures and cancers:

- a. Reproducible, easy and cost-effective fabrication
- b. Mechanical stability (especially in load-bearing implant conditions)
- c. Non-toxic (avoiding leaching of toxic metal ions)
- d. Substantial therapeutic loading and delayed release (catering to a wide-range of conditions and to achieve a long-term effect)
- e. Inherently bioactive (for long term osseointegration, after consumption of therapeutics)

### **1.3.3. Nano-Engineering Bone Implants: Titania Nanotubes**

To enable higher loading amounts and controlled local-release of active therapeutics, nano-engineering of the implant surfaces has been suggested<sup>67</sup>. After the advent of techniques such

as electrochemical anodization (EA), nano-tubular or nano-porous surfaces, such as porous silicon, nano-porous alumina and nano-tubular titania, have gained much popularity towards improving the therapeutic/bone-forming ability of implants<sup>50,68</sup>. Among these, fabrication of nano-tubular titania (TiO<sub>2</sub>) or titania nanotubes (TNTs) on titanium implant surfaces represents an ideal implant modification strategy, which has the potential to address challenges associated with conventional bone implants. Moreover, TNTs technology ensures easy integration into the current implant market, where titanium and its alloys comprise a large proportion.

Due to its properties, primarily corrosion resistance, biocompatibility, easy-to-tailor dimensions, cost-effective synthesis, and ease of functionalization, titania nanotubes (TNTs) fabricated as self-supporting membranes, on Ti substrates and as loose agglomerates, have been extensively explored for a variety of applications<sup>49</sup>. TNTs represent hollow, cylindrical, hexagonally ordered and vertically-oriented arrays of TiO<sub>2</sub>, as shown in **Figure 1.3**. The dimensions of these unique nanostructures in the form of tiny test-tubes, open at top and closed at bottom, can easily be tailored using fabrication strategies. Furthermore, they can be synthesized with diameters of 100-300 nm and lengths of 0.5-1000 μm<sup>50</sup>. Owing to their unique properties, they have been applied for numerous applications, including photocatalysis, purification, bio-sensing, bioactive surfaces, drug-eluting implants, and dye-sensitized solar cells<sup>49</sup>.

## **1.4. Fabrication of TNTs**

Titania nanotubes (TNTs) are 1-dimensional structures with tubular morphology, open at top and closed at bottom, which hexagonally self-order in an array onto Ti substrates or form as loose agglomerates in solution. They can be fabricated by three main methods: template-assisted, hydro/solvothermal and electrochemical anodization. For template-assisted

fabrication, various templates have been used, including molecular rod like assemblies of micelles, to more organised structures like nanoporous alumina<sup>69-70</sup>. The templates are coated with sol-gel or atomic layer deposition (ALD) to facilitate TNTs formation. However, the yield of TNTs is on or inside template structures and removal results in loose TNT agglomerates with a wide range of TNT lengths. Template-free approaches include the hydro/solvothermal method and electrochemical anodization. In the case of hydro/solvothermal methods, which reassemble in nanotubular morphology, TiO<sub>2</sub> particles are autoclaved in NaOH, however, the yield is in the form of TNT agglomerates with wide size distribution<sup>71-72</sup>. For the electrochemical anodization (EA) technique, TNTs structures form in the presence of fluoride-containing electrolytes under the influence of appropriate voltage. More recently, TNTs have also been fabricated using electrospinning strategy, whereby titanate precursors are coated onto polymeric fibers and later the polymers are decomposed via heat treatment, yielding hollow titania nanofibers or TNTs<sup>73-74</sup>. However, among the various approaches described for fabricating TNTs, EA stands out, mainly due to its ability to produce TNTs vertically self-ordered onto a Ti substrate with good control over the dimensions. This is essential, particularly for medical applications suited for bone implants, whereby Ti and its alloys are routinely used as implants/joint replacements, and EA enables growth of TNTs onto Ti substrates with the ability to tailor their characteristics.

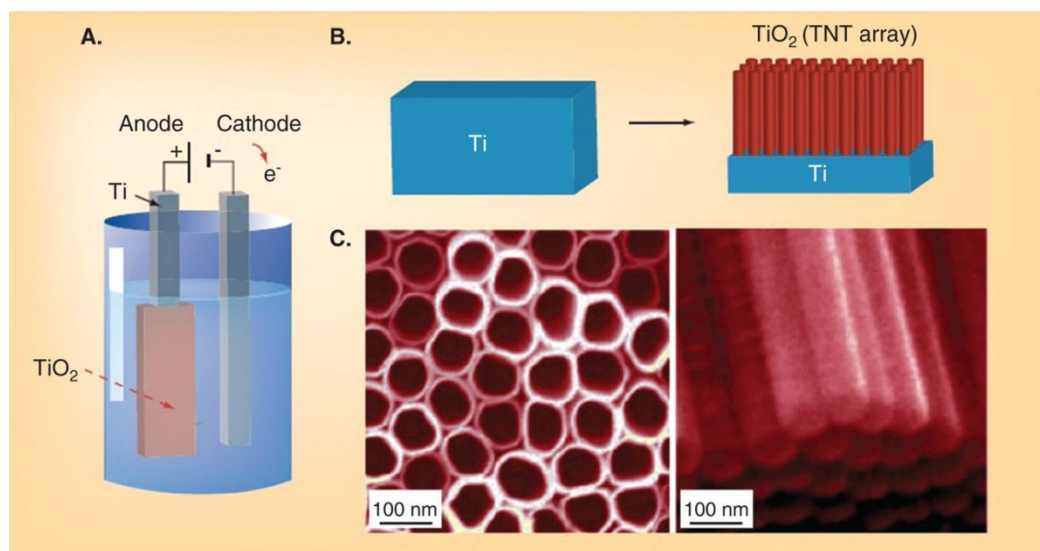


**Figure 1.3.** Electrochemical anodization of titanium to fabricate titania nanotubes (TNTs). (a) Scheme of electrochemical setup, (b) vertically arranged arrays of TNTs on Ti, and (c) SEM images showing open-pores and closed bottoms suitable for drug loading/releasing applications (with permission from [185]).

### 1.4.1. Electrochemical Anodization (EA)

EA is a century old industrial technique to fabricate oxide layers on the surfaces of metals, mainly to promote corrosion resistance, and for aesthetic appeal. The basic setup of EA involves an appropriate electrolyte, target metal substrate (working electrode or anode), and counter electrode (**Figure 1.3a**). When an adequate voltage is applied, metal (Ti) is oxidised to form metal oxide (equation 1) or is dissolved in to the electrolyte (equation 2). These reactions ultimately lead to hydrogen gas evolution at the counter electrode (equation 3).



Upon formation of  $\text{TiO}_2$ , there are three possibilities: (a) metal oxide forms ions that are completely dissolved in the electrolyte (no oxide film formation, equation 2), (b) formation of an insoluble oxide film (equation 1), and (c) competition between oxide dissolution and formation. In the last case, under the influence of suitable ions such as fluoride, a balance is maintained between oxide dissolution and formation (steady state equilibrium), resulting in the formation of a porous oxide film (equations 1 and 4). When these reaction kinetics are optimized, the yield is highly-organised nano-porous or nano-tubular arrangement<sup>75-76</sup>.





For a typical EA resulting in the formation of TNTs, a characteristic current-density plot (vs time) is obtained, as represented in **Figure 1.4a**, where three different regions corresponding to various stages of formation of TNTs can be identified <sup>49</sup>. Region-1 corresponds to the reaction in equation 1, whereby current continuously drops due to formation of oxide on the surface of the metal. At this stage, this oxide film is partially disrupted by ‘nano-scopic’ etch channels, yielding a porous initiation layer <sup>49</sup>. This is followed by region-2, where the porosity increases the surface area of the electrode and hence the current is also increased. At this time, the initiated pores compete among each other for the available current, until an optimized equilibrium state is achieved, where the pores share the current equally. In region-3 a steady-state equilibrium is established, stable pore growth begins and the current reaches a constant value.

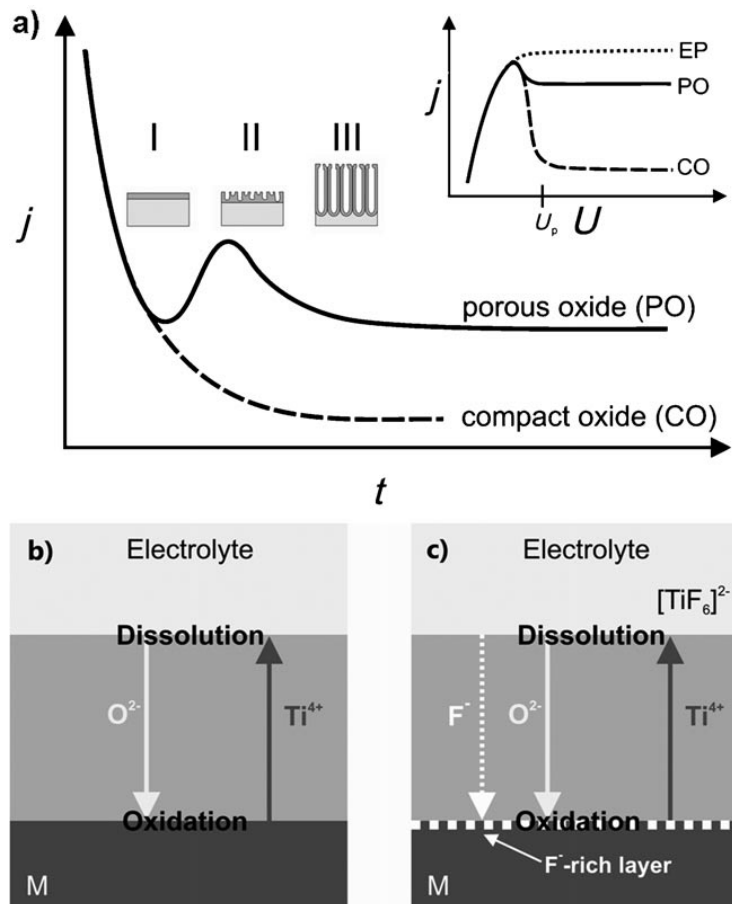


**Figure 1.4.** Characteristic features of electrochemical anodization of Ti to fabricate TNTs. (a) typical current-density ( $j$ ) vs time plot, compact-oxide/CO (---) forms for fluoride free electrolyte, and porous-oxide/PO (—) forms in fluoride containing electrolytes. Inset shows linear sweep voltamograms ( $j$ - $U$  plots) for electrolytes, containing different fluoride concentrations [very high: electro-polished/EP, very low: CO, intermediate: PO or TNT formation]. (b-c) Transport of active ions through the metal-oxide layer in the absence and presence of fluoride ions. (Adapted from [49]).

### 1.4.2. Progress in Ti Anodization

In 1999, Zwilling *et al.* pioneered the fabrication of TNTs using the EA technique, and since then many attempts have been made to improve the ordering of TNTs and achieving higher growth rates<sup>77-78</sup>. The initial studies only yielded TNTs with lengths of 0.5  $\mu\text{m}$ , due to extensive dissolution in the chromic acid electrolytes containing HF<sup>77</sup>. However, this study established the role of fluoride ions in self-ordering of the TNTs structures, but the resultant TNT yield lacked ordering and uniformity. This was followed by the 2<sup>nd</sup> generation of EA advancements, whereby pH controlled aqueous buffered electrolyte (with fluoride ions) significantly reduced the excessive dissolution and TNTs formed with lengths of 5-7  $\mu\text{m}$ <sup>79-81</sup>. These investigations also confirmed the relationship between nanotube characteristics (like size, organisation, crystal structure etc.) and the various anodization parameters like electrolyte composition, pH, voltage/current, time etc.<sup>79-81</sup>. This advancement led to the 3<sup>rd</sup> generation, where further increased growth rates (TNT lengths up to 1000  $\mu\text{m}$ ) were obtained by using non-aqueous polar organic solvents, such as dimethyl sulfoxide, formamide, ethylene glycol etc., in combination with fluoride ions<sup>82-83</sup>. The most optimized anodization conditions to fabricate highly-ordered, close-packed and long TNTs can be summarized as: anodization voltage of 80-120 V and organic viscous electrolytes. Furthermore, fabrication of TNTs has also been reported in fluoride-free electrolytes<sup>84</sup>.

Besides the advances in EA to fabricate high quality TNTs on Ti substrates, there remain some challenges that must be addressed to permit further optimization of the method. For instance, electrolyte ageing, which is anodization of dummy titanium foil repeatedly prior to anodizing target substrate, is not fully explored. While investigations have claimed that the use of aged/previously used electrolyte aids in fabricating high-quality TNTs, and contributes towards changing electrolyte characteristics and hence the TNT yield, there still remains scope for improvement<sup>49</sup>. The electrochemical systems used in these studies did not consider water absorption from the environment by the hygroscopic electrolyte, and the effect of ageing was not linked to structural stability/adherence of TNTs onto underlying substrates. Hence an in-depth study of the various anodization parameters, including electrolyte ageing, is desired to further optimize the anodization procedure to yield stable and well-adherent TNTs arrays. This can further aid in anodizing complex substrate geometries such as pins, wire, meshes etc., whereby occurrence of cracks and instabilities lead to delamination of the anodic film. It is noteworthy to mention here that for bone implant applications, mechanical stability is crucial and any defragmentation of TNTs can initiate tissue toxicity and lead to poor osseointegration.

Besides TNTs, alternate modified-TNTs and other TiO<sub>2</sub> nanostructures have also been fabricated as a result of various voltage or current oscillations during the EA process<sup>49,76</sup>. These include branched nanotubes, nanolace, inner-tubes, bamboo-type nanotubes, and multilayer nanotubes (**Figure 1.5**)<sup>85</sup>. However these altered morphologies of the TNTs have not as yet served any application. Very recently, to further enhance the EA process, the effect of UV-Vis irradiation on EA of Ti was investigated and the results confirmed the growth of larger diameter TNTs with thicker walls<sup>86</sup>. In a similar study, ultrasound forces were used during the fabrication procedure to promote TNT growth rates<sup>87</sup>.

Novel TNT structures as described above can offer interesting properties to otherwise straight cylindrical TNTs, especially for local therapeutic release applications suited for bone implants. By simply modulating the voltage or current during the anodization process, these structures with varied geometrical features can be generated, without any added complication. This simple methodology creates TNT structures with modulated dimensions in a periodic manner, corresponding to changes in the anodization voltage/current. This offers the ability to tailor TNT dimensions, including inner/outer diameter, branching of tubes, shape etc. For therapeutic applications, this can be translated into a modified available nanotubular volume. This vacant volume with modulated periodic features can enable improved drug releasing performance, mainly due to agglomeration of therapeutics inside the deliberately created restrictions in otherwise smooth straight pore nanotubes. Besides this, exploring the separation of loose nanotubes by breaking the tubular structures of modulated-TNTs, can offer interesting possibilities for drug encapsulation and targeted drug delivery.

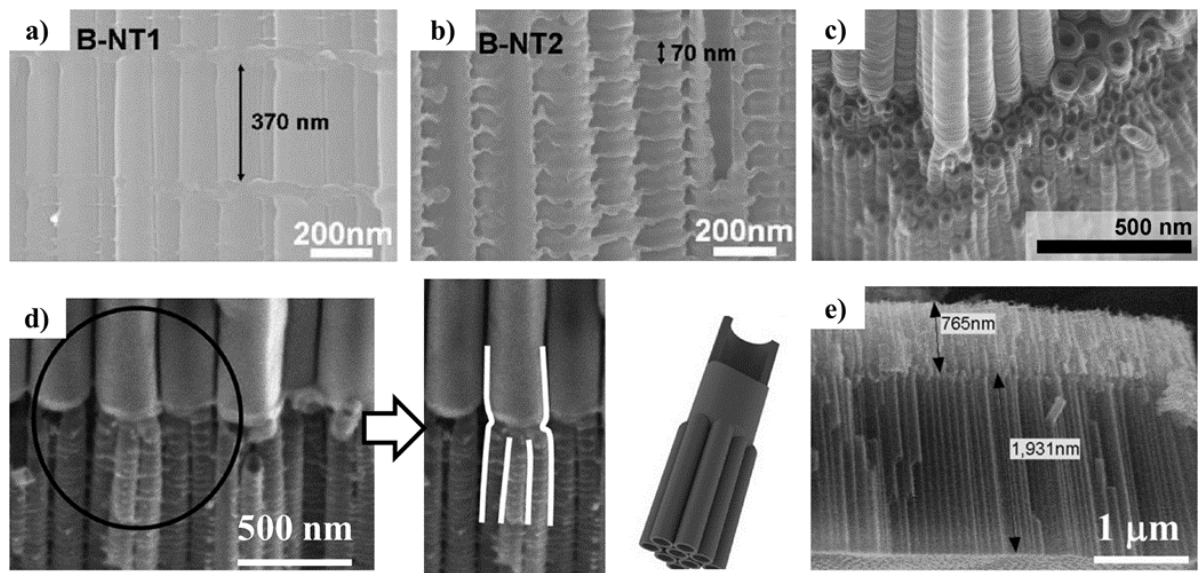


**Figure 1.5.** SEM images depicting the novel tubular  $\text{TiO}_2$  nano-structures fabricated using modified electrochemical anodization procedure. (a-b) Bamboo-type nanotubes with ability to tune segment size by voltage variation, (c-d) branched-nanotubes by voltage-stepping, and (e) hydrophobic and hydrophilic arrangement of nanotubes (Adapted from [76]).



### 1.4.3. TNTs on Complex Substrate Geometries

Research focused on TNT technology for bone implant applications generally involve TNTs fabricated on Ti flat foil substrates, whereby TNTs grow perpendicular to the substrate surface. Moreover the anodization optimizations have been performed for Ti flat substrates, which are easy to manage. However in the current bone implant technology, implants occur in various shapes and geometries such as pins, wires, screws, plates etc. Therefore to enable easy integration into the current implant market, TNT fabrication should be extended and optimized for more complex substrate geometries. This will require fabricating high quality and well adherent TNTs onto these complex substrates. Such advancements can ensure achieving 3-dimensional release from the implant surface. There are several reports showing fabrication of TNTs on meshes and wires, although for applications such as solar cells and filtration<sup>88-90</sup>.

In 2011 Yu *et al.* reported the fabrication of core-shell TNT structures by EA of Ti wires, followed by complete dissolution of the wire core, and these structures were proposed as photo-anodes for solar-cells<sup>88</sup>. Furthermore, Zeng *et al.* reported the fabrication of TNTs on Ti mesh by using a neutral electrolyte composed of ammonium sulphate and ammonium fluoride, and studied the influence of different anodization parameters on TNTs<sup>89</sup>. In another study, Sun *et al.* showed the influence of electrode orientation on TNTs fabricated by the anodization of hollow titanium cylinders<sup>90</sup>. These reports confirmed the fabrication of TNTs uniformly on the surface of various substrate geometries, however, optimization of anodization conditions on such complex substrate shapes and geometries has not been investigated. In addition, most studies have reported cracks in the anodic film formed on curved surfaces, which is due to competitive growth and volume expansion on a 3D circular surface. These cracks or instabilities must be controlled, and more research is demanded in this respect, particularly towards improving the adherence of the anodic film on such complex

substrates. This is important for the functioning and survival of the proposed applications, including electro-optics and bone implants, where delamination or breakage could lead to failure<sup>91</sup>.

#### **1.4.4. TNTs on Ti alloys**

Titanium alloys with Al, V, Ta, Zr have shown enhanced biomechanics as compared to commercially-pure Ti, and Ti alloys cover a large proportion of the implant market<sup>92</sup>. As a result, various surface modification techniques, including EA, have been extended to Ti alloys. Macak *et al.* anodized Ti alloys Ti-6Al-7Nb and Ti-6Al-4V, and obtained nanotubes composed of mixed oxides to lengths of several hundred nanometers<sup>93</sup>. Other researchers have reported similar results with Ti-28Zr-8Nb and Ti-35Zr<sup>94-95</sup>. Furthermore, rapid breakdown anodization (RBA) was utilised to synthesize oxide nanotubes on TiNb, TiZr and TiTa<sup>96</sup>. On the other hand, TiO<sub>2</sub> nanotubes or TNTs have also been fabricated on Ti alloys<sup>97-98</sup>. Nanotubes fabricated on biomedical alloys have also been proposed for drug delivery applications<sup>97</sup>. Briefly, the antibiotic minocycline hydrochloride was loaded inside TNTs fabricated on Ti-4Zr-22Nb-2Sn alloy *via* the immersion technique and the release kinetics were compared with different dimensions of nanotubes<sup>97</sup>.

### **1.5. Therapeutic Functions of TNTs/Ti Implants**

The vacant volume of the TNTs generated on Ti substrates can hold active therapeutics that can be released locally for extended periods of time, which can be controlled readily by adjusting the dimensions of the TNTs<sup>50</sup>. Furthermore, local drug delivery on a biocompatible surface modification on various Ti substrates and alloys means easy integration into current implants. Many studies have confirmed the local drug eluting abilities of TNTs, which were loaded with substantial amounts of antibiotics, proteins, growth factors etc., each representing varied solubilities, chemistries and catering to particular bone-implant challenges<sup>68</sup>. Also,

TNTs offer ease of chemical and biological functionalization, which could easily enhance drug loading/releasing abilities and modulate cellular behaviour. Various biocompatibility and toxicity studies carried out using TNTs have established their suitability for implantable applications<sup>99-100</sup>. More suited for bone implants, TNT-modified Ti surfaces have been shown to promote bone cell function, including adhesion and differentiation (**Figure 1.6**)<sup>101-102</sup>. Investigations with bacteria, endothelial cells, macrophages etc. on TNT-modified implants have suggested their ability to cater to implant-related challenges, such as infection, tissue integration, and inflammation<sup>102-105</sup>. Therefore, fabrication of TNTs on Ti implants represents a promising strategy to address complex implant challenges<sup>50,68</sup>. Moreover, as described earlier, implant failure can result from inadequate osseointegration and bacterial invasion<sup>106</sup>. On the other hand appropriate modulation of the immune responses or FBR (foreign body response) can enable implant acceptance and survival. In order to address the most common implant challenges, various therapeutics have been loaded inside of TNTs and their local release has been studied in various *in-vitro* and *in-vivo* settings<sup>68</sup>.

## 1.5.1. Modulation of Immune Responses

### 1.5.1.1. Foreign Body Response

Immediately following biomaterial implantation, ECM proteins and blood interact with the implant surface (**Figure 1.7**). The immune response is determined by the local environment at the site of implantation and the protein adsorption/conformation on the implant surface<sup>36,107</sup>. As a result, the implant surface modifications are aimed at minimising unfavourable interactions, thereby avoiding FBRs such as fibrous tissue encapsulation of implants<sup>108</sup>. However, it has been reported that modulating such responses in an appropriate manner is advantageous for the implant acceptance and osseointegration<sup>109-110</sup>. The tuning or modulation of immune responses can be realised by: (a) limiting functionality (adhesion and

activation) of macrophages by adequate surface roughness, and (b) surface incorporations of anti-inflammatory drugs or growth factors<sup>107</sup>.

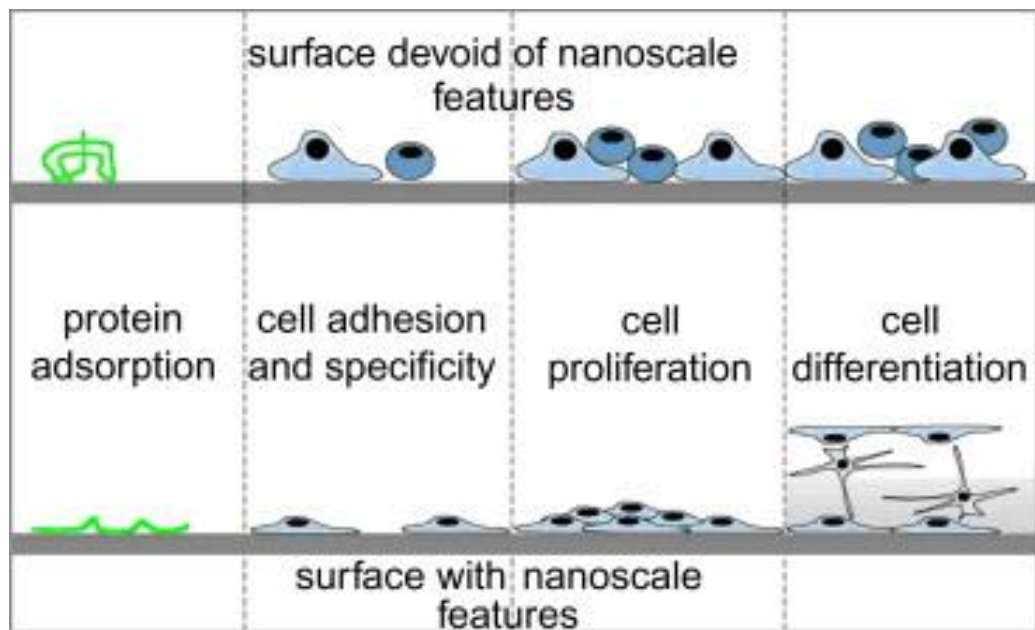


**Figure 1.6.** Schematic showing how cellular behaviour is modulated by nano-topography of the implant surface (with permission from [182]).

#### 1.5.1.2. Immune Responses on TNTs

In a study by Ainslie *et al.*, the ability of the nano-rough surface of titanium implants in reducing the inflammatory response was demonstrated<sup>110</sup>. They investigated and compared the immune reactions (human monocyte viability and morphology, inflammatory cytokines and reactive oxygen species generation) between smooth and nano-structured surfaces<sup>110</sup>. Furthermore, *in-vitro* short and long term immune responses were compared between TNTs and medical grade Ti, using human blood lysates (with leukocytes, thrombocytes and erythrocytes)<sup>111</sup>. Immune cells (macrophages, monocytes and neutrophils) showed significantly reduced cell functions (viability, adhesion, proliferation) for both short and long term on TNTs<sup>111</sup>. Also, very recently, an *in-vitro* study of TNTs and Ti with macrophages [RAW264.7] confirmed reduced inflammation in response to TNTs, suggesting the ability of

TNTs at modulating the macrophage responses <sup>104</sup>. These studies, along with other *in-vivo* investigations, whereby no fibrous encapsulation was observed for TNT implants, confirm the role of anodized nano-tubular surface in avoiding unwanted immune responses, which can result in excessive inflammation or, at the extreme, the need for total implant replacement

68,102

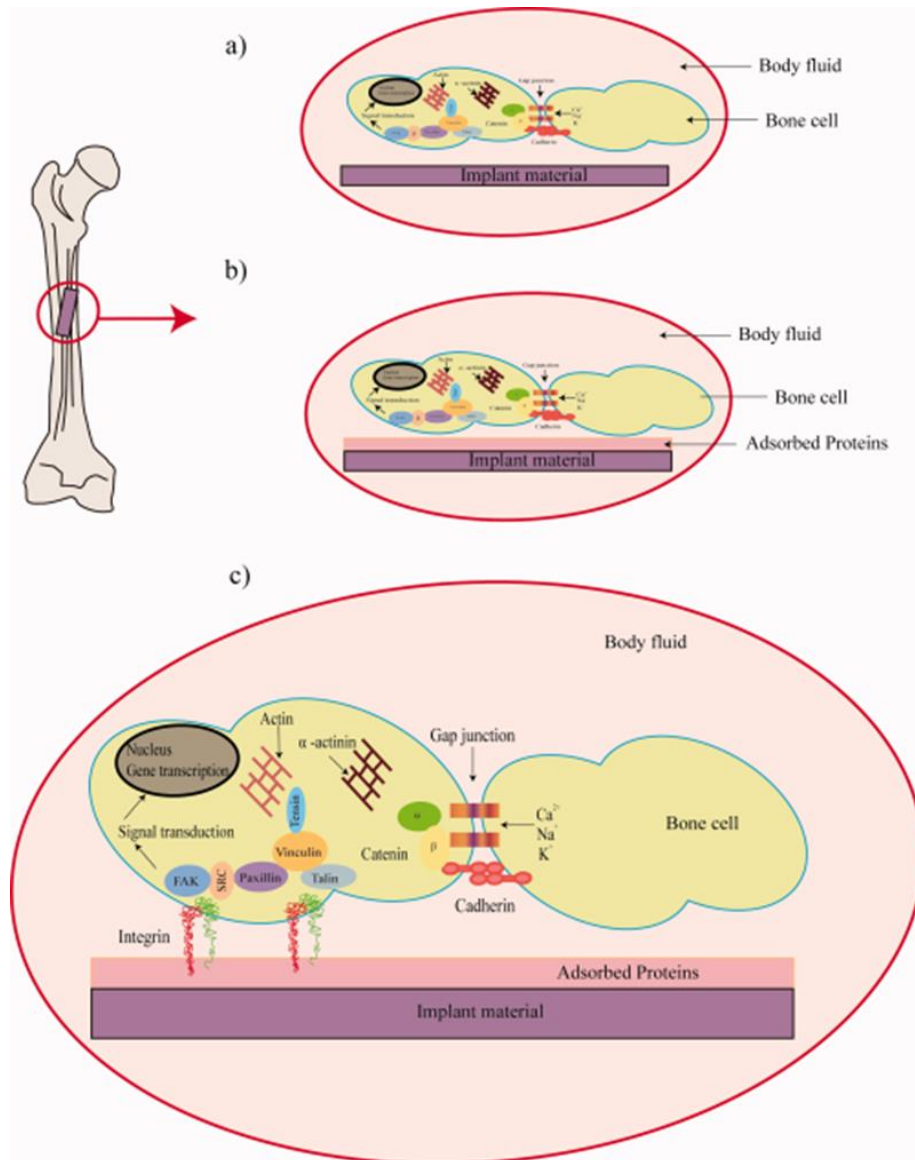


**Figure 1.7.** Schematic illustration of cellular interactions with the implant surfaces: (a) immediately after implant surgery, (b) protein adsorption/conformation on the surface, and (c) cellular attachment (with permission from [183]).

### ***1.5.1.3. Loading Anti-inflammatory Drugs***

Although TNTs by themselves have shown the ability to reduce excessive inflammation, various studies have shown substantial loading and local release of anti-inflammatory drugs from TNT modified implants. Aninwene *et al.* demonstrated the SBF deposited loading of dexamethasone inside TNTs and confirmed controlled drug release and enhanced osteoblastic functions<sup>67</sup>. Indomethacin is a commonly prescribed NSAID (non-steroidal anti-inflammatory drug) for pain and inflammation<sup>112</sup>. Our group has also extensively studied the enhanced loading and controlled release of indomethacin from TNT/Ti implants<sup>100,113,114</sup>. We have shown previously that advanced drug releasing features, like controlled release/multi-drug release of indomethacin, can be achieved by biopolymer coatings on drug-loaded TNTs and by micellar encapsulation of drugs<sup>113-114</sup>. Furthermore, alternative anti-inflammatory drugs, such as ibuprofen, sodium naproxen etc., have also been loaded using various strategies and their favourable release kinetics observed<sup>115-116</sup>.

## **1.5.2. Antibacterial Effects**

### ***1.5.2.1. Race to Invade Implant***

Studies have confirmed that smooth implant surfaces prevent bacterial attachment, but bone cell attachment, which is crucial for osseointegration, is also reduced<sup>117</sup>. Both bone cells and bacteria prefer rough surfaces, which provide ‘anchoring-points’, and thereby lead to successful attachment and adhesion<sup>1</sup>. As a result, modifying the surface roughness alone cannot be used to simultaneously reduce bacteria attachment and enhance bone cell function, in the case of bone implantation. In fact, post-implantation, pathogens may invade the traumatized bone site *via* the same mechanism as do the host immune cells<sup>118</sup>. There thus can be a ‘race’ between immune cells and bacteria to reach and invade the compromised implant site, and this may determine the fate of the implant<sup>119</sup>. The incidence of implant-associated

infections has been reported as 2-30% for transcutaneous fracture correction pins, and 2-5% for spinal implants<sup>120</sup>. The most common pathogens causing implant-related infections include: *S. aureus*, *S. epidermidis* and *Pseudomonas aeruginosa*<sup>121-122</sup>.

#### ***1.5.2.2. Treatment of Implant-Infection and Osteomyelitis***

As stated previously, osteomyelitis (OM) or deep bone infections are very serious medical challenges, and if untreated, can result in amputation and even death. Similarly, infection at the site of implantation can lead to OM. Prophylactic treatment involves simple antibiotic coatings on the surface of implants, as described previously. However, such coatings fail in a number of ways, including very high local concentration of antibiotic, which can be cytotoxic and impede osseointegration, unpredictable release kinetics, and the chance of rebound bacterial infection after the drug is consumed<sup>1</sup>. Therefore, prolonged local release is desired so as to assure long-term anti-bacterial effects.

#### ***1.5.2.3. TNTs and Bacterial Attachment***

TNTs represent a promising strategy for achieving local therapeutic release from the surface of implants, however, nanotopography can promote bacterial attachment as compared to rough and conventional Ti surfaces (**Figure 1.8**)<sup>123</sup>. TNTs in particular can lead to enhanced bacterial attachment *via* three possible mechanisms: (a) incorporated fluoride ions from anodization, (b) presence of dead bacteria, and (c) amorphous nature of TNTs<sup>123</sup>. While loading of substantial antibacterial compounds inside TNTs is a promising solution, many researchers have aimed at finding the most suitable TNT properties/enhancements to impede bacterial attachment. This concept combined with loading of antibiotics can further ensure a long term antibacterial effect. Ercan *et al.* reported the effect of tuning TNT dimensions and heat-treatment on attachment of bone-infection related bacteria<sup>124</sup>. The study suggested that large TNT diameters (60-80 nm) and heat-treatment (500°C for 2h) can significantly reduce

the number of attached live and dead bacteria. It is also noteworthy to mention here that dead bacteria on implant surfaces release proteins that can attract live bacteria, therefore, it is essential to reduce attachment of both live and dead bacteria<sup>125</sup>.

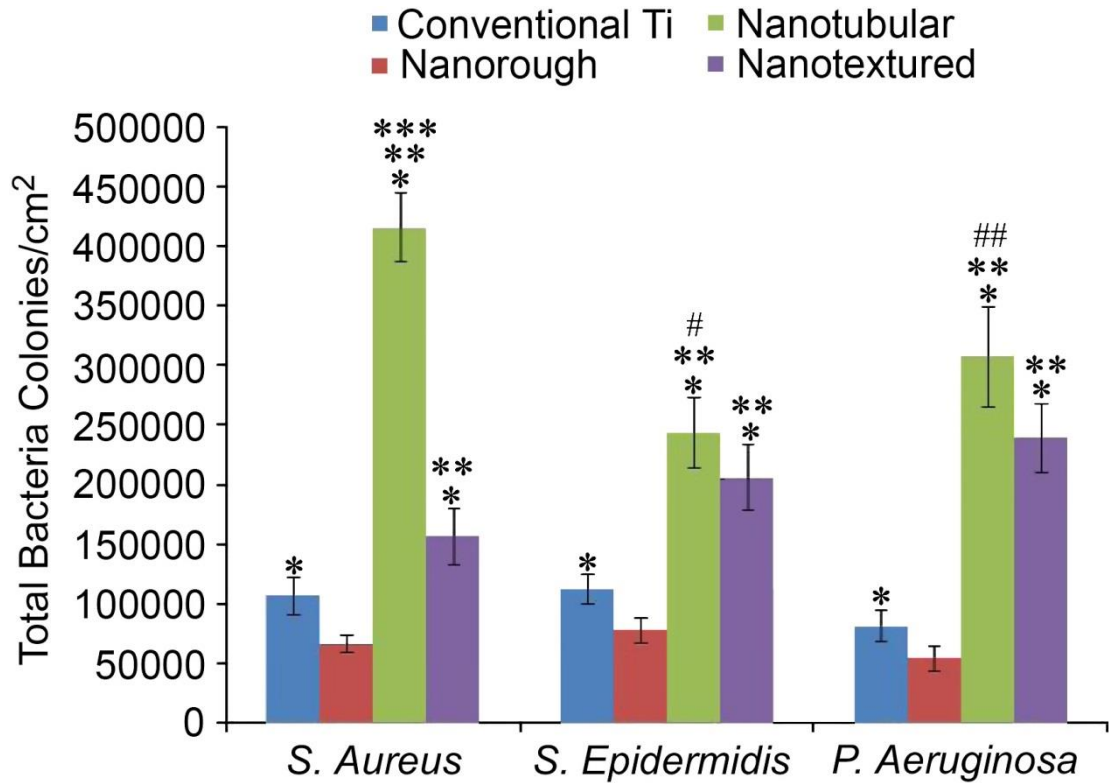


**Figure 1.8.** Evidence of increased bacterial attachment on nanotubular surfaces (TNTs) in comparison with conventional, nanorough and nanotextured Ti surfaces (adapted from [123]).

#### 1.5.2.4. Antibiotic Incorporated TNTs

To render implant surfaces bacteriostatic and bactericidal, various antibiotic formulations have been incorporated inside of TNTs/Ti surfaces<sup>50,68,102</sup>. These include antibiotics, metal ions, anti-microbial peptides (AMPs) and biopolymer coatings. Many independent reports have shown a reduction in the number of bacteria attached by locally releasing substantial amounts of antibiotics from TNTs. Popat *et al.* investigated the effect of different amounts of gentamicin loaded in TNTs against *S. epidermidis* adhesion<sup>102</sup>. They concluded that local antibiotic release did not interfere with osteoblastic functions, which is important in terms of



ensuring appropriate bone-implant bonding <sup>102</sup>. Similar claims have also been made by implantation of vancomycin-loaded TNTs in rats for 30 days <sup>126</sup>.

Antibiotic resistance is another challenge that must be addressed, as it makes even the most-potent antibiotics unable to eradicate invading pathogens, especially the methicillin-resistant *S. aureus* (MRSA) <sup>127</sup>. Repeated antibiotic treatments cannot act against such resistant bacteria, which can lead to serious consequences including deep-bone infection. Furthermore, repetitive or very high local release from implants can significantly reduce OI. This demands local release of alternate antibiotics that can effectively eradicate resistant-bacteria without adversely affecting OI. To address this, AMPs have been loaded inside TNTs to achieve maximum therapeutic effect against such resistant bacteria <sup>127-128</sup>. Almost 99.9% antibacterial activity of AMPs HHC-36 loaded TNTs was confirmed against *S. aureus* <sup>128</sup>.

#### ***1.5.2.5. TNTs with Metal Nanoparticles/Ions***

Metal species, especially silver ions and nanoparticles, which are potent antibacterial agents, have also been incorporated inside TNTs. Zhao *et al.* soaked TNTs in AgNO<sub>3</sub> solution, followed by UV-irradiation to incorporate Ag NPs <sup>129</sup>. Local release of Ag NPs from TNTs ensured short- and long-term (> 30 days) anti-bacterial activity <sup>129</sup>. This approach, however, can cause cytotoxicity due to NPs release, but this limitation can possibly be avoided by controlling the release kinetics of NPs from TNTs. Moreover, zinc ions loaded inside TNTs have been reported to provide both anti-bacterial and osseointegrating functionalities <sup>130</sup>.

#### ***1.5.2.6. Biopolymer Modified TNTs***

Bioactive polymers like chitosan offer many functions suitable for implant applications, including cost-effective synthesis, ease of modification, biodegradability, inherent anti-bacterial property and osseointegrating abilities <sup>131</sup>. As a result, various orthopaedic applications involving chitosan hydrogels, fibers, NPs, etc. have been suggested <sup>132-133</sup>. In

fact, chitosan modified titanium implants have shown superior anti-bacterial properties with improved bone cell adhesion <sup>134</sup>. This strategy has been extended to TNT/Ti implants to control drug release, while enhancing antibacterial and osteoblastic functions <sup>100,135</sup>. Another study demonstrated the ability of chitosan-coated selenium electrodeposited TNTs against *E. coli* activity <sup>135</sup>. This effect can be attributed to the dual antibacterial properties of chitosan and chitosan-degradation dependent release of potent therapeutics.

#### ***1.5.2.7. Advancing Antibacterial Effects using TNTs***

It has been well established that electric current can significantly cause cell damage and detachment, and this mechanism can be well applied for fabricating the next generation of antibacterial bone implants <sup>136</sup>. Ercan *et al.* utilised this approach to advance TNT implants seeded with *S. aureus* by electrically stimulating them each day (using 15 and 30 V for 1 hr) <sup>137</sup>. Enhanced biofilm formation was observed for TNT surfaces (in comparison with bare Ti surfaces), mainly due to promoted fibronectin adsorption on TNTs <sup>137</sup>. When the surfaces (both TNTs/Ti and bare Ti) were electrically stimulated, biofilm formation was reduced and this reduction was dependent on the voltage used (high voltage increased bactericidal effect) <sup>137</sup>. This unique strategy combined with TNT implants showed promising results, however, its effectiveness in actual traumatised bone tissue can only be confirmed after *in-vivo* studies, as electric stimulation might affect the health of bone cells.

### **1.5.3. Augmenting Osseointegration of Implants**

#### ***1.5.3.1. Osseointegration (OI)***

In order to ensure implant acceptance and survival, bone cell functions must be promoted at the bone implant interface in order to achieve osseointegration. Appropriate OI prevents implant loosening/micromotion and ultimately leads to enhanced bone healing rates <sup>138-139</sup>. As discussed previously, TNTs provide a nurturing micro-environment at the bone-implant

interface, whereby the bone cell functions such as attachment, adhesion and differentiation are promoted, leading to increased OI<sup>101,140</sup>. This observation is attributed to the ability of TNTs to absorb high amounts of vitronectin (protein that drives osteoblast adhesion) from serum.

### 1.5.3.2. TNTs and OI

Several *in-vitro* and *in-vivo* studies have established the osseointegrating abilities of TNTs<sup>50,68</sup>. Popat *et al.* demonstrated short- and long-term OI abilities of TNTs/Ti surfaces<sup>101</sup>. Enhanced functions of bone marrow stromal cells were confirmed, along with improved bioactivity of TNTs upon implantation in Lewis rats *in-vivo*<sup>101</sup>. Furthermore, no chronic inflammation or fibrosis was observed<sup>101</sup>. In another pioneering study, TNT implants were inserted into the skull of domestic pigs, and the results confirmed higher collagen type-1 expression and improved OI<sup>141</sup>. These and many other *in-vivo* investigations indicate that TNTs offer improved OI as compared to cp Ti and micro-/nano-rough surfaces<sup>105,141, 142</sup>.

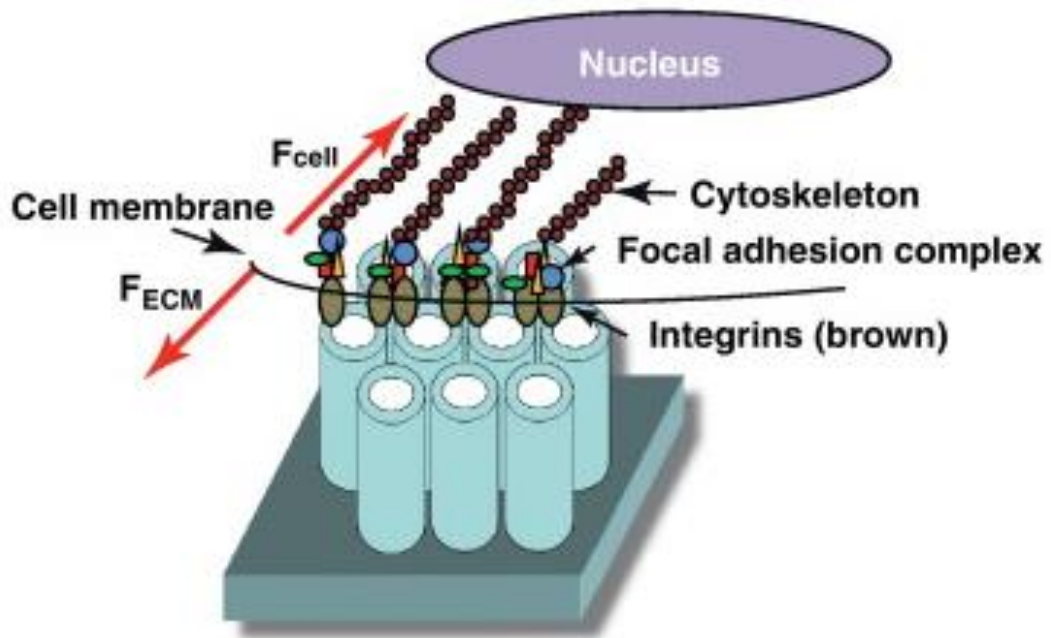


**Figure 1.9.** Illustration of mechanically-induced stress by TNTs surfaces, which can determine the extent of osseointegration for the bone implants (with permission from [184]).

### ***1.5.3.3. TNTs with Metal Ions and Biopolymers***

To upgrade OI features of TNTs, metal ions/nanoparticles (NPs) and bioactive polymers have been coupled with TNTs. In a novel study, Neupane *et al.* loaded gelatin-stabilised Gold NPs inside TNTs, and observed increased osteoblast adhesion and movement of cell filopodia <sup>143</sup>. Other studies have reported increased bone-forming features obtained from TNTs incorporated with zinc and strontium <sup>130,144</sup>. Our group has extensively utilised biopolymers, such as Chitosan and PLGA (poly lactic-co-glycolic acid), to delay release of therapeutics loaded inside TNTs and observed simultaneously enhanced osteoblastic functions <sup>100</sup>. Furthermore, Chen *et al.* electrodeposited selenium inside TNTs, followed by Chitosan modification, and the results revealed OI and anti-cancer features <sup>135</sup>. Although these strategies enable improved bone-forming abilities, the polymeric degradation kinetics and possible toxicity due to leaching of metal ions/NPs, needs to be investigated, especially for longer implantation periods.

### ***1.5.3.4. Incorporation of Hydroxyapatite inside TNTs***

To avoid possible limitations associated with metal ions and biopolymers, incorporation of hydroxyapatite (HA) on/inside TNTs can significantly improve OI. Kunze *et al.* suggested that anatase TNTs, in comparison with amorphous TNTs and TiO<sub>2</sub>, perform better for the growth of stable carbonated HA upon exposure to SBF (simulated body fluid) <sup>145</sup>. Electrodeposition was also utilised to incorporate HA, by exposing TNTs to alkaline treatment, followed by pulsed-electrodeposition of CaP and annealing to form stable and nanocrystalline HA <sup>146</sup>. Another strategy employed the alternate immersion of TNTs in solutions containing calcium hydroxide and diammonium hydrogen phosphate <sup>147</sup>. This alternate immersion method enables accelerated immobilisation of HA particles in an SBF environment, and allowed control over HA deposition weight and improved mineralisation rates <sup>147,148</sup>. Furthermore, HA incorporation into TNTs from SBF can allow for simultaneous

loading of therapeutics, thereby catering to both therapeutic as well as OI requirements of implants<sup>67</sup>.

#### ***1.5.3.5. Loading Proteins/Growth Factors inside TNTs***

There are different types of growth factors, catering to various aspects of OI and bone healing, which can be loaded inside TNTs to achieve maximum therapeutic effect<sup>149</sup>. Promoting OI and also bone-forming ability, especially in complicated situations like osteoporotic (OP) fractures, directly at the site of trauma can significantly improve bone-healing<sup>150</sup>. In such an attempt, BMP-2 (bone morphogenetic protein) was conjugated on polydopamine modified TNTs, and MSCs cultured in their presence revealed increased ALP activity and mineralization<sup>151</sup>. Furthermore, in a separate study, a multilayered coating of bioactive polymers gelatin and chitosan were formed on BMP-2 loaded TNTs to delay the release of proteins<sup>152</sup>. Bisphosphonates, known to reduce bone loss, especially in conditions like bone metastasis and Paget's disease, have also been incorporated inside TNTs/Ti implants to reduce bone resorption activity<sup>153-154</sup>. The bisphosphonates, pamidronate and ibadronate were loaded into TNTs, which were implanted into the tibiae of Wistar rats. After 2 and 4 weeks of implantation, enhanced expression of collagen type-1 and osteocalcin was reported<sup>154</sup>. In separate investigations, alternative bioactive molecules, including CNN2 (connective tissue growth factor) fragment, peptide sequence KRSR (lysine-arginine-serine-arginine), and the OP drugs raloxifene and alendronate incorporated inside TNTs showed improved OI<sup>150,155,156</sup>.

While the abovementioned studies showed promising results in *in-vitro* and *in-vivo* settings, longer duration studies of >6 months are desired to investigate the state of bone-implant bonding, especially when the loaded biomolecules have been consumed. Moreover, for complex therapeutic requirements like in OP fractures, a tiny implantable device capable of releasing active molecules directly inside the bone micro-environment in a 3D fashion, could provide improved therapeutic effect and fixation ability. Such in-bone therapeutic

implants should require minimal invasive surgery for implantation/placement, and should not require removal. This new generation of ‘fit-and-forget’ bone implants may address challenges associated with therapeutic demands of OP fractures, bone cancers and infections.

#### 1.5.4. TNTs for Complex Therapies

TNTs offer many advantages, such as ease of fabrication, biocompatibility, ability to tailor release of loaded therapeutics, ability to functionalize and favourable cellular activity, and as a result have been suggested for alternative therapies targeting complex disease conditions. Besides bone implants, titanium and its alloys have also been widely used as dental implants to fix root-canal infections and as dental prostheses. To achieve dental implant success, appropriate OI and prevention of bacterial infection are desired, and as a result various surface modification strategies have been suggested for dental implants<sup>157-158</sup>. In such an attempt, TNT modified Ti implants were modified with Ag NPs and the growth factor FGF-2 to reduce the chances of bacterial infection and simultaneously heal the surrounding tissues<sup>159</sup>. In another strategy, Lee *et al.* investigated the effect of bone formation for N-acetyl cysteine (NAC) incorporated in TNTs in *in-vitro* and *in-vivo* settings, and reported reduced inflammation and promoted bone formation<sup>160</sup>. To extend the TNT technology to dental implants, Demetrescu *et al.* confirmed promoted fibroblastic adhesion and improved stability of TNTs/Ti implants in saliva conditions, recreating the micro-environment for dental implant<sup>161</sup>.

TNTs have also been suggested as implants for releasing active chemotherapeutic agents directly inside tumours or cancer affected tissues. This strategy of LDD can avoid toxic and complex conventional treatments, including systemic chemotherapy and radiotherapy. Chen *et al.* electrodeposited Se inside TNTs followed by coating of chitosan to delay its elution, and reported inhibition of growth of cancerous osteoblasts, while promoting the functioning of healthy osteoblasts<sup>135</sup>. Alternatively, Kalbacova *et al.* utilized a photo-

catalytic feature of TNTs to kill cancerous cells, by UV irradiating the TNTs inside cancer cell cultures <sup>162</sup>. Furthermore, in a novel study, 3D mesoporous TNT-like fragments were fabricated as nano-vehicles to carry the potent anti-cancer therapeutic daunorubicin, and study with the hepatocarcinoma cell line revealed increased therapeutic uptake by cells <sup>163</sup>.

These novel investigations using TNTs as a platform to modify implant surfaces to achieve effective therapeutic action show promising results. However, there is ample scope for improvement in terms of designing easy-to-fabricate novel implants for in-bone and in-tumor therapeutics, achieving 3D release directly inside the affected tissue, and maintaining the minimally invasive surgery for placement and easy integration into the current implant market. Furthermore, there is enough potential to extend the TNT or other established nano/micro-technologies to address complex therapeutic challenges, for instance brain disorders and tumors.

## **1.6. Advancing Therapeutic Releasing Functions of TNTs**

The release of loaded therapeutics from TNTs follows Fick's first law of diffusion, whereby the release is mostly dependent on the size/mass of therapeutic molecules, their solubility, and interaction with TNTs <sup>113-114</sup>. As soon as the drug loaded open-pore TNTs come into contact with physiological fluids, a very rapid or burst release is expected due to a high diffusion gradient. This initial burst release (IBR), which is largely unavoidable for a nanoporous implant modification, can be disadvantageous, resulting in rapid consumption of loaded drugs and very high initial dosage, which can compromise OI and produce unnecessary tissue toxicity. Furthermore, in conditions like implant-related infections, early consumption of antibiotics can retrigger bacterial invasion. Hence, there is a need to further improve the drug release kinetics from the surface of TNTs/Ti implants, by enabling control over both the amount of drugs loaded and achieving their controlled sustained release for longer durations.

Further advancement in terms of triggered-release, bio-sensing and multi-drug release with TNT/Ti implants can cater to more complex therapeutic requirements of bone conditions. An illustration of the various TNTs drug-releasing advancements is presented in **Figure 1.10**.

### **1.6.1. Controlled Therapeutic Release from TNT/Ti Implants**

The release of loaded payloads from TNTs is governed by the diffusion gradient. The therapeutic release from nanoporous substrates mainly follows a biphasic fashion, whereby initial burst phase (1<sup>st</sup> few hrs) results in quick release of therapeutics present near the open end of the nanotubes/pores, which is followed by release of therapeutics loaded deep inside the nanotubes/pores. A very high initial burst release results from very high diffusion gradient as the implant is exposed to the external media, and can result in quick release of around 40-70 % of loaded therapeutics. This not only means early consumption of loaded therapeutics but can also cause local tissue toxicity. The idea is to load active molecules deep into the nanotubes and reduce/control the initial burst release phase. This is because the basic requirement of such implants is to maintain sufficient local concentration to have an appropriate therapeutic effect, which must be sustained for prolonged durations.

Other factors that determine the release kinetics include the interaction of drug with TNTs, therapeutic size/solubility, and implant size and these must also be taken into consideration to design/fabricate tailorable therapeutic TNT implants that can cater to specific conditions. Furthermore, growth factors/hormones must be protected from denaturation. Hence to prevent very high initial dosages and early consumption of therapeutics, which might lead to retriggered bacterial invasion and compromised osseointegration, the releasing ability of TNTs must be controlled to achieve prolonged favourable release patterns.



***1.6.1.1. Tailoring TNT Dimensions***

Since EA allows for controlling TNT dimensions *via* varying the anodization parameters, the same process can be used to control drug loading amounts and release kinetics. This strategy has been regarded as the simplest approach to addressing drug release challenges of nanoporous substrates<sup>114</sup>. By varying anodization time, various lengths of TNTs were fabricated, which were later used to control loading amounts and release kinetics of the potent anti-inflammatory drug Indomethacin<sup>114</sup>. Longer TNTs (as compared to short TNT tubes, but with same diameter) could load more drug, with a delayed overall release, which can be attributed to deeper loading of drugs in the longer TNTs<sup>164,165</sup>. However, when controlling loading/release by TNT dimensions, there is an inverse proportionality between loading amounts and delayed release, for example, wider TNTs can load more drug deeper inside the TNTs but since the pore size is large, IBR will be very high. Hence, alternative approaches are required, to reduce IBR. A simple strategy could be tailoring the geometry of TNTs (for e.g. fabricating branched or multi-layer nanotubes), to control drug release.

***1.6.1.2. Maximising Drug Occupancy of TNTs***

TNTs represent tubular capillary-like architecture with diameters and lengths in the range of 30-100 nm and 1-100  $\mu\text{m}$  respectively, where substantial loading of active molecules of varied chemistries, weights and solubilities can be very challenging. The key is to exploit the vacant volume of these ‘capillaries’ to load the maximum amount of drug. Furthermore, if the drugs are only present near the open ends of the TNTs or in the inter-TNT spaces, a very high IBR is expected. Moreover, to ensure appropriate therapeutic benefit, the loading should be deep in the TNTs structures. The most common loading procedures involve drop-casting, immersion, vacuum-assisted, and loading from SBF. Yao *et al.* have reported simultaneous recruitment of CaP crystals, when penicillin-based antibiotics were loaded from SBF, and achieved longer release as compared to physically adsorbed drugs<sup>166</sup>. Similar enhancements

were observed when the anti-cancer drug doxorubicin was loaded inside TNTs using vacuum suction<sup>167</sup>. The vacuum-assisted method in particular allows for loading therapeutics deep inside the TNT interior, as compared to soaking/immersion, which loaded therapeutics superficially near the TNTs open pores and inter-tube voids<sup>167</sup>. In another strategy, active antibiotics were loaded into silica xerogel prior to incorporation inside TNTs, to achieve maximum drug occupancy<sup>168</sup>.

### ***1.6.1.3. Encapsulation of Sensitive Drugs***

To load and locally release labile biomolecules, such as proteins or growth factors, it is crucial to maintain their stability and activity. In an attempt to achieve this, our group pioneered encapsulation of model drugs in polymeric micelles prior to their loading inside TNTs<sup>113-114</sup>. This strategy enables encapsulation of a wide variety of drugs with varied chemistries, solubilities and targeting different bone conditions. Briefly, as a model drug indomethacin was encapsulated in micelles [Pluronic F127®, TPGS: d- $\alpha$ -tocopheryl polyethylene glycol 1000 succinate, and others], and its *in-vitro* release was measured over 4-8 weeks<sup>114</sup>. Micellar encapsulation further allows tailoring of the loading/release by tuning TNT dimensions, size/properties of micelles etc. Furthermore, this technique was reported to further advance the TNT drug releasing functions by enabling loading/releasing of multiple therapeutics, and triggered release<sup>169-171</sup>.

### ***1.6.1.4. Functionalization of TNTs***

Chemically modifying TNTs to render the surface hydrophobic or hydrophilic can significantly change the drug-TNTs interaction, which in turn can influence both the loading amount and the release kinetics. To achieve this, prior to loading a hydrophobic model drug, TNTs were modified by self-assembling monolayers (SAMs) of 2-carboxyethyl-phosphonic acid (hydrophilic) and 16-phosphono hexadecanoic acid (hydrophobic)<sup>114</sup>. The release

studies revealed delayed release of drug for hydrophilic TNTs as compared to hydrophobic and untreated TNTs<sup>114</sup>. This technique employing SAMs is very versatile and can be used to immobilize various functionalities to the TNTs, which can further improve drug attachment and release.

#### ***1.6.1.5. TNTs Modified with Bioactive Polymers***

Combining biodegradable and osseointegrating polymers with drug eluting implant modifications of TNTs, could enable interesting characteristics especially towards improving release of drug payloads and simultaneously enhancing bone forming abilities. Furthermore, the ability to fabricate polymers in the form of coats, hydrogels, fibers, nanoparticles, etc. can be exploited to modify TNTs surfaces, to reduce or block the open pores of TNTs to slow drug release. Our group has extensively explored this area of TNT implant technology, whereby we have used plasma-polymerisation, dip-coating, and micellar-encapsulation to include new functionalities into the drug eluting TNTs<sup>100,114,172,173</sup>. To reduce the open pore size of TNTs (and also nanoporous alumina), an ultra-thin coat of plasma-polymerised poly(allylamine) was applied onto the drug loaded nanoporous substrates<sup>172-173</sup>. The release experiments confirmed delayed release for modified TNT implants, which can further be tuned by varying plasma conditions<sup>172-173</sup>. Furthermore, this strategy can also be used to impart selective functionalization and interfacial properties to the TNT surfaces, which can be used to improve release and modulate cellular interactions. However, with the use of plasma polymerisation, there are several challenges, such as time-consuming calibration, costly equipment and complex operation, which can limit its integration into the current implant market.

A simple alternative could be use of less complicated polymer modification techniques, such as dip-coating. Dip coating of the biopolymers chitosan and PLGA was made on drug loaded TNTs, in an attempt to cover the open pores of TNTs, to reduce IBR and

delay overall release<sup>100</sup>. Moreover, with dip-coating thickness of the polymer coat onto TNTs can be modified easily by varying the number of coats, coating speed, polymeric concentration etc. The results of doing so indicated reduced IBR and delayed overall release to over 30 days (as compared to 4 days for unmodified TNTs), with the ability to tune release kinetics, based on polymer thickness<sup>100</sup>. The release in this case was dependent on polymeric degradation and exposure of TNTs to the aqueous medium. Moreover, the biopolymer modification simultaneously enhanced osteoblastic functions<sup>100</sup>. In a similar study, gelatin and chitosan were multilayered onto BMP-2 loaded TNTs, to delay release of this labile but potent bone anabolic protein<sup>152</sup>. However, systems employing polymers require more investigation to closely link various parameters influencing degradation rate (especially *in situ* at the site of implantation), with the release of drugs incorporated inside TNTs, to aid in designing implant technologies to cater to a wide range of therapeutic needs. Likewise, alternative polymer modification technologies, such as electrospinning of polymeric nanofibers, coupled with TNTs, could provide a varied scale of nano-topography to further enhance the functionality of implants.

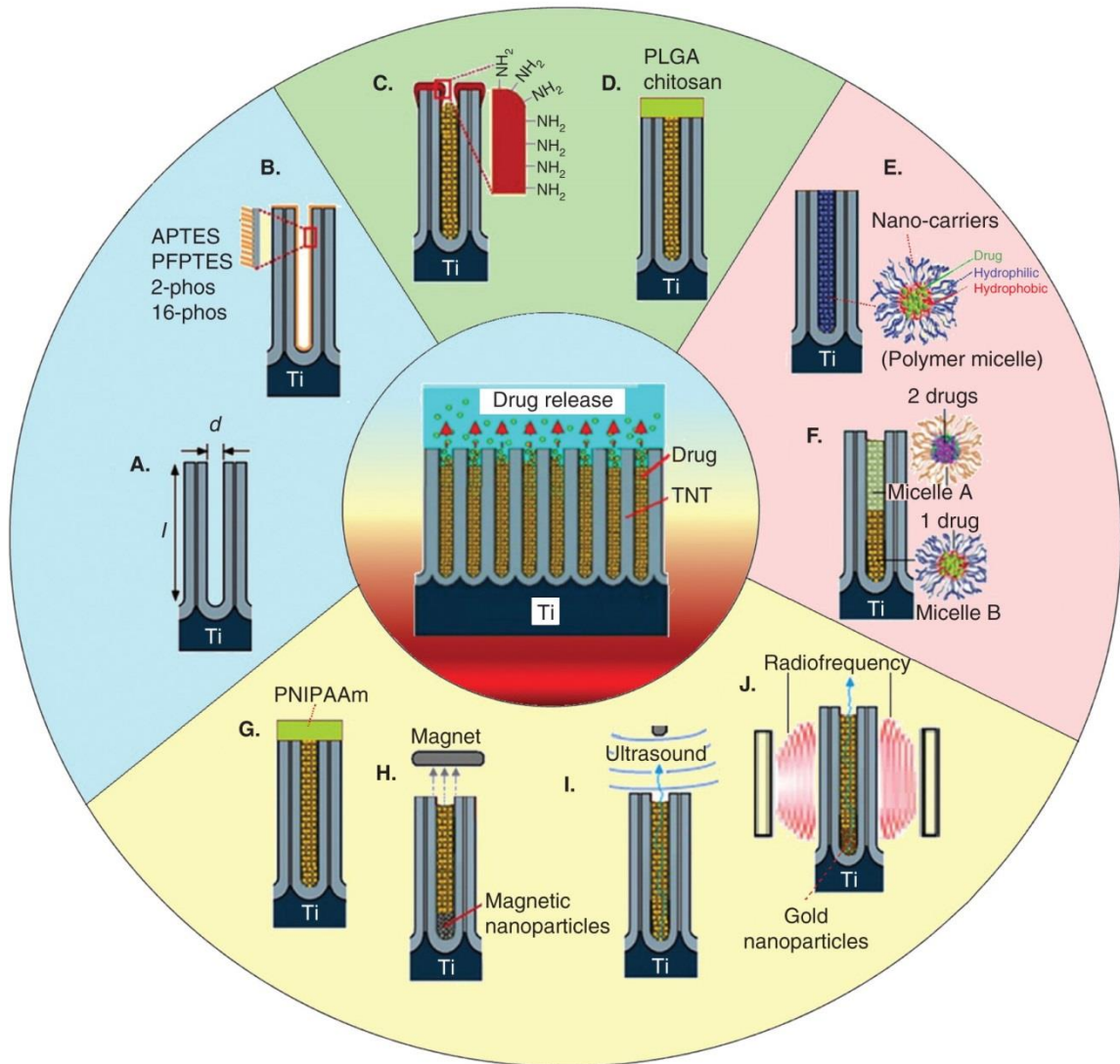


**Figure 1.10.** Schematic representation of various strategies employed to modify TNTs/Ti implants to: (a-e) control drug releasing kinetics, (f) enable loading of multiple therapeutics, and (j-g) stimuli responsive drug release (adapted from [186]).

### 1.6.2. TNTs for Triggered Therapeutic Release

For targeting complex bone conditions and implant failures, the new generation of drug-eluting bone implant should also be capable of addressing the needs of immediate drug release, especially in situations like bacterial infection where delayed release is not desirable. Hence, an advanced drug releasing implant, capable of releasing drug directly when it is desired *via* an external or internal trigger, could attend to these complex therapeutic

requirements. As a result, various TNT/Ti implant investigations have attempted to achieve triggered release upon stimulation by temperature, light, magnetic/electric field, ultrasonic trigger etc. Utilising the change in tissue environment (pH, temperature, oxygen content, sugar level etc.) upon onset of bacterial infection, inflammation or cancer, could be used as internal triggers to produce immediate local drug release <sup>174</sup>. In such an attempt, Cai *et al.* deposited a temperature-sensitive hydrogel composed of PNIPAAm (poly N-siopropylacrylamide) and PAAm (polyacrylamide) on Vitamin B2 loaded TNTs, and used temperature stimulated drug release <sup>175</sup>. In conditions like inflammation the local tissue temperature rises to 38.3-38.5°C, and the LCST (lower critical solution temperature) of polymer composite being 38°C, allowed for sudden release of the loaded therapeutics from TNT modified implants <sup>175</sup>. In another novel study, Shreshtha *et al.* loaded a fluorescent marker *via* silane coupling to magnetic TNTs (TNTs doped with magnetic NPs), and upon exposure to UV observed the sudden release of model drugs by chain-scission of anchoring groups <sup>176</sup>. A magnetic field approach has also been utilized to initiate quick release of indomethacin, *via* loading of micelle-encapsulated drugs into TNTs already containing magnetic NPs <sup>170</sup>. This novel magnetic trigger approach can also be linked with current magnetic diagnostic tools like NMR (nuclear magnetic resonance), however this strategy also has the limitation of accidental release of therapeutics upon exposure to routinely experienced magnetic fields.

To release drugs based on an electric field, Sirvisoot *et al.* electrodeposited polypyrrole conjugated with drugs on MWCNTs (multi-walled carbon nanotubes) modified TNTs/Ti implants, and observed around 80% release when an electric field was applied <sup>177-178</sup>. Other strategies for quick on-demand release, include ultrasonic irradiation (micelle encapsulate drugs in TNTs) and radiofrequency (drugs encapsulated in micelles loaded in TNTs containing gold NPs) <sup>171,179</sup>. Furthermore, both these approaches also reported easy

tuning of the trigger based on ultrasonic force (time, intensity, and amplitude) and radiofrequency (RF energy and amount of NPs) <sup>171,179</sup>. Although these triggered strategies did show quick release upon use of stimulation (internal or exterior), thorough *in-vivo* investigations are required to prove the usefulness of these triggers. Other challenges that these strategies must overcome include: release kinetics/possible toxicity of TNT modifications (polymers, NPs etc.), bone cell toxicity upon exposure to trigger/sudden release, long-term survival of triggered mechanism and avoiding accidental release. An alternative tactic could be fabricating TNTs with an in-built ability to respond to external/internal triggers, which could avoid possible limitations associated with multi-step chemical/physical modifications of TNTs/Ti implants.

### **1.6.3. TNTs for Multi-Therapy and Bio-Sensing**

Sometimes the therapeutic need of a bone condition might require simultaneous administration of multiple therapeutics, for e.g. avoiding bacterial attachment, while promoting bone forming ability. To address such challenges via TNTs/Ti technology, simple loading of multiple drugs inside TNTs might deactivate them, requiring a shielding strategy to avoid mixing. Our group addressed these complications by encapsulating two drugs with different solubilities: hydrophobic indomethacin/intraconazole and hydrophilic gentamicin, independently in regular and inverted polymeric micelles, respectively, prior to their loading inside TNTs in a layered fashion <sup>169</sup>. Upon immersion in PBS medium, the two immiscible drug containing micellar layers were released in a sequential pattern, with hydrophobic drugs/regular micelles (which were loaded later) releasing initially until 5 days, followed by release of hydrophilic drugs/inverted micelles (which were loaded initially inside TNTs) <sup>169</sup>.

Previous sections have described how drug loading can be improved to achieve delayed release for extended durations, and also on-demand triggered release. However diagnostic/sensing at the traumatized bone site adjacent to the bone implant could be used to

provide a clear picture of the state of bone healing, bacterial invasion or inflammation. Sirvisoot *et al.* designed a novel TNT implant by growing MWCNTs (multi-walled carbon nanotubes) inside the TNTs to improve bone cell activity and also include sensing functionality<sup>180-181</sup>. To prove the concept of sensing complex bone conditions such as inflammation or infection, the electrochemical signals from these modified implants inside the solution containing extracellular components released by osteoblasts were recorded and analysed<sup>181</sup>. These signals could then be linked with the health of the surrounding bone cells and any abnormalities related to trauma, such as inflammation or infection. Although this technology has produced promising results, more thorough *in-vivo* studies are required to test its applicability for sensing in complex multi-component traumatic bone micro-environment next to the bone implants.

#### **1.6.4. Challenges for TNTs/Ti Bone Implants for Improved Therapeutics**

The literature reviewed here summarizes the progress in exploring TNTs as a promising strategy towards modifying titanium bone implants, thereby improving implant acceptance/survival and also catering to complex therapeutic requirements of infections, osteoporotic fractures and cancers. It also indicates the challenges that still remain and must be addressed to advance the TNTs bone implant technology into clinical trials and enable its easy integration into the current implant market. Some of the key challenges are summarized below, and they serve as the objectives of this PhD project.

1. Fabricating novel TNT/Ti implants with the ability to tailor loading and release of therapeutics without the need of further modification.
2. Novel implants that require minimal invasive surgery for implantation (required for severe conditions such as deep bone infections, to achieve local delivery of therapeutics).



3. Fabrication of well-adherent and highly-ordered TNTs on various titanium substrates, to facilitate easy integration into the current implant market (which includes various implant materials: Ti and its alloys, often in complex geometries like: pins, screws, meshes, 3D-printed scaffolds, etc.).
4. Local drug delivery inside the bone microenvironment to successfully target complex conditions such as fixation of osteoporotic fractures, bone cancers, etc.
5. Monitoring the spread of therapeutics directly inside the bone micro-environment to inform the design of next generation of in-bone therapeutic implants.
6. Combining bioactive polymers with TNTs technology towards enhancing implant features.
7. Combining 3D printing technology with micro/nano-engineering to create unique custom-printed Ti implants.

## 1.7. Objectives

The broad aim of the work described in this thesis was to develop novel nano-engineered therapeutic and bone-forming implants based on titania nanotubes (TNTs), that enable effective 3D in-bone therapeutic effect, while maintaining cost-effective fabrication, minimally invasive implantation, and easy integration into the current implant market. The following points summarize the aims/objectives of this thesis:

1. To fabricate TNT with improved structural properties that can enable enhanced therapeutic loading and releasing abilities by:
  - Fabricating periodically-structured TNTs (P-TNTs) via voltage oscillations during the electrochemical anodization
  - Comparing drug loading and *in-vitro* drug release characteristics between P-TNTs and conventional TNTs

- Preparing loose TNTs/agglomerates by fracturing the P-TNTs as drug carriers
2. To develop advanced anodization conditions to fabricate stable and high-quality TNTs on curved surfaces by:
  - Understanding and optimizing the ageing conditions of the anodization electrolyte towards generating adherent and stable TNTs on complex substrate geometry of a Ti wire
  - Investigating the effect of other influencing parameters such as water content, anodization/voltage and substrate dimensions, towards finding the most optimized anodization conditions to anodize curved surfaces of Ti
3. To demonstrate the ability of TNTs/Ti wire implants as customizable in-bone therapeutic implants for complex conditions such as osteoporotic (OP) fractures by:
  - Investigating substantial loading and controlled *in-vitro* release of OP relevant drugs: indomethacin and parathyroid hormone (PTH)
  - Studying the therapeutic effect of PTH-loaded TNTs/Ti wire implants inside collagen gels containing human osteoblasts
  - Imaging the cellular spread morphology from collagen gel (to model bone tissue) onto TNT implants and the influence of micro-scale cracks on the anodic film
  - Analysing the stability of TNTs/Ti wire implants after *ex-vivo* implantation inside bovine trabecular bone cores
4. To investigate the *in-situ* formation of chitosan microtubes on TNTs/Ti wire implants upon immersion in PBS buffer by:
  - Comparing the effect of various parameters (substrate surface, immersion solution and pH, time of immersion, and thickness of chitosan coating) that can influence the formation of CMTs upon degradation of chitosan coatings on TNTs
  - Elucidating the mechanism of micro-tube formation on TNTs
5. To advance therapeutic features of TNT/Ti wire implants by:

- Magnesiothermic reduction of TiO<sub>2</sub> nanotubes (TNTs) into Ti while preserving the nanotubular morphology
  - Performing material characterizations to confirm effective conversion, and demonstrating the electrically conducting (proposed for electrical stimulation therapy) and drug releasing abilities of the titanium nanotube implant.
6. To combine 3D printing technology and electrochemical anodization to advance TNT implant technology by:
- Printing novel micro-rough Ti alloy substrates, followed by fabrication of TNTs while maintaining the micro-roughness
  - Testing bone cell adhesion and spreading onto these micro-/nano-rough implants
  - Elucidating the bone-forming/remodelling abilities of these implant by studying genetic expression

## 1.8 Thesis Structure

The thesis includes 9 chapters and the following summary briefly describes how specific objectives (as defined in the previous section) are addressed by each chapter, towards advancing bone implant technology using titania nanotubes.

**Chapter 1** describes in some detail bone implant technology, and the need to develop local drug releasing implants based on TNTs. It also describes the fabrication of TNTs, therapeutic release, and other advances in the field of nano-engineered Ti implants based on TNTs.

**Chapter 2** provides details on materials and methodologies including TNTs fabrication, modification, therapeutic loading/release, and various bone biology investigations to substantiate the applicability of TNTs/Ti as improved therapeutic implants.

**Chapter 3** demonstrates fabrication of new periodically-structured TNTs by voltage oscillations during anodization. This concept of structural engineering is explored as a strategy to improve drug releasing performances. Therapeutic loading and releasing abilities are compared between TNTs with periodically shaped and flat nanotube structures.

**Chapter 4** presents the optimization of electrochemical anodization parameters (especially ageing of electrolyte) towards fabricating stable and well-adherent high-quality TNTs on curved surfaces of Ti wires. This work is an important contribution toward improving TNTs fabrication technology and especially towards enabling easy integration of the TNTs into the current implant market.

**Chapter 5** explores a new concept of TNTs on Ti wires is presented as new bone therapeutic implants for treatment of osteoporotic (OP) fractures, by substantial loading/controlled release of OP therapeutic. The therapeutic effect on osteoblasts cultured in collagen gels, and demonstration of the stability by implantation in bovine trabecular bone cores, is also described. Furthermore, monitoring the release kinetics inside bone microenvironment *ex-vivo* using Zetos<sup>TM</sup> bone reactor system is also demonstrated.

**Chapter 6** reports *in-situ* degradation of chitosan coating on TNT/Ti wire implants into novel micro-tubular morphology, in the presence of phosphate buffer solution under optimized conditions of pH, substrate surface, thickness of coating and time of immersion.

**Chapter 7** presents the conversion of TiO<sub>2</sub> nanotubes (or TNTs) fabricated on Ti wires into Ti nanotubes (Ti NTs), to enable novel characteristics, such as electrically-conducting and drug-eluting titanium nanotube implant (proposed for electrical stimulation therapy).

**Chapter 8** shows the combination of 3D printing technology and anodization towards creating novel micro-rough Ti alloy implants decorated with TNTs. The behaviour of

osteoblasts on these novel TNT/3D substrates are compared with Ti 3D, rough Ti, polished Ti and bare TNTs.

**Chapter 9** summarizes the results of the investigations carried out to advance TNTs/Ti implant technology towards in-bone therapies, and provides a perspective for future applications of this technology.

The appendices provide the peer-reviewed articles that were published/submitted during the course of the PhD. **Appendix A** is the recent research article (in final stages of submission) that shows monitoring of therapeutic release directly inside the bone microenvironment *ex-vivo* using Zetos<sup>TM</sup> bone reactor. **Appendix B** is the peer-reviewed conference proceeding from 2013, which presents the *in-vitro* investigations using TNTs/Ti wire implants for targeting various bone conditions. **Appendix C** is the peer-reviewed review article published in 2012, as a part of extensive literature review. **Appendix D** is the recently published book chapter, which extensively reviews titania nanotube implants for local drug delivery applications.

## 1.9 References

1. Goodman, S. B.; Yao, Z.; Keeney, M.; Yang, F., The future of biologic coatings for orthopaedic implants. *Biomaterials* **2013**, *34*, 3174-3183.
2. Carter, D. R.; Beaupre, G. S.; Giori, N. J.; Helms, J. A., Mechanobiology of skeletal regeneration. *Clinical Orthopaedics and Related Research* **1998**, *335*, S41-55.
3. Liu, X.; Niebur, G. L., Bone ingrowth into a porous coated implant predicted by a mechano-regulatory tissue differentiation algorithm. *Biomechanics and Modeling in Mechanobiology* **2008**, *7*, 335-44.

4. Bishop, J. A.; Palanca, A. A.; Bellino, M. J.; Lowenberg, D. W., Assessment of compromised fracture healing. *Journal of the American Academy of Orthopaedic Surgeons* **2012**, *20*, 273-82.
5. Darouiche, R. O., Treatment of infections associated with surgical implants. *New England Journal of Medicine* **2004**, *350*, 1422-9.
6. Praemer, A.; Furner, S.; Rice, D., Musculoskeletal conditions in the United States. Rosemont, IL: *American Academy of Orthopedic Surgeons* **1992**.
7. Okazaki, Y.; Gotoh, E., Comparison of metal release from various metallic biomaterials in vitro. *Biomaterials* **2005**, *26*, 11–21.
8. Ostermann, P. A.; Henry, S. L.; Seligson, D., The role of local antibiotic therapy in the management of compound fractures. *Clinical Orthopaedics and Related Research* **1993**, *295*, 102–11.
9. Price, J. S.; Tencer, A. F.; Arm, D. M.; Bohach, G. A., Controlled release of antibiotics from coated orthopedic implants. *Journal of Biomedical Materials Research* **1996**, *30*, 281–6.
10. Paluska, S. A., Osteomyelitis. *Clinics in Family Practice* **2004**, *6*, 127–56.
11. Bisland, S. K.; Chien, C.; Wilson, B. C.; Burch, S., Pre-clinical in vitro and in vivo studies to examine the potential use of photodynamic therapy in the treatment of osteomyelitis. *Photochemical and Photobiological Sciences* **2006**, *5*, 31–8.
12. Qureshi, A. T; Terrell, L.; Monroe, W. T.; Dasa, V.; Janes, M. E.; Gimble, J. M.; Hayes, D. J., Antimicrobial biocompatible bioscaffolds for orthopaedic implants. *Journal of Tissue Engineering and Regenerative Medicine* **2014**, *8*, 386–95.
13. Mruk, A. L.; Record, K. E., Antimicrobial options in the treatment of adult staphylococcal bone and joint infections in an era of drug shortages. *Orthopedics* **2012**, *35*, 401–7.

14. Montanaro, L.; Testoni, F.; Poggi, A.; Visai, L.; Speziale, P.; Arciola, C. R., Emerging pathogenetic mechanisms of the implant-related osteomyelitis by *Staphylococcus aureus*. *International journal of Artificial Organs* **2011**, *34*, 781–8.
15. Yenson, A.; de Fries, H. O.; Deeb, Z. E., Actinomycotic osteomyelitis of the facial bones and mandible. *Journal of Otolaryngology - Head & Neck Surgery* **1983**, *9*, 173–6.
16. Hatzenbuehler, J.; Pulling, T. J., Diagnosis and management of osteomyelitis. *American Family Physician* **2011**, *84*, 1027–33.
17. Buchholz, H. W.; Engelbrecht, H., Depot effects of various antibiotics mixed with Palacos resins. *Der Chirurg* **1970**, *41*, 511–15.
18. Nelson, C. L.; Hickmon, S. G.; Harrison, B. H., Elution characteristics of gentamicin-PMMA beads after implantation in humans. *Orthopedics* **1994**, *17*, 415–6.
19. Moojen, D. J.; Hentenaar, B.; Charles Vogely, H.; Verbout, A. J.; Castelein, R. M.; Dhert, W.J., In vitro release of antibiotics from commercial PMMA beads and articulating hip spacers. *Journal of Arthroplasty* **2008**, *23*, 1152–6.
20. Thomas, M. V.; Puleo, D. A., Calcium sulfate: Properties and clinical applications. *Journal of Biomedical Materials Research Part B: Applied Biomaterials* **2009**, *88*, 597–610.
21. Ziran, B. H.; Smith, W. R.; Morgan, S. J., Use of calcium-based demineralized bone matrix/allograft for nonunions and posttraumatic reconstruction of the appendicular skeleton: preliminary results and complications. *Journal of Trauma* **2007**, *63*, 1324–8.
22. Greish, Y. E.; Brown, P. W., Phase evolution during the formation of stoichiometric hydroxyapatite at 37.4 degrees C. *Journal of Biomedical Materials Research Part B: Applied Biomaterials* **2003**, *67*, 632–7.
23. Johnell, O.; Kanis, J. A., An estimate of the worldwide prevalence and disability associated with osteoporotic fractures. *Osteoporosis International* **2006**, *17*, 1726–33.

24. Franzo, A.; Francescutti, C.; Simon, G., Risk factors correlated with post operative mortality for hip fracture surgery in the elderly: a population-based approach. *European Journal of Epidemiology* **2005**, *20*, 985-91.
25. Richards, J. B.; Zheng, H. F.; Spector, T. D., Genetics of osteoporosis from genome-wide association studies: advances and challenges. *Nature Reviews Genetics* **2012**, *13*, 576-88.
26. Kyllönen, L.; D'Este, M.; Alini, M.; Eglin, D., Local drug delivery for enhancing fracture healing in osteoporotic bone. *Acta Biomaterialia* **2015**, *11*, 412-34.
27. Barnes, G. L.; Kakar, S.; Vora, S.; Morgan, E. F.; Gerstenfeld, L. C.; Einhorn, T. A., Stimulation of Fracture-Healing with Systemic Intermittent Parathyroid Hormone Treatment. *Journal of Bone and Joint Surgery American volume* **2008**, *90*, 120-27.
28. Andreassen, T. T.; Ejersted, C.; Oxlund, H., Intermittent parathyroid hormone (1–34) treatment increases callus formation and mechanical strength of healing rat fractures. *Journal of Bone and Mineral Research* **1999**, *14*, 960-68.
29. Aspenberg, P.; Genant, H. K.; Johansson, T.; Nino, A. J.; See, K.; Krohn, K.; García-Hernández, P. A.; Recknor, C. P.; Einhorn, T. A.; Dalsky, G. P.; Mitlak, B. H.; Fierlinger, A.; Lakshmanan, M. C., Teriparatide for acceleration of fracture repair in humans: a prospective, randomized, double-blind study of 102 postmenopausal women with distal radial fractures. *Journal of Bone and Mineral Research* **2010**, *25*, 404-14.
30. Eswaramoorthy, R.; Chang, C. C.; Wu, S. C.; Wang, G. J.; Chang, J. K.; Ho, M. L., Sustained release of PTH(1–34) from PLGA microspheres suppresses osteoarthritis progression in rats. *Acta Biomaterialia* **2012**, *8*, 2254-62.
31. Liu, X.; Pettway, G. J.; McCauley, L. K.; Ma, P. X., Pulsatile release of parathyroid hormone from an implantable delivery system. *Biomaterials* **2007**, *28*, 4124-31.
32. Jeon, J. H.; Puleo, D. A., Alternating release of different bioactive molecules from a complexation polymer system. *Biomaterials* **2008**, *29*, 3591-98.



33. Yu, X.; Wang, L.; Jiang, X.; Rowe, D.; Wei, M., Biomimetic CaP coating incorporated with parathyroid hormone improves the osseointegration of titanium implant. *Journal of Materials Science: Materials in Medicine* **2012**, *23*, 2177-86.
34. Buchholz, H. W.; Elson, R. A.; Engelbrecht, E.; Lodenkämper, H.; Röttger, J.; Siegel, A., Management of deep infection of total hip replacement. *Journal of Bone and Joint Surgery* 1981, *63*, 342–353.
35. Wu, P.; Grainger, D. W., Drug/device combinations for local drug therapies and infection prophylaxis. *Biomaterials* 2006, *27*, 2450-67.
36. Geetha, M.; Singh, A. K.; Asokamani, R.; Gogia, A. K., Ti based biomaterials, the ultimate choice for orthopaedic implants –A review. *Progress in Materials Science* **2009**, *54*, 397-425.
37. Anselme, K., Osteoblast adhesion on biomaterials. *Biomaterials* **2000**, *21*, 667-81.
38. Bosco, R.; Van Den Beucken, J.; Leeuwenburgh, S.; Jansen, J., Surface engineering for bone implants: A trend from passive to active surfaces. *Coatings* **2012**, *2*, 95-119.
39. Bauer, S.; Schmuki, P.; Von Der Mark, K.; Park, J., Engineering biocompatible implant surfaces: Part I: Materials and surfaces. *Progress in Materials Science* **2013**, *58*, 261-326.
40. Hansson, S.; Norton, M., The relation between surface roughness and interfacial shear strength for bone-anchored implants. A mathematical model. *Journal of Biomechanics* **1999**, *32*, 829-836.
41. Kieswetter, K.; Schwartz, Z.; Hummert, T. W.; Cochran, D. L.; Simpson, J.; Dean, D. D.; Boyan, B. D., Surface roughness modulates the local production of growth factors and cytokines by osteoblast-like MG-63 cells. *Journal of Biomedical Materials Research* **1996**, *32*, 55-63.

42. Stea, S.; Savarino, L.; Toni, A.; Sudanese, A.; Giunti, A.; Pizzoferrato, A., Microradiographic and histochemical evaluation of mineralization inhibition at the bone-alumina interface. *Biomaterials* **1992**, *13*, 664-667.
43. Wennerberg, A., The importance of surface roughness for implant incorporation. *International Journal of Machine Tools and Manufacture* **1998**, *38*, 657-662.
44. Piattelli, A.; Degidi, M.; Paolantonio, M.; Mangano, C.; Scarano, A., Residual aluminum oxide on the surface of titanium implants has no effect on osseointegration. *Biomaterials* **2003**, *24*, 4081-4089.
45. Wennerberg, A.; Albrektsson, T.; Andersson, B.; Krol, J. J., A histomorphometric study of screw-shaped and removal torque titanium implants with three different surface topographies. *Clinical Oral Implants Research* **1995**, *6*, 24-30.
46. Wong, M.; Eulenberger, J.; Schenk, R.; Hunziker, E., Effect of surface topology on the osseointegration of implant materials in trabecular bone. *Journal of Biomedical Materials Research* **1995**, *29*, 1567-1575.
47. Cooper, L. F.; Zhou, Y.; Takebe, J.; Guo, J.; Abron, A.; Holmén, A.; Ellingsen, J. E., Fluoride modification effects on osteoblast behavior and bone formation at TiO<sub>2</sub> grit-blasted c.P. Titanium endosseous implants. *Biomaterials* **2006**, *27*, 926-936.
48. Liu, X.; Chu, P. K.; Ding, C., Surface modification of titanium, titanium alloys, and related materials for biomedical applications. *Materials Science and Engineering: R: Reports* **2004**, *47*, 49-121.
49. Roy, P.; Berger, S.; Schmuki, P., TiO<sub>2</sub> nanotubes: Synthesis and applications. *Angewandte Chemie International Edition* **2011**, *50*, 2904-2939.
50. Losic, D.; Simovic, S., Self-ordered nanopore and nanotube platforms for drug delivery applications. *Expert Opinion on Drug Delivery* **2009**, *6*, 1363-1381.
51. Yang, B.; Uchida, M.; Kim, H.-M.; Zhang, X.; Kokubo, T., Preparation of bioactive titanium metal via anodic oxidation treatment. *Biomaterials* **2004**, *25*, 1003-1010.

52. Sul, Y. T.; Johansson, C.; Wennerberg, A.; Cho, L. R.; Chang, B. S.; Albrektsson, T., Optimum surface properties of oxidized implants for reinforcement of osseointegration: Surface chemistry, oxide thickness, porosity, roughness, and crystal structure. *International Journal of Oral & Maxillofacial Implants* **2005**, *20*, 349-359.
53. Horbett, T. A.; Brash, L. J., Proteins at interfaces: Current issues and future prospects. In *Proteins at interfaces*, American Chemical Society **1987**, 1-33.
54. Sundgren, J. E.; Bodö, P.; Lundström, I., Auger electron spectroscopic studies of the interface between human tissue and implants of titanium and stainless steel. *Journal of Colloid and Interface Science* **1986**, *110*, 9-20.
55. Yoshinari, M.; Oda, Y.; Inoue, T.; Matsuzaka, K.; Shimono, M., Bone response to calcium phosphate-coated and bisphosphonate-immobilized titanium implants. *Biomaterials* **2002**, *23*, 2879-2885.
56. Tejero, R.; Anitua, E.; Orive, G., Toward the biomimetic implant surface: Biopolymers on titanium-based implants for bone regeneration. *Progress in Polymer Science* **2014**, *39*, 1406-1447.
57. Schmidmaier, G.; Wildemann, B.; Cromme, F.; Kandziora, F.; Haas, N. P.; Raschke, M., Bone morphogenetic protein-2 coating of titanium implants increases biomechanical strength and accelerates bone remodeling in fracture treatment: A biomechanical and histological study in rats. *Bone* **2002**, *30*, 816-822.
58. Barfeie, A.; Wilson, J.; Rees, J., Implant surface characteristics and their effect on osseointegration. *British Dental Journal* **2015**, *218*, E9.
59. Dorr, L. D.; Bloebaum, R.; Emmanuel, J.; Meldrum, R., Histologic, biochemical, and ion analysis of tissue and fluids retrieved during total hip arthroplasty. *Clinical Orthopaedics and Related Research* **1990**, *261*, 82-95.
60. Jacobs, J. J.; Skipor, A. K.; Patterson, L. M.; Hallab, N. J.; Paprosky, W. G.; Black, J.; Galante, J. O., Metal release in patients who have had a primary total hip arthroplasty. A

prospective, controlled, longitudinal study. *Journal of Bone and Joint Surgery American volume* **1998**, *80*, 1447-58.

61. Nichols K. G.; Puleo D. A., Effect of metal ions on the formation and function of osteoclastic cells in vitro. *Journal of Biomedical Materials Research* **1997**, *35*, 265-271.

62. Shirtliff, M. E.; Calhoun, J. H.; Mader, J. T., Experimental osteomyelitis treatment with antibiotic-impregnated hydroxyapatite. *Clinical Orthopaedics and Related Research* **2002**, *401*, 239–247.

63. Gabriel M.; Nazmi K.; Veerman E. C.; Nieuw Amerongen A. V.; Zentner A., Preparation of LL-37-grafted titanium surfaces with bactericidal activity. *Bioconjugate Chemistry* **2006**, *17*, 548-550.

64. Hendriks, J. G. E.; Van Horn, J. R.; Van Der Mei, H. C.; Busscher, H. J., Backgrounds of antibiotic-loaded bone cement and prosthesis-related infection. *Biomaterials* **2004**, *25*, 545-556.

65. Parvizi, J.; Saleh, K. J.; Ragland, P. S.; Pour, A. E.; Mont, M. A., Efficacy of antibiotic-impregnated cement in total hip replacement. *Acta Orthopaedica* **2008**, *79*, 335-341.

66. Anagnostakos, K.; Fürst, O.; Kelm, J., Antibiotic-impregnated PMMA hip spacers: Current status. *Acta Orthopaedica* **2006**, *77*, 628-637.

67. Aninwene, G. E.; Yao, C.; Webster, T. J., Enhanced osteoblast adhesion to drug-coated anodized nanotubular titanium surfaces. *International Journal of Nanomedicine* **2008**, *3*, 257-264.

68. Santos, A.; Aw, M. S.; Bariana, M.; Kumeria, T.; Wang, Y.; Losic, D., Drug-releasing implants: Current progress, challenges and perspectives. *Journal of Materials Chemistry B* **2014**, *2*, 6157-6182.

69. Zhang, M.; Bando, Y.; Wada, K., Sol-gel template preparation of TiO<sub>2</sub> nanotubes and nanorods. *Journal of Materials Science Letters* **2001**, *20*, 167-170.

70. Shin, H.; Jeong, D. K.; Lee, J.; Sung, M. M.; Kim, J., Formation of TiO<sub>2</sub> and ZrO<sub>2</sub> nanotubes using atomic layer deposition with ultraprecise control of the wall thickness. *Advanced Materials* **2004**, *16*, 1197-1200.
71. Chen, X.; Mao, S. S., Titanium dioxide nanomaterials: synthesis, properties, modifications, and applications. *Chemical Reviews* **2007**, *107*, 2891-959.
72. Ou, H.-H.; Lo, S.-L., Review of titania nanotubes synthesized via the hydrothermal treatment: Fabrication, modification, and application. *Separation and Purification Technology* **2007**, *58*, 179-191.
73. Li, D.; Xia, Y., Direct Fabrication of Composite and Ceramic Hollow Nanofibers by Electrospinning. *Nano Letters* **2004**, *4*, 933-938.
74. Nakane, K.; Shimada, N.; Ogihara, T.; Ogata, N.; Yamaguchi, S., Formation of TiO<sub>2</sub> nanotubes by thermal decomposition of poly(vinyl alcohol)-titanium alkoxide hybrid nanofibers. *Journal of Materials Science* **2004**, *42*, 4031-35.
75. Zhou, X.; Nguyen, N. T.; Özkan, S.; Schmuki, P., Anodic TiO<sub>2</sub> nanotube layers: Why does self-organized growth occur—A mini review. *Electrochemistry Communications* **2014**, *46*, 157–162.
76. Lee, K.; Mazare, A.; Schmuki, P., One-Dimensional Titanium Dioxide Nanomaterials: Nanotubes. *Chemical Reviews* **2014**, *114*, 9385–9454.
77. Zwilling, V.; Aucouturier, M.; Darque-Ceretti, E., Anodic oxidation of titanium and TA6V alloy in chromic media. An electrochemical approach. *Electrochimica Acta* **1999**, *45*, 921-929.
78. Zwilling, V.; Darque-Ceretti, E.; Boutry-Forveille, A.; David, D.; Perrin, M. Y.; Aucouturier, M., Structure and physicochemistry of anodic oxide films on titanium and TA6Valloy. *Surface and Interface Analysis* **1999**, *27*, 629-637.
79. Macak, J. M.; Tsuchiya, H.; Schmuki, P., High-aspect-ratio TiO<sub>2</sub> nanotubes by anodization of titanium. *Angewandte Chemie International Edition* **2005**, *44*, 2100-2102.

80. Macak, J. M.; Tsuchiya, H.; Taveira, L.; Aldabergerova, S.; Schmuki, P., Smooth anodic TiO<sub>2</sub> nanotubes. *Angewandte Chemie International Edition* **2005**, *44*, 7463-7465.
81. Macak, J. M.; Sirotna, K.; Schmuki, P., Self-organized porous titanium oxide prepared in Na<sub>2</sub>SO<sub>4</sub>/NaF electrolytes. *Electrochimica Acta* **2005**, *50*, 3679-3684.
82. Prakasam, H. E.; Shankar, K.; Paulose, M.; Varghese, O. K.; Grimes, C. A., A new benchmark for TiO<sub>2</sub> nanotube array growth by anodization. *Journal of Physical Chemistry C* **2007**, *111*, 7235-7241.
83. Paulose, M.; Prakasam, H. E.; Varghese, O. K.; Peng, L.; Popat, K. C.; Mor, G. K.; Desai, T. A.; Grimes, C. A., TiO<sub>2</sub> nanotube arrays of 1000 μm length by anodization of titanium foil: Phenol red diffusion. *Journal of Physical Chemistry C* **2007**, *111*, 14992-14997.
84. Allam N. K.; Grimes C. A., Formation of vertically oriented TiO<sub>2</sub> nanotube arrays using a fluoride free HCl aqueous electrolyte. *Journal of Physical Chemistry C* **2007**, *111*, 13028-13032.
85. Albu, S. P.; Kim, D.; Schmuki, P., Growth of aligned TiO<sub>2</sub> bamboo-type nanotubes and highly ordered nanolace. *Angewandte Chemie International Edition* **2008**, *120*, 1942-1945.
86. Smith, Y. R.; Sarma, B.; Mohanty, S. K.; Misra, M., Light-assisted anodized TiO<sub>2</sub> nanotube arrays. *ACS Applied Materials & Interfaces* **2012**, *4*, 5883-5890.
87. Neupane, M. P.; Park, I. S.; Bae, T. S.; Lee, M. H., Sonochemical assisted synthesis of nano-structured titanium oxide by anodic oxidation. *Journal of Alloys and Compounds* **2013**, *581*, 418-422.
88. Yu, J.; Wang, D.; Huang, Y.; Fan, X.; Tang, X.; Gao, C.; Li, J.; Zou, D.; Wu, K., A cylindrical core-shell-like TiO<sub>2</sub> nanotube array anode for flexible fiber-type dye-sensitized solar cells. *Nanoscale Research Letters* **2011**, *6*, 94.

89. Zeng, Q. Y.; Xi, M.; Xu, W.; Li, X. J., Preparation of titanium dioxide nanotube arrays on titanium mesh by anodization in  $(\text{NH}_4)_2\text{SO}_4/\text{NH}_4\text{F}$  electrolyte. *Materials and Corrosion* **2013**, *64*, 1001-1006.
90. Sun, L.; Wang, X.; Li, M.; Zhang, S.; Wang, Q., Anodic titania nanotubes grown on titanium tubular electrodes. *Langmuir* **2014**, *30*, 2835-2841.
91. Long, M.; Rack, H. J., Titanium alloys in total joint replacement—a materials science perspective. *Biomaterials* **1998**, *19*, 1621-1639.
92. Macak, J. M.; Tsuchiya, H.; Taveira, L.; Ghicov, A.; Schmuki, P., Self-organized nanotubular oxide layers on Ti-6Al-7Nb and Ti-6Al-4V formed by anodization in  $\text{NH}_4\text{F}$  solutions. *Journal of Biomedical Materials Research Part A* **2005**, *75A*, 928-933.
93. Feng, X. J.; Macak, J. M.; Albu, S. P.; Schmuki, P., Electrochemical formation of self-organized anodic nanotube coating on Ti-28Zr-8Nb biomedical alloy surface. *Acta Biomaterialia* **2008**, *4*, 318-323.
94. Yasuda, K.; Schmuki, P., Control of morphology and composition of self-organized zirconium titanate nanotubes formed in  $(\text{NH}_4)_2\text{SO}_4/\text{NH}_4\text{F}$  electrolytes. *Electrochimica Acta* **2007**, *52*, 4053-4061.
95. Jha, H.; Hahn, R.; Schmuki, P., Ultrafast oxide nanotube formation on TiNb, TiZr and TiTa alloys by rapid breakdown anodization. *Electrochimica Acta* **2010**, *55*, 8883-8887.
96. Liang, Y. Q.; Cui, Z. D.; Zhu, S. L.; Yang, X. J., Characterization of self-organized  $\text{TiO}_2$  nanotubes on Ti-4Zr-22Nb-2Sn alloys and the application in drug delivery system. *Journal of Materials Science: Materials in Medicine* **2011**, *22*, 461-467.
97. Wang, L.; Zhao, T. T.; Zhang, Z.; Li, G., Fabrication of highly ordered  $\text{TiO}_2$  nanotube arrays via anodization of ti-6al-4v alloy sheet. *Journal of Nanoscience and Nanotechnology* **2010**, *10*, 8312-8321.

98. Feschet-Chassot, E.; Raspal, V.; Sibaud, Y.; Awitor, O. K.; Bonnemoy, F.; Bonnet, J. L.; Bohatier, J., Tunable functionality and toxicity studies of titanium dioxide nanotube layers. *Thin Solid Films* **2011**, *519*, 2564-2568.
99. Boyan, B. D.; Hummert, T. W.; Dean, D. D.; Schwartz, Z., Role of material surfaces in regulating bone and cartilage cell response. *Biomaterials* **1996**, *17*, 137-146.
100. Gulati, K.; Ramakrishnan, S.; Aw, M. S.; Atkins, G. J.; Findlay, D. M.; Losic, D., Biocompatible polymer coating of titania nanotube arrays for improved drug elution and osteoblast adhesion. *Acta Biomaterialia* **2012**, *8*, 449-456.
101. Popat, K. C.; Leoni, L.; Grimes, C. A.; Desai, T. A., Influence of engineered titania nanotubular surfaces on bone cells. *Biomaterials* **2007**, *28*, 3188-3197.
102. Popat, K. C.; Eltgroth, M.; Latempa, T. J.; Grimes, C. A.; Desai, T. A., Decreased staphylococcus epidermis adhesion and increased osteoblast functionality on antibiotic-loaded titania nanotubes. *Biomaterials* **2007**, *28*, 4880-4888.
103. Peng, L.; Eltgroth, M. L.; Latempa, T. J.; Grimes, C. A.; Desai, T. A., The effect of TiO<sub>2</sub> nanotubes on endothelial function and smooth muscle proliferation. *Biomaterials* **2009**, *30*, 1268-1272.
104. Neacsu, P.; Mazare, A.; Cimpean, A.; Park, J.; Costache, M.; Schmuki, P.; Demetrescu, I., Reduced inflammatory activity of raw 264.7 macrophages on titania nanotube modified Ti surface. *International Journal of Biochemistry & Cell Biology* **2014**, *55*, 187-195.
105. Bjursten, L. M.; Rasmusson, L.; Oh, S.; Smith, G. C.; Brammer, K. S.; Jin, S., Titanium dioxide nanotubes enhance bone bonding in vivo. *Journal of Biomedical Materials Research Part A* **2010**, *92A*, 1218-1224.
106. Schroer, W. C.; Berend, K. R.; Lombardi, A. V.; Barnes, C. L.; Bolognesi, M. P.; Berend, M. E.; Ritter, M. A.; Nunley, R. M., Why are total knees failing today? Etiology of total knee revision in 2010 and 2011. *Journal of Arthroplasty* **2013**, *28*, 116-119.



107. Franz, S.; Rammelt, S.; Scharnweber, D.; Simon, J. C., Immune responses to implants – a review of the implications for the design of immunomodulatory biomaterials. *Biomaterials* **2011**, *32*, 6692-6709.
108. Ratner, B. D., The engineering of biomaterials exhibiting recognition and specificity. *Journal of Molecular Recognition* **1996**, *9*, 617-625.
109. Rungsiyakull, C.; Li, Q.; Sun, G.; Li, W.; Swain, M. V., Surface morphology optimization for osseointegration of coated implants. *Biomaterials* **2010**, *31*, 7196-7204.
110. Ainslie, K. M.; Tao, S. L.; Popat, K. C.; Daniels, H.; Hardev, V.; Grimes, C. A.; Desai, T. A., In vitro inflammatory response of nanostructured titania, silicon oxide, and polycaprolactone. *Journal of Biomedical Materials Research Part A* **2009**, *91*, 647-655.
111. Smith, B. S.; Capellato, P.; Kelley, S.; Gonzalez-Juarrero, M.; Popat, K. C., Reduced in vitro immune response on titania nanotube arrays compared to titanium surface. *Biomaterials Science* **2013**, *1*, 322-332.
112. Brown, J. C.; Klein, E. J.; Lewis, C. W.; Johnston, B. D.; Cummings, P., Emergency department analgesia for fracture pain. *Annals of Emergency Medicine* **2003**, *42*, 197-205.
113. Aw, M.; Gulati, K.; Losic, D., Controlling drug release from titania nanotube arrays using polymer nanocarriers and biopolymer coating. *Journal of Biomaterials and Nanobiotechnology* **2011**, *2*, 477-484.
114. Aw, M. S.; Kurian, M.; Losic, D., Non-eroding drug-releasing implants with ordered nanoporous and nanotubular structures: Concepts for controlling drug release. *Biomaterials Science* **2014**, *2*, 10-34.
115. Mandal, S. S.; Jose, D.; Bhattacharyya, A. J., Role of surface chemistry in modulating drug release kinetics in titania nanotubes. *Materials Chemistry and Physics* **2014**, *147*, 247-253.
116. Shokuhfar, T.; Sinha-Ray, S.; Sukotjo, C.; Yarin, A. L., Intercalation of anti-inflammatory drug molecules within TiO<sub>2</sub> nanotubes. *RSC Advances* **2013**, *3*, 17380-17386.

117. Harris, L. G.; Meredith, D. O.; Eschbach, L.; Richards, R. G., Staphylococcus aureus adhesion to standard micro-rough and electropolished implant materials. *Journal of Materials Science: Materials in Medicine* **2007**, *18*, 1151–6.
118. Hauck, C. R.; Ohlsen, K., Sticky connections: Extracellular matrix protein recognition and integrin-mediated cellular invasion by staphylococcus aureus. *Current Opinion in Microbiology* **2006**, *9*, 5-11.
119. Gristina, A., Biomaterial-centered infection: Microbial adhesion versus tissue integration. *Science* **1987**, *237*, 1588-1595.
120. Hickok, N. J.; Shapiro, I. M., Immobilized antibiotics to prevent orthopaedic implant infections. *Advanced Drug Delivery Reviews* **2012**, *64*, 1165-1176.
121. Costerton, J. W.; Stewart, P. S.; Greenberg, E. P., Bacterial biofilms: A common cause of persistent infections. *Science* **1999**, *284*, 1318-1322.
122. Rogers S. S.; Van Der Walle C.; Waigh T. A., Microrheology of bacterial biofilms in vitro: Staphylococcus aureus and pseudomonas aeruginosa. *Langmuir* **2008**, *24*, 13549-13555.
123. Puckett, S. D.; Taylor, E.; Raimondo, T.; Webster, T. J., The relationship between the nanostructure of titanium surfaces and bacterial attachment. *Biomaterials* **2010**, *31*, 706-713.
124. Ercan, B.; Erik, T.; Ece, A.; Thomas, J. W., Diameter of titanium nanotubes influences anti-bacterial efficacy. *Nanotechnology* **2011**, *22*, 295102.
125. Das, T.; Sharma, P. K.; Busscher, H. J.; Van Der Mei, H. C.; Krom, B. P., Role of extracellular DNA in initial bacterial adhesion and surface aggregation. *Applied and Environmental Microbiology* **2010**, *76*, 3405-3408.
126. Zhang, H.; Sun, Y.; Tian, A.; Xue, X. X.; Wang, L.; Alquhali, A.; Bai, X., Improved antibacterial activity and biocompatibility on vancomycin-loaded TiO<sub>2</sub> nanotubes: In vivo and in vitro studies. *International Journal of Nanomedicine* **2013**, *8*, 4379-4389.

127. Kazemzadeh-Narbat, M.; Kindrachuk, J.; Duan, K.; Jenssen, H.; Hancock, R. E. W.; Wang, R., Antimicrobial peptides on calcium phosphate-coated titanium for the prevention of implant-associated infections. *Biomaterials* **2010**, *31*, 9519-9526.
128. Ma, M.; Kazemzadeh-Narbat, M.; Hui, Y.; Lu, S.; Ding, C.; Chen, D. D. Y.; Hancock, R. E. W.; Wang, R., Local delivery of antimicrobial peptides using self-organized TiO<sub>2</sub> nanotube arrays for peri-implant infections. *Journal of Biomedical Materials Research Part A* **2012**, *100A*, 278-285.
129. Zhao, L.; Wang, H.; Huo, K.; Cui, L.; Zhang, W.; Ni, H.; Zhang, Y.; Wu, Z.; Chu, P. K., Antibacterial nano-structured titania coating incorporated with silver nanoparticles. *Biomaterials* **2011**, *32*, 5706-5716.
130. Huo, K.; Zhang, X.; Wang, H.; Zhao, L.; Liu, X.; Chu, P. K., Osteogenic activity and antibacterial effects on titanium surfaces modified with Zn-incorporated nanotube arrays. *Biomaterials* **2013**, *34*, 3467-3478.
131. Tejero, R.; Anitua, E.; Orive, G., Toward the biomimetic implant surface: Biopolymers on titanium-based implants for bone regeneration. *Progress in Polymer Science* **2014**, *39*, 1406-1447.
132. Khor, E.; Lim, L. Y., Implantable applications of chitin and chitosan. *Biomaterials* **2003**, *24*, 2339-2349.
133. Di Martino, A.; Sittinger, M.; Risbud, M. V., Chitosan: A versatile biopolymer for orthopaedic tissue-engineering. *Biomaterials* **2005**, *26*, 5983-5990.
134. Bumgardner, J. D.; Chesnutt, B. M.; Yuan, Y.; Yang, Y.; Appleford, M.; Oh, S.; McLaughlin, R.; Elder, S. H.; Ong, J. L., The integration of chitosan-coated titanium in bone: an in vivo study in rabbits. *Implant Dentistry* **2007**, *16*, 66-79.
135. Chen, X.; Cai, K.; Fang, J.; Lai, M.; Hou, Y.; Li, J.; Luo, Z.; Hu, Y.; Tang, L., Fabrication of selenium-deposited and chitosan-coated titania nanotubes with anticancer and antibacterial properties. *Colloids and Surfaces B: Biointerfaces* **2013**, *103*, 149-157.

136. Del Pozo, J. L.; Rouse, M. S.; Mandrekar, J. N.; Steckelberg, J. M.; Patel, R., The electricidal effect: Reduction of staphylococcus and pseudomonas biofilms by prolonged exposure to low-intensity electrical current. *Antimicrobial Agents and Chemotherapy* **2009**, *53*, 41-45.
137. Ercan, B.; Kummer, K. M.; Tarquinio, K. M.; Webster, T. J., Decreased staphylococcus aureus biofilm growth on anodized nanotubular titanium and the effect of electrical stimulation. *Acta Biomaterialia* **2011**, *7*, 3003-3012.
138. Chug, A.; Shukla, S.; Mahesh, L.; Jadwani, S., Osseointegration—molecular events at the bone–implant interface: A review. *Journal of Oral and Maxillofacial Surgery* **2013**, *25*, 1-4.
139. Vandamme, K.; Holy, X.; Bensidhoum, M.; Logeart-Avramoglou, D.; Naert, I. E.; Duyck, J. A.; Petite, H., In vivo molecular evidence of delayed titanium implant osseointegration in compromised bone. *Biomaterials* **2011**, *32*, 3547-3554.
140. Yao, C.; Perla, V.; Mckenzie, J. L.; Slamovich, E. B.; Webster, T. J., Anodized ti and Ti6Al4V possessing nanometer surface features enhances osteoblast adhesion. *Journal of Biomedical Nanotechnology* **2005**, *1*, 68-73.
141. Von Wilmsky, C.; Bauer, S.; Lutz, R.; Meisel, M.; Neukam, F. W.; Toyoshima, T.; Schmuki, P.; Nkenke, E.; Schlegel, K. A., In vivo evaluation of anodic TiO<sub>2</sub> nanotubes: An experimental study in the pig. *Journal of Biomedical Materials Research Part B: Applied Biomaterials* **2009**, *89B*, 165-171.
142. Xiao, J.; Zhou, H.; Zhao, L.; Sun, Y.; Guan, S.; Liu, B.; Kong, L., The effect of hierarchical micro/nanosurface titanium implant on osseointegration in ovariectomized sheep. *Osteoporosis International* **2011**, *22*, 1907-1913.
143. Neupane, M. P.; Park, I. S.; Bae, T. S.; Yi, H. K.; Uo, M.; Watari, F.; Lee, M. H., Titania nanotubes supported gelatin stabilized gold nanoparticles for medical implants. *Journal of Materials Chemistry* **2011**, *21*, 12078-12082.

144. Zhao, L.; Wang, H.; Huo, K.; Zhang, X.; Wang, W.; Zhang, Y.; Wu, Z.; Chu, P. K., The osteogenic activity of strontium loaded titania nanotube arrays on titanium substrates. *Biomaterials* **2013**, *34*, 19-29.
145. Kunze, J.; Müller, L.; Macak, J. M.; Greil, P.; Schmuki, P.; Müller, F. A., Time-dependent growth of biomimetic apatite on anodic TiO<sub>2</sub> nanotubes. *Electrochimica Acta* **2008**, *53*, 6995-7003.
146. Kar, A.; Raja, K. S.; Misra, M., Electrodeposition of hydroxyapatite onto nanotubular TiO<sub>2</sub> for implant applications. *Surface and Coatings Technology* **2006**, *201*, 3723-3731.
147. Kodama, A.; Bauer, S.; Komatsu, A.; Asoh, H.; Ono, S.; Schmuki, P., Bioactivation of titanium surfaces using coatings of TiO<sub>2</sub> nanotubes rapidly pre-loaded with synthetic hydroxyapatite. *Acta Biomaterialia* **2009**, *5*, 2322-2330.
148. Gu, Y. X.; Du, J.; Zhao, J. M.; Si, M. S.; Mo, J. J.; Lai, H. C., Characterization and preosteoblastic behavior of hydroxyapatite-deposited nanotube surface of titanium prepared by anodization coupled with alternative immersion method. *Journal of Biomedical Materials Research Part B: Applied Biomaterials* **2012**, *100B*, 2122-2130.
149. Vo, T. N.; Kasper, F. K.; Mikos, A. G., Strategies for controlled delivery of growth factors and cells for bone regeneration. *Advanced Drug Delivery Reviews* **2012**, *64*, 1292-1309.
150. Harmankaya, N.; Karlsson, J.; Palmquist, A.; Halvarsson, M.; Igawa, K.; Andersson, M.; Tengvall, P., Raloxifene and alendronate containing thin mesoporous titanium oxide films improve implant fixation to bone. *Acta Biomaterialia* **2013**, *9*, 7064–7073.
151. Lai, M.; Cai, K.; Zhao, L.; Chen, X.; Hou, Y.; Yang, Z., Surface functionalization of TiO<sub>2</sub> nanotubes with Bone Morphogenetic Protein 2 and its synergistic effect on the differentiation of mesenchymal stem cells. *Biomacromolecules* **2011**, *12*, 1097-1105.

152. Hu, Y.; Cai, K.; Luo, Z.; Xu, D.; Xie, D.; Huang, Y.; Yang, W.; Liu, P., Tio<sub>2</sub> nanotubes as drug nanoreservoirs for the regulation of mobility and differentiation of mesenchymal stem cells. *Acta Biomaterialia* **2012**, *8*, 439-448.
153. Koo, T.-H.; Borah, J.; Xing, Z. C.; Moon, S. M.; Jeong, Y.; Kang, I. K., Immobilization of pamidronic acids on the nanotube surface of titanium discs and their interaction with bone cells. *Nanoscale Research Letters* **2013**, *8*, 1-9.
154. Lee, S. J.; Oh, T. J.; Bae, T. S.; Lee, M. H.; Soh, Y.; Kim, B. I.; Kim, H. S., Effect of bisphosphonates on anodized and heat-treated titanium surfaces: An animal experimental study. *Journal of Periodontology* **2010**, *82*, 1035-1042.
155. Wei, H.; Wu, S.; Feng, Z.; Zhou, W.; Dong, Y.; Wu, G.; Bai, S.; Zhao, Y., Increased fibroblast functionality on CNN2-loaded titania nanotubes. *International Journal of Nanomedicine* **2012**, *7*, 1091-1100.
156. Sun, S.; Yu, W.; Zhang, Y.; Zhang, F., Increased preosteoblast adhesion and osteogenic gene expression on TiO<sub>2</sub> nanotubes modified with KRSR. *Journal of Materials Science: Materials in Medicine* **2013**, *24*, 1079-1091.
157. Adell, R.; Eriksson, B.; Lekholm, U.; Brånemark, P. I.; Jemt, T., Long-term follow-up study of osseointegrated implants in the treatment of totally edentulous jaws. *International Journal of Oral & Maxillofacial Implants* **1990**, *5*, 347-359.
158. Moiola, E. K.; Clark, P. A.; Xin, X.; Lal, S.; Mao, J. J., Matrices and scaffolds for drug delivery in dental, oral and craniofacial tissue engineering. *Advanced Drug Delivery Reviews* **2007**, *59*, 308-324.
159. Ma, Q.; Mei, S.; Ji, K.; Zhang, Y.; Chu, P. K., Immobilization of Ag nanoparticles/FGF-2 on a modified titanium implant surface and improved human gingival fibroblasts behavior. *Journal of Biomedical Materials Research Part A* **2011**, *98A*, 274-286.

160. Lee, Y. H.; Bhattarai, G.; Park, I. S.; Kim, G. R.; Kim, G. E.; Lee, M. H.; Yi, H. K., Bone regeneration around n-acetyl cysteine-loaded nanotube titanium dental implant in rat mandible. *Biomaterials* **2013**, *34*, 10199-10208.
161. Demetrescu, I.; Pirvu, C.; Mitran, V., Effect of nano-topographical features of Ti/TiO<sub>2</sub> electrode surface on cell response and electrochemical stability in artificial saliva. *Bioelectrochemistry* **2010**, *79*, 122-129.
162. Kalbacova, M.; Macak, J. M.; Schmidt-Stein, F.; Mierke, C. T.; Schmuki, P., TiO<sub>2</sub> nanotubes: Photocatalyst for cancer cell killing. *Physica Status Solidi Rapid Research Letters* **2008**, *2*, 194-196.
163. Li, Q.; Wang, X.; Lu, X.; Tian, H.; Jiang, H.; Lv, G.; Guo, D.; Wu, C.; Chen, B., The incorporation of daunorubicin in cancer cells through the use of titanium dioxide whiskers. *Biomaterials* **2009**, *30*, 4708-4715.
164. Gultepe, E.; Nagesha, D.; Sridhar, S.; Amiji, M., Nanoporous inorganic membranes or coatings for sustained drug delivery in implantable devices. *Advanced Drug Delivery Reviews* **2010**, *62*, 305-315.
165. Peng, L.; Mendelsohn, A. D.; Latempa, T. J.; Yoriya, S.; Grimes, C. A.; Desai, T. A., Long-term small molecule and protein elution from TiO<sub>2</sub> nanotubes. *Nano Letters* **2009**, *9*, 1932-1936.
166. Yao, C.; Webster, T. J., Prolonged antibiotic delivery from anodized nanotubular titanium using a co-precipitation drug loading method. *Journal of Biomedical Materials Research Part B: Applied Biomaterials* **2009**, *91B*, 587-595.
167. De Santo, I.; Sanguigno, L.; Causa, F.; Monetta, T.; Netti, P. A., Exploring doxorubicin localization in eluting TiO<sub>2</sub> nanotube arrays through fluorescence correlation spectroscopy analysis. *Analyst* **2012**, *137*, 5076-5081.

168. Han, C. M.; Lee, E. J.; Kim, H. E.; Koh, Y. H.; Jang, J. H., Porous TiO<sub>2</sub> films on Ti implants for controlled release of tetracycline-hydrochloride (TCH). *Thin Solid Films* **2011**, *519*, 8074-8076.
169. Aw, M. S.; Addai-Mensah, J.; Losic, D., A multi-drug delivery system with sequential release using titania nanotube arrays. *Chemical Communications* **2012**, *48*, 3348-3350.
170. Aw, M. S.; Addai-Mensah, J.; Losic, D., Magnetic-responsive delivery of drug-carriers using titania nanotube arrays. *Journal of Materials Chemistry* **2012**, *22*, 6561-6563.
171. Aw, M. S.; Losic, D., Ultrasound enhanced release of therapeutics from drug-releasing implants based on titania nanotube arrays. *International Journal of Pharmaceutics* **2013**, *443*, 154-162.
172. Simovic, S.; Losic, D.; Vasilev, K., Controlled drug release from porous materials by plasma polymer deposition. *Chemical Communications* **2010**, *46*, 1317-1319.
173. Vasilev, K.; Poh, Z.; Kant, K.; Chan, J.; Michelmore, A.; Losic, D., Tailoring the surface functionalities of titania nanotube arrays. *Biomaterials* **2010**, *31*, 532-540.
174. Collins, A. J.; Cosh, J. A., Temperature and biochemical studies of joint inflammation. A preliminary investigation. *Annals of the Rheumatic Diseases* **1970**, *29*, 386-392.
175. Cai, K.; Jiang, F.; Luo, Z.; Chen, X., Temperature-responsive controlled drug delivery system based on titanium nanotubes. *Advanced Engineering Materials* **2010**, *12*, B565-B570.
176. Shrestha, N. K.; Macak, J. M.; Schmidt-Stein, F.; Hahn, R.; Mierke, C. T.; Fabry, B.; Schmuki, P., Magnetically guided titania nanotubes for site-selective photocatalysis and drug release. *Angewandte Chemie International Edition* **2009**, *48*, 969-972.



177. Sirivisoot, S.; Pareta, R. A.; Webster, T. J., A conductive nanostructured polymer electrodeposited on titanium as a controllable, local drug delivery platform. *Journal of Biomedical Materials Research Part A* **2011**, *99A*, 586-597.
178. Sirivisoot, S.; Pareta, R.; Webster, T. J., Electrically controlled drug release from nanostructured polypyrrole coated on titanium. *Nanotechnology* **2011**, *22*, 085101.
179. Bariana, M.; Aw, M. S.; Moore, E.; Voelcker, N. H.; Losic, D., Radiofrequency-triggered release for on-demand delivery of therapeutics from titania nanotube drug-eluting implants. *Nanomedicine* **2013**, *9*, 1263-1275.
180. Sirivisoot, S.; Yao, C.; Xiao, X.; Sheldon, B. W.; Webster, T. J., Greater osteoblast functions on multiwalled carbon nanotubes grown from anodized nanotubular titanium for orthopedic applications. *Nanotechnology* **2007**, *18*, 365102.
181. Sirivisoot, S.; Webster, T. J., Multiwalled carbon nanotubes enhance electrochemical properties of titanium to determine in situ bone formation. *Nanotechnology* **2008**, *19*, 295101.
182. Mendonça, G.; Mendonça, D. B.; Aragão, F. J.; Cooper, L. F., Advancing dental implant surface technology – From micron-to nanotopography. *Biomaterials* **2008**, *29*, 3822–3835
183. Minagar, S; Wang, J; Berndt, CC; Ivanova, EP; Wen, C., Cell response of anodized nanotubes on titanium and titanium alloys—A review. *Journal of Biomedical Materials Research Part A* **2013**, *101A*, 2726–2739
184. Brammer, K. S.; Frandsen, C. J.; Jin, S., TiO<sub>2</sub> nanotubes for bone regeneration. *Trends in Biotechnology* **2012**, *30*, 315-322.
185. Gulati, K.; Aw, M. S.; Findlay, D.; Losic, D., Local Drug Delivery in Bone by Drug Releasing Implants: Perspectives of Nano-Engineered Titania Nanotubes. *Therapeutic Delivery*, **2012**, *3*, 857-873.

186. Losic, D.; Aw, M. S.; Santos, A.; Gulati, K.; Bariana, M., Titania Nanotube Arrays for Local Drug Delivery: Recent Advances and Perspectives. *Expert Opinion on Drug Delivery*, **2015**, *12*, 103-127.

## CHAPTER 2

---

# FABRICATION of TITANIA NANOTUBES on Ti for USE as BONE THERAPEUTIC IMPLANTS

**Karan Gulati**

School of Chemical Engineering, University of Adelaide, South Australia 5005, Australia

# CHAPTER 2: FABRICATION of TITANIA NANOTUBES on Ti for USE as BONE THERAPEUTIC IMPLANTS

## 2.1. Introduction and Objectives

A primary requirement for any bone implant modification is the use of biocompatible/biodegradable materials and scalable technology, which can ensure easy integration into the current implant market. Electrochemical anodization (EA) used to fabricate TNTs have been well researched and advanced, however, there is still scope for improvement, specially towards anodizing substrates with complex geometries, to meet specialised therapeutic needs. This chapter focuses on defining the design, fabrication strategies and therapeutic functionality of electrochemically anodized novel TNTs/Ti bone implants. This chapter also describes in detail the electrochemical setup, optimized anodization conditions, drug loading and tailoring *in-vitro* release, surface morphology characterization, and ultimately *ex-vivo* drug diffusion inside the bone micro-environment.

## 2.2. Fabrication of TNTs on Various Substrates

### 2.2.1 Ti Flat Foil Substrate

EA is most popular methodology to fabricate high-quality self-ordered TNTs suitable for multiple applications, and represents a cost-effective and scalable technology<sup>1</sup>. To fabricate TNTs, the electrochemical cell consists of 3 main components: Ti substrate (Ti flat foil), counter-electrode (dummy Ti foil, cathode) and appropriate electrolyte (1-3 % v/v water, 0.3 % w/v NH<sub>4</sub>F in ethylene glycol). This electrochemical cell is sealed to avoid moisture uptake

by the hygroscopic electrolyte, maintained at 25°C and placed on a magnetic stirrer. To prepare the electrolyte by means of ageing, anodization of dummy titanium (mechanically polished flat foil) was performed using a fresh/unused electrolyte. Each step of ageing corresponds to 2 h of anodization at 75 V, after which the sample (anode) was replaced with fresh polished Ti foil. An age of 10 h was considered appropriate to fabricate well-adherent and high-quality TNTs. Detailed investigations leading to optimization of electrolyte ageing are presented in **Chapter 4**. Prior to anodization, the Ti implant substrates were polished so as to obtain better ordering of the TNT arrays<sup>2-3</sup>. For flat Ti, mechanical polishing was performed, which included sand paper scrubbing (coarse and sand), followed by polishing with alumina powder paste made in deionized water (coarse and fine). After polishing, the Ti substrates were sonicated in ethanol and acetone.

The electrochemical setup designed to achieve successful fabrication of TNTs on Ti flat foil substrates is presented in **Figure 2.1**. For anodizing Ti flat foil substrates, the anodic holder comprises a plastic body with a copper connection that runs through it (**Figure 2.1a**), onto which various components of the electrode can be placed and secured with a clip (**Figure 2.1b-c**). Mechanically polished Ti foil (approx. size 1.2 x 1.2 cm<sup>2</sup>) is securely placed on top of Al foil, which covers the underlying copper plate. Onto this, the rubber and plastic components are placed with a hole that permits a circular area of diameter 1 cm of the underlying Ti to be exposed to the anodization electrolyte. Later, the anode and cathode (Ti foil strip) are immersed in the electrolyte containing transparent plastic container, which has a magnetic stirrer at the bottom. The distance between electrodes (2 cm), stirring speed and the temperature (25°C) is maintained throughout the anodization procedure. The setup is sealed at the top to avoid moisture uptake. The electrodes are then connected to the respective ports of the computer controlled power supply (Agilent) using Labview Program, as described elsewhere<sup>4</sup>.

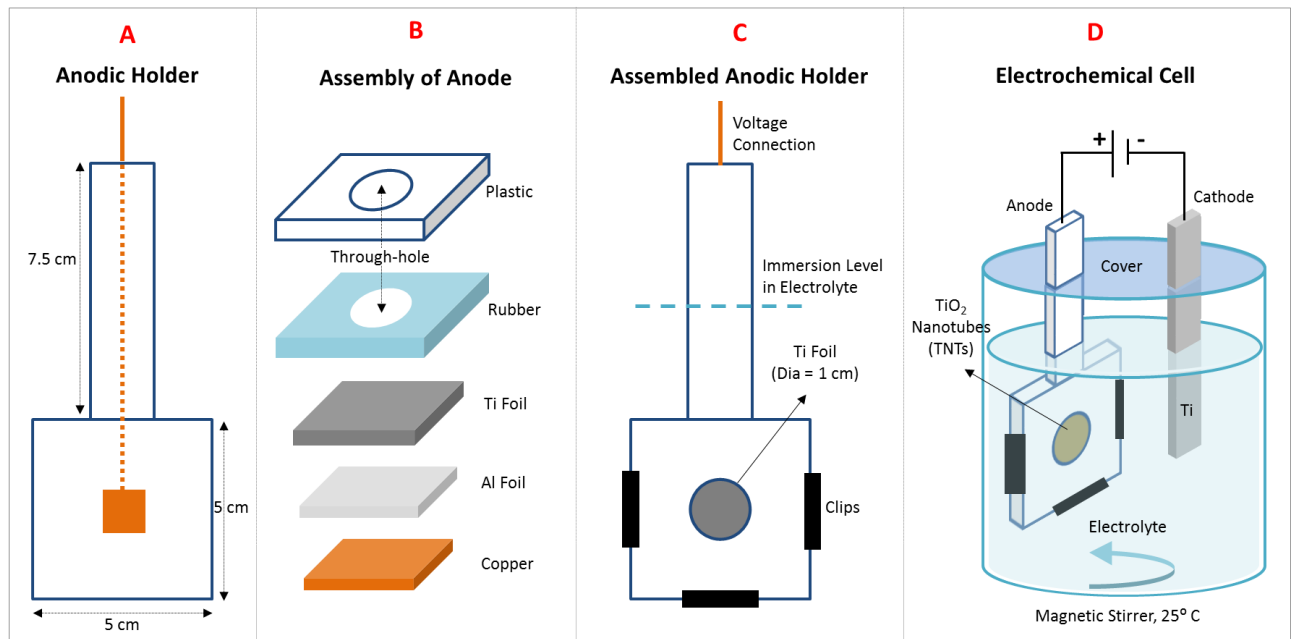


**Figure 2.1.** Schematic illustration of anodization setup used for fabricating TNTs on flat Ti foil substrate: (a) anodic holder design, (b) assembling various components of the anode holder, (c) final assembled anodic holder exposing 1 cm diameter circular area of mechanically polished Ti foil, and (d) sealed electrochemical cell with anode/cathode attached to computer-controlled power supply.

The anodization is carried out constant voltage (60-120 V) and the current density vs time plots are continuously monitored and recorded. To anodize a flat Ti foil substrate, a two-step anodization was adopted, with the 1<sup>st</sup> step involving 75 V for 2 h, followed by removal of the anodic film by sonication in methanol. This permitted a templated surface on the Ti substrate, suitable for the 2<sup>nd</sup> anodization step (75 V, various times), which results in improved ordering of the TNTs arrays. The two step anodization permits growth of highly ordered TNTs on flat foil substrates, however to achieve altered nanotube structures, such as periodic tailoring, a modified anodic profile was used with continuous voltage variation with time. The generation of periodically modulated TNTs structures is described in **Chapter 3**.

### 2.2.2. Ti Wires and 3D Printed Ti alloys

To fabricate high quality TNTs on complex Ti substrate geometries such as curved surface of Ti wires, an in depth evaluation of various contributing factors, including electrolyte ageing, water content, anodization voltage and time, and substrate dimensions, was performed. The investigations, as described in **Chapter 4**, lead to defining the most optimized anodization procedure, whereby well-adherent and highly ordered TNTs can be fabricated on curved surfaces of Ti wires. For Ti wires, electropolishing (EP) was performed prior to anodization, using perchloric acid electrolyte, containing butanol and ethanol (P:B:E = 1:6:9), maintained at 0 °C for 1-5 min at 25-40 V. The diameter of Ti wire used (0.50 or 0.80 mm) determined the time/voltage of EP. Afterwards, the implants were cleaned thoroughly in ethanol and acetone, and stored dry. For anodizing polished Ti wires, appropriately aged electrolyte (10 h aged, 1% v/v water and 0.3% w/v NH<sub>4</sub>F in ethylene glycol) was used in a 1 step procedure, carried out at 75 V for various times. For wires, no special anodic cell/holder was used, and a simple silicone tube was used as a mask to shield the wire from electrolyte, exposing only a specific length of the electropolished Ti wire (3-10 mm) for anodization. The schematic presented in **Figure 2.2** shows the electrochemical setup used to anodize Ti wires. This setup enables fabrication of TNTs all over the exposed curved surface area of Ti wires.

To anodize 3D printed Ti alloy, cleaned substrates (4 x 4 mm<sup>2</sup>) were attached to Ti wire *via* parafilm wrapping towards one of the corners. Later the implants were immersed as shown for Ti wires, where parafilm acted as a shield and Ti wire served as a connector to the power supply. A single anodization step was used at 60 V for various times. This resulted in TNT fabrication on both sides of the flat substrate and on the edges. No polishing step was performed prior to anodizing printed Ti alloys, so as to preserve the unique micro-scale topography (generated by random arrangement of Ti alloy micro-particles on flat substrate).

Furthermore anodization was used to add nano-structural topography while preserving the micro-scale features. Details are provided in **Chapter 8**.

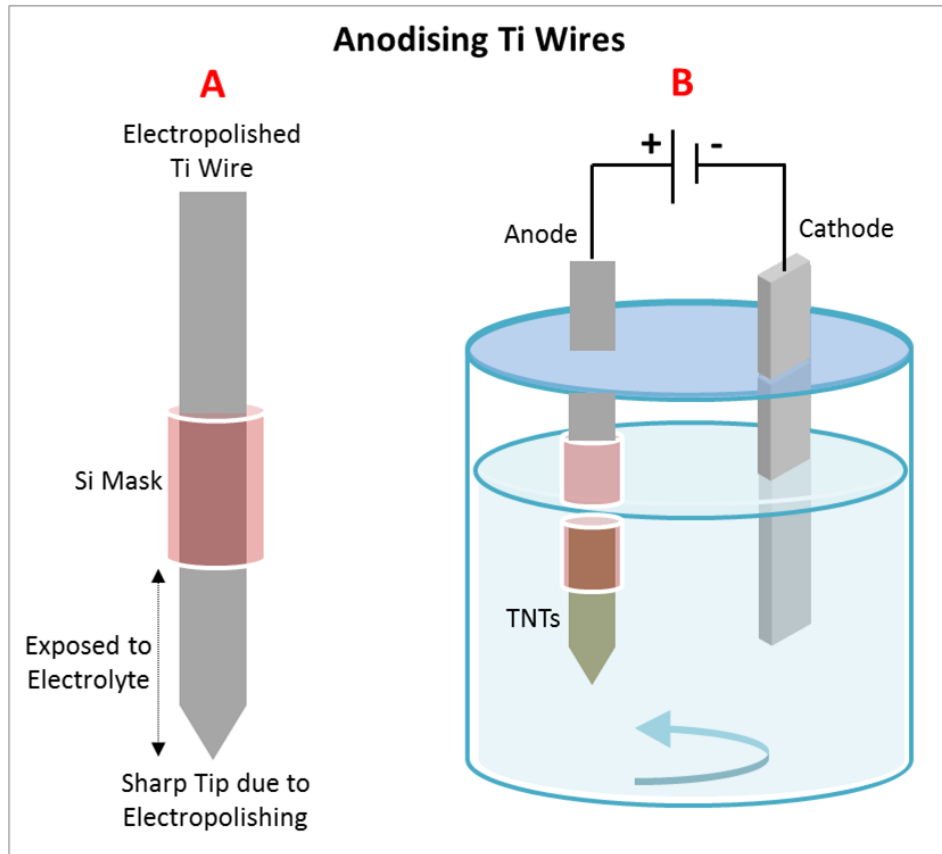


**Figure 2.2.** Scheme showing the electrochemical setup for anodizing Ti wires.

### 2.3. Therapeutic Loading inside TNTs

TNTs have been widely explored for use as therapeutic implants and many studies have shown that substantial amounts of drug can be loaded (various chemistries and catering to various conditions), and released locally<sup>5-6</sup>. To demonstrate their application for various bone conditions, different active therapeutics were loaded inside TNTs generated on Ti flat foil or wires. These include the non-steroidal anti-inflammatory drug indomethacin (Indo) and the potent osteoporotic therapeutic, parathyroid hormone (PTH). Prior to loading, the implant surfaces were sterilised using UV irradiation of all sides, for 30 min. The loading procedure used depended on the substrate choice: for TNTs generated on Ti flat foil, a drop of the drug



solution was placed onto the implants and allowed to dry. The steps were repeated until substantial amounts were loaded inside the implants. For TNTs/Ti wire, cleaned implants were immersed in drug solutions and the drug amounts loaded were found to directly correlate with the time of immersion. After loading, the surfaces of implants were gently wiped using a soft tissue to remove any surface accumulated drug.

To quantify the amount of drug loaded inside TNTs, firstly the characteristic decomposition peak of the particular therapeutic was evaluated using thermo-gravimetric analysis TGA Q500 (TA Instruments). Briefly, a known amount of the therapeutic was placed in the Pt pan and heated to  $> 500^{\circ}\text{C}$  in a  $\text{N}_2$  environment at the rate of  $10^{\circ}\text{C}/\text{min}$ . From the weight change vs temperature profile, the characteristic peak (temperature range at which decomposition occurs) of the drug was obtained. After this, the therapeutic loaded TNT implants were heated in the TGA furnace using the same conditions, and the characteristic peak, representing the therapeutic, was used to determine the amount loaded. Any background signal from TNTs alone was subtracted to obtain the correct loading amount.

### **2.3. Release of Therapeutics from TNTs *in-vitro***

Therapeutic loaded TNT/Ti samples were immersed in 5 ml phosphate buffered saline (PBS), maintained at pH 7.4 and  $25^{\circ}\text{C}$ . At predetermined time intervals, 3 ml aliquots were drawn and immediately replaced with fresh PBS solution. The 3 ml aliquots were used to measure absorbance, using Cary 60 Spectrophotometer at a wavelength which corresponds to the particular therapeutic used. Later this absorbance was used to calculate the concentration, based on the calibration curve, and a cumulative weight % vs time graph was plotted. A typical drug release profile is shown in **Figure 2.3**. Drug release in PBS is mainly driven by a diffusion gradient, and a biphasic release pattern is observed, whereby therapeutics present

near the open ends of TNTs are quickly released (initial burst release), which is followed by a sustained release pattern corresponding to the therapeutics that are present deep inside TNTs.

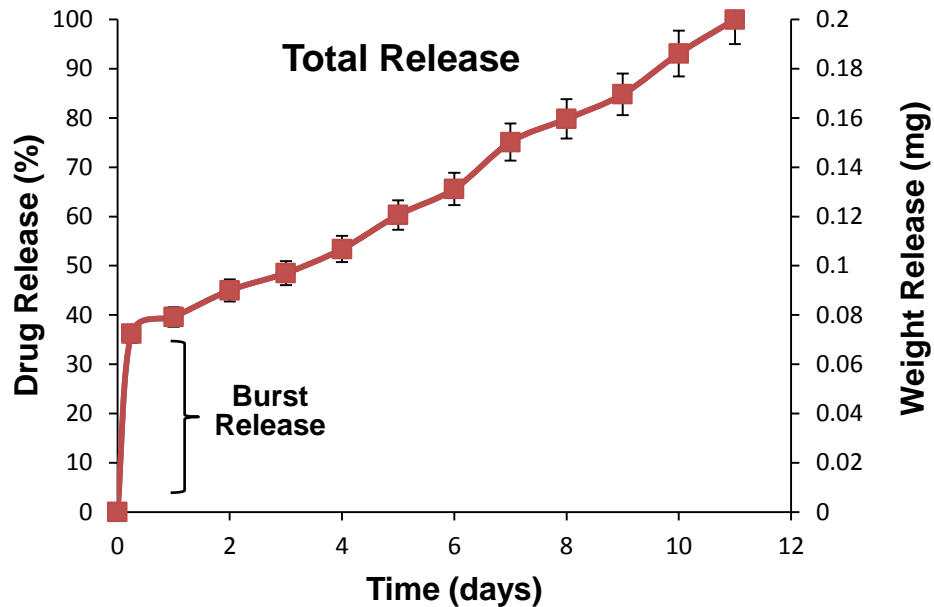


**Figure 2.3.** Release of gentamicin from TNTs/Ti wire, showing biphasic release pattern with initial burst release (1<sup>st</sup> 6 h) followed by total release until the entire loaded therapeutic is released into the PBS buffer (adapted with permission from [7]).

## 2.4. Strategies to Control Therapeutic Release

As described in **Chapter 1**, to achieve optimum release kinetics, the initial burst release must be reduced and overall release must be prolonged. To achieve this, two strategies were employed: periodic tailoring of TNTs structures *via* voltage oscillation (**Chapter 3**) and coating a thin layer of biopolymer on drug loaded TNTs/Ti wire (**Chapter 5**). For periodically tailored TNTs, the available vacant volume of TNTs was modulated so as to create restrictions in otherwise smooth nanotube walls. These in turn were expected to impede the diffusion of drug molecules. In another strategy, a thin film of bioactive and antibacterial polymer chitosan was coated onto indomethacin loaded TNTs/Ti wires, which served as an

extension to our previous work on TNTs/Ti flat foil<sup>4</sup>. The release in this case was dominated by the rate of chitosan degradation, which exposed the open pores of TNTs to the PBS. Furthermore, to investigate the fate of such biopolymer coatings, a systematic study was performed for chitosan coated TNTs/Ti wire immersed in PBS, to also simultaneously report the generation of chitosan micro-tubes on nanotubular structures (**Chapter 6**).

## 2.5. Experimental Setup to Confirm Bone Therapeutic Effects

The fabricated TNTs on Ti wires were proposed as in-bone therapeutic implants, capable of catering to wide range of complex bone conditions such as deep infections, osteoporotic fractures, cancers etc. To demonstrate the ability of the implant to effectively deliver therapeutics locally for maximised action, two separate experiments were designed. Firstly, parathyroid hormone (PTH) loaded TNTs/Ti wires (of various TNTs dimensions) were inserted into a collagen gel containing SaOS2 osteoblast-like cells. The release of PTH from TNTs and its effect on bone cells was evaluated in terms of genetic expression (**Chapter 5**). Secondly, to show the ability of the minimally invasive TNTs/Ti wire implants to release drugs inside the bone tissue itself, fluorescent dye Rhodamine B was loaded into implants followed by their insertion into bovine trabecular bone cores *ex-vivo*. The presented strategy in **Figure 2.4** shows the sequence of the experiment whereby trabecular bone cores were made from bovine sternum, followed by drilling a hole with a stainless steel pin and insertion of the dye loaded TNTs/Ti wire implant. The bone cores were then placed inside plastic perfusion chamber, which was perfused with culture media, using the Zetos<sup>TM</sup> system. The bone cores used represented three variants: intact with bone marrow, intact with bone marrow + anticoagulant (heparin), and with bone marrow removed. The release of dye at predetermined time intervals was measured using fluorescence microscopy (**Appendix A**).

Later, the implants were retrieved and examined under scanning electron microscopy (SEM) to reveal any structural deformities or delamination.

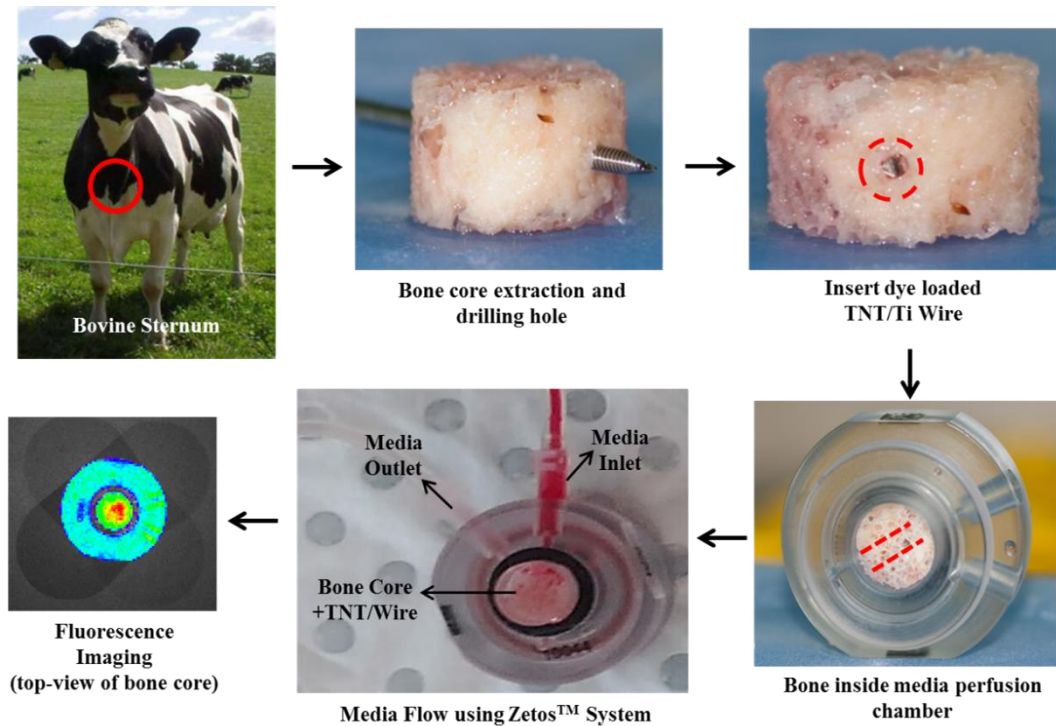


**Figure 2.4.** The photographic sequence showing the procedure for monitoring the release of therapeutics directly inside the bone micro-environment.

## 2.6 Structural Characterization of TNT implants

Structural morphology of the fabricated TNT/Ti implants was characterized using a field emission scanning electron microscope (SEM) (FEI Quanta 450). The samples were mounted on a holder with double-sided conductive tape and coated with a layer of platinum 5 nm thick. Images with a range of scan sizes at normal incidence and at a 30° angle were acquired from the top/bottom surfaces and cross sections. SEM images were subsequently analysed by ImageJ (public domain program developed at the RSB of the NIH). Furthermore, EDXS

(energy dispersive X-ray spectroscopy) of the nanotube samples, at top and cross-sections (after fracturing nanotube membrane) was also performed.

## 2.7 References

1. Roy, P.; Berger, S.; Schmuki, P., TiO<sub>2</sub> nanotubes: Synthesis and applications. *Angewandte Chemie International Edition* **2011**, *50*, 2904-2939.
2. Fan, M.; La Mantia, F., Effect of Surface Topography on the Anodization of Titanium. *Electrochemistry Communications* **2013**, *37*, 91–95.
3. Lu, K.; Tian, Z.; Geldmeier, J. A. Polishing Effect on Anodic Titania Nanotube Formation. *Electrochimica Acta* **2011**, *56*, 6014–6020.
4. Gulati, K.; Ramakrishnan, S.; Aw, M. S.; Atkins, G. J.; Findlay, D. M.; Losic, D., Biocompatible polymer coating of titania nanotube arrays for improved drug elution and osteoblast adhesion. *Acta Biomaterialia* **2012**, *8*, 449-456.
5. Losic, D.; Simovic, S., Self-ordered nanopore and nanotube platforms for drug delivery applications. *Expert Opinion on Drug Delivery* **2009**, *6*, 1363-1381.
6. Santos, A.; Aw, M. S.; Bariana, M.; Kumeria, T.; Wang, Y.; Losic, D., Drug-releasing implants: Current progress, challenges and perspectives. *Journal of Materials Chemistry B* **2014**, *2*, 6157-6182.
7. Gulati, K.; Aw, M. S.; Losic, D., Drug eluting Ti wires with titania nanotubes arrays for bone fixation and reduced bone infection. *Nanoscale Research Letters*, **2011**, *6*, 571-577.

## CHAPTER 3

---

# PERIODICALLY TAILORED TITANIA NANOTUBES for ENHANCED DRUG LOADING and RELEASING PERFORMANCES

**Karan Gulati**

School of Chemical Engineering, University of Adelaide South Australia 5005, Australia

**This chapter is based on the following peer-reviewed article:**

**K. Gulati, K. Kant, D. Losic** “Periodically Tailored Titania Nanotubes for Enhanced Drug Loading and Releasing Performances” *Journal of Materials Chemistry B*, 2015, **3**, 2553.

## Statement of Authorship

Title of Paper	Periodically tailored titania nanotubes for enhanced drug loading and releasing performances
Publication Status	<input checked="" type="checkbox"/> Published <input type="checkbox"/> Accepted for Publication <input type="checkbox"/> Submitted for Publication <input type="checkbox"/> Publication Style
Publication Details	<i>Journal of Materials Chemistry B</i> , 2015, 3, 2553.

### Principal Author

Name of Principal Author (Candidate)	Karan Gulati			
Contribution to the Paper	Under the supervision of D. Losic and D. Findlay, I developed, designed and performed the experiments, interpreted and processed the data and wrote the manuscript for submission			
Overall percentage (%)	80			
Signature		<table border="1"> <tr> <td>Date</td> <td>27 July 2015</td> </tr> </table>	Date	27 July 2015
Date	27 July 2015			

### Co-Author Contributions

By signing the Statement of Authorship, each author certifies that:

- i. the candidate's stated contribution to the publication is accurate (as detailed above);
- ii. permission is granted for the candidate to include the publication in the thesis; and
- iii. the sum of all co-author contributions is equal to 100% less the candidate's stated contribution.

Name of Co-Author	Krishna Kant			
Contribution to the Paper	I helped Karan Gulati (candidate) with designing the anodisation experiment of titanium to obtain periodically tailored titania nanotubes. I give consent for Karan Gulati to present this paper for examination towards the Doctorate of philosophy.			
Signature		<table border="1"> <tr> <td>Date</td> <td>27 July 2015</td> </tr> </table>	Date	27 July 2015
Date	27 July 2015			

Name of Co-Author	David Findlay			
Contribution to the Paper	I acted as secondary supervisor for the candidate and aided in development and design of the experiments and evaluation of manuscript for submission. I give consent for Karan Gulati to present this paper for examination towards the Doctorate of philosophy.			
Signature		<table border="1"> <tr> <td>Date</td> <td>27 July 2015</td> </tr> </table>	Date	27 July 2015
Date	27 July 2015			

Name of Co-Author	Dusan Losic		
Contribution to the Paper	I acted as primary supervisor of the candidate and aided in evaluation of experimental design and manuscript for submission. I give consent for Karan Gulati to present this paper for examination towards the Doctorate of philosophy.		
Signature		Date	27 July 2015

Please cut and paste additional co-author panels here as required.



Gulati, K., Kant, K., Findlay, D. & Losic, D. (2015). Periodically tailored titania nanotubes for enhanced drug loading and releasing performances. *Journal of Materials Chemistry B*, 3, 2553-2559.

NOTE:

This publication is included on pages 83 - 89 in the print copy of the thesis held in the University of Adelaide Library.

It is also available online to authorised users at:

<http://dx.doi.org/10.1039/c4tb01882f>

## CHAPTER 4

---

# OPTIMIZING ANODIZATION CONDITIONS for the GROWTH of TITANIA NANOTUBES on CURVED SURFACES

**Karan Gulati**

School of Chemical Engineering, University of Adelaide South Australia 5005, Australia

**This chapter is based on the following peer-reviewed article:**

**K. Gulati**, A. Santos, D. Findlay, D. Losic “Optimizing Anodization Conditions for the Growth of Titania Nanotubes on Curved Surfaces” *Journal of Physical Chemistry C*, 2015, **119**, 16033. **DOI:** 10.1021/acs.jpcc.5b03383.

## Statement of Authorship

Title of Paper	Optimizing Anodization Conditions for the Growth of Titania Nanotubes on Curved Surfaces
Publication Status	<input checked="" type="checkbox"/> Published <input type="checkbox"/> Accepted for Publication <input type="checkbox"/> Submitted for Publication <input type="checkbox"/> Publication Style
Publication Details	<i>Journal of Physical Chemistry C</i> , 2015, <b>119</b> , 16033.

### Principal Author

Name of Principal Author (Candidate)	Karan Gulati		
Contribution to the Paper	Under the supervision of D. Losic and D. Findlay, I developed, designed and performed the experiments, interpreted and processed the data and wrote the manuscript for submission		
Overall percentage (%)	80		
Signature		Date	27 July 2015

### Co-Author Contributions

By signing the Statement of Authorship, each author certifies that:

- i. the candidate's stated contribution to the publication is accurate (as detailed above);
- ii. permission is granted for the candidate to include the publication in the thesis; and
- iii. the sum of all co-author contributions is equal to 100% less the candidate's stated contribution.

Name of Co-Author	Abel Santos		
Contribution to the Paper	I helped Karan Gulati (candidate) with designing the experiments, elaborating on the role of various anodisation factors and improving the manuscript for submission. I give consent for Karan Gulati to present this paper for examination towards the Doctorate of philosophy.		
Signature		Date	27 July 2015

Name of Co-Author	David Findlay		
Contribution to the Paper	I acted as secondary supervisor for the candidate and aided in development and design of the experiments and evaluation of manuscript for submission. I give consent for Karan Gulati to present this paper for examination towards the Doctorate of philosophy.		
Signature		Date	27 July 2015

Name of Co-Author	Dusan Losic		
Contribution to the Paper	I acted as primary supervisor of the candidate and aided in evaluation of experimental design and manuscript for submission. I give consent for Karan Gulati to present this paper for examination towards the Doctorate of philosophy.		
Signature		Date	27 July 2015

Please cut and paste additional co-author panels here as required.

Gulati, K., Santos, A., Findlay, D. & Lasic, D. (2015). Optimizing anodization conditions for the growth of titania nanotubes on curved surfaces. *Journal of Physical Chemistry C*, 119(28), 16033-16045.

NOTE:

This publication is included on pages 93 - 109 in the print copy of the thesis held in the University of Adelaide Library.

It is also available online to authorised users at:

<http://dx.doi.org/10.1021/acs.jpcc.5b03383>

## CHAPTER 5

---

# TITANIA NANOTUBE (TNT) IMPLANTS LOADED with PARATHYROID HORMONE (PTH) for POTENTIAL LOCALIZED THERAPY of OSTEOPOROTIC FRACTURES

**Karan Gulati**

School of Chemical Engineering, University of Adelaide South Australia 5005, Australia

**This chapter is based on the following peer-reviewed article:**

**K. Gulati**, M. Kogawa, M. Prideaux, G. J. Atkins, D. M. Findlay, D. Losic. “Titania Nanotube (TNT) Implants Loaded with Parathyroid Hormone (PTH) for Potential Localized Therapy of Osteoporotic Fractures” *Journal of Material Chemistry B*, 2015 (Submitted)

## Statement of Authorship

Title of Paper	Titania nanotube (TNT) implants loaded with parathyroid hormone (PTH) for potential localized therapy of osteoporotic fractures		
Publication Status	<input type="checkbox"/> Published	<input type="checkbox"/> Accepted for Publication	
	<input checked="" type="checkbox"/> Submitted for Publication	<input type="checkbox"/> Publication Style	
Publication Details	<i>Journal of Material Chemistry B</i> , 2015		

### Principal Author

Name of Principal Author (Candidate)	Karan Gulati		
Contribution to the Paper	Under the supervision of D. Losic, D. Findlay and G. Atkins, I developed, designed and performed the experiments, interpreted and processed the data and wrote the manuscript for submission		
Overall percentage (%)	80		
Signature		Date	27 July 2015

### Co-Author Contributions

By signing the Statement of Authorship, each author certifies that:

- i. the candidate's stated contribution to the publication is accurate (as detailed above);
- ii. permission is granted for the candidate to include the publication in the thesis; and
- iii. the sum of all co-author contributions is equal to 100% less the candidate's stated contribution.

Name of Co-Author	Masakazu Kogawa		
Contribution to the Paper	I helped Karan Gulati (candidate) with designing/performing the collagen gel experiment and gene expression studies. I give consent for Karan Gulati to present this paper for examination towards the Doctorate of philosophy.		
Signature		Date	27 July 2015

Name of Co-Author	Matthew Prideaux		
Contribution to the Paper	I helped Karan Gulati (candidate) with designing the experiment, performing the statistical analysis on gene expression and improving the manuscript for submission. I give consent for Karan Gulati to present this paper for examination towards the Doctorate of philosophy.		

Signature		Date	27 July 2015
-----------	--	------	--------------

Name of Co-Author	David Findlay		
Contribution to the Paper	I acted as secondary supervisor for the candidate and aided in development and design of the experiments and evaluation of manuscript for submission. I give consent for Karan Gulati to present this paper for examination towards the Doctorate of philosophy.		
Signature		Date	27 July 2015

Name of Co-Author	Gerald Atkins		
Contribution to the Paper	I acted as external supervisor for the candidate and aided in development and design of the experiments and evaluation of manuscript for submission. I give consent for Karan Gulati to present this paper for examination towards the Doctorate of philosophy.		
Signature		Date	27 July 2015

Name of Co-Author	Dusan Losic		
Contribution to the Paper	I acted as primary supervisor of the candidate and aided in evaluation of experimental design and manuscript for submission. I give consent for Karan Gulati to present this paper for examination towards the Doctorate of philosophy.		
Signature		Date	27 July 2015

Please cut and paste additional co-author panels here as required.





Journal Name

ARTICLE

## Titania nanotube (TNT) implants loaded with parathyroid hormone (PTH) for potential localized therapy of osteoporotic fractures

Received 00th January 20xx,  
Accepted 00th January 20xx

DOI: 10.1039/x0xx00000x

www.rsc.org/

Karan Gulati<sup>a</sup>, Masakazu Kogawa<sup>bt</sup>, Matthew Prideaux<sup>bt</sup>, David M. Findlay<sup>b</sup>, Gerald J. Atkins<sup>b\*</sup> and Dusan Losic<sup>a\*</sup>

Healing of fractures in osteoporotic (OP) bone is problematic because of low bone stock. Here we propose a new strategy for potential treatment of OP fractures, via local delivery of hormones/drugs to the fracture site using the drug releasing fracture-fixation implants. The proposed implants were prepared in the form of small Ti wire/needle with nano-engineered oxide layer composed of array of titania nanotubes (TNTs). The prepared implants loaded with parathyroid hormone (PTH), an approved anabolic therapeutic for the treatment of OP, were inserted into a 3D collagen gel matrix containing human osteoblasts, to study the effect of their local release. Gene expression studies revealed a suppression of *SOST* and an increase in *RANKL* mRNA expression, confirming release of PTH from TNTs and its therapeutic action related to OP and bone fracture healing. The study of bone cell interaction with the surface of TNTs confirmed cellular spread morphology consistent with firm attachment and cell migration. Finally, the mechanical stability of the prepared implants was tested by their insertion into bovine trabecular bone cores *ex-vivo* followed by retrieval; which confirmed robustness of TNTs structure required for real bone implantation and fracture-fixation. This study proved the suitability of the TNT/Ti wire implants for bone therapy and potential enhancement of OP fracture healing.

### 1 Introduction

Osteoporosis (OP) is a pathological condition where the bones become fragile and fracture prone. It is characterized by a loss of bone mineral at a rate, which surpasses new bone formation. Millions of people worldwide are diagnosed with OP and low bone density each year.<sup>1</sup> This number is predicted to increase significantly due to negative life style factors, the increase in life expectancy and the ageing population. Fragility fractures can result in high morbidity or mortality, with mortality rates associated with hip-fractures during the first and the second year post fracture around 30 % and 40 %, respectively.<sup>2</sup> One in three women and one in five men over the age of 50 years are estimated to suffer from OP fracture, which represents a serious health and economic problem.<sup>3</sup>

Severe fractures in OP bone can be difficult to repair, due to insufficient bone stock and sub-optimal healing capacity, and often require prolonged hospitalization and invasive surgery.<sup>4</sup> The principal regulator for calcium metabolism in the human body, parathyroid hormone (PTH), is an approved anabolic therapeutic for the treatment of severe OP.<sup>5</sup> Animal studies and clinical trials have established the role of PTH systemic administration on reducing the OP fracture healing time.<sup>6-7</sup> Limitations associated with systemic administration of PTH include insufficient concentration at the traumatized bone tissue, high costs and poor patient compliance with

daily injections, prompting the development of local drug delivery strategies for PTH treatment of OP fractures.<sup>4</sup> Moreover a local PTH releasing implantable device could also be used to augment bone formation directly at the fracture site. Various attempts to achieve local delivery of PTH based on polymeric beads, co-polymer matrices and CaP coatings on Ti implants have been reported.<sup>8-11</sup> However, complex polymer degradation kinetics and their lack of mechanical support has made the polymeric drug releasing systems unsuitable for the load bearing conditions associated with implant fixation or total joint replacement. Novel biocompatible and osseointegrating implant modifications, with enhanced drug loading and releasing performance are desired to enable effective local therapeutic effect at the fracture site.

Drug-releasing implants based on titania (TiO<sub>2</sub>) nanotubes (TNTs) fabricated by electrochemical anodisation has been regarded as the most promising implant-modification strategy, as it offers many advantages including: tailorable drug loading, controllable drug release abilities (including extended release of several months and externally triggered release), excellent biocompatibility/osseointegration, and ease of surgical implantation.<sup>12-15</sup> This allows for a wide variety of bone implant functions, including localized drug delivery to treat bone-infection, bone inflammation, promote osseointegration, and localized cancer therapy.<sup>14-15</sup> Furthermore, many *in-vivo* investigations have established the suitability of TNTs/Ti as superior titanium bone implant modification, as compared to conventional, micro-rough and nano-rough Ti implant surfaces.<sup>16-17</sup> Moreover successful fabrication of TNTs on various substrate morphologies like curved surfaces (e.g. Ti wires) has enabled easy integration into the current implant technology, three-dimensional drug release inside the bone micro-environment, and also the ability to target complex in-bone conditions.<sup>18-19</sup> To prove the suitability of TNTs drug releasing implants for real medical applications, in our

<sup>a</sup> School of Chemical Engineering, The University of Adelaide, SA 5005 Australia

<sup>b</sup> Discipline of Orthopaedics and Trauma, The University of Adelaide, SA 5005, Australia

† These authors contributed equally to this work

\* Corresponding Authors:

Email: dusan.losic@adelaide.edu.au

Email: gerald.atkins@adelaide.edu.au

Electronic Supplementary Information (ESI) available.

See DOI: 10.1039/x0xx00000x

previous work we demonstrated several of these concepts using *in-vitro* and *ex-vivo* studies to extend/control the drug release for many model drugs (antibiotics, bone proteins, anti-cancer drugs etc.) relevant to bone infections and localized cancer therapy.<sup>20-21</sup> It is surprising that TNTs/Ti implants have not been explored for complex bone therapeutic requirements like in severe fractures of OP bones.

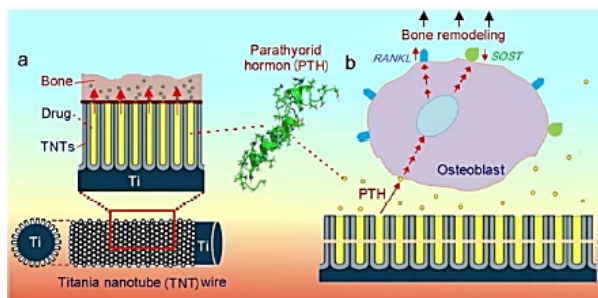


Fig 1. Scheme showing nano-engineered Ti wire implants proposed for osteoporotic fracture therapy (the scale is not real). (a) Structure of titania nanotubes (TNTs) prepared on Ti wires by electrochemical anodisation, loaded with drugs (PTH, parathyroid hormone), and (b) effect of local release of PTH from TNTs on human osteoblast cells embedded in a collagen-gel matrix and the expected genetic expression.

Recent studies have shown that local delivery of PTH directly at the fracture site can address compromised bone healing issues of the OP fractures.<sup>4</sup> To help solve this problem TNT/Ti based implants looks as promising solution for bone fixation or total joint replacement applications (especially in case of OP fractures), providing combined functionalities of drug-releasing and mechanical support.<sup>14,19</sup> In this context, we present this study aimed to explore the application of minimally invasive approach based on TNTs/Ti wire implants loaded with specific anabolic therapeutic for the localized OP treatment. Our approach is presented schematically in Fig. 1 showing the surface of bone fracture-fixation and drug-releasing wire made from Ti with layer of titania nanotubes (TNTs) nanoengineered by electrochemical anodisation process. These TNT/Ti wire implants were loaded with OP relevant drug (PTH) and inserted into a collagen gel matrix containing human osteoblasts cells in order to confirm their localized drug release performance and impact on bone cells. This was achieved by evaluation of genetic expression of *RANKL* (receptor activator of nuclear factor kappa-B ligand) and *SOST* (sclerostin), which can be directly related with the state of bone forming ability of the human osteoblasts. Imaging of the morphology of migrated bone cells onto TNT/Ti wire implants was also performed to show cellular attachment and interaction of bone cells with TNTs surface. Furthermore in order to optimize TNTs for proposed application it is critical to have maximized loading capacity and sustained drug release over a long period. Therefore the second objective of the study was focused on exploring the influence of nanotube dimensions (diameters and lengths) of TNTs on their drug loading capacity. A thin layer of chitosan was coated onto indomethacin (model anti-inflammatory drug) loaded TNTs, as a strategy to improve their drug releasing performance and achieve sustained release. Finally, to determine the ability of the TNT/Ti wire implants to withstand the forces experienced during fracture-fixation procedure, the implants were inserted into bovine trabecular bone core specimens (*ex-vivo*) and the surface morphology of the TNTs was examined. We believe this comprehensive study open new perspectives and valuable contribution toward the application of the TNTs/Ti wires as new fracture-fixation and drug releasing implant for alternative therapy to enhance fracture healing of severely OP bones.

## 2 Experimental

### 2.1 Fabrication of TNTs on Ti wire

High purity titanium wires (0.80 mm) were purchased from Nilaco (Japan). Ethylene glycol, ammonium fluoride (NH<sub>4</sub>F), perchloric acid, butanol, ethanol, and acetone were obtained from Sigma-Aldrich (Sydney, Australia). Ti wires were annealed at 500°C for 2 h. Annealed wires were sonicated in acetone and dried in N<sub>2</sub> prior to the polishing step. Electropolishing was performed in perchloric acid electrolyte (with butanol and ethanol) at 40 V using a special electrochemical setup maintained at 4°C. The wires were cleaned with deionized (DI) water and sonicated in acetone/ethanol. Electrochemical anodisation of the Ti wires was carried out by exposing a specific length of the Ti wire (via masking) to the ethylene glycol electrolyte (with 1 % water and 0.3 % NH<sub>4</sub>F) at 75 V maintained at 25°C.

### 2.2 Loading of parathyroid hormone inside TNTs

For cell studies, 5 mm Ti wire was anodised at 75 V for different times: 10 min (TNT-10) and 20 min (TNT-20). Post anodisation, the wires were sonicated in DI water for > 1 h and later dried in N<sub>2</sub>. Before loading PTH, all implants were sterilized for 1 h using UV irradiation. The TNT implants were then immersed thrice in 200 µl of 50 nM human recombinant PTH1-34 solution (in PBS) for 1 hr each. Controls included empty TNTs (no PTH loaded, only loaded with PBS), and empty TNTs + PTH in media (PBS loaded TNTs and same amount of PTH dispersed in media). TNT-10 and TNT-20 were loaded with 10 µl and 15 µl of the PTH solution, respectively.

### 2.3 SaOS2 3D cell culture

Human osteoblast-like SaOS2 cells (obtained from the American Type Culture Collection) were cultured in  $\alpha$ -MEM with 10% FCS, 10 mM HEPES, 0.2 M L-Glutamine and penicillin/streptomycin (all from Life Technologies) at 37°C with 5% CO<sub>2</sub>. Cells were seeded at a density of 2.5x10<sup>5</sup> in a type1 collagen gel (Cell Matrix, Nitta, Japan) in a 24-well plate (Nunc), as described previously.<sup>43</sup> After 24 h, culture medium was aspirated and TNT implants were inserted into the gel. TNTs (both TNT-10 and TNT-20) preloaded with PTH were inserted through the collagen gel matrix at an angle of approximately 30°. To provide structural support to the collagen gel, the implants were supported by sterilized plastic clips. Controls for the experiment were also similarly placed in the gel matrix: empty TNTs (no PTH, but loaded with same amounts of PBS); and empty TNTs with PTH present in medium, at an identical effective concentration to that present in the corresponding PTH-loaded implants. After implant placement, the media were replaced with differentiation medium ( $\alpha$ -MEM with 10% FCS, 10 mM HEPES, 0.2 M L-Glutamine, penicillin/streptomycin, 50 µg/ml ascorbate-2-phosphate and 1.8 mM potassium dihydrogen phosphate). After 24 h, RNA was harvested from each sample using Trizol reagent (Life Technologies, NY, USA).

### 2.4 Gene expression measurement by RT-PCR

RNA was extracted using the Trizol method, according to the manufacturer's instructions and as described elsewhere.<sup>26</sup> The quantity and quality of the RNA was measured by using NanoDrop spectrophotometer (Thermo Scientific, Waltham, MA, USA). 1 µg of RNA was reverse transcribed into cDNA using the iScript RT kit (BioRad, CA, USA). RT-PCR was performed using SYBR Green Fluor qPCR Mastermix (Qiagen, Limburg, The Netherlands), in a CFX Connect thermocycler (BioRad). Oligonucleotide primers for the amplification of human *SOST* and *RANKL* mRNA were designed in-house and synthesized by Geneworks (Thebarton, SA, Australia), as described elsewhere.<sup>43</sup> Relative gene expression was calculated using 2<sup>-ΔΔCt</sup> method and normalized to the expression of 18S rRNA.<sup>44</sup>

### 2.5 Improving drug loading and releasing performances



5 mm Ti wires were anodised at 75 V for 120 min (TNT-120). To enable substantial drug loading amounts, cleaned TNT implants were immersed in indomethacin solution in ethanol (1% v/v) for 24 h. TNTs were rotated occasionally to ensure even loading inside the TNTs. Later, the implant surface was cleaned gently with soft tissue to remove any surface accumulated drug. Quantification of the drug loading was achieved using thermo-gravimetric analysis (TGA), as described previously.<sup>21</sup> To delay the release of drug, a thin coat of chitosan solution [1% (w/v), chitosan + 0.8 vol. % acetic acid in DI water] was added onto the drug-loaded TNTs using a dip-coating technique. *In-vitro* drug release was performed in phosphate buffer solution (PBS) at pH 7.4 by measuring the absorbance of released drug at 320 nm using UV-Vis spectrophotometer (Cary 60, Agilent Technologies).<sup>21</sup> Briefly, TNTs (drug loaded TNTs and chitosan-coated drug loaded TNTs) were immersed in 5 ml of PBS, and at predetermined time intervals 3 ml aliquots were drawn and transferred to a 3 ml quartz cuvette (10 mm path length, Sterna Scientific, Australia) for absorbance analysis. The drug concentration for the corresponding absorbance values was calculated based on a calibration curve for indomethacin in PBS. Ultimately, the concentration was expressed as weight % released and plotted against time.

### 2.6 *Ex-vivo* bovine trabecular implantation

Trabecular bone cores (10 mm diameter and 5 mm height) were prepared from bovine sternum (harvested from a freshly slaughtered animal), as described previously.<sup>19</sup> Sterility and viability of the bone cores were maintained at all steps. The bone cores were washed in PBS to remove any residual bone marrow, without damaging cells within the bone matrix. Finally, the bone cores consisting of trabecular bone without any cartilage or bone marrow were used to test the mechanical stability of the implants. A hole was drilled into each bone core by using sterilized Kirschner wire (surgical grade stainless steel pin), followed by manual insertion of the TNT implants (TNT-120, anodised at 75 V for 120 min, length 10 mm). This was followed by perfusion of culture media for over 5 days using the Zetos™ bone bioreactor system, as described elsewhere.<sup>19</sup> Later the TNT implants were removed from the bone cores and their surface morphology was examined using SEM.

### 2.7 Surface characterization of TNT implants

Surface morphology of the TNT/Wire implants following their fabrication, after drug loading/drug release, chitosan coating and after implantation in the bovine bone core, was analysed using a field emission scanning electron microscope (FEI Quanta 450). The samples were mounted on a SEM holder with double-sided conductive tape and coated with a 5 nm thick layer of platinum. Images with a range of scan sizes at normal incidence and at a 30° angle were acquired from the top and bottom surfaces and from cross-sections.

### 2.8 Characterization of cellular morphology

SEM fixation of the cells cultured in the collagen matrix setup was also performed. Briefly, the implants (TNT-10 and TNT-20; empty, only loaded with PBS) with cells attached were immersed in glutaraldehyde/paraformaldehyde solution to fix the cells. Later, the cells were washed with PBS buffer (5 min) and treated with 70% and 90% EtOH for 15 min each. Then the surfaces were treated with 100% EtOH for 15 min (x 2 times), followed by immersion in HMDS (hexamethyldisilazane): 100% EtOH [1:1] solution for 10 min. The final treatment involved 100% HMDS solvent for 10 min (x 2 times). Finally the HMDS was removed and the samples were dried, and mounted on SEM holders for imaging.

### 2.9 Statistical analysis

Data analysis was performed using Graphpad Prism (Graphpad, CA, USA). For the purpose of comparing various experimental samples,

a one way analysis of variance (ANOVA) was used with a Bonferroni post-hoc test. a= significantly different to TNT-10 Empty and b= significantly different to TNT-20 Empty (P<0.05).

## 3 Results and Discussion

### 3.1 Characterization of nano-engineered TNT/Ti wire implants

Fig. 2 reveals the changes in surface morphology of the Ti wires during the electrochemical fabrication process and generation of oxide layer with vertically aligned TNTs. The commercially available Ti wires have an extremely micro-rough surface, which makes them unsuitable for anodisation [Fig. 2(a)]. To smoothen the surface [Fig. 2(b)], electropolishing was performed at 40 V for 1 min; followed by anodisation at 75 V for 20 min (TNT-20) to achieve TNTs layer with well-organized and perpendicularly oriented array of nanotubes [Fig. 2(c-d)]. As shown, TNTs cover the entire surface area of the Ti wire, including the top, which is sharpened as resulting from the etching during the electropolishing step [Fig. 2(c)]. The sharp tip of the implant which is uniformly covered with TNTs, can aid in implant insertion and placement inside the traumatized bone. Due to the volume expansion of the anodic film (TNTs) on curved surfaces, cracks occurred as can be observed in Fig. 2(d). However these structural features do not compromise the stability of the anodic film and can allow additional amounts of therapeutics to be loaded as proved in our previous work.<sup>18,19,22</sup> It is also noteworthy to mention here that sharpness/bluntness of the implant tip and the crack width of the anodic layer can easily be tailored, for e.g. by varying electropolishing (etching) and anodisation conditions. High resolution images presented in Fig. 2(e-f) confirms the unique geometry of TNTs structures with open tops and the closed bases which are perfect reservoirs suitable for loading large amount of drugs. The dimensions of TNTs formed for anodisation at 75 V for 20 min (TNT-20) were determined to be 65 ±4.1 nm diameter and 12 ±0.5 µm length.

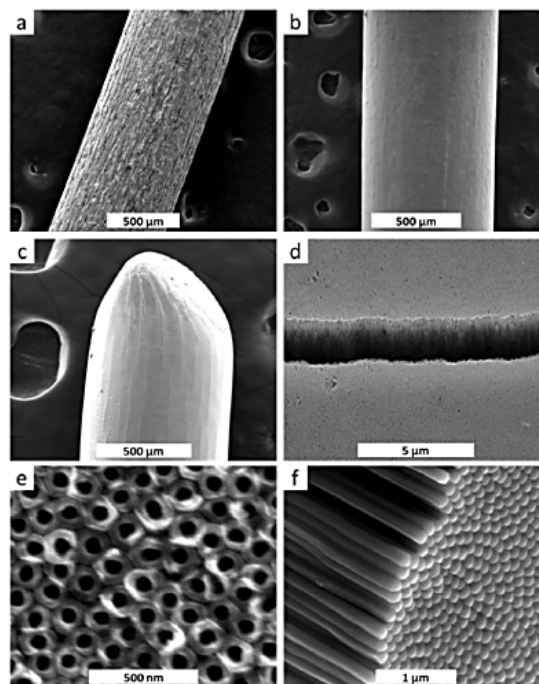




**Fig.2** Scanning electron microscopy (SEM) images showing fabrication of TNTs on Ti wires. (a) Rough surface of commercial Ti wire, (b) smooth surface obtained by electro-polishing process, (c) Ti wire (top) after electrochemical anodisation and formation of TNTs layer, (d) close-up of crack observed on the TNT anodic layer. High-magnification image of TNTs showing: (e) open tops and (f) closed-bottoms. The anodisation for Ti wire presented in this figure was performed at 75 V and 20 min (= TNT-20).

To maintain biologically relevant concentrations in the extracellular space for the required time, important criteria of the drug-releasing implants to be applied for localized drug delivery are to provide sufficient volume for drug loading, and enable their controllable release.<sup>15</sup> Moreover complex bone conditions demand various therapeutic dosages and release profiles to achieve maximum therapeutic effect. In this work a simple strategy to control drug loading capacity by altering the dimensions of TNTs structures by varying anodisation conditions is explored. Previous studies have shown that dimensions of TNTs can be controlled by several anodisation parameters including voltage, current, temperature etc.<sup>20</sup> In Fig. S1 (Supplementary information) we demonstrate that by controlling the time of anodisation we can tailor the dimensions of the TNTs (both diameter and length) on the curved surface of Ti wire. The dimensions of the nanotubes can control the drug loading and release kinetics, as discussed previously and optimization results will be presented in following section.<sup>20</sup> For the various investigations presented here, we used 3 different TNTs/Ti wire implants to demonstrate their suitability for various bone implant applications (summarized in Table S1, Supplementary Information). The motivation behind choosing various TNT/Ti wire implants (with different dimensions of TNTs) is to demonstrate the ability of the nano-engineered implant to be tailored easily, which in turn can cater to various therapeutic requirements and complex conditions.

### 3.2 Therapeutic effect of local release of parathyroid hormone (PTH) on human osteoblasts

To demonstrate the possible application of the nano-engineered implant for localized delivery of PTH to specific bone sites, human osteoblasts were suspended in a 3D collagen gel, into which PTH loaded TNT/Ti wires were inserted [Fig. 1(b)]. The idea here is to enhance bone healing rates for compromised bone conditions such as OP fractures, bypassing the inconvenience and the potential safety concern associated with systemic exposure of bone forming proteins/hormones such as PTH. For this study, Ti wires were anodised at 75 V for 10 min and 20 min (= TNT-10 and TNT-20 respectively) to yield nanotubes with diameters:  $58 \pm 3.2$  nm and  $65 \pm 4.1$  nm; and lengths:  $8 \pm 0.4$  and  $12 \pm 0.5$   $\mu$ m, respectively for TNT-10 and TNT-20, giving the loading volumes for 50 nM PTH solution:  $10.52 \pm 0.16$   $\mu$ l for TNT-10 and  $15.49 \pm 0.27$   $\mu$ l for TNT-20. This will translate into loading of 2.17 and 3.19 ng of PTH in TNT-10 and TNT-20 respectively. Smaller implant size and TNT dimensions were used to load very low but effective amount of PTH to quantify its effect on the bone cells. Moreover *in-vitro* release study of PTH in collagen gel is not performed for two reasons, firstly: the inability of established drug release monitoring techniques to accurately measure very low amount of drugs (in the range of nanograms), and secondly: the design of the experiment where the release of PTH inside the collagen gel matrix can be assumed to be impeded and slow, compared with *in-vitro* release (where PBS medium allow for rapid release). Also the focus of the study is to examine the effect of therapeutic release and hence its uptake on the surrounding bones cells.

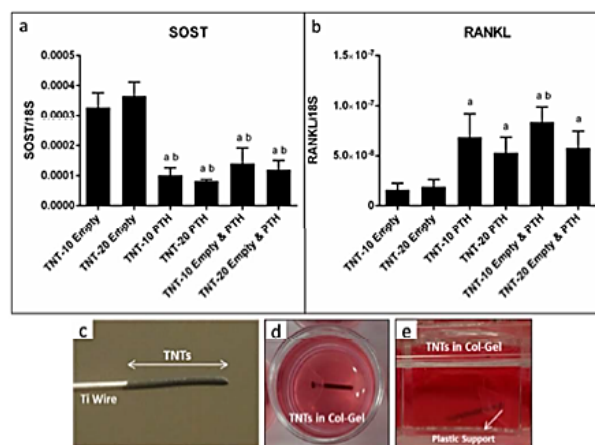


**Fig. 3** Gene expression results for the implantation of TNT/Ti wire pre-loaded with parathyroid hormone (PTH) inside the collagen-gel 3D matrix with osteoblast-like cells: (a) *SOST* and (b) *RANKL* mRNA expression. (c) Photograph of a TNT/Wire implant, (d) top and (e) cross-sectional views of the implant inserted in the collagen gel. Abbreviations used: TNTs: titania nanotubes on Ti wires, PTH: parathyroid hormone, Col-Gel: human osteoblasts embedded in 3D collagen gel, TNT-10: Anodised for 10 min, TNT-20: Anodised for 20 min, TNT (PTH): PTH Loaded TNTs, TNT (Empty) & PTH: Empty TNTs and PTH in Media, a= significantly different to TNT-10 Empty and, b= significantly different to TNT-20 Empty ( $P < 0.05$ ).

Studies have shown that at the cellular level, PTH actively binds to cells of the osteoblast lineage and regulates their differentiation and function.<sup>23</sup> Moreover it has been shown to enhance *RANKL* expression, which promotes osteoclast formation.<sup>24-25</sup> To quantify the effect of local PTH release directly inside the collagen gel matrix, we harvested RNA from the cells and analysed the expression of PTH sensitive genes, *SOST* and *RANKL*.<sup>26</sup> As shown in Fig. 3(a), PTH loaded TNTs significantly reduced *SOST* mRNA expression in the human osteoblasts, consistent with previous reports.<sup>26,27</sup> An increase in *RANKL* mRNA expression [Fig. 3(b)] was also consistent with the action of PTH on osteoblasts.<sup>26</sup> These results demonstrate that sufficient PTH was released from the nanotubes to effectively influence osteoblast gene expression.

Furthermore, these results may translate into enhancement of the bone formation during fracture repair, stimulated by local PTH release from TNTs.<sup>26</sup> Studies have shown that osteocyte-derived *RANKL* is crucial for bone remodelling, which can be related in our study towards enhancing the remodelling of the fractured bone via the localized PTH therapy from the TNT surface.<sup>28-29</sup> We propose that such novel implants can boost fracture healing mechanisms in complex situations like that of OP. More investigations in *ex-vivo* and *in-vivo* settings will further establish this effect, which will be a part of future studies.

### 3.3 Osteoblast migration from collagen gel onto TNTs

Another objective of the study was also to shine light on the possible mode of cellular migration and attachment of the bone cells on the TNT/Ti wire implants, whereby there exists a unique combination of nano-topographical anodic film (TNTs) with micro-scale cracks. SEM imaging was performed to investigate the interaction of osteoblasts with the TNTs. The collagen gel matrix was seeded with human osteoblasts and later pierced with TNT/Ti wire implants and incubated for 24 h. The empty implants samples (no PTH inside TNTs or in media)



were carefully removed from the gel and visualized under SEM to image cells adherent to the implant surfaces. It is also noteworthy to mention here that only empty TNTs' images are shown, as the 24 h time point was insufficient to appropriately study the effect of PTH release on cellular morphology and onset of mineralization.

Results presented in Fig. 4 shows the cellular spread morphology on the underlying cracks on the TNTs layer, which is characteristic of movement and migration. Moreover in the collagen-gel experiment, the bone cells were suspended in the 3D matrix, and their migration onto the TNT implant suggests that these implants can support cell viability and are an attractive surface for cell attachment. Such cellular features with elongated tails confirm that the cells are attracted onto the TNT surfaces and hence migrate from collagen gel matrix. Also the presence of cracks on the anodic film of the Ti wire did not appear to interfere with the cell attachment or migration, as seen in Fig. 5; cells were able to migrate around the cracks. These images also prove that the cracks do not compromise the mechanical stability of the implant and causes no resistance to bone cell migration and attachment.

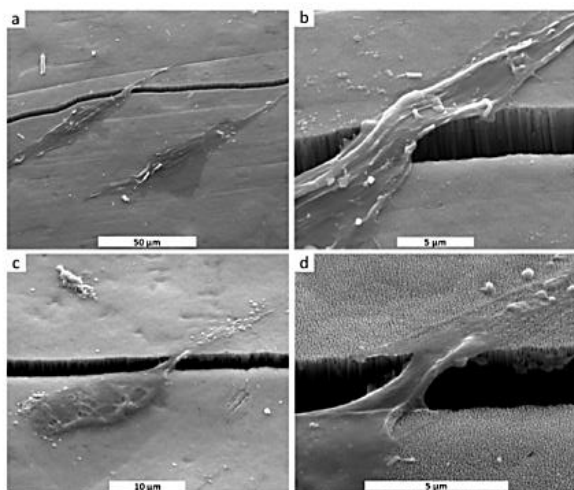


Fig. 4 SEM images showing the cellular morphology of human osteoblasts (consistent with cell movement/migration from collagen gel) on the TNT/Ti wire implants. The TNTs represent empty samples (containing only PBS): (a-b) TNT-10 and (c-d) TNT-20

The recruitment of bone cells also translates towards achieving quicker implant bonding which is very crucial for implant acceptance and survival, and also promotes bone healing rates.<sup>30</sup> Furthermore, studies have shown that when an implant is placed in the tissue inside the patient's body, quicker bone cell attachment ensures to a great extent prevention of any possible bacterial invasion.<sup>31</sup> In fact the cracks on the TNTs did not interfere with cellular movement and attachment, and can act like micro-scale pits for bone ingrowth and exchange of nutrients.<sup>32-34</sup> Moreover, there were no signs of TNT delamination or breakage, showing that the TNTs did not detach into toxic nano-debris. These results showcase the cell-recruiting and adhering nature of the nano-engineered implant, which could further enhance osseointegration of the implant. This clearly shows the well-optimized anodisation conditions utilized to fabricate high-quality and well-adherent anodic films on curved surfaces of Ti wire.

### 3.4 Osteoblast interaction with surface morphology of TNTs

Fig. 5(a-b) shows osteoblasts spreading onto the implant surfaces with clearly visible underlying TNT structures. The cell shape and degree of contact can easily be seen, which confirms firm attachment and anchoring.<sup>35</sup> Cell extensions and filopodial attachments are also seen, which establish that the cells adhere well onto the surface and thereby form firm and close contact with the TNTs. These observations translate into healthy environment of the bioactive TNT/Ti wire for cells to adhere and attach. In an attempt to further shine light on the cellular anchoring on the nanotube modified Ti wire implant, various areas of the implant were scanned. Fig. 5(c-d) shows the high-magnification SEM image of a single bone cell deeply anchored on the TNTs, and its attachment onto the TNTs sidewall via the crack on the anodic film. These stress fibers (SFs) which are the cellular response (in the form of cytoskeleton changes) in response to mechanical stimulation, denotes strong adherence. Reports have also suggested that such cellular extensions also contribute towards cell movement/migration, by attachment and release of such bonds with the implant surface.<sup>36-37</sup> These cell features also mean healthy cell environment for cell differentiation and also mineralization.<sup>30</sup>

It is known that the flexible cell membrane of the osteoblasts changes their shape in accordance with the local environment, and often binds via sub-micron range focal contacts/adhesion.<sup>38</sup> Furthermore, micro-scale cracks in a nanoscale rough anodic film (nanotubes) can significantly increase bone or implant contact area, and can serve towards

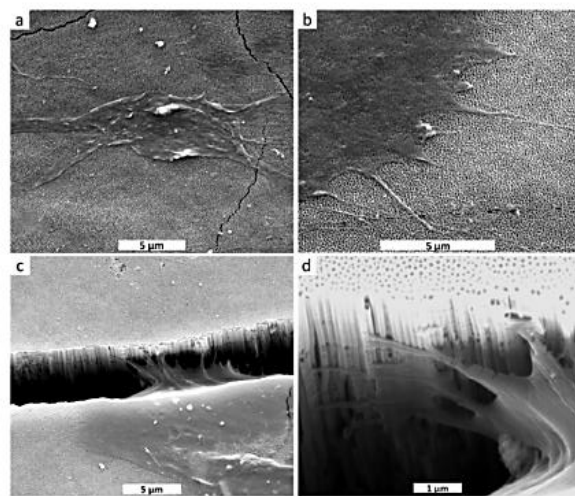


Fig. 5 Top-view SEM images showing osteoblast attachment onto the (a) TNT-10 and, (b) TNT-20 samples after removal from the collagen gel. The nanotubes represent empty samples, containing only PBS. (c-d) High-magnification SEM image of bone cell anchoring onto a crack in the anodic film of the TNT-20 implant.

physical interlocking of the cellular fibers on these surfaces.<sup>32</sup> Such micro-scale cracks on anodic film can also promote osseointegration by bone growth in micro/nano-cavities.<sup>33</sup> Other studies have also shown that micro-scale structures or pits, provide the most appropriate compression/stretching for the osteoblasts' mechanoreceptors, and can also aid in cell migration and nutrient transport.<sup>34</sup> The images presented in Fig. 5 and Fig. 6 also relates with previous reports, which claim that



micro-scale roughness can also augment osteoblast functions like: migration, adhesion, differentiation and matrix secretion.<sup>39</sup>

## 2.5 Enhancing drug loading/releasing abilities of TNT implants

To demonstrate the ability of the TNT wire implants to cater to a wide range of therapeutic requirements relevant to bone conditions such as OP, we performed study with another model drug (indomethacin) exploring strategies for improve drug loading and sustained drug release. Indomethacin which was used as a model hydrophobic drug, belongs to the category of NSAIDs (non-steroidal anti-inflammatory drugs), that help reduce swelling and manage pain, during the inflammatory phase of bone healing and post-implantation surgery.<sup>40</sup> It is also routinely prescribed for the treatment of inflammatory bone diseases, such as osteoarthritis and rheumatoid arthritis.<sup>40</sup> For some applications, to achieve an effective therapeutic effect and also to avoid the potent gastrointestinal side-effects, local release of indomethacin would be desirable.<sup>41</sup> It is also noteworthy to mention here that for bone forming proteins/growth-factors (like PTH), a very low dosage is required locally to enable desired effect; however for managing inflammation or infection, a relatively higher drug amounts for prolonged periods is required to achieve suitable therapeutic effect. The motivation here was to demonstrate the ability of implant to enable loading of substantial drug amounts, so as to effectively target conditions like: infection, inflammation and even cancer, whereby a continuous and prolonged local therapy is required, and failure of achieve this can easily re-trigger bacterial invasion and cancer metastasis.

In order to explore drug amounts, wider/longer TNTs were chosen as presented TNTs were fabricated on Ti wires at 75 V for 120 min (TNT-120), and were  $90 \pm 6.5$  nm in diameter (with wide inter-nanotube gaps) and  $32 \pm 2.8$   $\mu\text{m}$  in length [Fig. 7(a-b)]. TGA (thermo-gravimetric analysis) investigation confirmed a loading of  $320.54 \pm 10.6$   $\mu\text{g}$  of indomethacin in the TNTs. A very high loading amount can be attributed to longer/wider TNTs and was also due to the presence of large cracks on the anodic film and the inter-nanotube distance. The amount of drug loaded can be readily tuned by various anodisation parameters such as voltage/time of anodisation, water content of electrolyte etc., by which the TNT dimensions can be manipulated, as shown in Table S2 (Supplementary Information). We have previously reported that TNT dimensions/structure, drug encapsulation inside polymeric micelles, and biopolymer modification can be applied to enhance drug loading amounts and delay the release kinetics.<sup>20,21,42</sup> Such modifications can further allow advanced drug releasing features, such as loading multiple drugs, triggered and sequential release.<sup>14</sup>

The release of loaded drugs from TNTs is observed to be biphasic, with drug loaded near the open ends of the TNTs released initially (initial burst release or IBR), followed by the drug loaded deep inside TNTs (total release). For unmodified TNTs loaded with indomethacin, in the IBR phase around 74% (237.44  $\mu\text{g}$ ) of the payloads was released [Fig. 6(d)]. Very quick release of large amounts of drugs can cause local tissue toxicity, and can also impair osseointegrating abilities of the implant. Also it means wastage of large amounts of drugs, which for instance in an antibiotic release model could mean re-triggering the bacterial invasion. Beyond IBR, the total release of indomethacin from TNTs lasted for  $\sim 10$  days [Fig. 7(c)]. In an attempt to control very high release amounts due to diffusion gradient, which can cause local tissue toxicity, a thin

layer of biopolymer was coated onto the drug loaded TNTs. We have previously demonstrated the role of biopolymer coating in

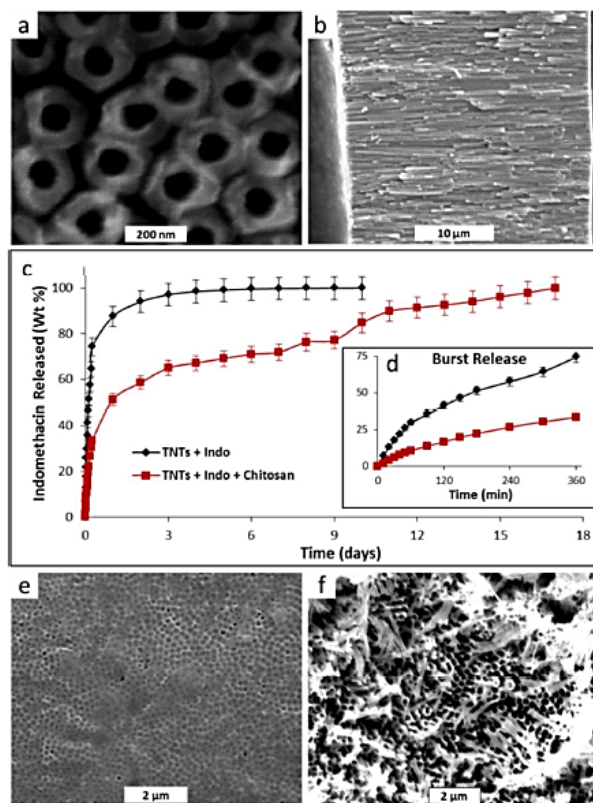


Fig. 6 SEM images showing surface features of the TNT/Ti wires (TNT-120) used for indomethacin (indo) release *in-vitro*. (a) Open pores of TNTs showing gaps between individual nanotubes, and (b) cross-section confirming a length of  $\sim 32$   $\mu\text{m}$ , which allows for very high loading amounts ( $>320$   $\mu\text{g}/\text{implant}$ ). Drug release plots for indo-loaded TNTs: (c) total release and (d) initial burst release (1<sup>st</sup> 6 h). Chitosan coated TNTs: (e) thin coat of chitosan on indo-loaded TNTs (before release experiment), and (d) clear signs of chitosan degradation and visible open pores of TNTs (after completion of the drug release experiment).

delaying release from TNTs fabricated on Flat Ti foil; however in the current study we extended the same technology to TNT/Ti wire implants as they present a more suitable geometry specially towards achieving in-bone therapeutic effect in a uniform 3D fashion.<sup>21</sup> Dip coating of chitosan was performed once and resulted in a very thin coat of chitosan of around  $250 \pm 10.23$  nm. The SEM image in Fig. 6(e) shows the top-view of the chitosan-coated drug-loaded TNTs, with a clear evidence of the underlying TNT structures. As seen from the release plots [Fig. 7(c-d)], chitosan coating of the TNTs reduced the initial burst release (from  $>74$  % to  $< 34$  %) and also delayed the overall release from  $\sim 10$  days to  $>17$  days. While the release of drug from bare TNTs is primarily diffusion based, for TNTs that are coated with polymers such as chitosan, drug release also depends on the degradation/dissolution kinetics of the polymer film.<sup>21</sup> As the polymer degrades the pores are exposed to the surrounding buffer, and the payloads were released as a result of diffusion gradient. Fig. 6(f) shows the top-view of the degraded polymer coating on the implant (after termination of



drug release), with the underlying TNTs clearly visible. Release kinetics can further be tailored by controlling the thickness of the biopolymer film, which has been reported earlier for the TNTs fabricated on flat Ti foil.<sup>21</sup> Table S3 (Supplementary Information) summarizes the various drug release characteristics compared between the two TNT systems: bare TNTs and chitosan-coated TNTs. It is also noteworthy to mention that, the use of chitosan can add further functionalities to TNT implants, due to its inherent anti-bacterial and bone-forming properties.

## 2.6 Ex-vivo bone implantation of TNT/Ti wire implants

For any fracture healing situation, the modified implant surface should not only encourage bone formation and hence the osseointegration, but also should be able to withstand insertion into the bone. Failure or fatigue in such conditions will not only cause the fixation to fail but also the release of debris from the implant surface can cause local tissue toxicity as reported elsewhere.<sup>14</sup> Briefly the marrow-free trabecular bone cores were pierced with stainless steel medical grade pins (Kirschner wire), followed by insertion of the TNT wire implants, and later were perfused with culture media using Zetos bone reactor system for 5 days.<sup>19</sup> After termination of the experiment the implants were removed, which was followed by SEM imaging of the implant surface to check any surface deformities or delamination in the anodic TNT layers. As shown in Fig. 7, the nanotube structures were able to survive bone implantation, without delamination of the TNT layer. This study established the mechanical stability and robustness of the TNT/Ti wire implants suitable for placement inside the traumatized bone via minimal invasive surgery. Such novel implants can sustain the forces experienced during mechanical handling and surgical placement; however ongoing study with *in-vivo* implantation will fully establish the implant suitability and safety.

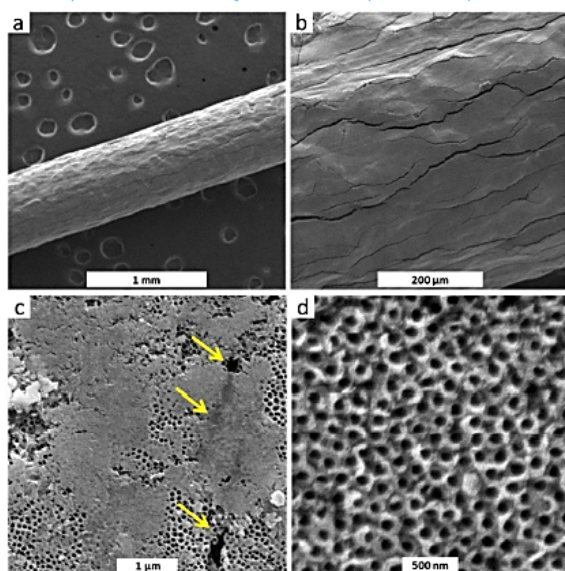


Fig. 7 SEM images of the TNTs after performing the insertion inside the bovine trabecular bone core *ex-vivo*. (a-b) The anodic film is seen stable even for presence of cracks and anodisation performed at 75 V for 120 min (TNT-120), (c) high-magnification image showing TNTs covered with media depositions and possible extracellular secretions from cells (arrows points towards the underlying cracks of the anodic film), and (d) close-up of the TNTs showing stable structure.

To summarize, the investigations presented in this study demonstrated the applicability of the TNTs fabricated on Ti wires as customizable in-bone therapeutic implants. Table S4 (Supplementary information) briefly sums up the various studies carried out using nano-engineered Ti wires, and the inference from the results that suggest its suitability for drug releasing bone implants. To conclude, high-quality, mechanically stable and easy-to-tailor TNTs fabricated on Ti wires, can be applied towards achieving an enhanced therapeutic effect to potentiate localized bone healing, for example in conditions such as fragility fracture in OP patients.

## 4 Conclusions

Present work demonstrated the potential Ti wires with nano-engineered TNTs layer as customizable fracture-fixation wire implants that enable effective therapeutic action and promote bone cell activities. The optimization of anodisation conditions permitted fabrication of high-quality and easy-to-tailor nanotube structures on curved surface of Ti wires, which can enable integration of this technology into current orthopaedic implants. In an attempt to achieve local therapeutic action for complex bone conditions such as osteoporotic fractures, the effect of TNTs loaded with a parathyroid hormone (PTH) on human osteoblastic cells cultured in a 3D collagen-gel matrix was demonstrated. The finding indicated that bone cells respond to the drug released from the TNTs, in this case PTH, which promoted a gene expression profile consistent with previous observations for osteoblast lineage cells. The cellular morphology on the implants confirmed the migration and firm attachment of the cells on the underlying nanotube surface. Furthermore substantial amounts of therapeutics ( $>25 \mu\text{g}/\text{mm}^2$ ) can be loaded inside the TNTs which can be controlled by anodisation conditions using simple parameters like anodisation time. *In-vitro* investigations established that release performances of TNTs/Ti wire implants can be significantly improved in terms of achieving sustained release ( $\sim 3$  weeks) using a thin coat of biopolymer such as chitosan. Also TNT implants inserted inside trabecular bone *ex vivo* retained their structural integrity, indicating their suitability for fracture-fixation *in vivo* application. These results suggest that cost-effective and easy-to-customize TNT/Ti wire implants are suited for various localized bone-therapy applications, such as targeting inflammation/infection and potential fracture-fixation application for treatment of complex bone conditions such as osteoporotic fractures.

## Acknowledgements

The authors acknowledge the financial support of ARC DP 120101680, FT 110100711, and The University of Adelaide. Also acknowledged is the characterization support from Ms Lyn Waterhouse and Mr Ken Neubauer, at The Adelaide Microscopy, The University of Adelaide.

## References

- 1 O. Johnell and J. A. Kanis, *Osteoporos. Int.*, 2006, **17**, 1726.
- 2 A. Franzo, C. Francescutti and G. Simon, *Eur. J. Epidemiol.*, 2005, **20**, 985.
- 3 J. B. Richards, H. F. Zheng and T. D. Spector, *Nat. Rev. Genet.*, 2012, **13**, 576
- 4 L. Kyllönen, M. D'Este, M. Alini and D. Eglin, *Acta Biomater.*, 2015, **11**, 412.
- 5 G. L. Barnes, S. Kakar, S. Vora, E. F. Morgan, L. C. Gerstenfeld and T. A. Einhorn, *J. Bone Joint Surg. Am.*, 2008, **90**, 120.

ARTICLE

Journal Name

- 6 T. T. Andreassen, C. Ejersted and H. Oxlund, *J. Bone Miner. Res.*, 1999, **14**, 960.
- 7 P. Aspenberg, H. K. Genant, T. Johansson, A. J. Nino, K. See, K. Krohn, P. A. García-Hernández, C. P. Recknor, T. A. Einhorn, G. P. Dalsky, B. H. Mitlak, A. Fierlinger and M. C. Lakshmanan, *J. Bone Miner. Res.*, 2010, **25**, 404.
- 8 R. Eswaramoorthy, C. C. Chang, S. C. Wu, G. J. Wang, J. K. Chang and M. L. Ho, *Acta Biomater.*, 2012, **8**, 2254.
- 9 X. Liu, G. J. Pettway, L. K. McCauley and P. X. Ma, *Biomaterials*, 2007, **28**, 4124.
- 10 J. H. Jeon and D. A. Pulco, *Biomaterials*, 2008, **29**, 3591.
- 11 X. Yu, L. Wang, X. Jiang, D. Rowe and M. Wei, *J. Mater. Sci. Mater. Med.*, 2012, **23**, 2177.
- 12 K. C. Papat, M. Eltgroth, T. J. Latempa, C. A. Grimes and T. A. Desai, *Biomaterials*, 2007, **28**, 4880.
- 13 K. C. Papat, L. Leoni, C. A. Grimes and T. A. Desai, *Biomaterials*, 2007, **28**, 3188.
- 14 D. Losic, M. S. Aw, A. Santos, K. Gulati and M. Bariana, *Exp. Op. Drug Deliv.*, 2015, **12**, 103.
- 15 K. Gulati, M. S. Aw, D. Findlay and D. Losic, *Ther. Deliv.*, 2012, **3**, 857.
- 16 L. M. Bjursten, L. Rasmusson, S. Oh, G. C. Smith, K. S. Brammer and S. Jin, *J. Biomed. Mater. Res. A*, 2010, **92A**, 1218.
- 17 C. Von Wilmsky, S. Bauer, R. Lutz, M. Meisel, F. W. Neukam, T. Toyoshima, P. Schmuki, E. Nkenke and K. A. Schlegel, *J. Biomed. Mater. Res. B Appl. Biomater.*, 2009, **89B**, 165.
- 18 K. Gulati, M. S. Aw and D. Losic, *Nanoscale Res. Lett.*, 2011, **6**, 571.
- 19 M. S. Aw, K. A. Khalid, K. Gulati, G. J. Atkins, P. Pivonka, D. M. Findlay and D. Losic, *Int. J. Nanomedicine*, 2012, **7**, 4883.
- 20 M. S. Aw, M. Kurian and D. Losic, *Biomater. Sci.*, 2014, **2**, 10.
- 21 K. Gulati, S. Ramakrishnan, M. S. Aw, G. J. Atkins, D. M. Findlay and D. Losic, *Acta Biomater.*, 2012, **8**, 449.
- 22 K. Gulati, G. J. Atkins, D. M. Findlay and D. Losic, Proc SPIE 8812, Biosensing and Nanomedicine VI, 88120C (September 11, 2013); doi:10.1117/12.2027151.
- 23 A. H. Tashjian and R. F. Gagel, *J. Bone. Miner. Res.*, 2006, **21**, 354.
- 24 J. E. Compston, *Bone*, 2007, **40**, 1447.
- 25 T. Ishizuya, S. Yokose, M. Hori, T. Noda, T. Suda, S. Yoshiki and A. Yamaguchi, *J. Clin. Invest.*, 1997, **99**, 2961.
- 26 M. Prideaux, A. R. Wijenayaka, D. D. Kumarasinghe, R. T. Ormsby, A. Evdokiou, D. M. Findlay and G. J. Atkins, *Calcif. Tissue Int.*, 2014, **95**, 183.
- 27 H. Keller and M. Kneissel, *Bone*, 2005, **37**, 148.
- 28 B. Chalidis, C. Tzioupis, E. Tsiroidis and P. V. Giannoudis, *Exp. Opin. Investig. Drugs*, 2007, **16**, 441.
- 29 T. Nakashima, M. Hayashi, T. Fukunaga, K. Kurata, M. Oh-Hora, J. Q. Feng, L. F. Bonewald, T. Kodama, A. Wutz, E. F. Wagner, J. M. Penninger and H. Takayanagi, *Nat. Med.*, 2011, **17**, 1231.
- 30 K. Anselme, *Biomaterials*, 2000, **21**, 667.
- 31 V. Saini, D. A. Marengi, K. J. Barry, K. S. Fulzele, E. Heiden, X. Liu, C. Dedic, A. Maeda, S. Lotinun, R. Baron and P. D. Pajevic, *J. Biol. Chem.*, 2013, **288**, 20122.
- 32 A. Gristina, *Science*, 1987, **237**, 1588.
- 33 T. Albrektsson and A. Wennerberg, *J. Prosthodont.*, 2004, **17**, 536.
- 34 Y. T. Sul, C. Johansson, E. Byon and T. Albrektsson, *Biomaterials*, 2005, **26**, 6720.
- 35 D. M. Findlay, K. Welldon, G. J. Atkins, D. W. Howie, A. C. Zannettino and D. Boby, *Biomaterials*, 2004, **25**, 2215.
- 36 K. Burrige, *Nature*, 1981, **294**, 691.
- 37 E. Crowley and A. F. Horwitz, *J. Cell Biol.*, 1995, **131**, 525.
- 38 M. J. Dalby, M. O. Riehle, H. Johnstone, S. Affrossman and A. S. Curtis, *Cell Biol. Int.*, 2004, **28**, 229.
- 39 B. D. Boyan, T. W. Hummer, D. D. Dean and Z. Schwartz, *Biomaterials*, 1996, **17**, 137.
- 40 P. A. Elchidana and S. G. Deshpande, *J. Control. Release*, 1999, **59**, 279.
- 41 J. C. Brown, E. J. Klein, C. W. Lewis, B. D. Johnston and P. Cummings, *Ann. Emerg. Med.*, 2003, **42**, 197.
- 42 M. Aw, K. Gulati and D. Losic, *Biomater. Nanobiotechnol.*, 2011, **2**, 477.
- 43 G. J. Atkins, K. J. Welldon, A. R. Wijenayaka, L. F. Bonewald and D. M. Findlay, *Am. J. Physiol. Cell. Physiol.*, 2009, **297**, C1358.
- 44 G. J. Atkins, K. J. Welldon, C. A. Holding, D. R. Haynes, D. W. Howie and D. M. Findlay, *Biomaterials*, 2009, **30**, 3672.



## ***Supplementary Information***

# **Titania nanotube (TNT) implants loaded with parathyroid hormone (PTH) for potential localized therapy of osteoporotic fractures**

Karan Gulati<sup>a</sup>, Masakazu Kogawa<sup>b†</sup>, Matthew Prideaux<sup>b†</sup>, David M. Findlay<sup>b</sup>  
Gerald J. Atkins<sup>b\*</sup> and Dusan Losic<sup>a\*</sup>

<sup>a</sup> *School of Chemical Engineering, The University of Adelaide, SA 5005 Australia*

<sup>b</sup> *Discipline of Orthopaedics and Trauma, The University of Adelaide, SA 5005, Australia*

\*Corresponding Authors

*Prof Dusan Losic*

School of Chemical Engineering,  
The University of Adelaide,  
SA 5005 Australia,  
Phone: +61 8 8013 4648,  
Email: [dusan.losic@adelaide.edu.au](mailto:dusan.losic@adelaide.edu.au)

*Prof Gerald J. Atkins*

Discipline of Orthopaedics and Trauma,  
The University of Adelaide,  
SA 5005, Australia  
Email: [Gerald.Atkins@adelaide.edu.au](mailto:Gerald.Atkins@adelaide.edu.au)

† These authors contributed equally to this work.

**Journal of Materials Chemistry B**

**Table S1**

Summary of the various implants fabricated and the planned OP-fracture relevant investigations carried out. Using varied anodisation conditions different dimensions of the TNTs were fabricated to show the wide range of bone implant applications.

Objective	Implant Study	TNT/Ti Wire	Anodisation Voltage/Time	TNTs' Length/Diameter
Effect of local release of PTH on human bone cells	Gene expression of cells fixed in 3D collagen gel, implanted with PTH-loaded TNTs	TNT-10 and TNT-20	75 V 10 min	8 ±0.4 µm / 58 ±3.2 nm
Cell behaviour on TNTs	Imaging cellular migration/attachment (from collagen gel) onto TNTs		75 V 20 min	12 ±0.5 µm / 65 ±4.1 nm
Enhancing drug loading/releasing performances of TNTs	Chitosan coating on Indo-loaded TNTs	TNT-120	75 V 120 min	32 ±2.8 µm / 90 ±6.5 nm
Stability of TNTs	<i>Ex-vivo</i> trabecular bone core implantation			

**Journal of Materials Chemistry B**

**Table S2**

Variation of drug loading amounts for model drug Indomethacin based on different TNT dimensions of the nano-engineered implant. 5 mm Ti wire (0.8 mm diameter) was anodised at 75 V for various times.

Time of Anodisation (min)	TNT Length ( $\mu\text{m}$ )	TNT Diameter (nm)	Amount of Drug Loaded ( $\mu\text{g}/\text{implant}$ )	Drug Loading Capacity ( $\mu\text{g}/\text{mm}^2$ )
10	8 $\pm$ 0.4	58 $\pm$ 3.2	38.32 $\pm$ 3.4	2.93
20	12 $\pm$ 0.5	65 $\pm$ 4.1	81.45 $\pm$ 5.2	6.24
60	21 $\pm$ 1.7	82 $\pm$ 2.2	188.25 $\pm$ 8.8	14.41
120	32 $\pm$ 2.8	90 $\pm$ 6.5	320.54 $\pm$ 10.6	24.49

**Table S3**

Comparison of drug release characteristics between bare TNTs and chitosan-coated TNTs. 5 mm of Ti wire was anodised at 75 V for 120 min (TNT-120) to demonstrate the ability of the implants to load substantial amounts of therapeutics.

Indomethacin Loaded TNTs	TNTs Only	TNTs + Ch Coating
Amount of Drug Loaded	320.54 $\pm$ 10.6 $\mu\text{g}$ per implant	
Drug Loading Capacity	24.49 $\mu\text{g}/\text{mm}^2$	
Initial Burst Release (1 <sup>st</sup> 6hrs)	74.20 $\pm$ 4 %	33.56 $\pm$ 5 %
	237.44 $\mu\text{g}$	107.39 $\mu\text{g}$
	39.57 $\mu\text{g}/\text{hr}$	17.90 $\mu\text{g}/\text{hr}$
Time for 100% Release	10 days	17 days
Release Rate Total	8.26 $\mu\text{g}/\text{day}$	12.51 $\mu\text{g}/\text{day}$

**Journal of Materials Chemistry B**

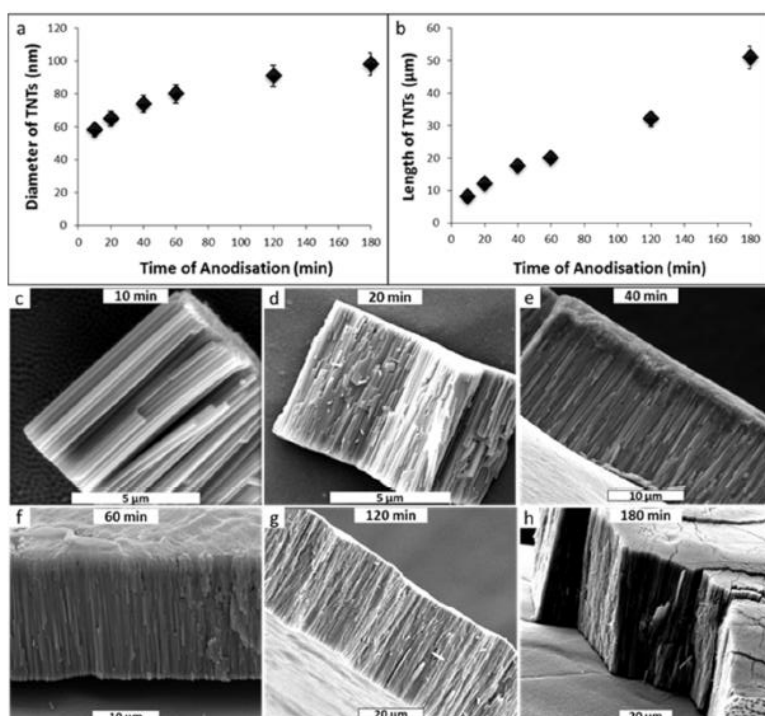
**Table S4**

Summary of the various investigations carried out to prove suitability of the TNT/Ti wire implants to be applied for complex therapeutic requirements like that of a severe osteoporotic fracture.

Study	Parameters Investigated	Inference	Proposed Bone Implant Application
Fabrication of TNTs on Ti wires	Various time of anodisation	Successful fabrication of stable/easy-to-tailor TNTs on curved surface of Ti wire	Easy integration of TNTs into fixation pins, screws, plates etc.
3D Collagen gel experiment	Influence of local release of PTH from TNTs on bone cells	Gene expression indicates improved therapeutic effect	Enhanced fracture fixation for compromised bone conditions like OP
Bone cells' morphology on TNTs	Cellular attachment and anchoring on TNTs	Cells migrate, spread and anchor on the TNT modified implants	Cell viability and non-toxic TNTs
Enhancing drug loading/releasing abilities of TNTs	Biopolymer modification and <i>in-vitro</i> drug release	Reduced initial burst release and delayed total drug release	Ability to cater wide range of therapeutic requirements
<i>Ex-vivo</i> bone implantation of TNTs/Ti wire	Mechanical stability	TNTs structure is not damaged	Ability to withstand forces experienced during implant handling and bone placement

**Journal of Materials Chemistry B**

Figure S1 F Controlling dimensions of nanotubes on Ti wire by time of anodisation: (a-b) increase of diameter and length of TNTs with time, and (c-h) variation in lengths from  $\sim 8 \mu\text{m}$  to  $>50 \mu\text{m}$  for various times. Anodisation was performed at 75 V on 0.80 mm electropolished Ti wire.



## CHAPTER 6

---

# ***IN-SITU* TRANSFORMATION of CHITOSAN FILMS into MICROTUBULAR STRUCTURES: a NEW BIO-INTERFACE for BONE IMPLANTS**

**Karan Gulati**

School of Chemical Engineering, University of Adelaide South Australia 5005, Australia

**This chapter is based on the following peer-reviewed article:**

**K. Gulati, L. Johnson, R. Karunakaran, D. Findlay, D. Losic** “*In-Situ* Transformation of Chitosan Films into Microtubular Structures: A New Bio-Interface for Bone Implants” *Biomacromolecules*, 2015 (Submitted).

## Statement of Authorship

Title of Paper	<i>In-situ</i> transformation of chitosan films into microtubular structures: a new bio-interface for bone implants
Publication Status	<input type="checkbox"/> Published <input type="checkbox"/> Accepted for Publication <input checked="" type="checkbox"/> Submitted for Publication <input type="checkbox"/> Publication Style
Publication Details	<i>Biomacromolecules</i> , 2015

### Principal Author

Name of Principal Author (Candidate)	Karan Gulati		
Contribution to the Paper	Under the supervision of D. Losic and D. Findlay, I developed, designed and performed the experiments, interpreted and processed the data and wrote the manuscript for submission.		
Overall percentage (%)	80		
Signature		Date	27 July 2015

### Co-Author Contributions

By signing the Statement of Authorship, each author certifies that:

- i. the candidate's stated contribution to the publication is accurate (as detailed above);
- ii. permission is granted for the candidate to include the publication in the thesis; and
- iii. the sum of all co-author contributions is equal to 100% less the candidate's stated contribution.

Name of Co-Author	Lucas Johnson		
Contribution to the Paper	I helped Karan Gulati (candidate) with designing the chitosan degradation experiment and improving the discussion of underlying mechanism. I give consent for Karan Gulati to present this paper for examination towards the Doctorate of philosophy.		
Signature		Date	27 July 2015

Name of Co-Author	Ramesh Karunakaran		
Contribution to the Paper	I helped Karan Gulati (candidate) with the synthesis of magnetic nanoparticles and improving the discussion of chitosan transformation into micro-tubes. I give consent for Karan Gulati to present this paper for examination towards the Doctorate of philosophy.		



Signature		Date	27 July 2015
-----------	--	------	--------------

Name of Co-Author	David Findlay		
Contribution to the Paper	I acted as secondary supervisor for the candidate and aided in development and design of the experiments and evaluation of manuscript for submission. I give consent for Karan Gulati to present this paper for examination towards the Doctorate of philosophy.		
Signature		Date	27 July 2015

Name of Co-Author	Dusan Losic		
Contribution to the Paper	I acted as primary supervisor of the candidate and aided in evaluation of experimental design and manuscript for submission. I give consent for Karan Gulati to present this paper for examination towards the Doctorate of philosophy.		
Signature		Date	27 July 2015

Please cut and paste additional co-author panels here as required.



Gulati, K., Johnson, L., Karunagaran, R., Findlay, D. & Losic, D. (2016). In-Situ transformation of chitosan films into microtubular structures on the surface of nanoengineered titanium implants. *Biomacromolecules*, 17(4), 1261-1271.

NOTE:

This publication is included on pages 129 - 163 in the print copy of the thesis held in the University of Adelaide Library.

It is also available online to authorised users at:

<http://dx.doi.org/10.1021/acs.biomac.5b01037>

## CHAPTER 7

---

# CHEMICAL REDUCTION of TITANIA (TiO<sub>2</sub>) into CONDUCTIVE TITANIUM (Ti) NANOTUBES ARRAYS for COMBINED DRUG-DELIVERY and ELECTRICAL STIMULATION THERAPY

**Karan Gulati**

School of Chemical Engineering, University of Adelaide South Australia 5005, Australia

**This chapter is based on the following peer-reviewed article:**

**K. Gulati**, S. Chandrasekaran, N. H. Voelcker, D. M. Findlay, D. Losic “Chemical Reduction of Titania (TiO<sub>2</sub>) into Conductive Titanium (Ti) Nanotubes Arrays for Combined Drug-Delivery and Electrical Stimulation Therapy” *Chemical Communications*, 2015. (Final Stages of Submission)

## Statement of Authorship

Title of Paper	Chemical reduction of titania (TiO <sub>2</sub> ) into conductive titanium (Ti) nanotubes arrays for combined drug-delivery and electrical stimulation therapy
Publication Status	<input type="checkbox"/> Published <input type="checkbox"/> Accepted for Publication <input type="checkbox"/> Submitted for Publication <input checked="" type="checkbox"/> Publication Style
Publication Details	<i>Chemical Communications</i> , 2015

### Principal Author

Name of Principal Author (Candidate)	Karan Gulati		
Contribution to the Paper	Under the supervision of D. Losic, D. Findlay and N. H. Voelcker, I developed, designed and performed the experiments, interpreted and processed the data and wrote the manuscript for submission		
Overall percentage (%)	80		
Signature		Date	30 July 2015

### Co-Author Contributions

By signing the Statement of Authorship, each author certifies that:

- i. the candidate's stated contribution to the publication is accurate (as detailed above);
- ii. permission is granted for the candidate to include the publication in the thesis; and
- iii. the sum of all co-author contributions is equal to 100% less the candidate's stated contribution.

Name of Co-Author	Soundarrajan Chandrasekaran		
Contribution to the Paper	I helped Karan Gulati (candidate) with the magnesiothermic conversion of nanotube implants, and improving the manuscript for submission. I give consent for Karan Gulati to present this paper for examination towards the Doctorate of philosophy.		
Signature		Date	30 July 2015

Name of Co-Author	Nicolas H. Voelcker		
Contribution to the Paper	I acted as external supervisor for the candidate and aided in development and design of the experiments and evaluation of manuscript for submission. I give consent for Karan Gulati to present this paper for examination towards the Doctorate of philosophy.		

Signature		Date	30 July 2015
-----------	--	------	--------------

Name of Co-Author	David Findlay		
Contribution to the Paper	I acted as secondary supervisor for the candidate and aided in development and design of the experiments and evaluation of manuscript for submission. I give consent for Karan Gulati to present this paper for examination towards the Doctorate of philosophy.		
Signature		Date	30 July 2015

Name of Co-Author	Dusan Losic		
Contribution to the Paper	I acted as primary supervisor of the candidate and aided in evaluation of experimental design and manuscript for submission. I give consent for Karan Gulati to present this paper for examination towards the Doctorate of philosophy.		
Signature		Date	30 July 2015



Journal Name

COMMUNICATION

## Chemical reduction of titania (TiO<sub>2</sub>) into conductive titanium (Ti) nanotubes arrays for combined drug-delivery and electrical stimulation therapy

Received 00th January 20xx,  
Accepted 00th January 20xx

DOI: 10.1039/x0xx00000x

www.rsc.org/

Karan Gulati,<sup>a</sup> Soundarrajan Chandrasekaran,<sup>b</sup> Nicolas H. Voelcker,<sup>b</sup> David M. Findlay,<sup>c</sup> and Dusan Losic\*<sup>a</sup>

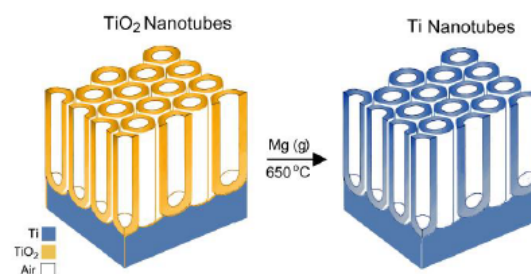
The conversion of titania (TiO<sub>2</sub>) nanotubes into titanium (Ti) while preserving their nanotubular structure is demonstrated. Their application as wire implants for combined local drug delivery and electrical stimulation therapy is proposed.

Electrical stimulation therapy (EST) to treat bone fracture (nonunions and delayed unions) is approved for clinical use, and various *in-vitro* and *in-vivo* studies have established its role in accelerating bone healing.<sup>1</sup> Several EST strategies have been used to administer low level of current (DC), directly to the trauma site using surgical placement of electrodes (cathode at fracture site, and anode at adjacent tissue).<sup>2</sup> It has been reported that this process can induce cellular functions including stimulations of fibroblast activities, Ca influx and increased number of growth factor receptor sites.<sup>1-2</sup> In addition, studies have shown that EST reduce presence of bacteria in wounds, edema formation and improve tissue perfusion causing significant increase in the transcutaneous oxygen pressure.<sup>1-2</sup> Although EST has shown enormous success in clinical applications, there is still a scope for improvement, for instance combination with localized drug delivery (LDD) to provide maximum therapeutic effect. This can be achieved using conductive drug-releasing implants with ability to release desired therapeutics (antibiotics/proteins) inside the traumatized bone, while simultaneously providing electrical stimulation.

Drug-releasing implants based on electrochemically engineered titania (TiO<sub>2</sub>) nanotubes (NTs), which can easily be fabricated on Ti implants of varied geometries, have been extensively explored for addressing various bone therapeutic challenges.<sup>3</sup> Owing to its cost-effective synthesis, improved bioactivity, promoted bone cell functions, ability to load therapeutics, and proven technologies to achieve delayed/triggered release, TiO<sub>2</sub> NTs fabrication have emerged as a very promising bone implant modification strategy.<sup>4</sup> More recently, TiO<sub>2</sub> NTs technology has been extended to Ti wires, pins and needles, and has been proposed as minimally-invasive, 3-

dimensionally therapeutic releasing bone implants.<sup>5-6</sup> These implantable devices have also opened opportunities towards catering multiple challenges simultaneously, for example: fracture fixation and therapeutic release to combat infection/inflammation and compromised bone healing. However, the layer composed of TiO<sub>2</sub> NTs on Ti implants is not conductive, which limits another very attractive option, to combine their drug releasing function with electrical stimulation therapy.

To address these limitations and enable EST while simultaneously delivering active therapeutics locally, inside the micro-environment of the traumatized bone, we present a simple fabrication approach to convert layer of TiO<sub>2</sub> NTs into conducting Ti NTs using Ti wire as a model implant. Our approach is presented in Scheme 1.



Scheme 1 Representation of conversion of TiO<sub>2</sub> nanotubes fabricated on Ti wires, into Ti nanotubes using magnesiothermic reduction process.

The process involves electrochemical anodisation of Ti wires (diameter 0.80 mm, length 5.0 mm) to fabricate oxide layer with array of TiO<sub>2</sub> NTs on the surface. These TiO<sub>2</sub> nanotubes were reduced into Ti using modified magnesiothermic reduction process.<sup>7</sup> The idea is to reduce TiO<sub>2</sub> into Ti while preserving the nanotubular architecture, in order to make conductive Ti wire implants with Ti nanotube arrays on the surface. Structural characterization and elemental analysis was performed to confirm conversion of TiO<sub>2</sub> into Ti, with preserved structures. Conductivity measurements were also performed to prove successful oxide to metal conversion. Finally *in-vitro* drug release studies were carried

<sup>a</sup> School of Chemical Engineering, University of Adelaide, SA 5005 Australia. Email: dusan.losic@adelaide.edu.au

<sup>b</sup> Mawson Institute, University of South Australia, SA 5095, Australia.

<sup>c</sup> Discipline of Orthopaedics and Trauma, University of Adelaide, SA 5005, Australia



out to establish the suitability of the modified implant for proposed fracture healing applications in combination with EST.

Electrochemical anodisation, which represents a cost-effective and scalable technology, was used to fabricate TiO<sub>2</sub> NTs on the surface of electro-polished Ti wire.<sup>5</sup> Using ethylene glycol electrolyte (with 1% v/v water, and 0.3% w/v NH<sub>4</sub>F) in a specially designed electrochemical cell, successful fabrication of high-quality TiO<sub>2</sub> nanotubes on the curved surface of the Ti wire was achieved. This is confirmed by SEM (scanning electron microscopy) characterization showing images with typical structures of nanotube arrays (Fig. 1a). Anodisation condition using 75 V and 20 min, yielded nanotubes with ~ 12 μm length and ~ 65 nm diameter, but their dimensions (diameters, length) could easily be tailored using various anodisation parameters as previously reported.<sup>5</sup>

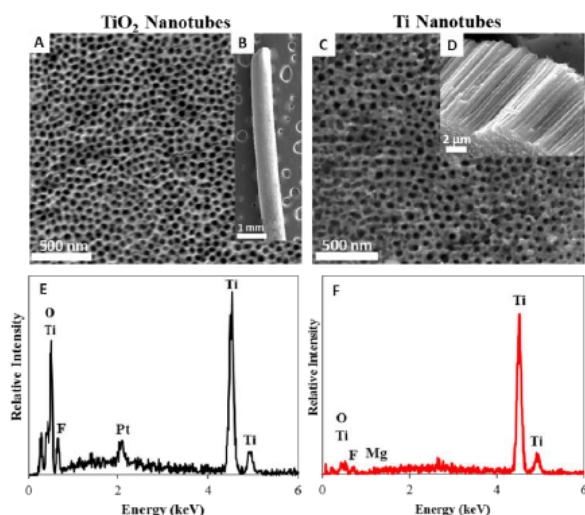


Fig. 1 Conversion of TiO<sub>2</sub> into Ti nanotubes by magnesiothermic reduction process: (a) SEM image showing the top-view of TiO<sub>2</sub> NTs structures [inset (b) TiO<sub>2</sub> NTs wire implant at low magnification], (c) top-view of Ti NTs structures after conversion process. (d) Cross-sectional SEM image showing that Ti nanotubes retain the nanostructural features of TiO<sub>2</sub> nanotubes. (e-f) comparative EDXS analysis for TiO<sub>2</sub> NTs and Ti NTs confirms transformation of oxide into metallic nanotubular layer.

To achieve reduction of TiO<sub>2</sub> layer with nanotube structures into Ti, a modified magnesiothermic reduction process was employed, as described previously.<sup>7</sup> SEM image of the converted Ti NTs presented in Fig. 1c-d, confirms successful transformation of oxide into metallic layer while preserving the nanotube structures. Furthermore, SEM imaging of Ti NTs samples was performed without using any conductive coating and shows no charging effect which proves that sample is conductive.

Comparative EDXS (energy dispersive X-ray spectroscopy) plots of the TiO<sub>2</sub> nanotubular layer, before and after conversion, taken from the cross-section are presented in Fig. 1e-f. Plots for TiO<sub>2</sub> NTs show significant peaks for Ti and O, confirming oxide layer with presence

of F and Pt. It is noteworthy to mention here that F ions, which are present in the anodisation electrolyte, often get incorporated into the nanotube structures. Studies have shown that presence of F ions on implants can significantly improve bone cell functions, which are crucial for bone-implant bonding and bone healing.<sup>8</sup> On the other hand; Pt was used to coat the samples prior to SEM imaging, to make the surface conducting. EDXS graph from Ti NTs (Fig. 1f) shows significant Ti and minor O/Mg peaks. These observations establish successful reduction of TiO<sub>2</sub> into Ti. The presence of small oxygen peak can be explained by re-oxidation of Ti in air after sample preparation. The incorporation of Mg from reduction process is also observed but with minor quantity showing almost successful removal after reduction process. This observation can also be attributed to cracks on the anodic film that occur when anodising curved surface of titanium substrates, which can easily allow for incorporation of Mg/F species.<sup>5</sup> For the unavoidable presence of Mg species into the Ti NTs, the suitability for bone implant applications is not affected, as studies have shown the role of Mg ions in upregulation of bone cell functions.<sup>9</sup>

The comparative X-ray diffraction (XRD) graphs taken from the TiO<sub>2</sub> and Ti NTs presented in Fig. 2a-b, shows clear evidence of successful conversion of TiO<sub>2</sub> into Ti, with stronger presence of Mg in the nanotube structures. Weak signals for Ti are seen for TiO<sub>2</sub> nanotubes, and on the contrary, clear evidence for Ti is seen for converted nanotubes (Ti NTs). Prominent peaks can be seen for Ti and MgO complexes as a result of magnesiothermic process.

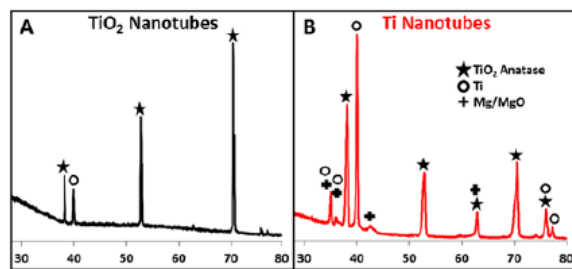


Fig. 2 XRD plots comparing the structural composition between (a) TiO<sub>2</sub> NTs and (b) Ti NTs. Analysis performed based on PDF card numbers 9008517/9002991 and published work.<sup>10</sup> X-axis and y-axis represents 2θ (degrees) and relative intensity respectively.

To confirm if the converted Ti NTs represents a conducting surface suitable for the proposed EST for promoting fracture healing rates, 4-probe conductivity meter was used to measure sheet resistance of Ti and TiO<sub>2</sub> NTs, compared with bare Ti and Cu. The results presented in Fig. 3 reveal very low values of sheet resistance for Ti NTs, which closely matches to conducting control samples: Ti and Cu. However, the resistance of TiO<sub>2</sub> NTs is several orders higher. Since the sheet resistance is inversely related to conductance, it can be confirmed that the non-conducting oxide layer with TiO<sub>2</sub> NTs was successfully converted to conducting Ti NTs. The presented results show that Ti NTs/Ti wire implants can be used as electrodes for EST to stimulate bone cells to upregulate healing mechanisms.

More investigations in this regard will be reported in future, using *ex-vivo* and *in-vivo* models.

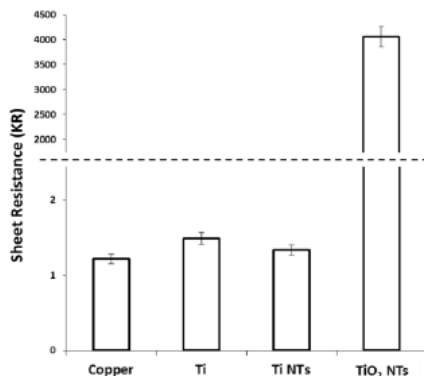


Fig. 3 Sheet resistance of TiO<sub>2</sub> NTs before and after conversion into Ti NTs (Cu and Ti were used as controls). Sheet resistance (Ohm/Sq) values inversely relate to conductance of the material, confirming transformation of non-conducting TiO<sub>2</sub> NTs to conducting Ti NTs.

Finally drug loading and releasing abilities of the Ti NTs/Ti wire implant was demonstrated using hydrophilic dye Rhodamine B (Rh B) as a drug model. Dye is used as simple drug model, however, the 'vacant' nanotubes could be loaded with any drug, protein or growth factor, catering towards specific bone condition, as we have demonstrated with TiO<sub>2</sub> NTs in our previous studies.<sup>4</sup> Thermogravimetric analysis (TGA) confirmed a loading amount of ~80 µg, which is comparable with loading in TiO<sub>2</sub> NTs, showing no changes in drug loading performance after the conversion process. It is worth noting that drug loading could further be controlled by varying immersion times, drug concentration or nanotube dimensions.<sup>4</sup>

The drug release graph from Ti NTs/Ti wire implant is presented in Fig. 4. The graph shows the release of around ~65 µg of model drug (~80% of the total amount loaded) in 1<sup>st</sup> 6 hrs, which is comparable with TiO<sub>2</sub> NTs. This release profile shows considerable burst release caused due to drug present on and near the top of the nanotubes, and inside the cracks of the anodic film. The purpose of this experiment was to show that prepared Ti NTs are functional for drug-releasing applications. However, with further optimizations, advanced features including maximised drug loading, controlled release, and triggered release, which have been demonstrated previously for TiO<sub>2</sub> NTs can also be integrated into Ti NTs systems.<sup>4,12</sup>

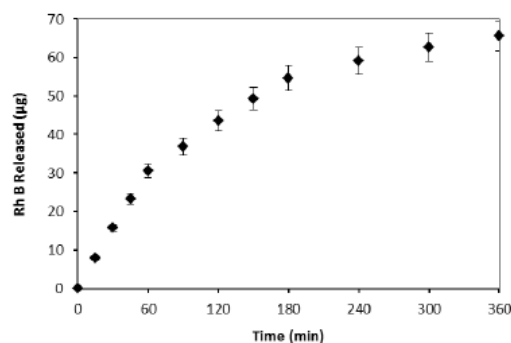


Fig. 4 *In-vitro* release profile of model drug (Rhodamine B) from Ti NTs/Ti wire implants.

Furthermore, to prove that EST process can be achieved from the prepared conducting Ti NTs implants, without affecting the drug releasing abilities, a special *in-vitro* release experiment was performed by applying small DC voltage during release process. Voltage of 10 V for 1 min in cycles with a gap of 10 min at 120 and 300 min time intervals was selected, to monitor any changes in the release behaviour. It is noteworthy to mention here that, any sudden change in release kinetics can adversely affect bone healing, for instance: very high concentration can cause local tissue toxicity, and below optimum dosages could retrigger conditions such as bacterial invasion. The results for electrically-stimulated drug-release showed no difference in the release kinetics of the loaded dye, as compared with the release without any stimulation. This certifies that the drug-releasing and electrically conducting functions can be combined into a single nano-engineered Ti wire implant, and can be applied for EST with localized drug delivery. This solution can address the complex therapeutic needs for instance combating infection while also simultaneously enabling quicker bone healing via electrical stimulation.

In conclusion, this study presents new advances to the TiO<sub>2</sub> nanotubes implant technology, by successfully converting TiO<sub>2</sub> into Ti, while retaining the nanotubular morphology and providing electrical conducting property. The advantage of these new Ti NTs/Ti wire implants is their minimally invasive implantation towards fracture fixation, and use as electrode in electrical stimulation therapy with simultaneous local release of therapeutics. Furthermore, the conducting therapeutic wire implants also qualifies as drug releasing neural prostheses, which can be used to electrically stimulate specific deep lying brain regions to address complications such as: Parkinson' disease.<sup>13</sup>

The support from the University of Adelaide and University of South Australia is gratefully acknowledged.



## Notes and references

**Experimental:** High purity titanium wires (diameter 0.80 mm) were purchased from Nilaco (Japan). Rhodamine B, ethylene glycol, NH<sub>4</sub>F, perchloric acid, butanol, ethanol, and acetone were obtained from Sigma-Aldrich (Sydney, Australia). Ti wires were annealed at 500°C for 2 h, followed by sonication in acetone and drying in N<sub>2</sub>. Electropolishing was performed in perchloric acid electrolyte (with butanol and ethanol, P:B:E = 1:6:9) at 40 V/1 min maintained at 4°C. The wires were cleaned with deionized (DI) water and sonicated in acetone/ethanol. Electrochemical anodisation of the Ti wires was carried out by exposing specific length (5 mm) of the Ti wire (via masking) to the ethylene glycol electrolyte [with 1 % (v/v) water and 0.3 % (w/v) NH<sub>4</sub>F] at 75 V/ 20 min maintained at 25°C.<sup>5</sup>

For magnesiothermic conversion of TiO<sub>2</sub> nanotubes into Ti, Mg and TiO<sub>2</sub> NTs/Ti wire implants were mixed (in the weight ratio of 0.5:1) and placed into tube furnace, which was heated to 650°C at the rate of 10°C/min for 7 h, under argon gas (99.995 %) flow.<sup>7</sup> After cooling down, the contents (Mg and implant) were mixed thoroughly, and the heating procedure was repeated. Afterwards the implants were washed in HCl/HF solutions to remove impurities (MgO and TiO<sub>2</sub>). The cleaned implants (now Ti NTs) were stored in glove box with argon gas (99.997 %).

Surface characterization of the TiO<sub>2</sub> and Ti NTs implants was performed using a field emission scanning electron microscope/SEM (FEI Quanta 450). Furthermore, EDXS of the nanotube samples, at top and cross-sections (after fracturing nanotube membrane) was also performed. XRD spectra of the samples were recorded on a Rigaku Miniflex 600 instrument. Sheet resistance of the nanotubes (TiO<sub>2</sub> and Ti), along with controls of bare Ti and Cu was acquired using 4-point probe conductivity meter (Jandel RM3000).

For loading Rhodamine B (RhB), clean nanotube samples were immersed in RhB solution (50 mg/ml in water) for 2 h, followed by wiping of the excess dye using soft tissue and drying. To quantify the amount of dye loaded inside the nanotubes, the loaded samples were heated to 500°C (at the rate of 10°C/min) in TGA instrument (TA Instruments Q500), followed by analysis of the weight change. Later the Ti NTs samples loaded with RhB were immersed in 5 ml PBS (pH 7.4, 25°C), and at predetermined time intervals 3 ml aliquots were drawn (and replaced with fresh PBS) and the absorbance was measured at 555 nm using Cary 60 spectrophotometer. The drug concentration/weight for the corresponding absorbance values was calculated based on the calibration curve and plotted against time. For electrical stimulation at specific time intervals during *in-vitro* release, Ti NTs (as cathode) and bare Ti wire (immersed in PBS, as anode) were connected to power supply and 10 V was applied for 1 min (3 cycles, separated by 10 min).

1. (a) J. C. Gan and P. A. Glazer, *Eur. Spine J.*, 2006, **15**, 1301; (b) C. Goldstein, S. Sprague and B. A. Petrisor, *J. Orthop. Trauma*, 2010, **24**, 62.
2. (a) R. K. Aaron, D. M. Ciombor and B. J. Simon, *Clin. Orthop.*, 2004, **419**, 21; (b) M. W. Otter, K. J. McLeod and C.T. Rubin, *Clin. Orthop. Relat. Res.*, 1998, **355**, S90.
3. (a) K. C. Popat, M. Eltgroth, T. J. Latempa, C. A. Grimes and T. A. Desai, *Biomaterials*, 2007, **28**, 4880; (b) K. C.

- Popat, L. Leoni, C. A. Grimes and T. A. Desai, *Biomaterials*, 2007, **28**, 3188.
4. (a) D. Losic, M. S. Aw, A. Santos, K. Gulati and M. Bariana, *Exp. Op. Drug Deliv.*, 2015, **12**, 103; (b) K. Gulati, M. S. Aw, D. Findlay and D. Losic, *Ther. Deliv.*, 2012, **3**, 857; (c) A. Santos, M. S. Aw, M. Bariana, T. Kumeria, Y. Wang and D. Losic, *J. Mater. Chem. B*, 2014, **2**, 6157.
  5. K. Gulati; A. Santos; D. Findlay; D. Losic. *J. Phys. Chem. C*, 2015, **119**, 16033.
  6. (a) K. Gulati, M. S. Aw and D. Losic, *Nanoscale Res. Lett.*, 2011, **6**, 571; (b) M. S. Aw, K. A. Khalid, K. Gulati, G. J. Atkins, P. Pivonka, D. M. Findlay and D. Losic, *Int. J. Nanomedicine*, 2012, **7**, 4883; (c) K. Gulati, G. J. Atkins, D. M. Findlay and D. Losic, *Proc SPIE* 8812, 88120C (September 11, 2013); doi:10.1117/12.2027151.
  7. (a) Z. Bao, M. R. Weatherspoon, S. Shian, Y. Cai, P. D. Graham, S. M. Allan, G. Ahmad, M. B. Dickerson, B. C. Church, Z. Kang, H. W. Abernathy Iii, C. J. Summers, M. Liu and K. H. Sandhage, *Nature*, 2007, **446**, 172; (b) S. Chandrasekaran, M. J. Sweetman, K. Kant, W. Skinner, D. Losic, T. Nann and N. H. Voelcker. *Chem. Commun.*, 2014, **50**, 10441.
  8. L. F. Cooper, Y. Zhou, J. Takebe, J. Guo, A. Abron, A. Holmén and J. E. Ellingsen, *Biomaterials*, 2006, **27**, 926.
  9. (a) T Okuma, *Nutrition* 2001, **17**, 679; (b) P. A. Revell, E. Damien, X. S. Zhang, P. Evans and C. R. Howlett. *Key Eng. Mater.*, 2004, **254–256**, 447.
  10. L. Zhao, H. Wang, K.Huo, L. Cui, W. Zhang, H. Ni, Y. Zhang, Z. Wu and P. K. Chu, *Biomaterials*, 2011, **32**, 5706.
  11. K. Gulati, S. Ramakrishnan, M. S. Aw, G. J. Atkins, D. M. Findlay and D. Losic, *Acta Biomater.*, 2012, **8**, 449.
  12. (a) M. S. Aw, M. Kurian and D. Losic, *Biomater Sci.*, 2014, **2**, 10; (b) M. S. Aw, J. Addai-Mensah and D. Losic, *Chem. Commun.*, 2012, **48**, 3348; (c) M. S. Aw, J. Addai-Mensah and D. Losic, *J. Mater. Chem.*, 2012, **22**, 6561; (d) S. Sirivisoot and T. J Webster, *Nanotechnology*, 2008, **19**, 295101.
  13. (a) J. A. Sorkin, S. Hughes, P. Soares and K. C. Popat, *Mater. Sci. Eng. C*, 2015, **49**, 735; (b) K. Gulati, M. S. Aw and D. Losic, *Int. J. Nanomedicine*, 2012, **7**, 2069.



## CHAPTER 8

---

# 3D PRINTED TITANIUM IMPLANTS with COMBINED MICRO PARTICLES and NANOTUBE TOPOGRAPHY PROMOTE INTERACTION with HUMAN OSTEOBLASTS and OSTEOCYTE-LIKE CELLS

**Karan Gulati**

School of Chemical Engineering, University of Adelaide South Australia 5005, Australia

**This chapter is based on the following peer-reviewed article:**

**K. Gulati, M. Kogawa, M. Prideaux L. Lima-Marques, G. J. Atkins, D. M. Findlay, D. Losic** “3D Printed Titanium Implants with Combined Micro Particles and Nanotube Topography Promote Interaction with Human Osteoblasts and Osteocyte-Like Cells” *Biomaterials*, 2015 (Under Review).

## Statement of Authorship

Title of Paper	3D printed titanium implants with combined micro particles and nanotube topography promote interaction with human osteoblasts and osteocyte-like cells
Publication Status	<input type="checkbox"/> Published <input type="checkbox"/> Accepted for Publication <input checked="" type="checkbox"/> Submitted for Publication <input type="checkbox"/> Publication Style
Publication Details	<i>Biomaterials</i> , 2015

### Principal Author

Name of Principal Author (Candidate)	Karan Gulati		
Contribution to the Paper	Under the supervision of D. Losic, D. Findlay and G. Atkins, I developed, designed and performed the experiments, interpreted and processed the data and wrote the manuscript for submission		
Overall percentage (%)	80		
Signature		Date	27 July 2015

### Co-Author Contributions

By signing the Statement of Authorship, each author certifies that:

- i. the candidate's stated contribution to the publication is accurate (as detailed above);
- ii. permission is granted for the candidate to include the publication in the thesis; and
- iii. the sum of all co-author contributions is equal to 100% less the candidate's stated contribution.

Name of Co-Author	Matthew Prideaux		
Contribution to the Paper	I helped Karan Gulati (candidate) with the gene expression studies, performing the statistical analysis and improving the manuscript for submission. I give consent for Karan Gulati to present this paper for examination towards the Doctorate of philosophy.		
Signature		Date	27 July 2015

Name of Co-Author	Masakazu Kogawa		
Contribution to the Paper	I helped Karan Gulati (candidate) with bone cell adhesion studies and fixation of implants for imaging. I give consent for Karan Gulati to present this paper for examination towards the Doctorate of philosophy.		

Signature		Date	27 July 2015
-----------	--	------	--------------

Name of Co-Author	Luis Lima-Marques		
Contribution to the Paper	I helped Karan Gulati (candidate) with 3D printing of the titanium alloy substrates. I give consent for Karan Gulati to present this paper for examination towards the Doctorate of philosophy.		
Signature		Date	27 July 2015

Name of Co-Author	Gerald Atkins		
Contribution to the Paper	I acted as external supervisor for the candidate and aided in development and design of the experiments and evaluation of manuscript for submission. I give consent for Karan Gulati to present this paper for examination towards the Doctorate of philosophy.		
Signature		Date	27 July 2015

Name of Co-Author	David Findlay		
Contribution to the Paper	I acted as secondary supervisor for the candidate and aided in development and design of the experiments and evaluation of manuscript for submission. I give consent for Karan Gulati to present this paper for examination towards the Doctorate of philosophy.		
Signature		Date	27 July 2015

Name of Co-Author	Dusan Losic		
Contribution to the Paper	I acted as primary supervisor of the candidate and aided in evaluation of experimental design and manuscript for submission. I give consent for Karan Gulati to present this paper for examination towards the Doctorate of philosophy.		
Signature		Date	27 July 2015

Please cut and paste additional co-author panels here as required.

**3D printed titanium implants with combined micro particles and nanotube topography promote interaction with human osteoblasts and osteocyte-like cells**

Karan Gulati<sup>1\*</sup>, Matthew Prideaux<sup>2\*</sup>, Masakazu Kogawa<sup>2</sup>, Luis Lima-Marques<sup>3</sup>,

Gerald J. Atkins<sup>2†</sup>, David M. Findlay<sup>2†</sup>, Dusan Losic<sup>1†✉</sup>

<sup>1</sup>School of Chemical Engineering, University of Adelaide, SA, Australia

<sup>2</sup>Discipline of Orthopaedics & Trauma, University of Adelaide, SA, Australia

<sup>3</sup>The Institute for Photonics and Advanced Sensing, University of Adelaide, SA, Australia

\*Equal first author status

†Equal senior author status

✉Corresponding author: Prof. DusanLosic,

School of Chemical Engineering,

The University of Adelaide,

Adelaide, SA5005 Australia,

Phone: +61 8 8013 4648,

Email: *dusan.losic@adelaide.edu.au*

## **Abstract**

The success of material implantation into bone is governed by effective osseointegration, requiring biocompatibility of the material and the attachment and differentiation of osteoblastic cells. To enhance cellular function in response to the implant surface, micro- and nano-scale topography have been suggested as essential. In this study, we present a new bone implants based on 3D-printed titanium alloy (Ti6Al4V), with a unique topography composed of micron sized spherical particles and nano sized cavities with vertically aligned titania nanotubes (TNTs). These new type of implants were prepared by combination of 3-d printing and anodisation processes, which are scalable, simple and low-cost. The osseointegration properties of fabricated implants, examined using human osteoblasts, showed enhanced adhesion of osteoblasts compared to titanium materials commonly used as orthopaedic implants. Gene expression studies at early (day 7) and late (day 21) stages of culture were consistent with the Ti substrates inducing an osteoblast phenotype conducive with effective osseointegration. These implants with the unique combination of micro- and nano-scale topography are proposed as a new generation of multi-functional bone implants, suitable for addressing many orthopaedic challenges including implant rejection, poor osseointegration, inflammation, drug delivery and bone healing.

## **Keywords**

3D printing, titanium, titania nanotubes, bone implants, osteoblast phenotype

## 1. Introduction

Titanium (Ti) and its alloys have been used for many decades as bone implants, mainly due to their corrosion resistance and appropriate biomechanical properties [1]. Besides providing mechanical support and function, a bone implant must also serve as a substrate for various protein and cellular interactions, that determine the extent of bone to implant bonding (osseointegration) and the rate of peri-implant bone healing. As a result, the implant surface, being the first site of contact with the surrounding tissue, plays an important role in determining the fate of the implant. The porosity and pore size of a biomaterial intended for bone implant applications, are important determinants of its osteogenic properties *in vitro* and *in vivo* [2]. The surface chemistry or energy of the implant material also influences the nature of the interaction with bone cells, in particular by the extent to which the material binds extracellular matrix proteins, such as vitronectin and fibronectin, either present in the serum or synthesized by the bone cells themselves [3]. In addition, the surface topography of implant materials influences osteoblast attachment and influences subsequent osteogenesis, thought due in part to bone being a material with natural micro- and nanoscale topographical features. As a result, various surface modification strategies have been utilised to enhance the surface roughness of implant materials, including sand-blasting, acid-etching, plasma reaction and electrochemical anodisation [4]. These approaches render the implant surface micro- to nano-rough, with electrochemical anodisation offering good control over the structural characteristics. In fact *in vitro* and *in vivo* investigations, together with mathematical modelling, have established that micrometer roughness, particularly hemispherical pits (1.5  $\mu\text{m}$  deep and 4  $\mu\text{m}$  wide), provides the optimal surface features to enhance integration with the surrounding tissue [5]. Other studies conclude



that implants having roughened surfaces with irregular morphologies promote high levels of cellular attachment at the bone-implant contact region [6].

A number of reports have shown that nano-scale roughness and topography further improves bone cell interaction compared to micro-scale roughness [7]. Moreover these surface characteristics, which relate to the bioactivity of the implant could also be enhanced by coating with hydroxyapatite (HAP) and biomolecules, such as growth factors [1,4]. A further advancement on Ti implants based on the electrochemical anodisation and the fabrication of self-ordered and bioactive nano-tubular (TNTs) or nano-porous titania structures (TNTs) was achieved [4,8]. Nano-cavity topography with TNTs offer significantly improved characteristics compared to the micro- and nano-rough implant surfaces, including biocompatibility, cell adhesion, and drug loading/release capabilities [1,4,8]. Furthermore, the anodization process permitted close control over the dimensions of the nanotubes by various means, such as time, current, voltage, pH and electrolyte composition, which in turn can modulate the cellular response and the drug loading and release properties [9-11]. Another feature of TNTs fabricated by this process was the presence of fluoride ions, which was shown to enhance bone cell functionality [12]. Cell adhesion also influences cell morphology, the rate of cell proliferation and the extent of differentiation. When bone cells come into contact with the implant surface they firstly attach, adhere and spread, which is influenced by the orientation of the molecules adsorbed onto the implant [3].

Recent advancements in medical implant technology include rapid prototyped or 3D printed implants composed of various polymers, ceramics and metals, which closely mimic the biomechanics of the surrounding tissue [13-17]. Metal counterparts are more suited for load bearing conditions, such as fracture fixation and joint replacement. Using 3D printing to

fabricate Ti implants allows close control over the resulting structural parameters in terms of pore shape, size and number, and the inter-connectedness of the structure as a whole, and this has proved beneficial for osseointegration [18-19].

Based on previous studies showing enhanced bone cell functions on the implants with micro-rough surface and nanotube structures we proposed that their combination could provide further enhancement and create new bone implants with advanced properties. Hence, the aim of this work was to demonstrate a new approach to fabricate these implant with dual micro and nanotopography and explore their interaction with human osteoblasts and osteocyte-like cells compared with conventional implant surfaces. These new Ti implants based on micro-spherical particles and nanotube arrays were fabricated by a combination of 3D printing of Ti and electrochemical anodisation process. The fabrication process and corresponding implant with dual micro (particle) and nano (nanotubes) topography is schematically presented in **Fig. 1**. The 3D printing technology (**Fig. 1a**) was used to fabricate Ti implants (alloy Ti6Al4V) with the desired shape and micro-scale rough surface composed of randomly dispersed spherical microparticles (**Fig. 1b**). These 3D printed implants decorated with micro particles were then electrochemically anodised to generate anodic layer with nano topography composed with vertically aligned titania nanotube (TNTs) or nanopore structures (**Fig. 1d**). The short- and long-term response of human osteoblasts to these prepared implants was compared with other titanium materials commonly used as orthopaedic implants. The cell adhesion in relation to surface topography, morphology and gene expression was evaluated in order to compare the phenotype of osteoblast-like cells on the different Ti substrates and show significant impact of combined micro and nano topography.



## 2. Materials and Methods

### 2.1 3D printing of Ti implants with micro-particle topography

Titanium alloy (Ti6Al4V Grade 5, termed in the text as Ti) in the form of strips (4x4 mm<sup>2</sup>) was printed with a selective laser melting machine: 3D System ProX 200 (Phenix Systems PXM), equipped with 300W Laser (1070 nm at 50% power), in the presence of an Argon atmosphere: (~500 ppm O<sub>2</sub>). The alloy powder material used in the selective laser melting printer has the following particle size distribution characteristics, as measured by a Malvern Mastersizer: D[4,3] = 22.27 μm, D[3,2] = 17.31 μm, D[v,0.9] = 31.32 μm, D[v,0.5] = 24.07 μm, D[v,0.1] = 10.69 μm; where D[4,3] indicates the equivalent spherical volume diameter mean, or the De Broncker mean diameter, D[3,2] is the equivalent surface area mean diameter or the Sauter mean diameter, D[v,0.9] indicates the 90 % of the volume distribution below the value, D[v,0.5] indicates the volume 50% value of the distribution, and D[v,0.1], indicates the 10% of the volume distribution below the value.

A manufacturing layer thickness of 30 μm was achieved by forming a film of powder material, which was then selectively melted using laser, into the required form. This process was repeated to produce the desired number of melted layers, thereby enabling the formation of the three-dimensional object. The printing technology involving selective laser melting resulted in a unique morphology, whereby micro-scale spherical particles of the Ti alloys (of varied dimensions) were randomly arranged onto a flat Ti alloy surface (**Fig. 1**), via adhesion of partially melted or trapped particles onto the Ti surface from the non-melted build material volume. The Ti strips were removed from the build plate, and then thoroughly cleaned by wiping and ultra-sonication in ethanol, to remove any non-adhered spherical particles from the outer surface. The resulting implants are referred to as “Ti 3D” throughout the study.

## *2.2 Fabrication of titania nanotube topography on Ti 3D printed implants*

Ti 3D samples were cleaned using ultra-sonication in acetone and ethanol to remove surface debris, followed by drying in N<sub>2</sub> (Ti 3D samples). TNTs were fabricated using a special electrochemical anodisation setup that permits the generation of an oxide layer with TNTs structures on both sides. The setup involved a counter electrode of Ti flat foil and Ti 3D implant immersed in ethylene glycol electrolyte, containing 1 % water (v/v) and 0.3 % NH<sub>4</sub>F (w/v), maintained at 25 °C, on a magnetic stirrer. A constant voltage of 60 V was applied for 20 min, and current/voltage signals were recorded using a computer-controlled power supply (Agilent) and Labview software (National Instruments, USA) [9]. Post-anodisation, the prepared TNT 3D samples were washed with deionized water and dried in N<sub>2</sub> (TNT 3D Samples).

## *2.3 Preparation of control substrates*

Four comparative model substrates were prepared and investigated as controls in order to evaluate influence of dual topography on cell adhesion and gene expression properties. These substrates include: rough and polished Ti foil (model of clinically used Ti implants), 3D printed Ti alloy (model of micro-particle topography) and TNTs fabricated on Ti foil (model of nanotube topography). Titanium foil (99.6 % purity, thickness 0.25 mm) supplied by Sigma-Aldrich (Sydney, Australia) was used for the preparation of various surface roughness samples and as substrates for TNTs fabrication. Ti foil was cut into a size similar to the Ti 3D samples, and cleaned with acetone and ethanol (Rough Ti Samples). Later, the samples were smoothed using mechanical polishing followed by cleaning with acetone/ethanol (Polished Ti Samples). The electrochemical anodisation was performed using the conditions described above (TNT Ti Samples).

## *2.4 Structural characterization of prepared implants*

Surface morphology characterisation of the prepared samples was performed using a field emission scanning electron microscope (SEM, FEI Quanta 450). The samples were mounted on a SEM holder with double-sided conductive tape and coated with 5 nm thick layer of platinum. Images with a range of scan sizes at normal incidence and at a 30 degree angle were acquired from the top and bottom surfaces and cross-sections.

### *2.5 Cell culture and adhesion*

Human osteoblast-like cells (NHBC) were obtained from a single patient and processed as described previously [20]. Cells were cultured in  $\alpha$ -MEM (Gibco® by Life Technologies™) with 10 % FBS, 0.2 M L-Glutamine and 100  $\mu$ M ascorbate 2-phosphate at 37 °C/5% CO<sub>2</sub> in a humidified incubator [20]. All experiments were performed on 2<sup>nd</sup> passage cells, which were enzymatically removed from culture dishes using collagenase-1 and dispase, and plated onto tissue culture plastic.

Prior to the cell attachment study, all the samples were sterilized using UV irradiation for 30 min on both sides. Each of the samples (in triplicate) was placed in a single well of the 48-well plate followed by the addition of 500  $\mu$ l of the cell suspension containing  $5 \times 10^4$  cells. After 1h, unattached cells were removed by vigorous pipetting with PBS and the remaining cells were stained with crystal violet [21]. The quantification was performed by measuring the optical density (OD) of the cell lysates at 570 nm, which directly corresponds to the number of cells attached onto the sample surface [21].

### *2.6 Characterization of cell morphology on implants by confocal microscopy*

Cell morphology was assessed essentially as previously described, with some modifications [22]. After 24 h of incubation of cells on various surfaces, cells were fixed (4%

w/v paraformaldehyde/PBS, 20 min) and the samples were then blocked with goat serum (2.5% in PBS) for 1h. This was followed by permeabilisation with Triton X-100 (0.5 % in PBS) on ice for 5min and staining with Phalloidin-TRITC (10µg/ml in PBS; Sigma Chemical Co., St. Louis, MO, USA) at room temperature in the dark for 1h. After washing (3x PBS) the cells were incubated with DAPI (4',6-diamidino-2'-phenylindole dihydrochloride) (1µg/ml in methanol; Roche Diagnostics, Castle Hill, NSW, Australia) for 10 min. After washing with PBS (3x) the samples were mounted in glycerol (50 % in PBS) and examined by confocal microscopy (Leica). Images were taken using a water immersion 40x objective (numerical aperture = 1.5). Phalloidin was excited with Green HeNe 543 nm laser line and the emission was viewed through a long pass barrier filter (E570P). The images were analysed using Confocal Assistant software (Todd Clarke Brelje, USA).

### *2.7 SaOS2 cell culture and gene expression studies*

Human osteoblast-like SaOS2 cells (obtained from the American Type Culture Collection) were cultured as previously described [23]. Implants were placed into 12 well plates and SaOS2 cells were seeded at a density of  $2 \times 10^4/\text{cm}^2$  on the surface of the implant. After 24 h, culture medium was removed and replaced with differentiation medium ( $\alpha$ -MEM with 10% FCS, 10 mM HEPES, 0.2 M L-Glutamine, penicillin/streptomycin, 50 µg/ml ascorbate-2-phosphate and 1.8 mM potassium dihydrogen phosphate) [23]. The cells were cultured in differentiation media for up to 21 days, with the media replaced every 3 days. After 7 and 21 days of differentiation, RNA was harvested from the samples using Trizol reagent (Life Technologies, NY, USA), as described elsewhere [23].

The quantity and quality of the RNA was measured by using a NanoDrop spectrophotometer (Thermo Scientific, Waltham, MA, USA). 1 µg of RNA was reverse



transcribed into cDNA using the iScript RT kit (BioRad, CA, USA). RT-PCR was performed using SYBR Green Fluor qPCR Mastermix (Qiagen, Limburg, The Netherlands), in a CFX Connect thermocycler (BioRad). Oligonucleotide primers for the amplification of human *DMPI*, *SOST*, *OCN*, *TNAP*, *RANKL* and *OPG* mRNA were designed in-house and synthesised by Geneworks (Thebarton, SA, Australia), as described elsewhere [22,23]. Relative gene expression was calculated using 2- $\Delta\Delta$ Ct method and normalized to the expression of *18SrRNA* [23].

### *2.8 Characterization of cell morphology on implants using scanning electron microscopy (SEM)*

Cells were fixed after culturing for the times indicated on various implant surfaces for the purpose of imaging using SEM. Briefly, the implants with cells attached were immersed in glutaraldehyde/paraformaldehyde solution to fix the cells. The cells were then washed with PBS buffer (5 min) and then sequentially dehydrated in ethanol (70 %, 90 % EtOH for 15 min each followed by two 15 min washes in 100 % EtOH). Samples were then immersed in hexamethyl disilazane (HMDS):100%EtOH (1:1) solution for 10 min and then twice in 100% HMDS for 10 min. The samples were then air-dried, and mounted on SEM holders as described earlier. Electron dispersive spectroscopy (EDS) analysis of the implants was also performed using SEM to characterise the mineral deposited on the various implant surfaces [24].

### *2.9 Statistical analysis*

Data analysis was performed using Graphpad Prism (Graphpad, CA, USA). For the purpose of comparing various experimental samples, a one way analysis of variance (ANOVA) was used with a Bonferroni post-hoc test.

## **3. Results**

### *3.1 Surface morphology of prepared 3-D Ti implants with dual topography*

The typical morphology of Ti implants with micro-particles topography prepared by 3D printing and characterised by SEM is presented in **Fig. 2**. SEM images show that Ti surface is completely covered by spherical Ti micro-particles of various sizes randomly distributed on the surface (**Fig. 2a-b**). Their arrangement is irregular, with a wide range of sizes for the particles, as depicted in the size distribution plot in **Fig. 2d**. The ‘peak-and-valley’ surface topography, ranging from approximately 5  $\mu\text{m}$  to 20  $\mu\text{m}$  for micro-particles with the inter-particle distance ranging from 1  $\mu\text{m}$  to more than 100  $\mu\text{m}$ . The average diameter of Ti micro particles was estimated to be  $\sim 12$   $\mu\text{m}$ . Most micro-particles, which appeared strongly attached to the underlying Ti surface, were interconnected although some isolated micro-particles were also observed (**Fig. 2b-c**).

The SEM images showing introduction of nanotube topography on 3D printed Ti after anodisation process are summarised in **Fig. 3**. Firstly, these images confirm that micro-particles survived the anodisation process and that the entire surface including micro-particles and the underlying Ti surface were composed of TNTs structures. Characteristic cracks are apparent on the surface of the Ti micro-particles as well as the underlying Ti surface (**Fig. 3a-d**). These cracks arise as a result of radial outgrowth of nanotubes on the curved surfaces of the Ti particles and the irregular/unpolished flat Ti surface. This is consistent with our previous observations on anodising curved surfaces of Ti [25-27]. It is worth noting that these cracks or pits do not compromise the stability of the anodised layer and can be controlled using various anodisation parameters: water content, voltage/time of anodisation, and age of electrolyte. Thus, the printed surface consisted of two distinct features: micro-particles and flat surface, which are both upon by anodization process modified with titania oxide layer composed of TNTs (**Fig. 3c-h**). The

anodisation was performed at 60 V for 20 min, which yielded TNTs with an average diameter of  $32 \pm 4$  nm (on Ti micro-particles) and  $40 \pm 4$  nm (on underlying flat Ti). Open pores TNTs on an irregular micro-scale printed surface is evident from the SEM images (**Fig. 3**). The dimensions of the TNTs can be further tailored using various anodisation parameters, and we have demonstrated the effect of different anodisation times (Supporting Information, **Fig.S1**). Besides Ti 3D (**Fig. 2**) and TNT 3D (**Fig. 3**), alternate Ti surfaces including Ti Rough, Ti Polish (mechanically polished) and TNTs on Flat Ti foil (TNT Ti) were also compared (Supporting Information **Fig. S2**).

### *3.2 Comparative study of osteoblast adhesion on control surfaces*

Osteoblast (NHBC) adhesion assays demonstrated that TNTs fabricated on Ti 3D (TNT 3D) significantly outperformed other Ti surfaces tested (**Fig. 4a**). The closest performance in terms of cell adhesion was TNT Ti, consistent with the significant influence of nanotube topography on cell adhesion. Cell adhesion was found to be: TNT 3D>TNT Ti>Ti 3D >Rough Ti> Polish Ti. Representative SEM images are presented in **Fig. 4b-c** and show osteoblasts spread and focally attached to the various structural features of the TNT 3D implant. Confocal imaging of NHBC after a 24 h incubation on the various substrates also showed cells attaching and spreading on the surfaces. As shown in **Fig. 5** (and in **Fig. S3** and **S4**, Supporting Information) the cell morphology differed greatly on the various surfaces. The cellular spread morphology appeared to correlate with the surface roughness of the samples, with more rapid attachment and spread overall evident for the TNT Ti 3D sample. The comparative images showing morphology of the attached cells on the TNT-modified substrates, TNT 3D and TNT Ti are represented in the high magnification confocal images in **Fig. 5**. On the TNT Ti the cells appear attached in a largely 2D orientation with evidence of dendritic extensions. On the TNT

3D surfaces, stress fibres and focal adhesions are evident, and together with the SEM analysis (**Fig. 4a-b**), this suggests a strong cell anchoring on 3D printed structures interdigitating with the micro-scale Ti particles and with cracks on the anodic film, which is likely to translate into effective osseointegration.

### *3.3 Gene expression in SaOS2 cells cultured on Ti surfaces*

To further investigate the biocompatibility of the TNT modified 3D implants with respect to osteoblast function, we utilised the SaOS2 osteosarcoma cell line, which we have validated as a model for studying human osteoblast differentiation and transition to a mature osteocyte-like stage [23]. Gene expression analysis at early (7 day) and late (21 day) differentiation stages was performed for genes that characterise osteoblast maturity and functionality. After 7 days, the relative expression of the mature osteocyte markers *DMP1* and *SOST* was elevated in cells cultured on TNT 3D compared with the other substrates (**Fig. 6**), suggesting earlier cell differentiation on this substrate. The relative expression of other markers of osteoblast differentiation, *OCN* and *TNAP*, did not differ between substrates. However, the expression of most genes on most substrates tested changed markedly with long-term culture. From day 7 to 21, the expression of *OCN*, *DMP1* and *SOST* mRNA all increased to a similar extent on most substrates, with the exception of Ti TNT, which exhibited altered expression for each of these genes (**Fig. 6**). The expression of the osteoclastogenic inhibitory factor osteoprotegerin (*OPG*) was decreased on TNT 3D, and as a result, the ratio of *RANKL:OPG* mRNA was increased relative to all other substrates tested (**Fig. 7**). Interestingly, the expression of both *RANKL* and *OPG* did not change with time in cells cultured on TNT 3D, whereas the *RANKL:OPG* mRNA ratio increased markedly on all other surfaces (**Fig. 7**), suggesting that TNT 3D may promote a



more stable degree of bone remodelling, which in turn is likely to be more conducive to osseointegration.

### *3.4 Morphological features of SaOS2 cells on implants on day 7 and day 21*

The morphology of SaOS2 cells attached after 7 and 21 days of culture on the TNT-3D implants is shown in **Fig. 8** and **9**, respectively. At 7 days, osteoblastic extensions can be seen between individual micro-particles (**Fig. 8a-b**), and also penetrating into the micro-scale cracks (that occur on the surface of anodised Ti micro-particles) (**Fig. 8c-f**). These observations suggest that the surface topography of the TNT 3D implants, with micro-scale ‘peaks and valleys’, in combination with nanoporous modification (TNTs), creates a surface that promotes firm anchoring of the osteoblasts. Control samples showed an increase in cell number and the appearance of cellular extensions (**Fig. S5**, Supporting Information).

After 21 days of culture, the images presented for the TNT-3D implant in **Fig. 9** indicate an increased number of cells adherent on the implant (as compared to day 7), along with presence of complex filopodial extensions. EDS analysis of chemical composition (**Fig. 9d**) indicates mineralisation of the extracellular matrix on the surface of the implant, with clear peaks observed for Ca and P. The cellular morphology and functions again signify the synergistic action of dual-topography of TNT 3D implants in achieving strong attachment of the osteoblasts, confirming the possible effect of mechanical stimulation.

## **4. Discussion**

Appropriate surface roughness of implants, promotes bone cell functions, including adhesion, proliferation and differentiation, which are considered to be the primary requirements

in order to achieve successful bone implants integration and timely bone healing [1,10,11]. Previous reports have suggested that Ti implants with micro-scale, nano-scale and their combination enhance osteoblastic cell functions [7, 28-39]. The ability to control the dimensions of these structures allows the potential to generate implants with specialised features, such as reduced bacterial attachment and biofilm formation, modulating localised immune responses, as well as bone cell functionality. Some of these parameters are associated with the implant acceptance and survival [4,8]. More rapid bone cell attachment onto the implant surface can reduce bacterial colonisation and reduce risks for the rejection of the implant caused by infection or inflammation [30]. However, the fabrication of these implants with reproducible, micro and nanostructured features to control their physicochemical properties of the structures is challenging.

In order to address the abovementioned challenges we have developed new Ti implants with unique dual micro- and nano-topography composed of micro-particles and titania nanotubes. The implants were prepared using simple, low cost and scalable technologies based on 3D printing and electrochemical allows tailoring the implants with desired shapes (plates, wires, screws etc) at macro scale and specific features on surface with micro to nano-scale (**Fig. 1-3**). Our results showed that 3 D printing technology is successfully used to fabricate Ti alloy with unique topography composed of randomly arranged micro-particles on surface. These micro-particles of various sizes (between 5 - 20  $\mu\text{m}$ ) create a ‘peak and valley’ like surface topography and the vacant spaces in-between them range from approximately 1  $\mu\text{m}$  up to 100  $\mu\text{m}$ . Importantly, the micro-particles were well bonded to the underlying surface. To create a nano-scale surface with nano cavities (TNTs) in combination with the micro-scale with spherical topography, electrochemical anodisation technique was successfully used to generate nanotubes

on these 3D printed Ti substrates. This represents a very cost effective and scalable methodology that could be readily be integrated into the current implant market [4]. The anodisation of micro-particles present on the Ti 3D implant resulted in fabrication of TNTs with cracks in the anodic film, which occurs due to a volume expansion phenomenon of the metal-oxide on the metal surface [4]. Previous studies have indicated that cells tend to elongate or stretch on nanotube surfaces, due mainly to open pores in the TNTs and the inter-nanotube distances [11]. Also, the presence of fluoride ions (from the anodisation electrolyte) in the TNTs may enhance bone cell activity [12]. It is also noteworthy that TNTs have previously demonstrated efficacy for drug loading and release, and that the presence of micro-scale cracks on the TNTs does not compromise the mechanical stability of the implant [25-27]. These cracks can, however, be managed by controlling the anodisation parameters [31]. In the current study, TNT 3D implants showed cracks in the anodic film in the range of 0.5 to 3  $\mu\text{m}$ , which varied even on the same implant surface due to the presence of various sized micro-particles. The unique fabrication technique imparts an extremely irregular implant topography and roughness in the scale between 50 nm and 100  $\mu\text{m}$ , which is 3-dimensional due to the peak and valley-like architecture created by presence of micro-particles.

It is well established that the first contact between cells and the biomaterial is decided by its surface features (including topography, chemistry, surface energy etc.), which significantly influences osteoblastic functions, such as attachment, adhesion and spreading [3]. This in turn influences the ability of cells to proliferate and differentiate in contact with the implant. A lack of osseointegration may lead to impaired bonding and implant loosening, which is one of the most common causes of implant failure [4]. This issue is potentially more challenging in conditions such as osteoporotic fractures, diabetic patients and other bone ailments [1-2]. Also, it

has been reported that nano-scale roughness, particularly nano-tubular/porous morphologies, promotes osseointegration in comparison to bare or micro-rough surfaces [7]. Our findings of superior osteoblast adhesion to TNT Ti 3D and TNT Ti surfaces compared to the underivatized Ti are consistent with previous studies indicating improved osseointegration imparted by TNTs surfaces [32-34]. With this desirable surface topography enhanced bioactivity, and ability to load drugs (proteins, antibiotics, anti-inflammatory drugs) by inside the TNTs, make these new implant applicable to implant scenarios where, for example, faster bone healing or preventing inflammation or bone infection is needed [4].

When bone cells come in contact with the implant surface they firstly attach and spread, depending upon the orientation of the adsorbed molecules on the implant [3]. Other factors that influence osteoblast activity include mechanical stimulation [3]. Morphological analysis of attached cells on all Ti surfaces indicated an elongated fibroblastic appearance, similar to osteoblastic cells cultured on tissue culture plastic (**Fig. S3** and **S4**, Supporting Information) [20]. However, differences were observed between TNT 3D and TNT Ti samples, with respect to cell shape, the degree of contact with the surface and contact guidance. Cells on TNT Ti 3D surfaces showed many complex filopodia-like extensions and formed close contact with the various surface features. For TNTs 3D, stress fibres, which are cytoskeletal responses to mechanical stimulation, could also be seen, signifying the force-generating nature of the unique micro and nano topography of Ti particles [35]. Reports indicate that such stress fibres denote strong adherence, which can contribute towards cell migration by creating the force required to release the cell tail and move the rear forward [36-37].

The extracellular matrix (ECM), which consists of a variety of interacting molecular assemblies, creates a local micro-environment nurturing for proper cellular functioning and



anchorage [38]. Furthermore, attachment of osteoblasts to the ECM induces mechanical forces and the cells respond to it by developing isometric tensions (resulting in stressed cell matrices), which have been demonstrated to enhance cell proliferation in comparison to unstressed cells [39]. This effect in turn influences cellular architecture and modulates gene expression [40]. Analysis of TNT 3D surfaces after long-term SaOS2 culture revealed extensive osteoblast interactions via cytoplasmic protrusions and filopodial attachments to ECM (**Fig. 8** and **Fig 9**). This observation is in accord with studies showing that complex topographies in micro-scale enable induction and regulation of specific integrin sub-units present on the osteoblast cell surface [41]. On the other hand, cell-to-biomaterial interactions occur at the nano-scale, and the nano-topography of the implant can modulate osteoblast morphology and differentiation state [42].

Gene expression analysis revealed an early increase in the *RANKL:OPG* mRNA ratio in SaOS2 cells cultured on TNT 3D, driven by suppressed OPG expression, relative to the other materials tested. This, however, did not increase further with long-term culture, whereas a marked increase in the expression of this ratio occurred in the other samples. The ratio of *RANKL* to *OPG* expression by the osteoblast/osteocyte determines its capacity to support bone resorption [43]. It is now well accepted that bone resorbing osteoclasts also provide critical signals that stimulate osteoblastic bone formation [44]. For this reason, it is likely that some osteoclastic activity is desirable for osseointegration to occur. Monjo and colleagues demonstrated a positive correlation between the osteoclastic reorption markers *TRAP*, calcitonin receptor and  $H^+$ -ATPase and pull-out strength in a rabbit osseointegration model [45]. Interestingly, many studies have shown that well-known osteoclast inhibitors, the bisphosphonates, improve osseointegration [46]. However, some of this effect is likely due to an

independent osteogenic effect of these agents and may not be due simply to inhibition of osteoclast formation [47]. Indeed, in many instances inhibition of osteoclastogenesis may be incomplete [48]. While the significance of changes in the *RANKL:OPG* mRNA ratio observed in this study are not yet fully understood, it is plausible that a sustained and steady bone remodelling response as seen in TNT 3D cultures is compatible with osseointegration in the face of superior osteoblast adhesion and differentiation.

Of the numerous studies to date that have considered responses of osteoblasts to implant materials, few have considered those of osteocytes, despite these cells being the predominant bone cell type and being critical for controlling bone metabolism [49-50]. A recent study by Du and colleagues demonstrated the close contact between Ti and osteocyte processes in a dental implant model [51]. The SaOS2 model used in this study is useful in this regard as it provides a human-relevant osteoblast-osteocyte transition model [23]. The expression of the genes *OCN*, *SOST* and *DMP1* are associated with osteocyte differentiation. In this study, early increases in the levels of *SOST* and *DMP1* mRNA were observed on TNT 3D implants, suggestive of enhanced osteocyte differentiation. The expression of *SOST* increased during the 21 day culture period to a similar extent on all substrates, although to a significantly lesser extent on TNT Ti. Likewise, *DMP1* and *OCN* expression increased similarly on most substrates. Overall, these data indicate the biocompatibility of Ti-based implants in being permissive of osteoblast differentiation through to the mature osteocyte stage. It will be of interest in future studies to examine the responsiveness of established osteocytes to drugs and other osteotropic compounds deliverable by virtue of TNTs [4].

## **5. Conclusion**

The current study shows that a unique combination of micro-scale and nano-topography achieved by electrochemical anodisation of 3D printed Ti implants provides an outstanding cell adhesion substrate for human osteoblastic cells and promotes an osteogenic gene expression profile. The 3D printed Ti alloy produced irregular micro-scale topography due to the presence of micro-particles randomly arranged on a flat substrate. The titania nanotubes (TNTs) were generated by anodisation process on 3-D printed Ti surface including micro-particle which enabled additional ‘nano-topography’, while preserving the micro-particle arrangement. The resultant implant surface with dual topography: micro-scale with 3D printed irregular micro-spherical particles and nanoscale with titania nanotubes (stable, easy-to-tailor), was compared with control Ti substrates (smooth, micro-rough, micro-particles and TNTs) for osteoblastic functions. Enhanced bone cell function based on cellular adhesion and biocompatibility of the TNTs 3D implant surfaces were observed. Furthermore, this approach allows printing of specific implant geometries to meet custom surgical needs, coupled with the ability to load and locally-release active therapeutics. We propose that such custom-printed TNTs 3D implants combined with their drug-releasing capabilities and localized drug delivery can address multiple challenges of bone implants.

### **Acknowledgements**

The authors acknowledge the financial support of ARC DP 120101680, FT 110100711, and The University of Adelaide. This work was performed in part at the OptoFab node of the Australian National Fabrication Facility utilizing Commonwealth and SA State Government funding. Also acknowledged is the characterization support from Ms Lyn Waterhouse, Dr. Agatha Labrinidis and Mr Ken Neubauer, at The Adelaide Microscopy, The University of Adelaide.



## Supporting Information

Supporting Information is available from the Elsevier Online Library or from the author.

## References

1. K.C. Popat, L. Leoni, C.A. Grimes, T.A. Desai, Influence of engineered titania nanotubular surfaces on bone cells, *Biomaterials* 28 (2007) 3188-3197.
2. V. Karageorgiou, D. Kaplan, Porosity of 3D biomaterial scaffolds and osteogenesis, *Biomaterials* 26 (2005) 5474–5491.
3. K. Anselme, Osteoblast adhesion on biomaterials, *Biomaterials* 21 (2000) 667-681.
4. D. Losic, M.S. Aw, A. Santos, K. Gulati, M. Bariana, Titania nanotube arrays for local drug delivery: Recent advances and perspectives, *Expert Opin. Drug Deliv.* 12 (2015) 103-127.
5. S. Bauer, P. Schmuki, K. Von Der Mark, J. Park, Engineering biocompatible implant surfaces: Part I: Materials and surfaces, *Prog. Mater. Sci.* 58 (2013) 261-326.
6. K.T. Bowers, J.C. Keller, B.A. Randolph, D.G. Wick, C.M. Michaels, Optimization of surfaces morphology for enhanced osteoblast responses in vitro, *Int. J. Oral Maxillofac. Implants* 7 (1992) 307–310.
7. T.J. Webster, J.U. Ejiogor, Increased osteoblast adhesion on nanophase metals: Ti, Ti6Al4V, and CoCrMo, *Biomaterials* 25 (2004) 4731-4739.
8. K. Gulati, M.S. Aw, D. Findlay, D. Losic, Local drug delivery to the bone by drug-releasing implants: Perspectives of nano-engineered titania nanotube arrays, *Ther. Deliv.* 3 (2012) 857-873.

9. K. Gulati, S. Ramakrishnan, M.S. Aw, G.J. Atkins, D.M. Findlay, D. Losic, Biocompatible polymer coating of titania nanotube arrays for improved drug elution and osteoblast adhesion, *Acta Biomater.* 8 (2012) 449-456.
10. K.C. Popat, M. Eltgroth, T.J. Latempa, C.A. Grimes, T.A. Desai, Decreased staphylococcus epidermis adhesion and increased osteoblast functionality on antibiotic-loaded titania nanotubes, *Biomaterials* 28 (2007) 4880-4888.
11. N. Wang, H. Li, W. Lü, J. Li, J. Wang, Z. Zhang, Y. Liu, Effects of TiO<sub>2</sub> nanotubes with different diameters on gene expression and osseointegration of implants in minipigs, *Biomaterials* 32 (2011) 6900-6911.
12. L.F. Cooper, Y. Zhou, J. Takebe, J. Guo, A. Abron, A. Holmén, J.E. Ellingsen, Fluoride modification effects on osteoblast behavior and bone formation at TiO<sub>2</sub> grit-blasted c.p. titanium endosseous implants, *Biomaterials* 27 (2006) 926–936.
13. G.E. Ryan, A.S. Pandit, D.P. Apatsidis, Porous titanium scaffolds fabricated using a rapid prototyping and powder metallurgy technique, *Biomaterials* 29 (2008) 3625–3635.
14. A. Cheng, A. Humayun, D.J. Cohen, B.D. Boyan, Z. Schwartz, Additively manufactured 3D porous Ti-6Al-4V constructs mimic trabecular bone structure and regulate osteoblast proliferation, differentiation and local factor production in a porosity and surface roughness dependent manner, *Biofabrication* 6 (2014) 045007-18.
15. Y. Xiong, C. Qian, J. Sun, Fabrication of porous titanium implants by three-dimensional printing and sintering at different temperatures, *Dent. Mater. J.* 31 (2012) 815–820.
16. F.C. Fierz, F. Beckmann, M. Huser, S.H. Irsen, B. Leukers, F. Witte, Ö. Degistirici, A. Andronache, M. Thie, B. Müller, The morphology of anisotropic 3D-printed hydroxyapatite scaffolds, *Biomaterials* 29 (2008) 3799–3806.

17. U. Gbureck, E. Vorndran, F.A. Müller, J.E. Barralet, Low temperature direct 3D printed bioceramics and biocomposites as drug release matrices, *J. Control. Release* 122 (2007) 173–180.
18. M.A. Lopez-Heredia, E. Goyenvalle, E. Aguado, P. Pilet, C. Leroux, M. Dorget, P. Weiss, P. Layrolle, Bone growth in rapid prototyped porous titanium implants, *J. Biomed. Mater. Res. A* 85A (2008) 664–673.
19. S. Maleksaeedi, J.K. Wang, A. El-Hajje, L. Harb, V. Guneta, Z. He, F.E. Wiria, C. Choong, A.J. Ruys, Toward 3D printed bioactive titanium scaffolds with bimodal pore size distribution for bone ingrowth, *Procedia CIRP* 5 (2013) 158 – 163.
20. D.M. Findlay, K. Welldon, G.J. Atkins, D.W. Howie, A.C.W. Zannettino, D. Bobyn, The proliferation and phenotypic expression of human osteoblasts on tantalum metal, *Biomaterials* 25 (2004) 2215–2227.
21. S. Gronthos, A.C.W. Zannettino, S.E. Graves, S. Ohta, S.J. Hay, P.J. Simmons, Differential cell surface expression of the STRO-1 and alkaline phosphatase antigens on discrete developmental stages in primary cultures of human bone cells, *J. Bone Miner. Res.* 14 (1999) 47–56.
22. A. Evdokiou, S. Bouralexis, G.J. Atkins, F. Chai, S. Hay, M. Clayer, D.M. Findlay, Chemotherapeutic agents sensitize osteogenic sarcoma cells, but not normal human bone cells, to Apo2L/ TRAIL-induced apoptosis, *Int. J. Cancer* 99 (2002) 491–504.
23. G.J. Atkins, K.J. Welldon, A.R. Wijenayaka, L.F. Bonewald, D.M. Findlay, Vitamin K promotes mineralization, osteoblast-to-osteocyte transition, and an anticatabolic phenotype by  $\gamma$  carboxylation-dependent and -independent mechanisms, *Am. J. Physiol. Cell. Physiol.* 297 (2009) C1358-67.

24. M. Prideaux, A.R. Wijenayaka, D.D. Kumarasinghe, R.T. Ormsby, A. Evdokiou, D.M. Findlay, G.J. Atkins, SaOS2 Osteosarcoma Cells as an In Vitro Model for Studying the Transition of Human Osteoblasts to Osteocytes, *Calcif. Tissue Int.* 95 (2014) 183-193.
25. K. Gulati, M.S. Aw, D. Losic, Drug-eluting Ti wires with titania nanotube arrays for bone fixation and reduced bone infection, *Nanoscale Res. Lett.* 6 (2011) 571-6.
26. M.S. Aw, K.A. Khalid, K. Gulati, G.J. Atkins, P. Pivonka, D.M. Findlay, D. Losic, Characterization of drug-release kinetics in trabecular bone from titania nanotube implants, *Int. J. Nanomedicine*, 7 (2012) 4883–4892.
27. K. Vasilev, Z. Poh, K. Kant, J. Chan, A. Michelmore, D. Losic, Tailoring the surface functionalities of titania nanotube arrays, *Biomaterials*, 31 (2010), 532-540
28. G. Mendonça, D.B. Mendonça, L.G. Simões, A.L. Araújo, E.R. Leite, W.R. Duarte, F.J. Aragão, L.F. Cooper, The effects of implant surface nanoscale features on osteoblast specific gene expression, *Biomaterials* 30 (2009) 4053-62.
29. L. Bren, L. English, J. Fogarty, R. Policoro, A. Zsidi, J. Vance, J. Drelich, C. White, S. Donahue, N. Istephanous, K. Rohly, Effect of surface characteristics of metallic biomaterials on interaction with osteoblast cells, *Proc. 7th World Biomaterials Congress* (2004). Page 1121.
30. A. Gristina, Biomaterial-centered infection: Microbial adhesion versus tissue integration, *Science* 237 (1987) 1588-1595.
31. K. Gulati, A. Santos, D. Findlay, D. Losic, Optimizing Anodization Conditions for the Growth of Titania Nanotubes on Curved Surfaces, *J. Phy. Chem. C* (2015) DOI: 10.1021/acs.jpcc.5b03383

32. L.M. Bjursten, L. Rasmusson, S. Oh, G.C. Smith, K.S. Brammer, S. Jin, Titanium dioxide nanotubes enhance bone bonding in vivo, *J. Biomed. Mater. Res. A*, 92A (2010) 1218-1224.
33. C. Von Wilmsky, S. Bauer, R. Lutz, M. Meisel, F.W. Neukam, T. Toyoshima, P. Schmuki, E. Nkenke, K.A. Schlegel, In vivo evaluation of anodic tio<sub>2</sub> nanotubes: An experimental study in the pig, *J. Biomed. Mater. Res. B Appl. Biomater.* 89B (2009) 165-171.
34. S. Oh, S. Jin, Titanium oxide nanotubes with controlled morphology for enhanced bone growth, *Mater. Sci. Eng. C* 26 (2006) 1301-1306.
35. K. Burrige, E.S. Wittchen, The tension mounts: Stress fibers as force-generating mechanotransducers, *J. Cell Biol.* 200 (2013) 9–19.
36. K. Burrige, Are stress fibres contractile? *Nature* 294 (1981) 691–692.
37. E. Crowley, A.F. Horwitz, Tyrosine phosphorylation and cytoskeletal tension regulate the release of fibroblast adhesions, *J. Cell Biol.* 131 (1995) 525–537.
38. B. Geiger, A. Bershadsky, R. Pankov, K.M. Yamada, Transmembrane extracellular matrix—cytoskeleton crosstalk, *Nat. Rev. Mol. Cell Biol.* 2 (2001) 793–805.
39. E. Cukierman, R. Pankov, K.M. Yamada, Cell interactions with three-dimensional matrices, *Curr. Opin. Cell Biol.* 14 (2002) 633–639.
40. M.A. Wozniak, K. Modzelewska, L. Kwong, P.J. Keely, Focal adhesion regulation of cell behavior, *Biochim. Biophys. Acta*, 1692 (2004) 103-119.
41. L. Feller, Y. Jadwat, R.A.G. Khammissa, R.Meyerov, I.Schechter, J. Lemmer, Cellular Responses Evoked by Different Surface Characteristics of Intraosseous Titanium Implants, *Biomed. Res. Int.* 2015 (2015) 171945-52.



42. P. Tambasco De Oliveira, A. Nanci, Nanotexturing of titanium-based surfaces upregulates expression of bone sialoprotein and osteopontin by cultured osteogenic cells, *Biomaterials* 25 (2004) 403–413.
43. D.M. Findlay, G.J. Atkins, Relationship between serum RANKL and the expression of RANKL mRNA in bone, *Osteoporos. Int.* 22 (2011) 2597-2602.
44. K. Ikeda, S. Takeshita, Factors and mechanisms involved in the coupling from bone resorption to formation: how osteoclasts talk to osteoblasts, *J. Bone Metab.* 21 (2014) 163-7.
45. M. Monjo, J.M. Ramis, H.J. Ronold, S.F. Taxt-Lamolle, J.E. Ellingsen, S.P. Lyngstadaas, Correlation between molecular signals and bone bonding to titanium implants, *Clin. Oral Implants Res.* 24 (2013) 1035-43.
46. J. Arnoldi, A. Alves, P. Procter, Early tissue responses to zoledronate, locally delivered by bone screw, into a compromised cancellous bone site: a pilot study, *BMC Musculoskelet. Disord.* 15 (2014) 97-106.
47. B. Pan, L.B. To, A.N. Farrugia, D.M. Findlay, J. Green, S. Gronthos, A. Evdokiou, K. Lynch, G.J. Atkins, A.C. Zannettino, The nitrogen-containing bisphosphonate, zoledronic acid, increases mineralisation of human bone-derived cells in vitro, *Bone* 34 (2004) 112-23.
48. J. Astrand, P. Aspenberg, Reduction of instability-induced bone resorption using bisphosphonates: high doses are needed in rats, *ActaOrthop. Scand.* 73 (2002) 24-30.
49. G. Thalji, L.F. Cooper, Molecular assessment of osseointegration in vitro: a review of current literature, *Int. J. Oral Maxillofac. Implants* 29 (2014) 171-99.
50. G.J. Atkins, D.M Findlay, Osteocyte regulation of bone mineral: a little give and take, *Osteoporos. Int.* 23 (2012) 2067-79.



51. Z. Du, S. Ivanovski, S.M. Hamlet, J.Q. Feng, Y. Xiao, The Ultrastructural Relationship Between Osteocytes and Dental Implants Following Osseointegration, *Clin. Implant Dent. Relat. Res.* (2014) doi: 10.1111/cid.12257

## Figures and Figure Legends

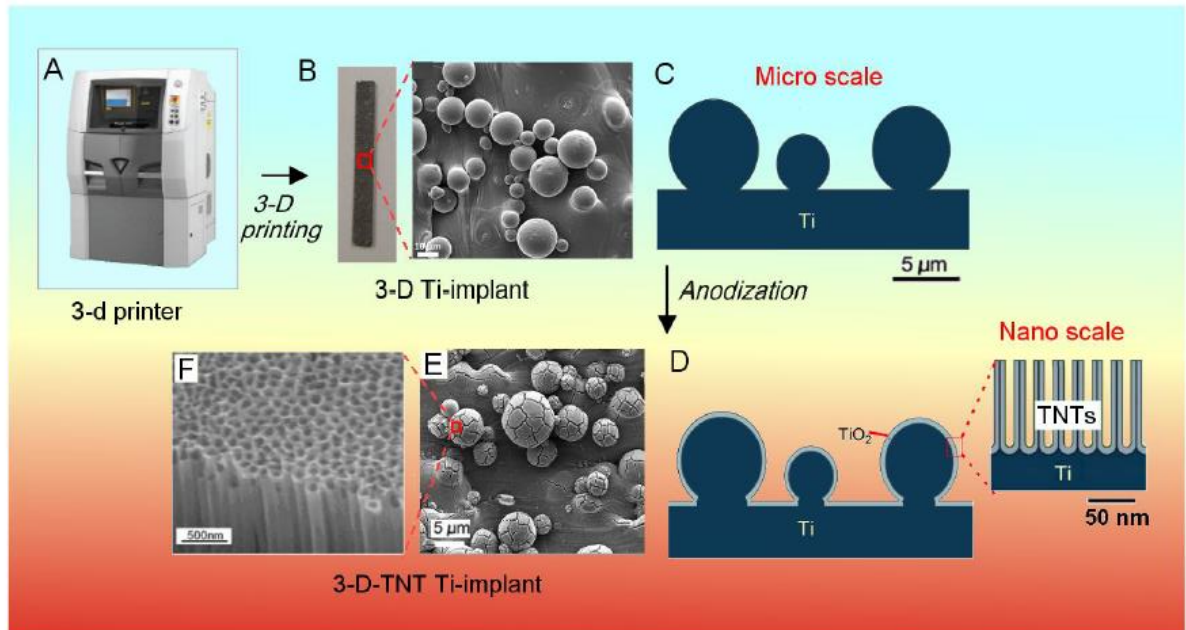


**Fig. 1.** Scheme showing fabrication of new TNT 3D printed Ti implants with unique micro-topography (spherical micro-particles) and nano-topography (titania nanotubes) fabricated by a combined 3D printing and anodisation process.

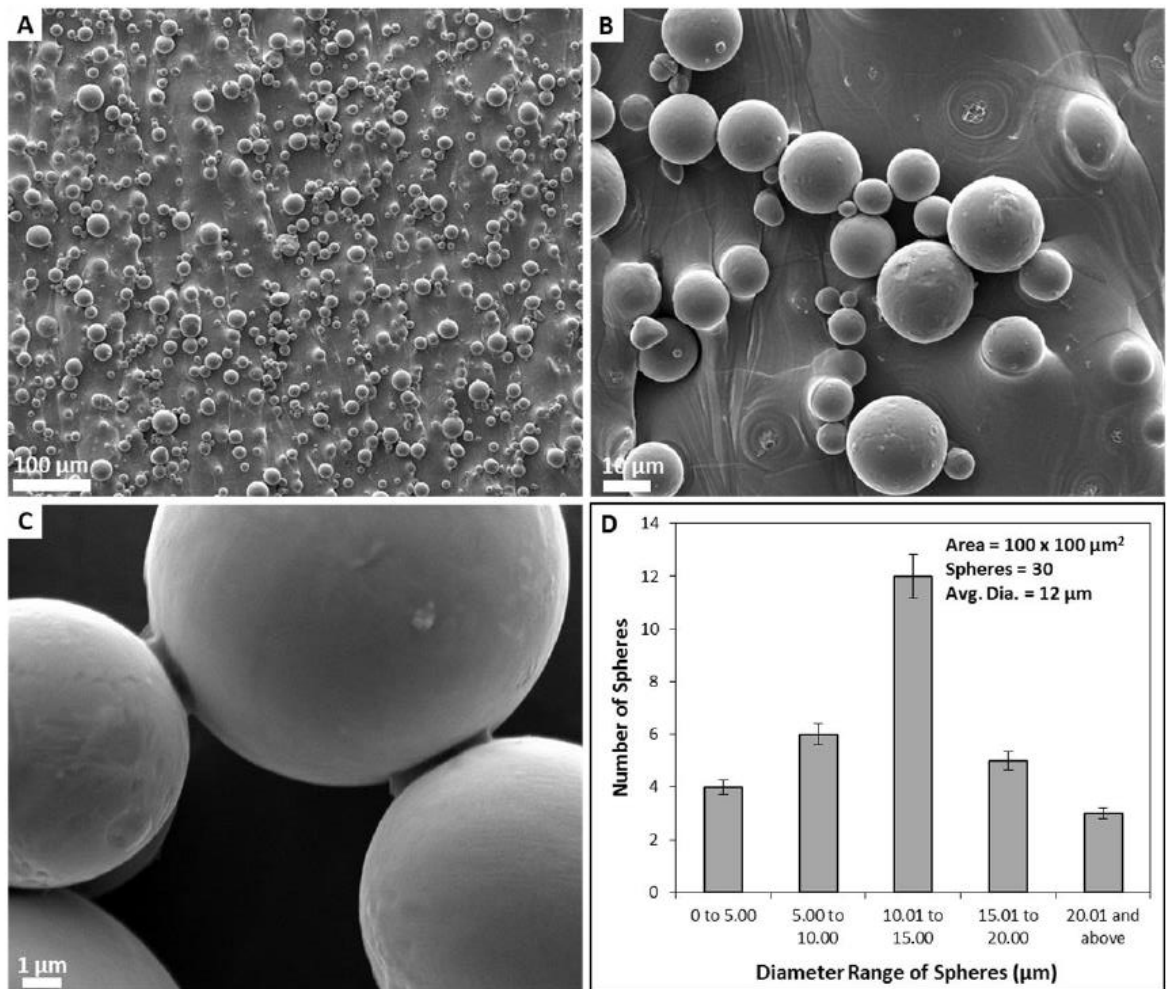


**Fig. 2.** Surface characterisation of 3D printed Ti. (a-c) SEM images showing the top surface of the Ti 3D with Ti micro spherical particles of varied diameters randomly covering the entire Ti surface, and (d) size distribution chart of the Ti particles calculated from SEM images.

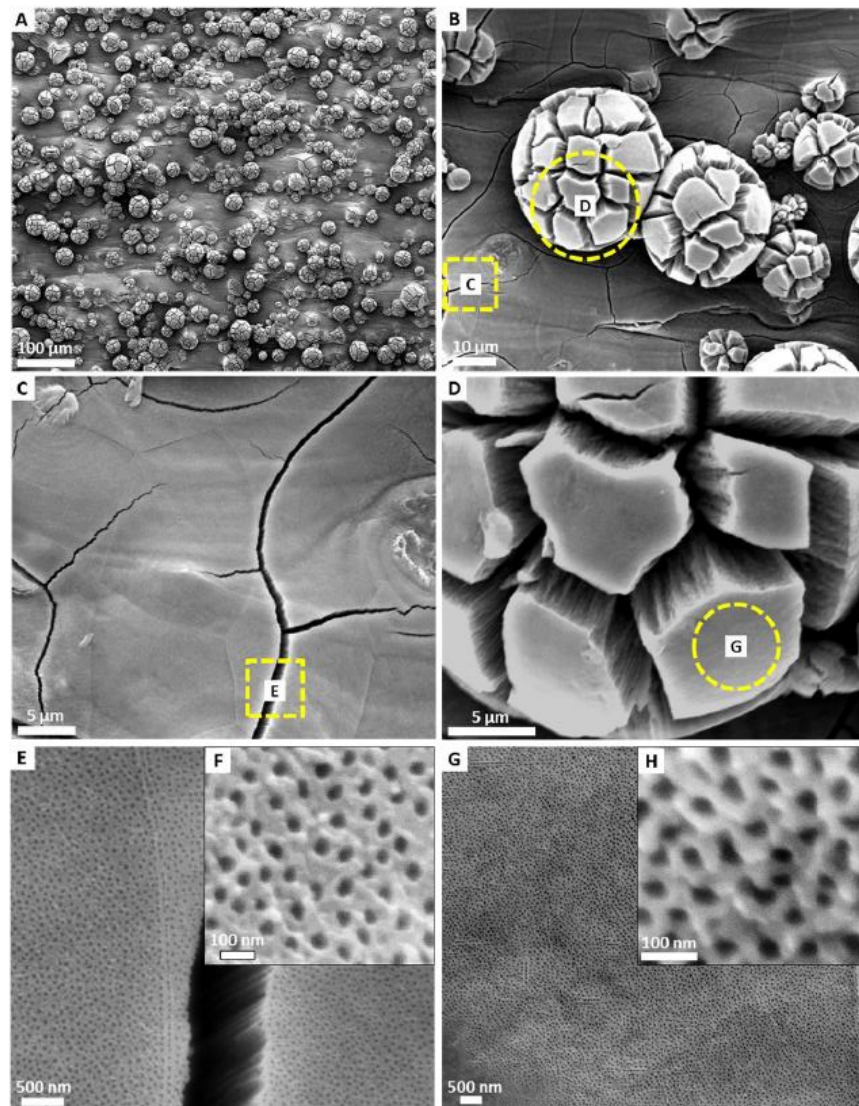


**Fig. 3.** SEM images of anodised 3D printed Ti confirming the introduction of nano-scale topography of oxide layer composed of titania nanotubes (TNTs) covering the surface of the Ti particles and the underlying Ti surface. (a) top-view showing the preserved 3D printed micro-particles on Ti surface covered with TNTs layer formed by anodization process, (b-d) characteristic cracks inside nanotube layer on micro particles and (b,d) and underlying Ti surface (b,c). These cracks are formed due radial growth on the curved surface, (e -h) well-ordered TNTs structure formed on the both Ti underlying surface and Ti particles.



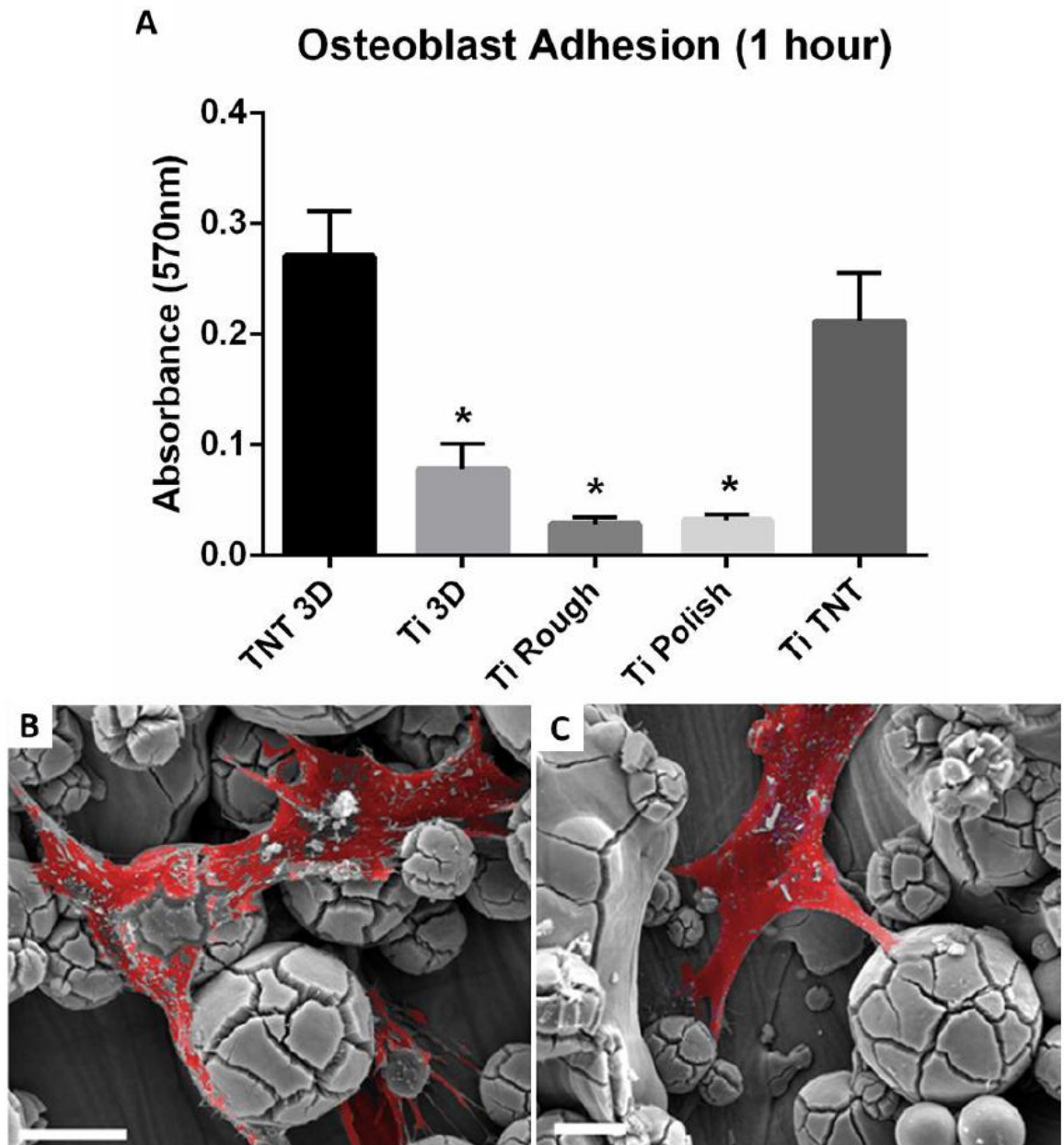


**Fig. 4.** Osteoblast adhesion on TNT 3D printed Ti implants. (a) Crystal violet staining at 1 h, representing osteoblast adhesion on various Ti surfaces. Data shown are means of triplicate assays  $\pm$  standard deviation (SD). Significant differences to the level of adhesion on TNT 3D are indicated by asterisks ( $p < 0.001$ ). (b-c) Osteoblasts (coloured red) adherent (24 h) on nanotubes fabricated on micro-rough 3D printed Ti (TNTs 3D). Scale bars represent 10  $\mu\text{m}$ .

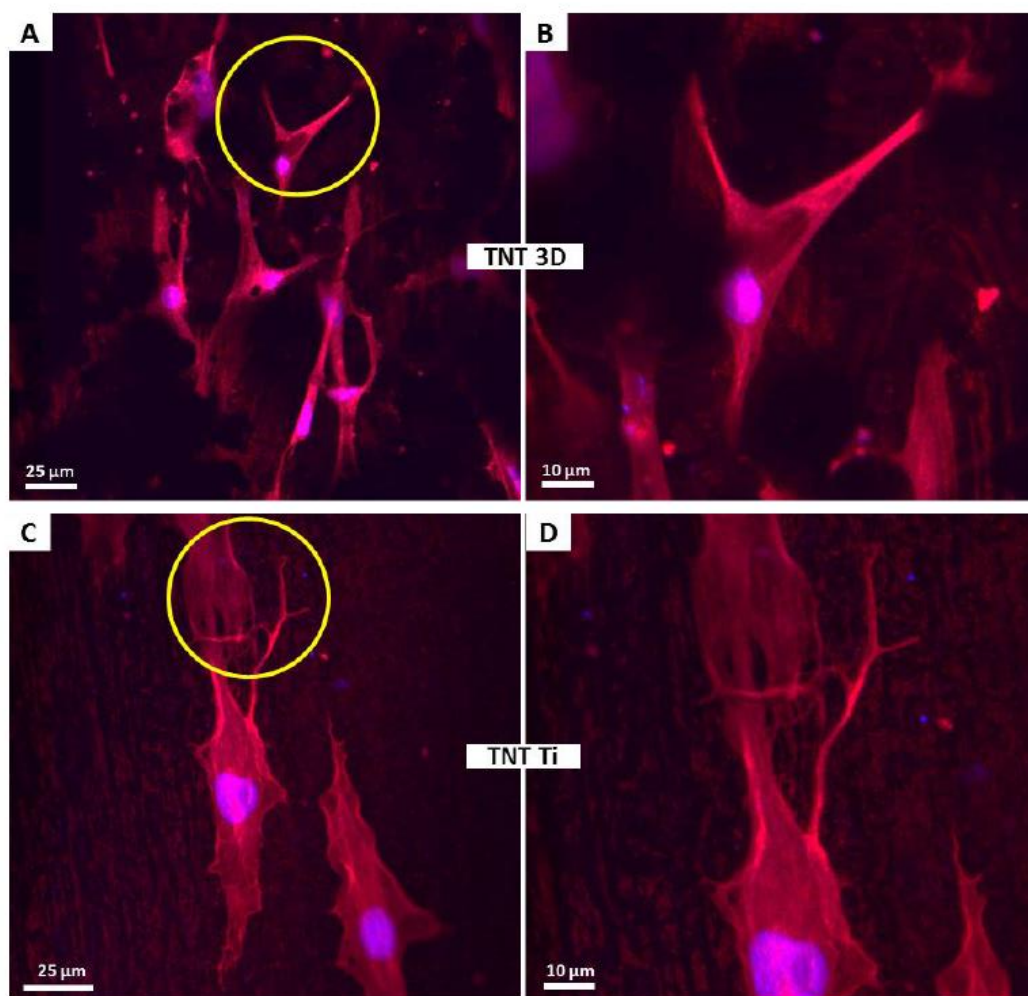


**Fig. 5.** High magnification confocal microscopy images showing the spread and adhering morphology of osteoblasts [Phalloidin (red, cytoskeleton) and DAPI (blue, nuclei) stained], on: (a-b) TNTs fabricated on Ti 3D (TNT 3D), and (c-d) TNTs on flat Ti Foil (TNT Ti).



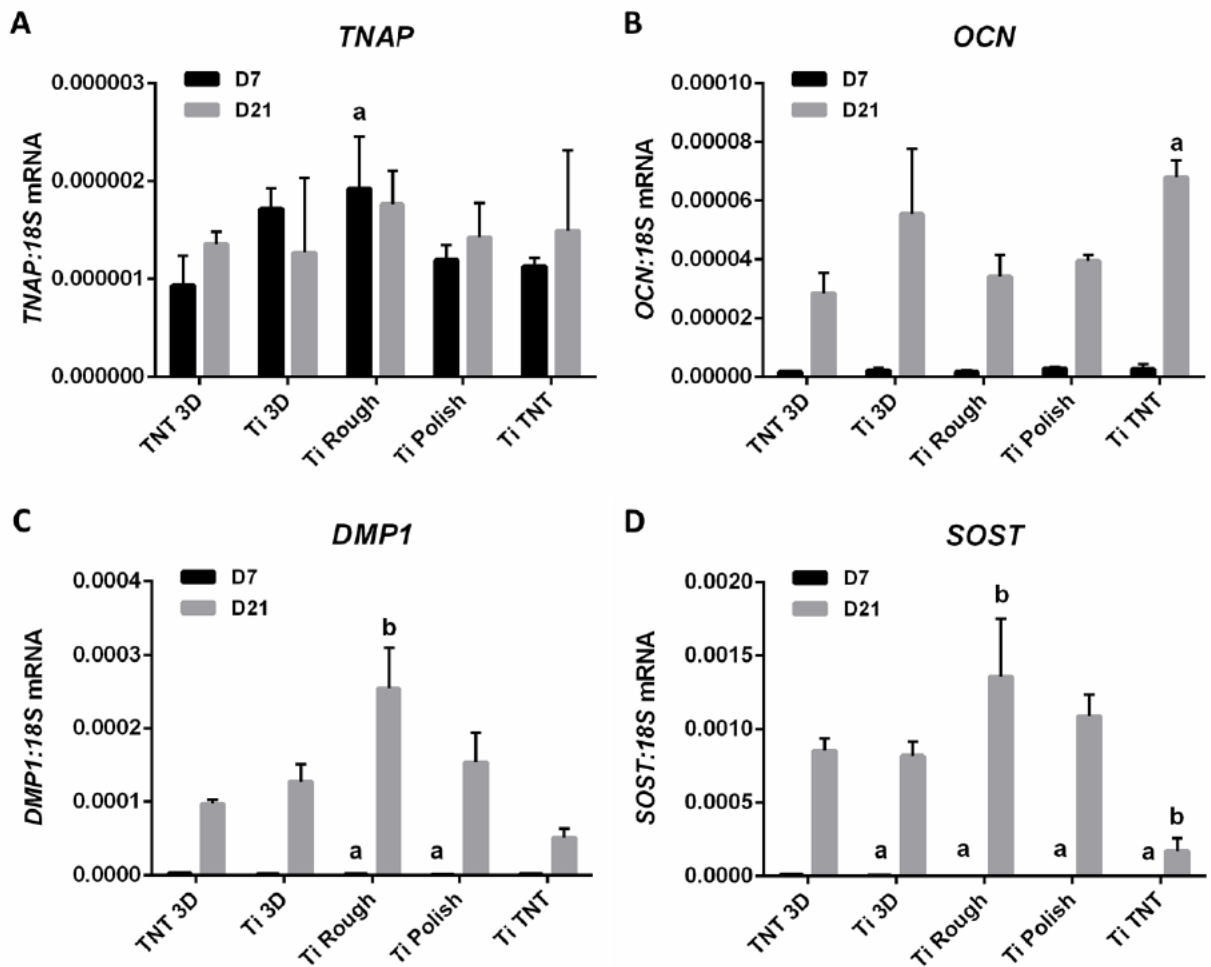


**Fig. 6.** Gene expression of osteogenic and differentiation markers in SaOS2 cells cultured on various Ti implant surfaces for 7 and 21 days. Real-time RT-PCR analysis was performed for a) *TNAP*, b) *OCN*, c) *DMP1* and d) *SOST* mRNA relative to the expression of *18S* rRNA in each sample. Data shown are means of experimental triplicates  $\pm$  standard deviation (SD). Significant differences to the level of gene expression on TNT 3D on day 7 are indicated by a ( $p < 0.05$ ). Significant differences to the level of gene expression on TNT 3D on day 21 are indicated by b ( $p < 0.05$ ).

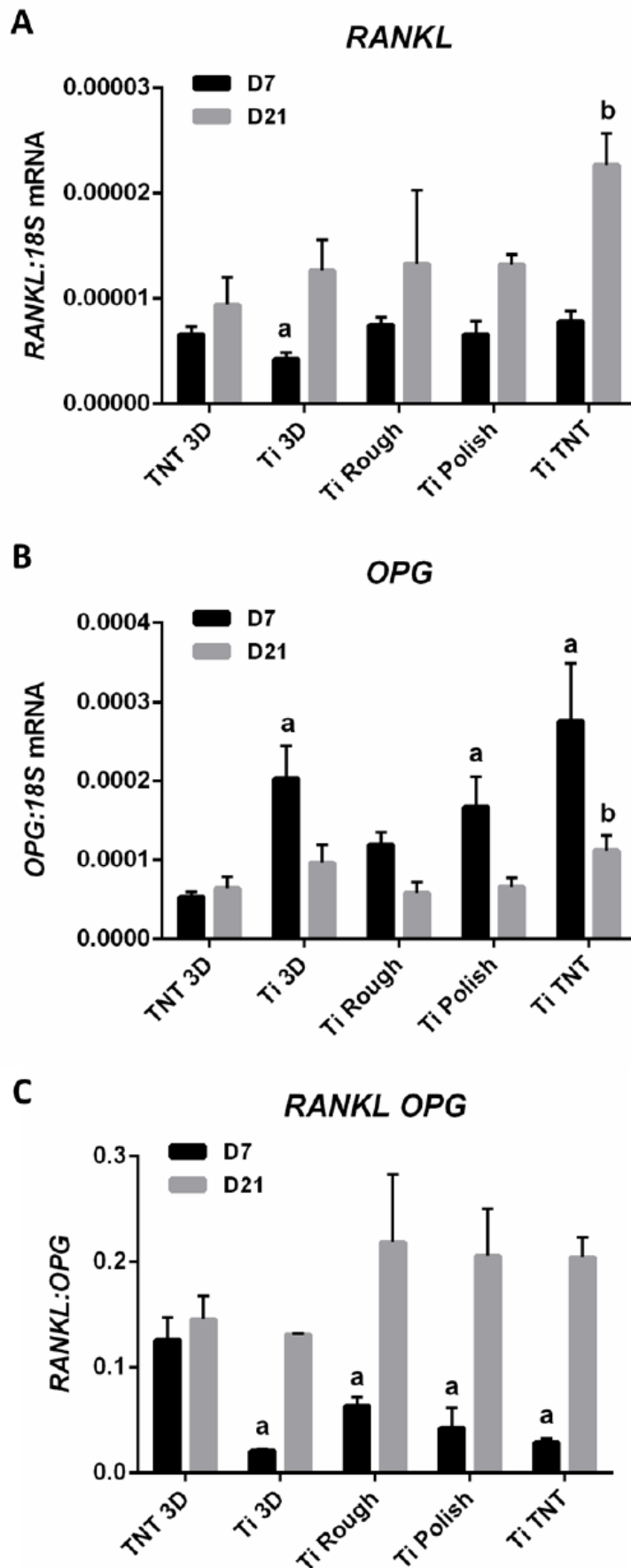


**Fig. 7.** Expression of bone resorption related genes in SaOS2 cells cultured on various Ti implant surfaces for 7 and 21 days. Real-time RT-PCR analysis was performed for a) *RANKL* and b) *OPG* relative to the expression of *18S* rRNA in each sample, and the ratio of *RANKL:OPG* mRNA was then calculated (c). Data shown are means of experimental triplicates  $\pm$  standard deviation (SD). Significant differences to the level of gene expression on TNT 3D on day 7 are indicated by a ( $p < 0.05$ ). Significant differences to the level of gene expression on TNT 3D on day 21 are indicated by b ( $p < 0.05$ ).

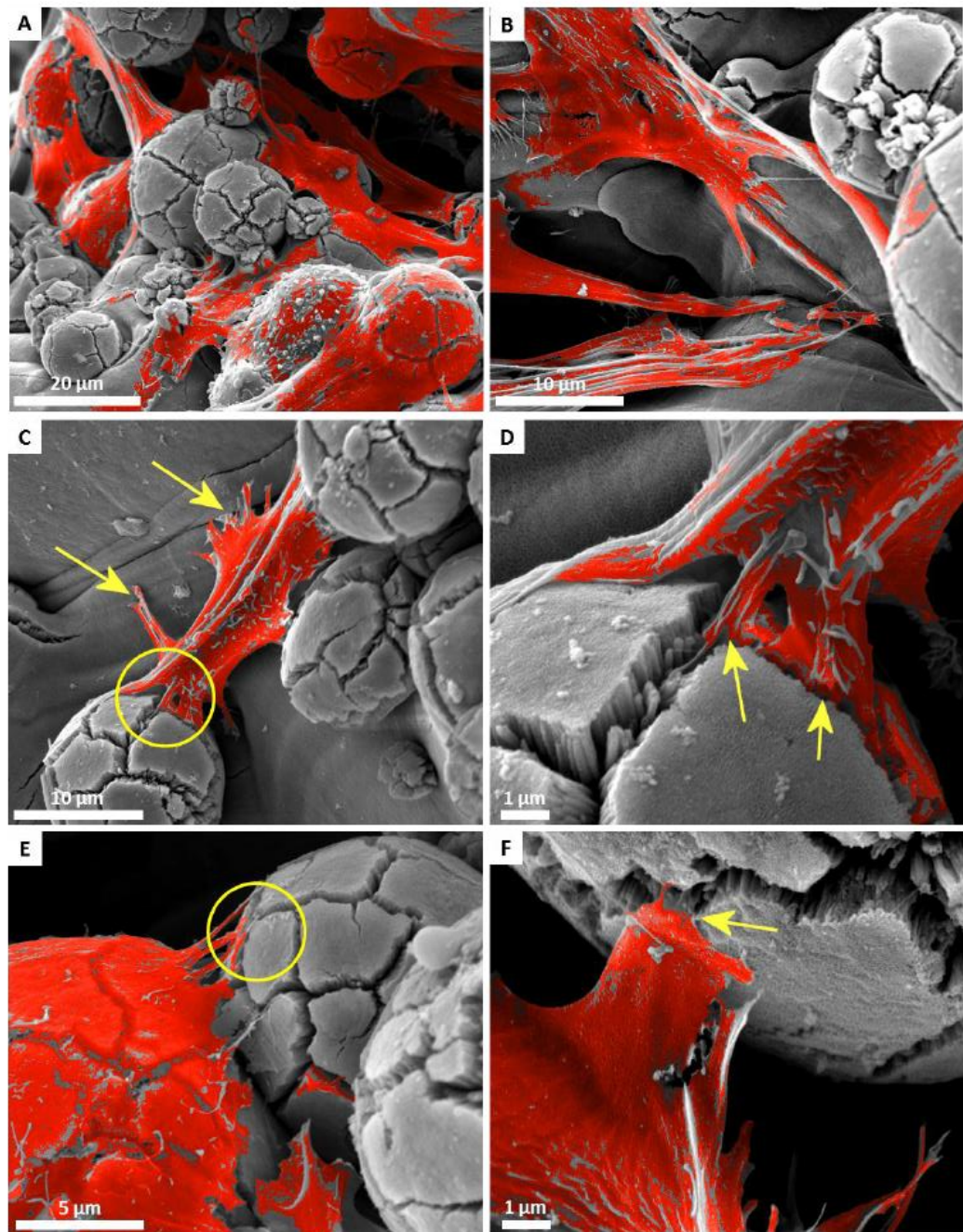


**Fig. 8.** SEM analysis showing SaOS2 cell attachment (red) on TNT 3D implants after 7 day incubation. Cells can be seen firmly attached on the TNT 3D implant surfaces and inside the cracks, which arise during anodisation of the curved surfaces.



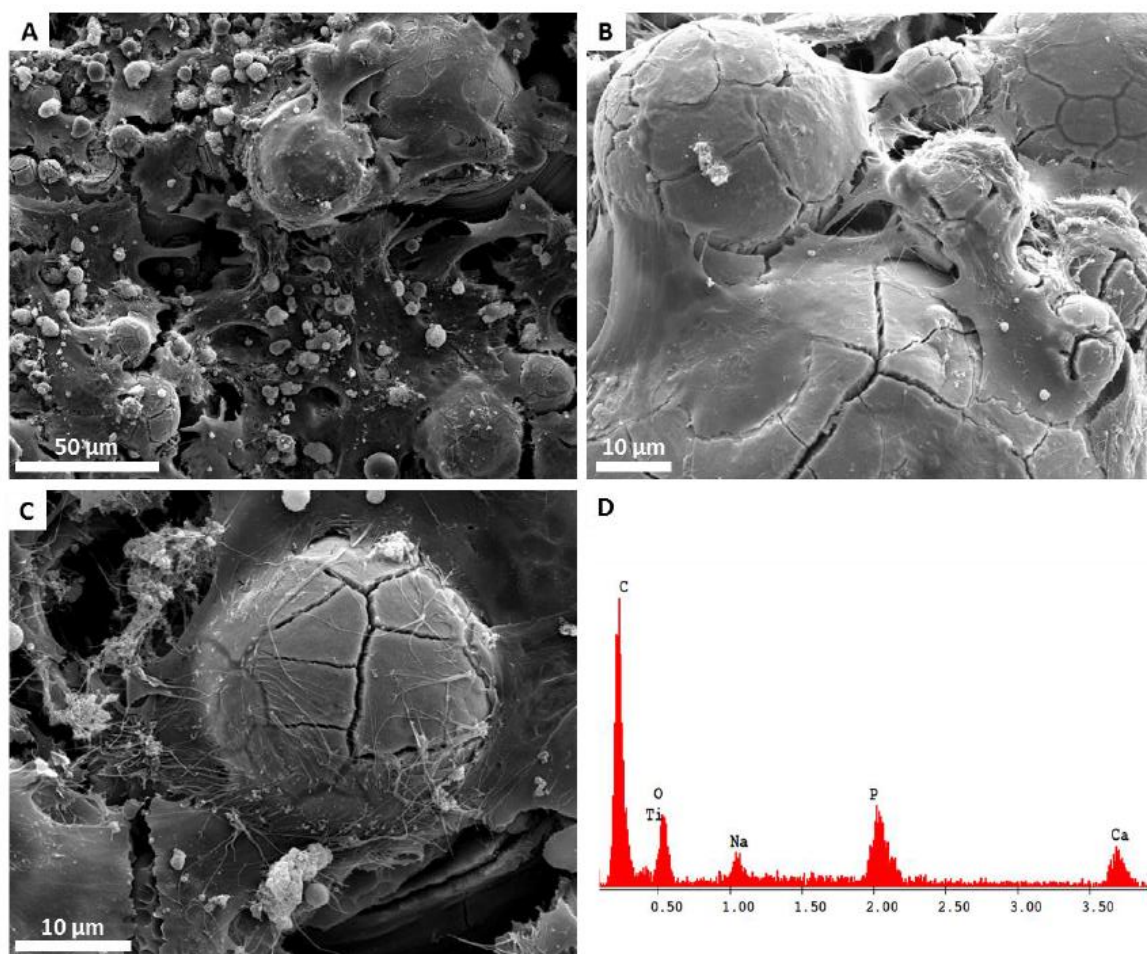


**Fig. 9.** SaOS2 cells cultured on TNT 3D implants for 21 days confirm mineralisation and ECM matrix deposition. (a-c) SEM images showing cell attachment and mineralized matrix deposition, and (d) EDS analysis revealing the presence of Ca and P on the TNT 3D surface.

## Supporting Information

### **3D printed titanium implants with combined micro particles and nanotube topography promote interaction with human osteoblasts and osteocyte-like cells**

Karan Gulati<sup>1\*</sup>, Matthew Prideaux<sup>2\*</sup>, Masakazu Kogawa<sup>2</sup>, Luis Lima-Marques<sup>3</sup>,

Gerald J. Atkins<sup>2†</sup>, David M. Findlay<sup>2†</sup>, Dusan Losic<sup>1†✉</sup>

<sup>1</sup>School of Chemical Engineering, University of Adelaide, SA, Australia

<sup>2</sup>Discipline of Orthopaedics & Trauma, University of Adelaide, SA, Australia

<sup>3</sup>The Institute for Photonics and Advanced Sensing, University of Adelaide, SA, Australia

\*Equal first author status

†Equal senior author status

✉Corresponding author: Prof. Dusan Losic,

School of Chemical Engineering,

The University of Adelaide,

Adelaide, SA5005 Australia,

Phone: +61 8 8013 4648,

Email: *dusan.losic@adelaide.edu.au*



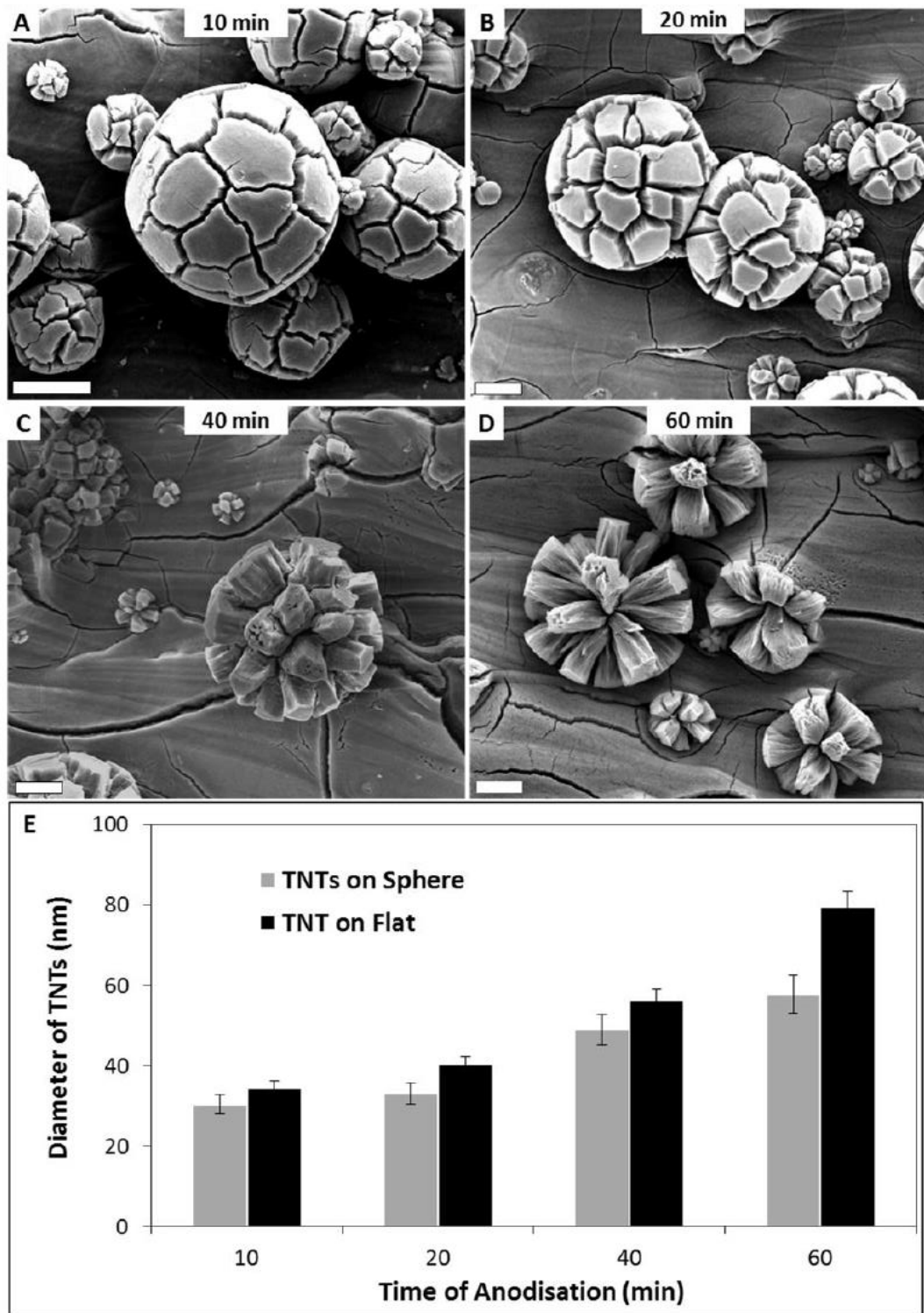


**Fig. S1.** Controlling the surface features of the anodised TNT 3D printed Ti implants by varying the time of anodisation. (a-d) SEM images showing the fabricated TNTs on 3D Ti at different times: 10, 20, 40 and 60 min, each resulting in increased TNT diameter wider cracks on the Ti spheres. (e) Plot showing the various diameters corresponding with the time of anodisation. All scales represent 10  $\mu\text{m}$ .

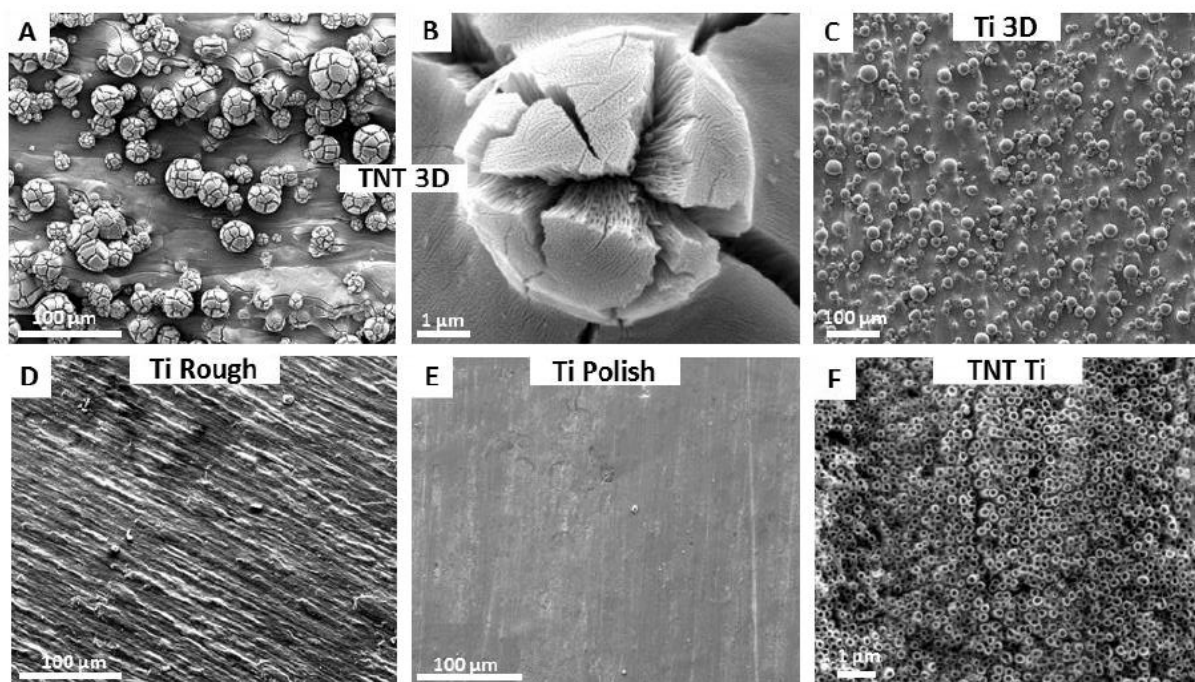


**Fig. S2.** SEM images showing the top-view of various Ti implants used to study bone cell adhesion, attachment and gene-expression. (a-b) TNT 3D, (c) Ti 3D, (d) Ti Rough, (e) Ti Polish, and (f) TNT Ti.

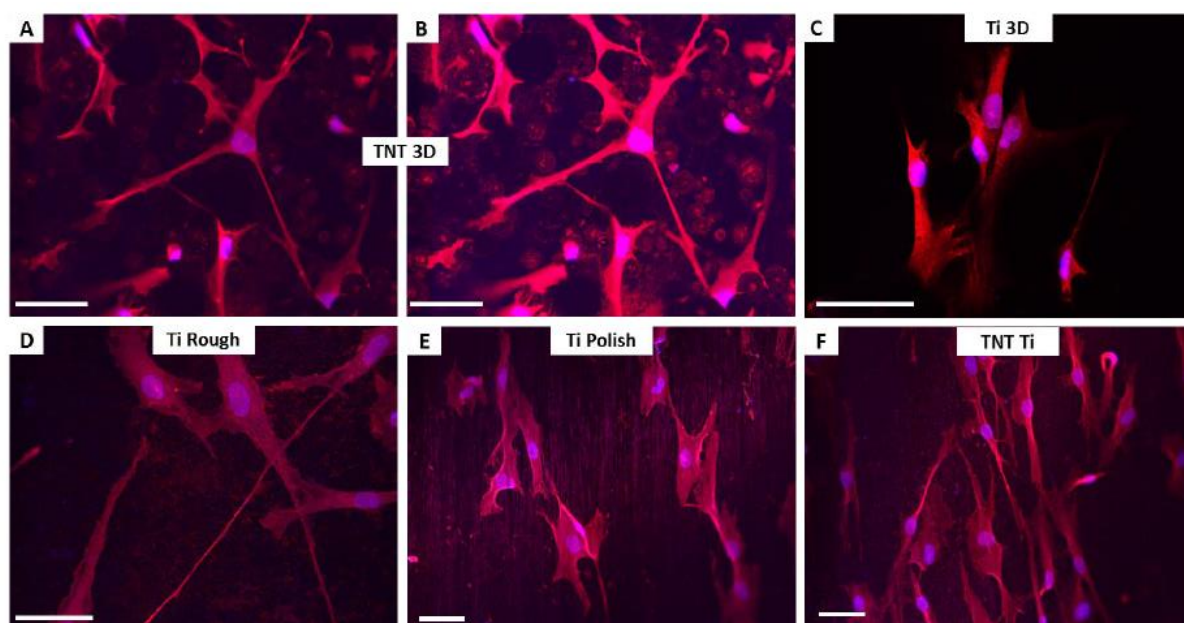


**Fig. S3.** Confocal microscopy images showing spread of osteoblasts after 24 hrs of culturing on various Ti surfaces: (a) TNT 3D, (b) TNT 3D image enhanced to show underlying Ti spheres, (c) Ti 3D, (d) Ti Rough, (e) Ti Polish, and (f) TNT Ti. Phalloidin (red, cytoskeleton) and DAPI (blue, nuclei) stains show the clear spreading and morphological features of the adhered cells. Interconnections between cells and presence of stress fibers are also evident. All scale bars represent 50 μm.



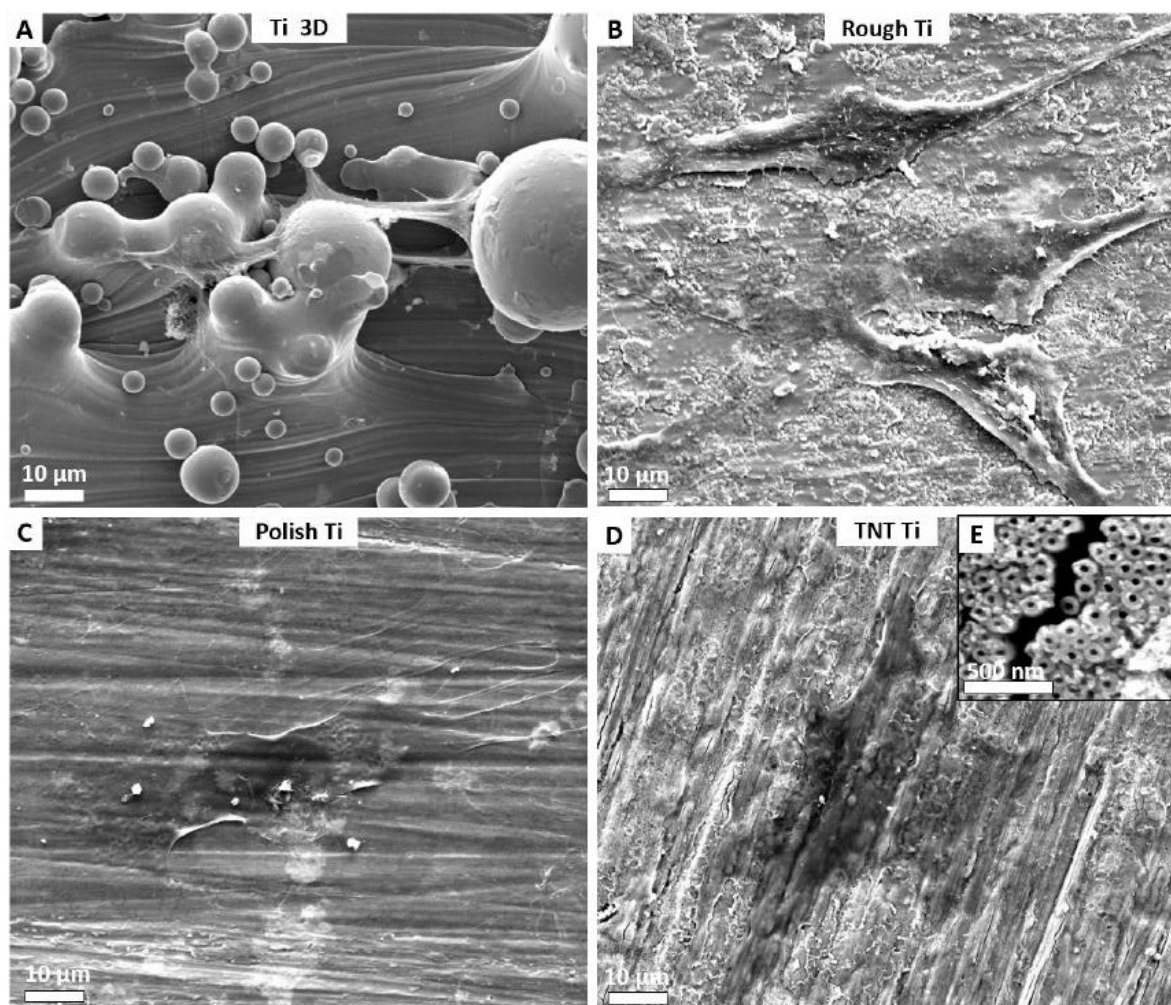


**Fig. S4.** NHBCs adhesion on the various implants surfaces after culturing for 24 hrs. (a) Ti 3D, (b) Rough Ti, (c) Polish Ti and (d) TNT Ti.



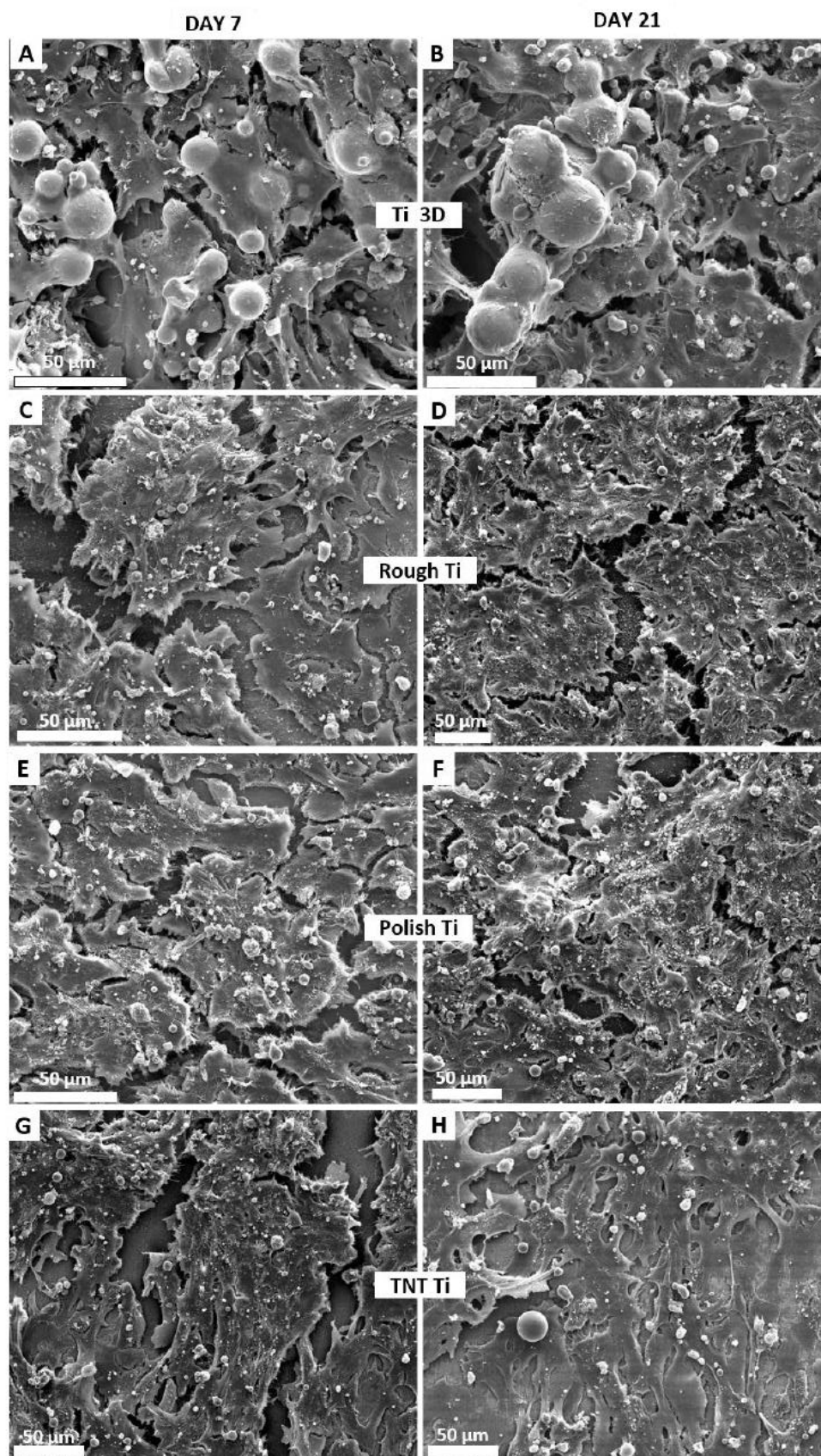


**Fig. S5.** SaOS2 adhesion and ECM formation on the various implants surfaces after culturing for 7 day and 21 day. (a-b) Ti 3D, (c-d) Rough Ti, (e-f) Polish Ti and (g-h) TNT Ti.

## CHAPTER 9

---

# CONCLUSIONS and RECOMMENDATIONS for FUTURE WORKS

**Karan Gulati**

School of Chemical Engineering, University of Adelaide, South Australia 5005, Australia



## 9.1 Conclusions

The work described in this thesis sought to advance titania nanotube technology towards enabling novel titanium bone implant solutions catering to complex bone therapeutic needs. Initially, in-depth knowledge of the electrochemical anodization (EA) technique to fabricate titania nanotubes (TNTs), and the need of localised drug delivery and modulation of cellular responses in traumatized bone conditions, permitted design of novel implant designs that can improve current implant technology and cater to a wide range of bone conditions. By optimizing EA conditions, the TNT bone implant technology was advanced by: generating periodically tailored nanotube structures, stable TNTs on complex Ti substrates such as Ti wires and unique architecture with TNTs on micro-rough 3D printed Ti alloys with dual micro-/nano-topography. These stable and easy-to-tailor TNTs/Ti implants were tested to achieve improved drug loading and controlled therapeutic release, optimized local therapeutic action, enhanced bone cell function: adhesion/attachment and gene expression, and ultimately release inside the bone microenvironment *ex-vivo*. Furthermore, additional functionalities were imparted to TNTs/Ti implants by virtue of conversion of titania (TiO<sub>2</sub>) into Ti (preserving nanotube structures) and investigating chitosan degradation on TNTs into micro-tubular structures in phosphate buffer. These led to novel implant concepts: electrically conducting drug releasing implants and *in-situ* generation of chitosan micro-tubes on TNTs structures, which open new possibilities for future research. Moreover, the fabrication and modification strategies employed in the abovementioned investigations represent easy, cost-effective and tailorable technologies, which can be integrated into the current implant market and also can address a wide range of bone traumas including: bone cancers, infections, osteoporotic fractures etc. The following summarizes the specific conclusions from the major investigations carried out as a part of this PhD thesis.

### 9.1.1. Periodically Tailored Titania Nanotubes for Enhanced Drug Loading and Releasing Performances

To advance the drug loading and releasing abilities of the titania nanotube implants, periodic-tailoring of the nanotube structures was performed. The following points summarize the conclusions drawn from this study:

1. Periodic oscillation of the voltage signal during the anodization process resulted in formation of periodic segments (P-TNTs) in the otherwise straight nanotubes. Alteration in voltage during the anodization process corresponded to the pore-size during the growth of the TNTs, which can be further tailored to design various TNT structures. A linear increase of voltage from 60 to 100 V and a sudden drop from 100 to 60 V reduced the outer diameter of the nanotubes from ~ 175 nm to ~ 130 nm for each oscillation.
2. Hydrophobic anti-inflammatory drug, indomethacin, routinely prescribed for pain/inflammation associated with bone implants and osteoporotic fractures, was loaded in P-TNTs and TNTs (with similar lengths/open-pore diameters) and its release kinetics into PBS *in-vitro* was monitored. For P-TNTs, a higher drug loading capacity ( $\uparrow$  9 %), reduced initial burst release ( $\downarrow$  35%), and delayed overall release ( $\uparrow$  >300%) was confirmed, with the possibility to tune loading/release to match specific therapeutic needs.
3. Further modifying the anodization profile by introducing rectangular voltage signals with high voltage differences (cycles of constant 100 V for 5 m and sudden drop to 20 V for 1 m), permitted huge differences in the growth rates of nanotubes and thereby generation of 'weak' spots in the nanotube arrays. Upon sonication for small intervals, the P-TNTs could be broken at these structural defects or weak points, into smaller nanotube fragments and single nanotubes. These loose TNTs fragments or bundles could be used as therapeutic vehicles for targeted or localized therapies.

### 9.1.2. Optimizing Anodization Conditions for the Growth of Titania Nanotubes on Curved Surfaces

To enable easy integration of the TNTs technology into the current implant market, which involves implants in different shapes/geometries such as: pins, screws, plates, meshes, etc., optimization of the anodization parameters was performed to achieve fabrication of well-ordered and stable TNTs on complex substrate geometry of Ti wire. The following points summarize the conclusions drawn from this study:

1. Anodization electrolyte was aged by anodizing dummy titanium foil in a moisture-controlled electrochemical cell, and various ages of the electrolyte (1% v/v water, 0.3 % w/v  $\text{NH}_4\text{F}$  in ethylene glycol), including fresh (no ageing performed) to > 30 h aged, were systematically studied. To identify key changes that occur in the electrolyte when ageing of anodization electrolyte is performed, reduction in conductivity and increase in Ti ion concentration of the electrolyte with ageing was linked with the stability of the anodic film on Ti wires. Briefly, appropriately aged electrolyte (~ 10 hr aged) resulted in stable anodic films on Ti wires, as compared to fresh/unused electrolyte, which yielded anodic films with severe cracks that cause delamination.
2. Alternate anodization parameters, including water content of the electrolyte, anodization voltage and time, and substrate dimensions, were also studied towards obtaining optimized anodization conditions (~ 1% v/v water, 75 V, 10-40 m, for reduced cracks: 0.80 mm Ti wire), that yield stable/well-adherent anodic films with high-quality TNTs.
3. Finally, this chapter enables fabrication of highly ordered TNTs that are well-adherent onto the underlying curved surface of the Ti substrate, which can improve integration of TNT technology into various medical implants.

### 9.1.3. Titania Nanotube (TNT) Implants Loaded with Parathyroid Hormone (PTH) for Potential Localized Therapy of Osteoporotic Fractures

To enable maximized therapeutic effect locally inside the bone micro-environment, this chapter shows the potential of TNTs/Ti wire for addressing challenges associated with conventional treatments for complex bone ailments such as osteoporotic (OP) fractures. The following points summarize the conclusions drawn from this study:

1. Based on optimized anodization procedures, stable TNTs were fabricated on Ti wires and were used as a platform to demonstrate the therapeutic effect of the OP drug, parathyroid hormone (PTH), and indomethacin, used for skeletal inflammatory conditions.
2. By tuning the electrochemical anodization parameters (for instance time of anodization), the dimensions of TNTs could easily be tailored, which in turn allowed loading of various amounts of active therapeutics inside them. Substantial drug loading and delayed release kinetics, upon coating of chitosan onto drug loaded TNTs/Ti wires, was demonstrated.
3. TNTs/Ti wires pre-loaded with PTH were inserted inside 3D collagen gel containing human osteoblast-like SaOS2 cells. Gene expression studies revealed suppression of *SOST* and upregulation of *RANKL*, which confirmed the effect of localised 3D elution of potent OP therapeutic on the cells.
4. Bone cell spread morphology on the TNTs/Ti wires removed from the collagen gel, demonstrated cellular migration and firm attachment, and the presence of cracks in the anodic film did not interfere with the cellular functions.
5. TNT/Ti wire implants were inserted into bovine trabecular bone cores *ex-vivo*, and the surface morphology examination upon retrieval established the mechanical stability of TNTs on Ti wires, which is crucial for load-bearing conditions such as implantation procedures and fracture-fixation.

### **9.1.4. *In-Situ* Transformation of Chitosan Films into Microtubular Structures: A New Bio-Interface for Bone Implants**

This chapter focused on determining the fate of chitosan coatings on TNT/Ti implants, which is usually employed to advance drug releasing/bone-forming/anti-bacterial properties, in the presence of phosphate buffer saline (PBS). It also reports and explains the self-degradation of such modifications into micro-tubular architecture on TNTs *in-situ* in PBS maintained at pH 7.4. The following points summarize the conclusions drawn from this study:

1. TNTs fabricated on Ti wires by electrochemical anodization, were modified by dip-coating chitosan, and the SEM results confirmed even coating of the open pores of TNTs with chitosan. This was followed by immersion in PBS (maintained at 25 °C and pH 7.4) to determine the degradation of the chitosan film.
2. Phosphate buffered saline-induced gelation/precipitation of chitosan film on TNTs and their reformation into micro-tubular structures (chitosan micro-tubes/CMTs) was reported, thereby generating a micro-rough surface onto nano-tubular TNTs.
3. Various contributing parameters, including the role of substrate surface topography, immersion solution and pH, chitosan coating thickness and the time of immersion, were investigated to determine the possible mechanism for the self-formation of CMTs on TNTs.
4. The results indicated that CMTs form on TNTs/Ti wires when the chitosan dip-coated implants were immersed in PBS (pH 7.4) for a minimum of 3 weeks.
5. This study showing formation of micro-tubular architecture composed of chitosan on titania nanotubes, generating dual micro-/nano-features, has considerable potential for the fabrication of advanced bone-therapeutic implants.

### **9.1.5. Chemical Reduction of Titania (TiO<sub>2</sub>) into Conductive Titanium (Ti) Nanotubes Arrays for Combined Drug-Delivery and Electrical Stimulation Therapy**

This chapter highlighted the magnesiothermic conversion of TiO<sub>2</sub> NTs (or TNTs) into titanium while preserving the nanotubular morphology, in an attempt to impart unique properties such as electrically-conducting and drug releasing implants. The following points summarize the conclusions drawn from this study:

1. TNTs fabricated on Ti wires were reduced at high temperatures (650 °C) in the presence of magnesium, to enable conversion of TiO<sub>2</sub> into Ti. SEM imaging and EDXS analysis of the implants before and after magnesiothermic conversion revealed successful conversion of TiO<sub>2</sub> into Ti, while maintaining the nanotube morphology.
2. XRD (x-ray diffraction) and EDXS of the resultant Ti nanotubes (Ti NTs) also confirmed strong signals for presence of Ti (and reduced TiO<sub>2</sub>) and also incorporation of magnesium oxides. Conductivity measurements of TNTs and Ti NTs established the electrically conducting nature of the modified implant (Ti NTs), which was proposed for electrical stimulation therapy (EST) to enable quicker fracture healing rates.
3. Furthermore, Ti NTs were loaded with Rhodamine B dye to showcase substantial drug loading and local-releasing features of the modified implant. *In-vitro* release was performed in PBS, and at pre-determined time intervals voltage was applied to the implant (as a cathode, 10 V for 1min x 3 cycles) to investigate the effect of electric field on the drug releasing behavior. The results confirmed that the release kinetics was not affected when voltage was applied. Ti NTs/Ti wires were proposed as simultaneous EST and drug releasing implants.



### **9.1.6. 3D Printed Titanium Implants with Combined Micro Particles and Nanotube Topography Promote Interaction with Human Osteoblasts and Osteocyte-Like Cells**

This chapter reported the fabrication of unique Ti alloy bone implants by combining 3D printing technology with electrochemical anodization, to create novel micro/nano-rough implants that promote bone cell function. The following points summarize the conclusions drawn from this study:

1. Using 3D printing, Ti alloy (Ti6Al4V) implants were fabricated with micro-topography (Ti 3D), whereby spherical Ti alloy micro-particles (diameter 5–20  $\mu\text{m}$ ) were randomly arranged on the underlying flat substrate. The inter-particle distance ranged from 1-100  $\mu\text{m}$ , with the surface of the implant creating micro-scale ‘peak and valley’ architecture.
2. Anodization was performed on Ti 3D implants to fabricate nanotubes (TNTs 3D), while preserving the micro-scale features. Bone cell functions were compared between TNT 3D (nanotubes on 3D micro-rough), Ti 3D (3D micro-rough), Ti Rough (micro-rough, flat Ti), Ti Polish (mechanically polished, smooth flat Ti), and TNTs Ti (TNTs on flat polished Ti).
3. Cell adhesion studies with human osteoblast-like cells (NHBC) revealed maximum cell attachment in 1h to TNT 3D implants, as compared to other implant surfaces. SEM and Confocal imaging of the cell spreading on TNT 3D surfaces confirmed firm attachment with clear evidence of stress-fibres, possibly due to mechanical stimulation by 3D micro/nano-rough topography.
4. Gene expression studies of human osteoblast-like SaOS2 cells cultured on these implant surfaces, for short- (7 day) and long-term (21 day), revealed a profile consistent with effective osseointegration and promotion of cellular function.

## 9.2. Recommendations for Future work

The investigations and the results presented in this thesis advance the knowledge of TNT technology for bone implant therapeutic applications. Future studies aimed at confirming the findings of these investigations in animal models *in vivo* can significantly contribute towards integrating TNTs into the current bone implant market. The following points outline possible future directions in the field of TNTs as bone therapeutic implants:

1. Although numerous claims have been made for the mechanical robustness of nano-engineering strategies for modifying titanium bone implants, mechanical testing, especially for long-term *in vivo* placement (> 6 months) is required to prove the applicability of such approaches. This will also ascertain if there are any nanoparticulates or toxic ions leaching from the implant surface, which might compromise bone cell functions and impair bone healing.
2. While *ex vivo* bone systems such as Zetos<sup>TM</sup> permit studying the spread of therapeutic payloads from the surface of modified implants directly inside the bone micro-environment, future studies aimed at investigating the optimum therapeutic requirements directly inside the traumatized tissue are required. Moreover, studying the role of stress/strain on bone implants using Zetos<sup>TM</sup>, mimicking the forces experienced by movement or body weight, will provide real insight towards designing the next generation of bone implants, ensuring their success in load-bearing conditions.
3. Long-term anti-bacterial efficacy of antibiotic incorporated implants is also important, especially in the *in vivo* setting, catering to re-triggered bacterial infection, development of antibiotic resistance and biofilm formation. While current TNT technology aims at delaying release to 6-8 weeks, more advancement is desired to maintain anti-bacterial effect for the life time of the implant or until successful osseointegration has been established. Moreover anti-bacterial modification of implants should not in any way impair the normal bone cell functions.

4. It will be important to apply biopolymers with dual functionalities, for example chitosan with bone forming and anti-bacterial functions to TNTs/Ti implant technology, with a thorough understanding of biopolymer consumption and cellular functions, at the implant-bone interface in animal models *in-vivo*. Inclusion of poly-electrolyte complexes with added therapeutics can further delay the release kinetics so that a long-term therapeutic effect can be achieved.
5. Designing novel *ex vivo* models to study diffusion of therapeutics directly inside the bone from nano-engineered implants. While currently available systems include tumor spheroids, 3D matrigel/collagen matrices, etc., they do not match the complexity of a traumatized bone micro-environment. The Zetos<sup>TM</sup> bone reactor system is well established and animal studies is another alternative, however these strategies represent costly and cumbersome procedures. An alternative 3D *ex vivo* model, in which real bone is mimicked in porous architecture, bone marrow and cells, could advance the initial in-depth testing of new therapeutic implants prior to proceeding into animal studies *in vivo*.

## APPENDIX A

---

# ***EX-VIVO* IMPLANTATION of NANO-ENGINEERED IMPLANTS: INVESTIGATING DRUG DIFFUSION and INTEGRATION inside the BONE MICROENVIRONMENT**

**Karan Gulati**

School of Chemical Engineering, University of Adelaide, South Australia 5005, Australia

S. Rahman\*, **K. Gulati\***, M. Kogawa, G. J. Atkins, P. Pivonka, D. M. Findlay, D. Losic “*Ex-Vivo* Implantation of Nano-Engineered Implants: Investigating Drug Diffusion and Integration inside the Bone Microenvironment” *Journal of Biomedical Materials Research Part A*, 2015 (**Equal Contribution**). (Final Stages of Submission)

***Ex-Vivo* Implantation of Nano-Engineered Implants: Investigating Drug Diffusion and Integration inside the Bone Microenvironment**

Shafiur Rahman<sup>1\*</sup>, Karan Gulati<sup>1\*</sup>, Masakazu Kogawa<sup>2</sup>, Gerald J. Atkins<sup>2</sup>, Peter Pivonka<sup>3</sup>,  
David M. Findlay<sup>2</sup>, Dusan Losic<sup>1</sup>✉

<sup>1</sup>School of Chemical Engineering, University of Adelaide, SA, Australia

<sup>2</sup>Discipline of Orthopaedics & Trauma, University of Adelaide, SA, Australia

<sup>3</sup>Australian Institute for Musculoskeletal Science, University of Melbourne, VIC, Australia

\*Equal first author status

✉Corresponding Author: Prof. Dusan Losic,

School of Chemical Engineering,

The University of Adelaide,

Adelaide, SA5005 Australia,

Phone: +61 8 8013 4648,

Email: *dusan.losic@adelaide.edu.au*

**Keywords:** local drug delivery, bone therapy, titania nanotubes, drug-releasing implants, drug diffusion, bio-interaction

## **Abstract**

Local drug delivery from the surface of bone implants has been recognized as a promising solution that bypasses the need of systemic drug administration. However with complex conditions such as deep bone infections, osteoporotic fractures and osteosarcoma, there is need of extensive therapeutic action directly inside the bone microenvironment. In this study we present nano-engineered Ti wire implants with titania (TiO<sub>2</sub>) nanotubes (TNTs), as minimally invasive therapeutic implants with ability to release potent drugs directly inside the traumatized bone tissue. Electrochemical anodisation was performed on tiny Ti wires (diameter 0.80 mm and length 10 mm) to uniformly fabricate TNTs all over the surface area of the wire, followed by loading of fluorescent dye, and placement inside bovine trabecular bone core *ex-vivo* using Zetos<sup>TM</sup> perfusion system. To advance the study and closely relate with real traumatized tissue, three bone cores were considered: marrow removed, with marrow, and with marrow and anticoagulant. Release of dye inside the bone cores was monitored using fluorescence imaging, and revealed different patterns/release rates based on type of bone core studied. Furthermore scanning electron microscopy (SEM) of the implants after retrieval from bone cores confirmed integration of the implant with the bone tissue, and survival of the nanotubular topography. Additional histology investigations showed the presence of viable osteocyte along the implantation area. This study advances the TNTs technology towards in-bone therapeutics and aids in design of customized implants with predictable release kinetics inside the bone micro-environment.



## 1. INTRODUCTION

Treating bone diseases, such as osteomyelitis, inflammation or cancer, using systemic therapy remains the common approach.<sup>1</sup> However, the success of such therapies appears to be limited, mainly due to limited drug distribution in bone, the lack of selectivity, and the inability to maintain an optimum drug concentration at the target site for prolonged duration. To overcome these limitations local delivery has been recognized as an alternative approach, offering sustained drug release, a continuous high local drug concentration and reduced systemic drug levels, minimizing potential ‘off-target’ effects.<sup>2-4</sup> Numerous bone implants and bone substitutes such as acrylic polymer, poly(lactic-co-glycolic acid), collagen, hyaluronan, chitosan, fibrin, silk, hydroxyapatite, ceramics and calcium phosphate cements, in different forms such as membranes, granules, hydrogels, matrices and sponges, have been explored as local drug delivery carriers.<sup>5-9</sup> However, many of these materials, even accepted for clinical use, have several disadvantages which limits their broader applications. These include a lack of mechanical support, rigidity and a large variation of porosity, causing undesirable initial burst drug release and uncontrollable and un-reproducible release kinetics. To address these limitations new nano-engineered materials as bone implants, with controllable pore size, porosity, and tunable surface functionality have been explored in recent years.<sup>3,10</sup> The expectations of these new materials are that they exhibit improved bioactivity, favor tissue regeneration and bone integration, provide sustained and controlled drug delivery ability and surgically less-invasive implantation. Titania nanotubes (TNTs) generated on titanium (Ti) surfaces have emerged as a promising drug-releasing material to have these requirements, with many valuable features, including high surface area, controllable pore dimensions, mechanical rigidity, biocompatibility and excellent integration particularly with bone tissue.<sup>11-14</sup> In this regard, extensive research has been performed in recent years to demonstrate their biocompatibility with bone cells, ability to act as drug releasing therapeutic implants and delivery of variety of drugs for bone therapy including antibiotics, anti-inflammatory, anticancer and growth factors.<sup>15</sup> Several approaches to control drug release from TNTs including sustained drug release over several months, sequential, multi-drug and externally triggered drug release were developed by our group showing TNT drug releasing implants as attractive devices for clinical applications.<sup>16-19</sup>

However, most of the existing studies on TNTs were performed on planar Ti substrates which appear to be inconvenient for insertion into bone and require a large surgical intervention. Therefore, development of an effective delivery device, with a minimally invasive strategy, is important to ensure effective local treatment for bone disease. In the search for a suitable alternative, our group has developed small, Ti based nanoengineered wire implants with TNTs on the curved surfaces, which can be conveniently inserted into bone.<sup>20,21</sup> Importantly, the payload from these implants is expected to be released in a three-dimensional (3-D) fashion, ensuring maximal exposure of the surrounding bone and bone marrow.

In our previous study, it was revealed that TNT-Ti wire implants could release the drug payload in a marrow-less bone model and their release could be monitored using an *in situ* fluorescence imaging technique.<sup>22</sup> This study indicated that the multi-directional distribution of drug within the porous architecture of bone is possible. However the marrow-less bone model does not present the real bone environment to confirm drug delivery distribution inside the bone relevant to *in vivo* conditions. Drug delivery and its distribution into bone depends on the presence of bone marrow, which has a high fat content and occupies the large pore spaces of the complex porous architecture of cancellous bone.<sup>3,23,24</sup> Presence of marrow will have obvious impact on the drug distribution in bone and will determine whether adequate drug concentration can be achieved at the sites of disease. The drug distribution, release behavior and stability of wire implants within the bone marrow environment has not been explored previously and it is essential to perform this study before considering *in vivo* and clinical studies of these implants.

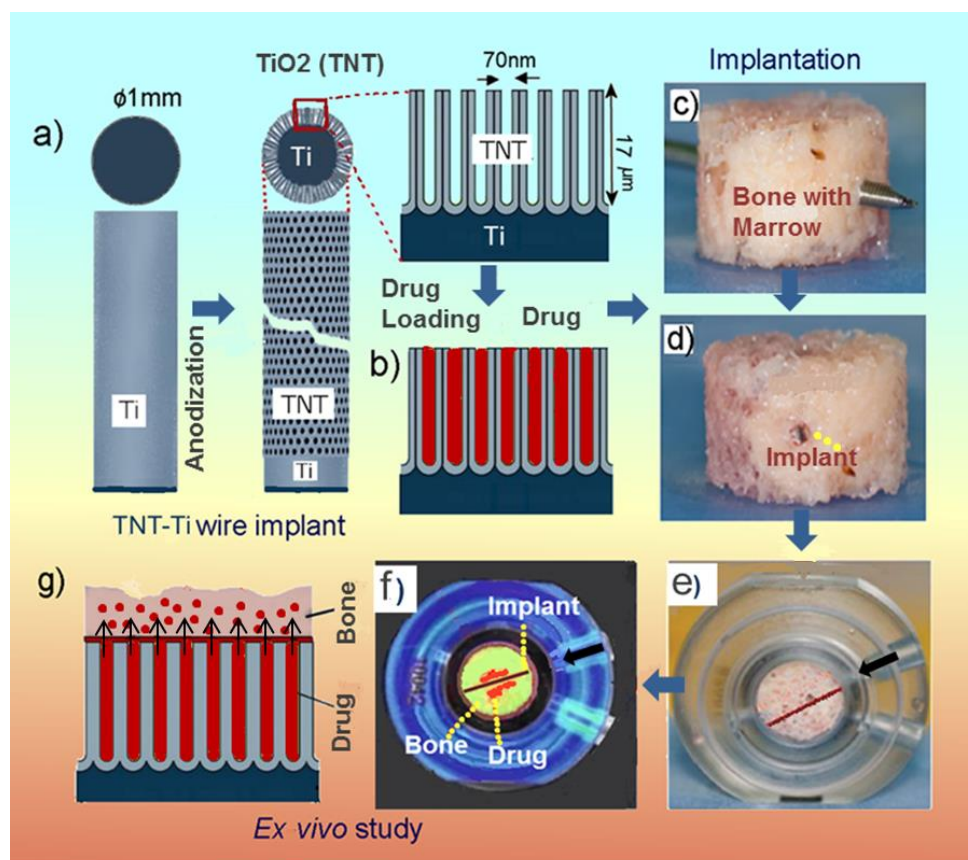


**Figure 1.** Scheme showing the fabrication of TNT-Ti wire implants and the *ex-vivo* bone perfusion studies. a) TNT-Ti wire implant fabrication, b) cross section with formed nanotubes and drug loading, c-d) needle puncture approach for insertion of the drug-loaded TNT-Ti wire implants into bone marrow explants, e) insertion in Zetos chamber, and f-g) monitoring of *ex vivo* drug release inside the bone.

Therefore, the aim of this study was to examine the *ex vivo* performance of drug-loaded TNT-Ti implants in trabecular bone containing bone marrow, with respect to drug release behavior, and implant stability and interaction. An overall scheme of proposed study is outlined in Figure 1. We proposed to establish the *ex vivo* experiments using the Zetos bone bioreactor<sup>23,24</sup> with bone inserted with TNT-Ti wire implants loaded with model drug. This work was specifically focused to explore impact of bone marrow on drug release compared with marrow-less bone. The addition of anticoagulant heparin used to inhibit blood coagulation was also explored to investigate the influence in drug distribution in bone marrow. The implants taken out of bone after study were examined to determine stability and integrity of TNTs structures, bone materials adhesion on their surface and histology of bone being in contact with implants.

## **2. EXPERIMENTAL SECTION**

### **2.1. Materials**

Ti (99.99 %) wires (diameter 0.8 mm) were supplied by Nilaco (Japan). Ethylene glycol, lactic acid, acetone, ammonium fluoride, rhodamine B ( $C_{28}H_{31}ClN_2O_6$ , 97 %), and heparin were obtained from Sigma-Aldrich Pty Ltd (St Louis, MO, USA) and used without further purification. High-purity ultra-grade Milli-Q® water (18.2 MΩcm resistivity) (EMD Millipore Corporation, Billerica, MA) with additional filtration (0.22 μm) was used for the preparation of all reagents.

### **2.2. Nanofabrication of TNT-Ti wire implants**

Ti wires were mechanically polished using commercially available sand paper, cleaned by sonication for 30 min each in water and acetone and then air-dried. Electrochemical polishing of mechanically cleaned wires was performed by a mixture of perchloric acid, butanol and ethanol (v/v, 1:9:6) at a constant voltage of 20 V for 3 min in a custom-built cell consisting of stainless steel wire as a counter electrode to obtain wires with a smooth surface. The wires were then rinsed with water, air-dried and partially protected with a pipette tip to expose only 9 mm length for electrochemical anodization, using methods described elsewhere with modification.<sup>25</sup> In brief, a single step anodization was performed using a mixture of 1.5 M lactic acid, 0.1 M ammonium fluoride, ethylene glycol and 2.5 % water maintained at 60 °C and a constant voltage of 60 V with a microprocessor-controlled power supply (Agilent) using a specially designed cell containing a Ti cathode. After 20 minutes of anodization, Ti wire with a TNT surface layer was removed from the cell, cut into 1 cm lengths, cleaned with water and air-dried for future use.

### **2.3. Structural Characterization**

Prepared TNT-Ti samples were examined by light microscopy. Structural characterization of the TNT-Ti wires before drug loading and post-experimentally was carried out using a field emission scanning electron microscope (SEM) (Quanta 450, Eindhoven, The Netherlands), equipped with energy dispersive X-ray spectroscopy (EDS) employed for surface composition analysis. To the sample

surfaces were mounted on a SEM sample holder using double-sided conductive tape, and coated with a 3–5 nm thick layer of platinum. Images, with a range of scan sizes at normal incidence and at a 30° angle, were acquired from the top and bottom surfaces, and cross-sections and EDS spectra were collected from different areas of interest.

#### **2.4 Drug loading and *in vitro* drug release**

Rhodamine B (RB) as a model drug was dissolved in water (50 mg/mL) and loaded into the anodized TNT-Ti implants using a technique described elsewhere.<sup>19</sup> In brief, implants were fully immersed in the RB solution in a glass vial, sonicated for 5 min and then allowed to soak for 2 h with gentle shaking every 30 min to promote drug loading. The implants were then dried in air and kept under vacuum for 2 h, followed by gently removing any excess drug from the wire surfaces using a soft tissue wetted with phosphate buffered saline (PBS; pH 7.4). The implants were sterilized using low-temperature hydrogen peroxide gas plasma (Sterrad® 100NX™ System, Advanced Sterilization Products, Irvine, CA, USA). For *in vitro* drug-release study the RB-loaded TNT–Ti wires were immersed in 5 mL of PBS (pH 7.4) at room temperature using a procedure described previously.<sup>20</sup> Briefly, aliquots of buffer solution were analyzed every 30 min up to the first 6 h and then every 24 h until drug is completely released from implants (13 days). The aliquots were measured for absorbance at 551<sub>nm</sub> using a UV spectrophotometer following previously described procedure.<sup>22</sup>

#### **2.5. *Ex vivo* study in a bone bioreactor**

*Preparation of bovine trabecular bone cores:* Three types of bone samples, bone core with marrow (type 1), heparin (30 unit/mL, 1 mg equivalent to 180 USP units) treated bone core with marrow (type 2) and bone core without marrow (type 3), were prepared from the sternum of a freshly slaughtered 13-month-old steer. Prior to processing, collected sternums were harvested and kept in cold sterile saline (0.85 %) to prepare type 1 and 3 and in a heparin mixed cold sterile saline (0.85 %) to prepare type 2 bone cores. Bone processing was conducted using sterile apparatus and equipment. In general, soft tissues and cartilage were removed from the sternum, which was then manually cut into sagittal

sections using a surgical saw and prepared sections were transferred into prewash medium, consisting of high-glucose Dulbecco’s Modified Eagle Medium (Life Technologies Corporation, Carlsbad, CA, USA), with 20 mM of 4-(2-hydroxyethyl)-piperazineethanesulfonic acid, 2.4 mg/mL benzylpenicillin, 3.2 mg/mL gentamicin sulfate, and 4 µg/mL amphotericin B. Bone cylinders of 10 mm diameter from the prewashed bone sections were prepared using an industrial drilling machine (Model G0517 Mill/Drill, Grizzly Industrial Inc, Muncy, PA, USA) and a custom-made diamond drill bit immersed in cold sterile saline (0.85%) or heparin mixed sterile saline (0.85%) in a custom polyoxymethylene drilling jig to prevent desiccation and/or thermal necrosis. Finally, the bone cylinders were mounted onto another custom-made platform and milled to 5 mm thickness using a 10 mm diameter tungsten carbide bit, again keeping the bone pieces immersed in cold sterile saline solution. The resulting types 1 and 2 bone cores consisted of uniform trabecular bone filled with marrow and without any visible cartilage. However, type 3 bone cores were prepared by removing marrow under pressure from type 1 bone cores using a dental water jet (WP-450A; Water Pik, Inc, Fort Collins, CO, USA). All bone cores were stored in separate prewash medium at 4°C prior to use for *ex vivo* study.

*Ex vivo drug release in trabecular bone:* Three bone cores of each type (1, 2 and 3) were used in this study. A hole was drilled through the middle of each bone core using a sterilized surgical grade stainless steel sharp 1.1 mm diameter pin Kirschner wire, and then RB loaded TNT–Ti implants were carefully inserted into the hole prior to placing the bone into secured custom-made bone culture chambers, aligning the implant with the perfusion inlet. Bone culture chambers were then connected to a multi-channel perfusion pump at 37°C and the appropriate culture medium was perfused through the bone samples at a constant rate of 7 ml/h (Figure 4). The perfused media were replaced every three days throughout the experiment. To measure the concentration of RB released from the TNT–Ti wires as fluorescence intensity, which directly corresponds to the concentration, an image of each entire bone core was captured at 1, 2, 4, 6 h and then every 24 h up to 264 h (11 days) using an *in vivo* imaging system (Xenogen IVIS 100, Caliper Life Sciences, Hopkinton, MA, USA). The fluorescence imaging mode was set at 5 sec exposure time, medium-size binning, open emission filter and 25 cm view field, with 2×2 (width by height) pixel count and a subject area of 0.76 cm<sup>2</sup>. The captured images



were finally processed using a Living Image® (version 2.50.1) software to derive fluorescence intensity data representing the concentration of released RB.

## **2.6. Evaluation of stability and integration of TNT-Ti implants into bone**

At the end of the *ex vivo* study, bone cores with inserted TNT-Ti implants were carefully removed from the perfusion chamber and immersed into 20 mL of fixation solution (1.4% w/v paraformaldehyde) at room temperature for 24 h to preserve morphological details. Samples were then placed in a slow decalcifying solution (10 % EDTA, 5% paraformaldehyde and 50% PBS, (v/v), pH 8) for 3 days before transferring into fast decalcifying media (5 % EDTA, 9.5 % HNO<sub>3</sub>, (v/v)) for 24 h. The samples were placed on photographic film (AGFA Structurix D4 film) and exposed to 35 kV for 2½ min in a Faxitron 804 (Faxitron Company, Illinois, USA) to confirm decalcification. The soft bone core samples were then carefully cross-sectioned for two samples, 1) one with visible implant inserted into bone and 2) with clear groove caused by circular implant surface. Sample 1 was treated using ethanol to prepare for SEM (discussed in section 2.2) to observe any morphological damage on the implant surface due to insertion, any organic deposition and bone implant contact, while sample 2 was used to prepare for histological study. For histological analysis, the decalcified samples were embedded into paraffin wax, cut into sections of 5 µM thickness using a microtome (Leica microsystems, Germany) and collected on silane-coated slides. The sections were dewaxed using histolene, hydrated using ethanol and water, and stained using haematoxylin for nuclear staining before washing in tap water, blueing using 5% ammonia water and differentiating using 1% HCl. The slides were again washed, counterstained using eosin, dehydrated using ethanol and cleared using histolene, before finally mounting in permanent mounting media. The prepared slides were then observed for osteocytes or other cells adjacent to the implant position or along the edge of the drill hole used for the TNT-Ti wire insertion using a Leica microscope (Olympus).

## 2.7. Statistical analysis

Student *t*-test (two-tailed) and two-way analysis of variance, followed by Tukey’s multiple comparison test, were used to analyze *ex vivo* drug release data. A value for \* $p < 0.05$  and \*\*\* $p < 0.001$  were considered significant in each case.

## 3. RESULTS AND DISCUSSION

### 3.1 Characterization of TNT-Ti wire implants

To fabricate TNT-Ti wire implants, an anodization process using lactic acid at 60 °C was adopted and compared with previous work where different electrolyte and two-step process was used.<sup>20–22</sup> Unlike previously published methods a single step technique enabled use of low voltage current (60 V) and a short period of time (20 min) to prepare about 15–20 μm thick layer of nanotubes around a 0.8 mm thick Ti wire. Our results showed that the anodization of wire requires different optimization conditions as compared to planar Ti surfaces. A series of SEM images of prepared TNT structures are presented in Figure 2. Digital photos of the prepared wire implants showed a characteristic golden brown colour with smooth surface texture and a stable oxide layer, deemed suitable for handling (Figure 2a, inset). A low-resolution SEM image confirmed the growth of a TNT layer around the curved surface of 0.9 cm length at the 1 cm long Ti wire. TNT layers exhibit small vertical cracks (0.5–1 μm wide) across the entire wire (Figure 2a). These cracks were also observed in our previous work<sup>18–22</sup> and they are usually caused by the radial growth of TNTs across the wire length. However, these cracks were shown do not compromise the adherence and stability of the TNTs and provide additional microstructure which is known to be beneficial for bone cell adhesion. TNT layers prepared by this method compared with TNTs prepared by anodization using only ethylene glycol electrolyte appear to be smoother and have smaller cracks.<sup>18–20</sup> High-resolution SEM images of the top, cross-section, and bottom surface of the showed a densely packed 17±2 μm thick layer of uniform and vertically aligned nanotubes of 70±5 nm diameters (Figure 2c).

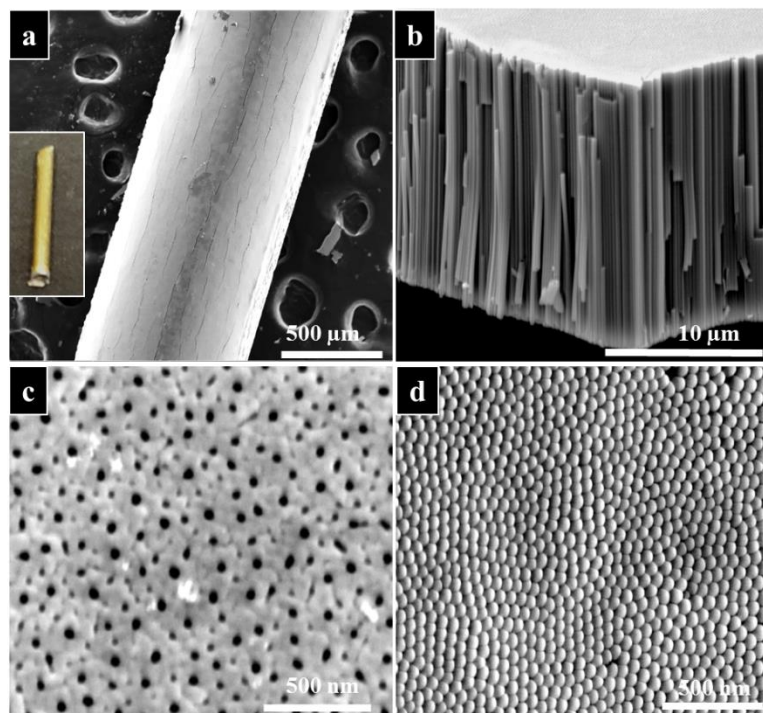


**Figure 2.** Structural morphology of TNT-Ti wire implants. SEM images of a) prepared TNT-Ti wire implants, with an inset digital image of the whole implant, b) a cross-sectional view showing TNT length or thickness, c) the top surface showing the nanotube opening and d) bottom surface showing closed end of the nanotubes taken by removing TNT layer from wire.

It is interesting that TNTs have more porous than tubular morphology usually obtained using other electrolytes (Figure 2c). The growth rate of 850 nm/min confirmed reasonable fast production time of only 20 minutes to make implants of 17-19  $\mu\text{m}$  thickness, which can be extended if fabrication TNTs with longer thickness is required. The SEM image of bottom surface shows a uniformly closed bottom of TNTs across the entire structure (Figure 2d). These results demonstrate that the applied method with lactic acid as electrolyte is an excellent method for fast and reproducible preparation of TNT-Ti wire implants with robust TNT layers. Therefore the method potentially can be translated for scalable production of implants based on conventional Ti implants in the form of screws, plates and prostheses, currently used in clinical practice.

### 3.2 Drug loading and *in vitro* drug release from TNT-Ti implants

Drug loading and *in vitro* drug release of the drug loaded implant is presented in Table 1 and Figure 3. The results show that TNT-Ti wire implants with  $70 \pm 5$  nm diameter and  $17 \pm 2$   $\mu\text{m}$  layer thickness

were able to load  $25.6 \pm 1.5$   $\mu\text{g}$  of drug after 2 h of immersion into the RB solution. However it should be noted that drug loading if required can be increased by increasing the pore diameters, thickness of TNTs, time of loading and surface chemistry.<sup>14,15</sup> We have already shown in our previous study that drug loading can be significantly increased to  $>300$   $\mu\text{g}$  on TNT-Ti wire implants with increasing diameters (140 nm) and thickness and 50  $\mu\text{m}$ .<sup>22</sup> Thus, these TNT-Ti implants could be customized to meet specific requirements for implantable drug delivery in bone, depending on the required dosage, properties of drugs, and proposed bone therapy.

**Table 1.** Summary of drug loading and *in vitro* release from TNT-Ti wire implants

Nanotube length ( $\mu\text{m}$ )	Nanotube diameter (nm)	Drug loading ( $\mu\text{g}$ )	Drug loading capacity ( $\mu\text{g}/\text{mm}^2$ )	Cumulative burst release in 6 h (%)	Cumulative release in 13-14 days (%)
$17 \pm 2$	$70 \pm 5$	$25.6 \pm 1.5$	$2.9 \pm 0.8$	$37.3 \pm 4.3$	$100 \pm 0.7$

A biphasic drug-release pattern was observed with *in vitro* release study, the first phase showing an initial burst release in the first 24 h, followed by the second phase of slow release of the remaining drug (Figure 3). The initial burst denoted by the straight portion of the curve, showed a release of about 37.5 % in first 6 h and 65 % by 24 h in buffer solution, could be regarded as a first-order release. This indicates that initial burst release could be reduced by using a small (70 nm) tube diameter when considering that our previous study showed an initial 65 % release of the same drug in 6 h with 140 nm diameter tubes, although with different dimensions and drug loading.<sup>22</sup> This initial fast release could be attributed to the fast diffusion of the drug molecules physisorbed on the top and upper parts of the TNTs.

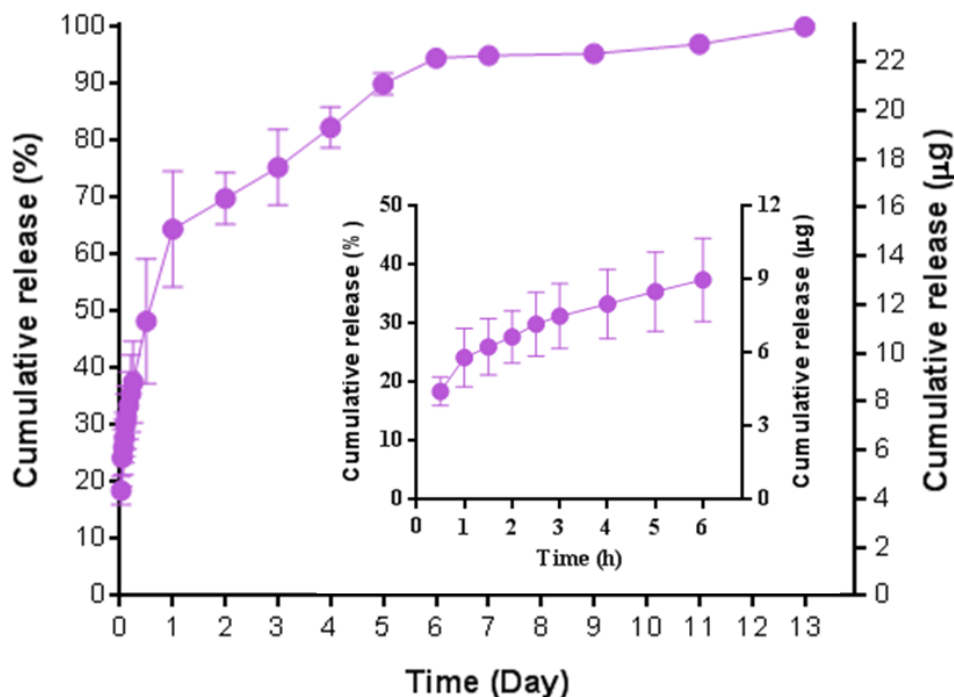


**Figure 3.** *In vitro* drug release of RB from TNT-Ti wire implants into PBS (pH 7.4). Graph indicating cumulative percentage (%) and amount released over 13 days, with an inset graph showing the first 6 h release (burst release). Data represent mean  $\pm$  SD, n=3.

Within the second phase of cumulative release, the implants showed two phases, first a slow increasing phase starting at 24 h up until 6 days and releasing about 30 % of the rest of the drug before reaching almost a steady phase until 11 days. This slow and steady release could be due to diffusion of molecules from the deep areas of the tube structures and is considered to be zero-order release, based on the Fickian diffusion law, when release rate, due to a reduction in concentration gradient, decreases as a function of time.<sup>26</sup> A zero-ordered pattern observed with any pharmaceutical dosage is considered an ideal profile of drug release because of constant drug elution rate.<sup>27</sup> These results acquired using TNT-Ti wire implants prepared with the new method are in agreement with our previous reports and showed suitable drug-releasing characteristics of the implant for local drug delivery applications.<sup>18-22</sup> Furthermore, the release kinetics can easily be tailored as demonstrated previously, by employing biopolymer modification of TNTs or drug encapsulation in polymeric micelles.<sup>17</sup>

### 3.3 *Ex vivo* drug delivery in bone studied using a bone reactor Zetos

In the next part of our study, we used individual bone cores inserted with drug loaded TNT-Ti implants inside bone chambers with peristaltic pump-driven media perfusion to investigate delivery of drug into trabecular bone cores, and the effect of marrow on the drug release and on bone integration of the implant (Figure 4a). Considering possible blood coagulation inside the marrow-containing bones, the use of anticoagulant treated bone marrow was also evaluated for *ex vivo* drug release. This bioreactor system can be utilized for studying different aspects of local drug delivery into bone, including release of drug, surface interaction and integration of biomaterials, implant stability and with the Zetos loading component, mimicking load bearing situations of bone.<sup>23,24</sup> The prepared TNTs-Ti implants were easy to insert and remove from the bone and their handling was associated with unchanged surface morphology, mechanical stability and excellent adherence of the TNT layer. An example of colour change due to release of the drug into the bone structure is shown in Figure 4b(i–iii). This change in colour clearly indicates release of drug from TNT structure and the subsequent diffusion and spread across the bone. *In situ* measurement of drug release drug were monitored by fluorescence Xenogen

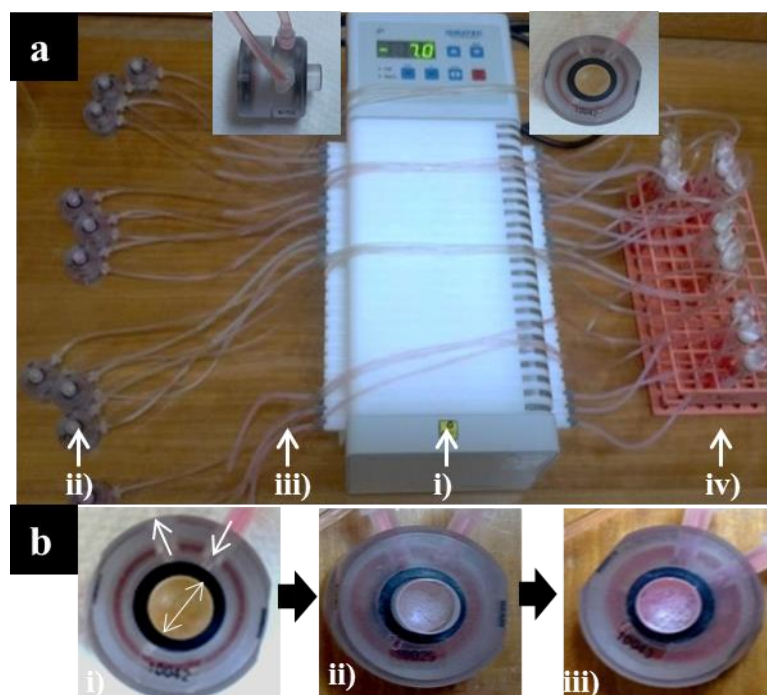


**Figure 4.** *Ex vivo* study set-up with bone bioreactor and image analysis for drug release from TNT-Ti wires. a) Bone bioreactor Zetos system includes i) peristaltic pump to flow media ii) chamber with bone core, inset



showing side and closer views iii) tubing for media inlet and outlet and iv) holder with fitted test tube to contain culture media. b) Typical representation of i-iii) visual observation of RB release from implants (white line indicating direction and position) into bone chambers using digital images acquired at i) time 0, ii) time 30 min and iii) time 1 h, indicating gradual increase of colour intensity representing model drug (RB) release.

imaging at predetermined time intervals until 11 days of the experiment and summarized in Figure 5. This figure shows the change in fluorescence intensity corresponding to the drug diffusion inside the trabecular bone core with and without of bone marrow. The fluorescence intensity change in the images confirmed the gradual release of drug from TNT-Ti wires into the bone. This non-destructive approach to monitor and measure drug release could be an important tool to guide the optimization of drug dose required to treat a disease, by allowing quantification and persistence of local drug concentrations, and also to optimize and the design of the drug-delivery implants in bone.

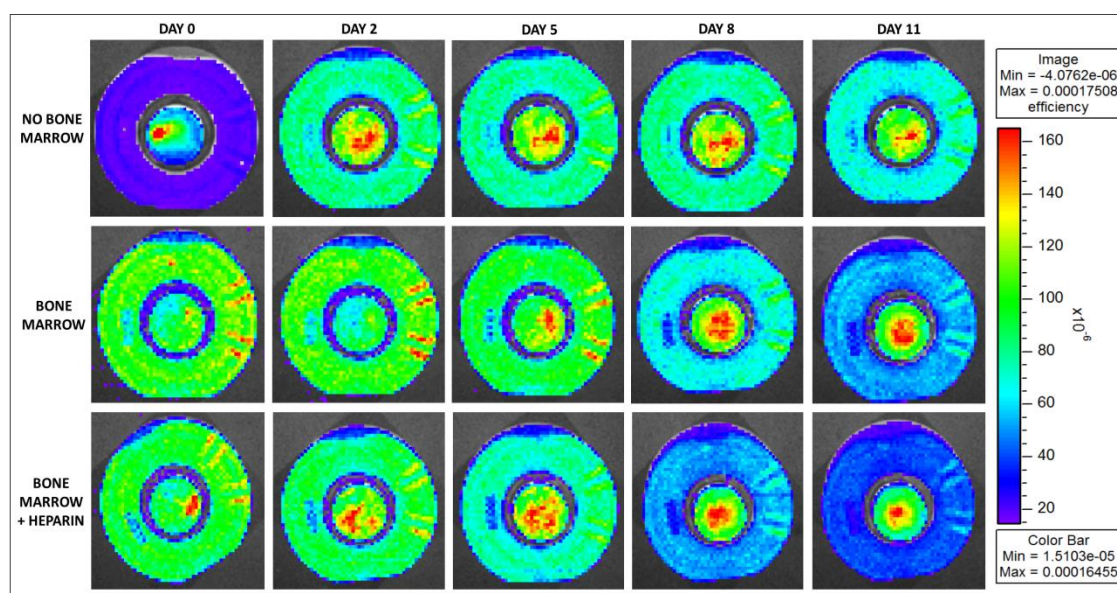


**Figure 5.** Change in fluorescence intensity corresponding to the drug diffusion inside the *ex-vivo* trabecular bone cores. Each figure represents the fluorescence signal from the drug, however for quantification, only the bone cores (inner circle) were analyzed and the background signal was subtracted. The image clearly indicates the spread of dye from the TNT/Ti Wire implant (inserted inside the bone matrix) for different bone samples considered. (Only day 0, 2, 5, 8 and 11 images are shown here)

Fluorescence intensities, which correspond to the concentrations of drug released into each of the three types of bone samples, measured from the images are presented in Figure 6(a–b). The data showed a similar trend with changes in fluorescence intensity for all three types of implanted bone, including the initial high levels evident at 30 min. The subsequent inconsistent pattern of the release may be

attributed to the variable nature of the internal bone microarchitecture of each bone core and the variable media flow as a result of this. The graph also indicates that drug release inside bone has a similar trend to *in vitro* initial burst release (Figure 3b), with *ex vivo* release showing initial very strong fluorescence intensity of about 2.0 au, decreasing to less than 0.25 au after 6 h.

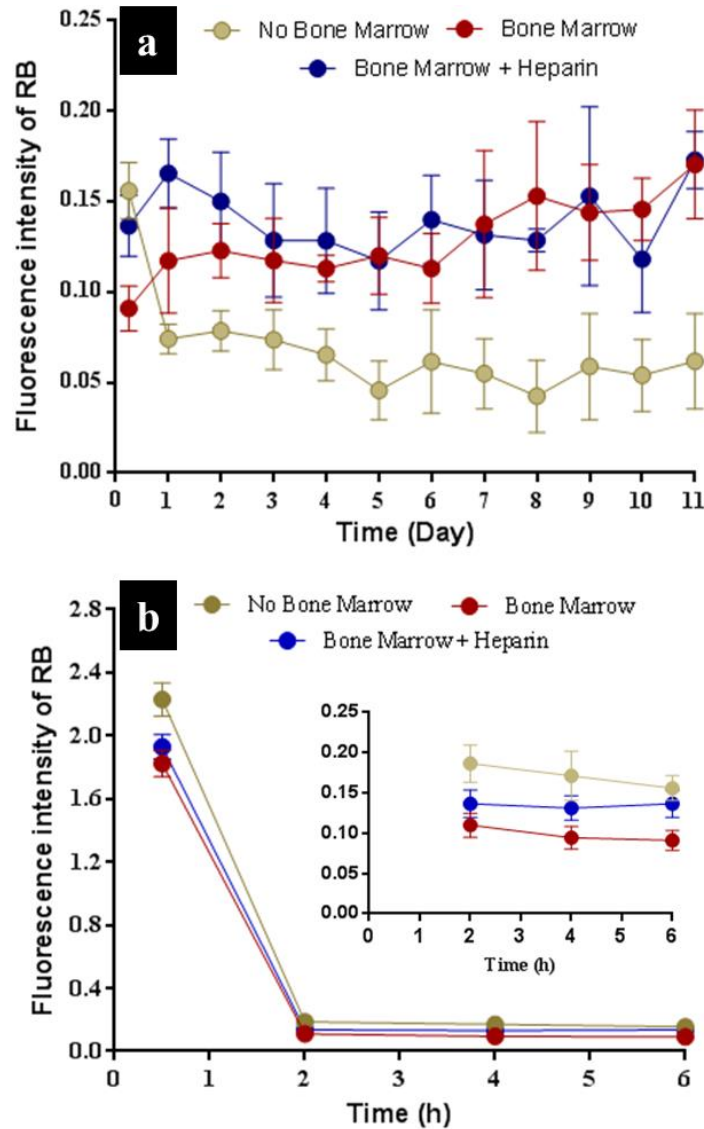


**Figure 6.** *Ex vivo* release profile of RB from TNT-Ti wire implants into marrow-less bone, and marrow- and heparin-treated marrow containing bone. Graph a) showing changes of fluorescence intensities (corresponds to concentration) of released RB measured over 11 days using an live *in vivo* imaging system and b) showing release pattern observed in first 6 h, with an inset showing graph expansion. Student *t*-test (two-tailed) and two-way analysis of variance, followed by Tukey’s multiple comparison test, were used to analyze the data with values for \* $p < 0.05$  and \*\*\* $p < 0.001$  and described into text. Data represents mean  $\pm$  SD,  $n=3$ .

After this time, fluorescence intensities remained mostly steady with little fluctuation over the 11 days experimental period. This indicated consistent and gradual release of drug, which could be considered

to display zero order kinetics similar *in vitro* observations. Compared to marrow-containing bone (including heparin treated), the first 6 h of release showed relatively higher fluorescence intensity, with a highest observed data of 2.2 au just after 30 min, in marrow-less bone. However, this initial high intensity reduced to less than 0.2 au after 60 min and remained similar up until 6 h (Figure 6b). This finding clearly indicates that a significantly ( $^{***} p < 0.001$ ) higher portion of drug was released in first 6 h in marrow-less bone compared to other groups. After one day the intensity further reduced to less than 0.1 (0.05–0.1) au and remained within the range over the 11 days of observation. This very low level of intensity indicates that a small fraction of drug was released constantly in marrow-less bone. The release of a reduced drug amount in marrow-less bone is due to uninterrupted perfusion, of the drug into the porous architecture of the bone, caused mainly by absence of marrow content. As a result of this, drug molecules were able to freely move and spread into pore spaces and be cleared from the bone with the perfused media flow. The clearance of the released drug by the media perfusion also led to a high concentration gradient near the implant and hence increased diffusive drug transport from the implants. This would explain the initial high amount of drug release observed in the first 6 h, with a sustained low release for an extended period observed later on.

On the other hand, marrow-containing bone showed an initial fluorescence intensity of 1.8 au after 30 min, which reduced to 0.1 au after 60 min and remained similar up until 6 h of observation (Figure 6b). This indicates a relatively lower amount of drug release compared to marrow-less bone in first 6 h. However, after one day the intensity was found to be increased to more than 0.1 (0.1–0.15) au and remained within the range with little fluctuation over 11 days of drug release. Each time point of measurement after one day showed significantly ( $^{***} p < 0.001$ ) higher fluorescence intensity in marrow-containing bone compared to marrow-less bone. This in turn showed the maintenance of a significantly higher overall level ( $^{***} p < 0.001$ , compared to marrow-less bone) of intensity until 11 days of release. This result clearly shows that a significant drug-retention or high level of drug was persistent in marrow-containing bone, presumably reflecting the *in vivo* scenario. The persistent increased level of drug is believed mostly due to interrupted perfusion of drug through the porous structure of the bone. Unlike marrow-less bone this interruption was primarily due to presence of

marrow content, including fat and other tissue, acting as barrier and restraining diffusion of the drug molecules across the bone.

In addition, coagulated blood inside the bone, particularly the portion of red-bone marrow, could potentially also act as a diffusion barrier. The anticoagulant heparin was used to inhibit blood coagulation and was anticipated to enhance perfusion of the drug. The heparin treated marrow-containing bone samples showed an initial fluorescence intensity of 1.9 au after 30 min, which reduced to 0.15 au after 60 min and remained steady until 6 h of drug release (Figure 6b). Compared to non-treated marrow-containing bone, this heparin treated group showed relatively higher drug level only at 4 and 6 h time points of measurement but showed significantly ( $^{***}p < 0.05$ , avg mean) higher overall level of release for up until the entire 6 h period. However, there was no significant difference observed in their overall level of release profiles up until 11 days of experiment. The very short term retention of higher drug level or drug release in the presence of heparin indicates very mild effect of the anticoagulant. Their overall non-significant differences also suggest that coagulation did not impair diffusion in the marrow-containing bone models. Rather, the presence of marrow served primarily to aid retention and therefore exposure of the local microenvironment to the test drug.

From these results, we can conclude that drug molecules released from TNTs is quickly diffused inside the empty porous bone core and cleared from it. However, drug diffusion is impeded in bone cores with either heparin treated or non-treated marrow but high retention of released drug can be achieved compared to marrow-less bone. An overall summary of these drug diffusion results is also presented in Table S2.

### **3.4 Stability and integration of TNT-Ti implants into bone**

For the application of local drug delivery via bone implants in orthopaedics, it is critical to evaluate the interaction of the implant material with the bone and bone marrow. In order to demonstrate the interaction, bone cores with inserted implants were treated to preserve their morphology at the end of *ex vivo* release study and then decalcified for easy cross-sectioning. Digital and SEM images showing the surface stability and morphology of the implants within bone are presented in Figure (7–9).

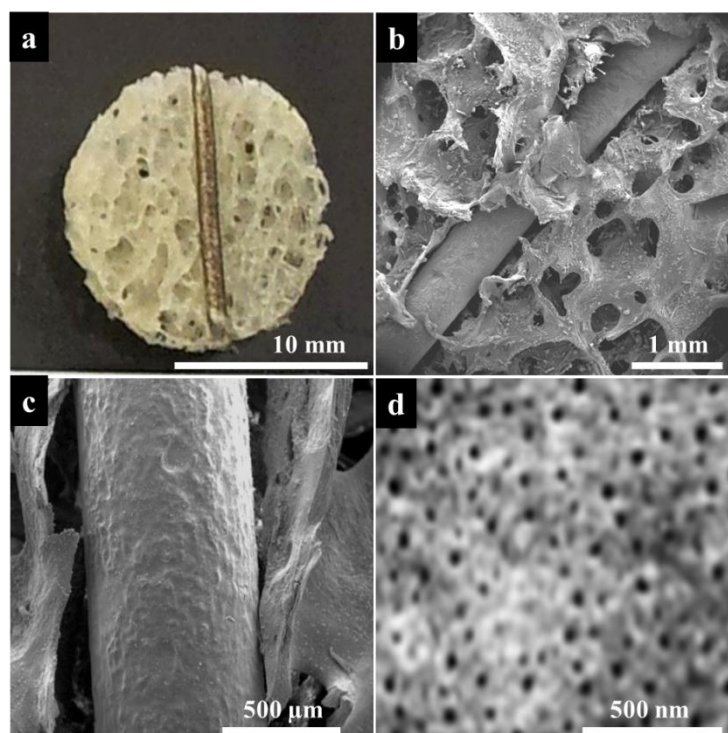


**Figure 7.** Stability and interaction of TNT-Ti wire implants in marrow-less bone. Cross sectional a) digital and b–d) series of SEM images showing porous bone structure with placement of the inserted implant, with unchanged surface morphology and clear nanotubes. The bone core samples with inserted TNT-Ti wire were collected at the end of *ex vivo* study, decalcified, cross sectioned, and specially coated with platinum for imaging purpose.

These images from inserted implants at the end of experiment confirmed no change in their characteristic colour even after 11 days of media perfusion (Figure 7a, 8a, 9a). Both low and high magnification SEM images revealed their unchanged surface texture and nanotubular morphology, also confirming that the implant insertion process did not affect their surface. TNT layers were also strong enough to withstand insertion pressure and displayed no evident damage upon extraction from the bone (data not shown). In the absence of marrow, the implants showed minimal contact and interaction with the surrounding bone and all of their TNTs appeared to be open, although with a possibility of some adhesion due to adsorption of bone material during insertion of the TNT-Ti wires (Figure 7b–d).



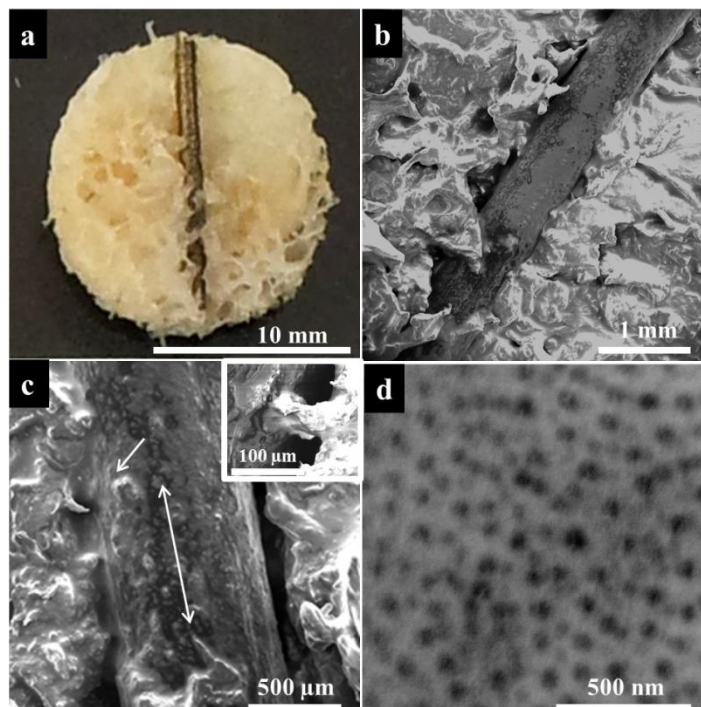


**Figure 8.** Stability and interaction of TNT-Ti wire implants in bone in presence of marrow. Cross sectional a) digital and b–d) SEM images showing porous bone with placement of the inserted implant, with surface showing organic deposit (white single and double headed arrows indicating adhesion and middle of the implant) and firm attachment in the inset as well as nanotube mouths. The bone core samples, having inserted TNT-Ti wire, were collected after the *ex vivo* study, decalcified, cross sectioned, and coated for imaging.

In the presence of marrow, the implants within bone appeared to have more secure placement and contact and some apparently firm attachments with the surrounding bone and bone marrow were observed (Figure 8b–d, 9b–d). Contrary to marrow-less bone, implants in bone marrow also showed some visible deposits, which could be due to adhesion and deposition of different bone cells, blood cells and marrow contents.<sup>28,29</sup>



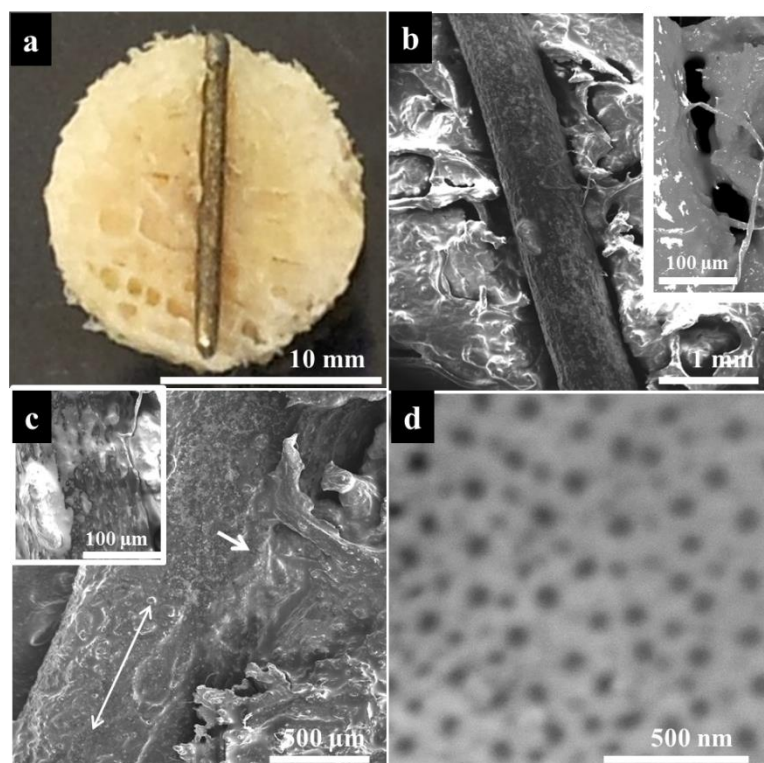


**Figure 9.** Stability and interaction of TNT-Ti wire implants in bone in presence of heparin treated marrow. Cross sectional a) digital image and b–d) series of SEM images showing porous bone structure with placement of the inserted implant, with firm attachment in the inset, with surface showing integration (white single and double headed arrows indicating integration and middle of the implant) and organic adhesion or deposit in the inset as well as nanotube mouths. With inserted TNT-Ti wire the bone core samples were collected at the end of *ex-vivo* study, decalcified, cross sectioned, and coated with platinum for imaging using SEM.

Moreover, although TNTs in some areas appeared to remain open even after 11 days of drug release, some blocked TNTs were observed, including those which cannot be seen under the thick adhesions or deposits. Interestingly, implants in the heparin treated bone marrow appeared to be fused with the bone at some areas (Figure 9b–c). However, at this stage it is difficult to estimate the surface area covered with the deposits, or the proportion of blocked TNTs, which could be explored in future studies.

EDS analysis performed on these implants to confirm the chemical composition of aggregates on their surface is presented in Figure S1. In comparison to bare implant surface showing presence of ‘Ti’ and similar to decalcified bone, all three types of implanted bone presented with common spectra. However, implants in the presence of marrow indicated the presence of ‘Fe’, in addition to ‘C’ and ‘O’ elements. The presence of ‘Fe’, an important component of haemoglobin, indicates adhesion of red

blood cells or their contents to the implant. This is consistent with several previous studies describing attachment of different molecules such as extracellular matrix, growth hormones, proteins and cells such as bone cells and blood cells upon contact with biomaterials of porous structures.<sup>30–34</sup> These EDS analysis are used as an qualitative indication of changes of surface chemistry on TNTs and more more appropriate techniques are required to confirm more details about expressed organic compounds from bone cells on TNTs surface. This attachment of various biological molecules including bone cells have been regarded beneficial to induce bone growth on to the implant surface of nanotubular structure such as TNT, leading to integration into body.<sup>35–38</sup>

To demonstrate that proposed needle puncture guided insertion of the implant into bone, contact of the implant with the bone and media perfusion preserves the viability of bone cells adjacent to the implant, histological analysis of decalcified bone using H&E staining was undertaken and is presented in Figure 10(a–d). Microscopic observation of these samples revealed the presence of mostly viable osteocytes along the edge of the drilled hole and contact of the implant in all types of bone cores tested even after 11 days of the *ex vivo* study. However, it was difficult to observe the presence of other bone cell types such as osteoblast and osteoclast using this staining technique. Overall, the results indicate that our drilling and implant insertion technique is minimally invasive.

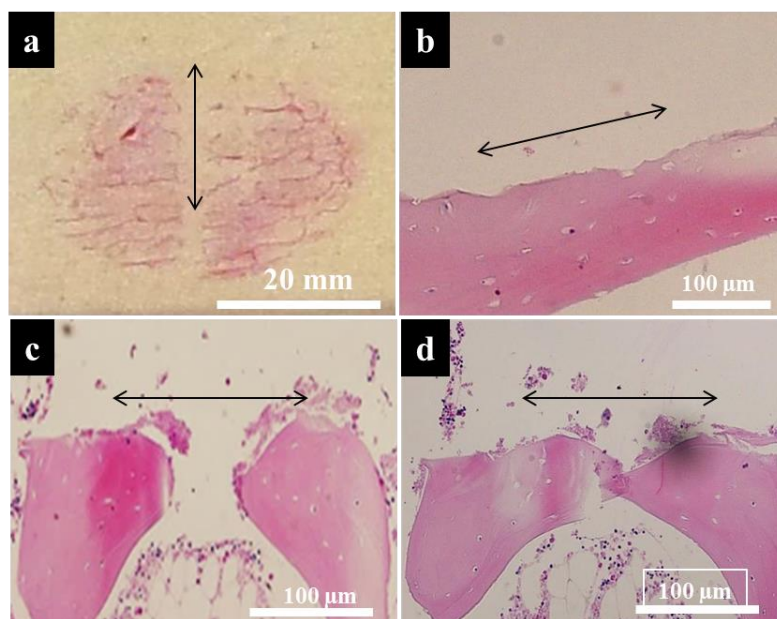


**Figure 10.** Histology of bone cores inserted with TNT-Ti wire implants. a) Digital image indicating a representative hematoxylin-eosin stained histology sample, with a double headed black arrow to locate implant

position. Light microscopic b–d) images showing presence of viable osteocytes (black dot in small white circle) along the drilled areas in b) absence of marrow c) presence of marrow and d) presence of heparin treated marrow. At the end of *ex vivo* study the bone core samples with inserted TNT-Ti wire were collected, decalcified, cross sectioned, and coated with platinum for imaging using SEM.

#### **4. CONCLUSION**

In this work, we demonstrated that simple and scalable preparation of nano-engineered TNT-Ti wire implants of small pore diameters and controllable pore lengths with drug loading ability can be undertaken by adopting and optimizing an established lactic acid-based anodization process. A simple needle puncture was shown to be an effective technique for implanting prepared drug releasing wire implants into cancellous bone. The Zetos bone reactor was successfully used to monitor *in situ* release of loaded drugs from the implants into the bone and bone marrow environment. This condition is very close to real *in vivo* bone conditions and provides option to monitor drug release from the implants for an extended period using a non-destructive live imaging technique. This study revealed that distribution of drug from the implants in presence of bone marrow results in reduced drug perfusion or distribution and increased retention compared to absence of bone marrow. Considering the microenvironment and interfacial properties of bone marrow, we speculate that distribution of drug will be influenced by the size and hydrophobicity/hydrophilicity of the molecules and this fact will be explored in our future study. The physical or surface stability of the implants after implantation and drug release study is confirmed. However, the surface of the implants appeared to have biological deposits and it is likely that these could facilitate their integration into bone over the time. The presented wire implantation approach is proposed to be minimally invasive with preserving the viability of surrounding osteocytes, which is potentially important to avoid a bone remodeling response adjacent to the inserted implants. Overall, this study indicates a great potential of this method to directly apply TNT-Ti therapeutic implants for localized bone therapy for a number of bone disease scenarios.

## **ACKNOWLEDGMENTS**

The authors acknowledge the financial support of the Australian Research Council (FT110100711 and DP 120101680) and the University of Adelaide for this work. Authors also acknowledge the technical support from Dr Agatha Labrinidis at The Adelaide Microscopy, The University of Adelaide.

## **ASSOCIATED CONTENT**

### **Supporting Information**

S1) SEM-EDS characterization of bone materials deposited on the TNT-Ti wire implants surfaces and a table summarising and Table S2) Factors influencing drug diffusion inside the bone microenvironment.

### **Notes**

The authors declare no competing financial interest.

## **REFERENCES**

1. Wu P, Grainger DW. Drug/device combinations for local drug therapies and infection prophylaxis. *Biomaterials* **2006**, 27(11), 2450–2467.
2. Buchholz HW, Elson RA, Engelbrecht E, Lodenkamper H, Rottger J, Siegel A. Management of deep infection of total hip replacement. *J. Bone Jt Surg. Br.* **1981**, 63, 342–353.
3. Porter JR, Ruckh TT, Popat KC. Bone tissue engineering: a review in bone biomimetics and drug delivery strategies. *Biotechnol. Prog.* **2009**, 25(6), 1539–1560.
4. Ginebra MP, Traykova T, Planell JA. Calcium phosphate cements: competitive drug carriers for the musculoskeletal system? *Biomaterials* **2006**, 27(10), 2171–2177.
5. Passuti N, Gouin F. Antibiotic-loaded bone cement in orthopaedic surgery. *Jt Bone Spine* **2003**, 70(3), 169–174.
6. Zalavras CG, Patzakis MJ, Holtom P. Local antibiotic therapy in the treatment of open fractures and osteomyelitis. *ClinOrthopRelat Res.* **2004**, 427, 86–93.
7. Colilla M, Manzano M, Vallet-Regi M. Recent advances in ceramic implants as drug delivery systems for biomedical applications. *Int. J. Nanomed.* **2008**, 3(4), 403–414.

8. Hoppe A, Güldal NS, Boccaccini AR. A review of the biological response to ionic dissolution products from bioactive glasses and glass-ceramics. *Biomaterials* **2011**, 32(11), 2757–2774.
9. Liu H, Webster TJ. Nanomedicine for implants: a review of studies and necessary experimental tools. *Biomaterials* **2007**, 28(2), 354–369.
10. Losic D, Velleman L, Kant K, Kumeria T, Gulati K, Shapter JG, Beattie DA, Simovic S, Self-ordering electrochemistry: a simple approach for engineering nanopore and nanotube arrays for emerging applications, *Aust. J. Chem.* **2011**, 64,294–01.
11. Roy P, Berger S, Schmuki P. TiO<sub>2</sub> nanotubes: synthesis and applications. *Angew Chem. Int. Ed. Engl.* **2011**, 50(13), 2904–2939.
12. Rani S, Roy SC, Paulose M, Varghese OK, Mor GK, Kim S, Yoriya S, Latempa TJ, Grimes CA. Synthesis and applications of electrochemically self-assembled titania nanotube arrays. *Phys Chem Chem Phys* **2010**, 12(12), 2780–800.
13. Ghicov A, Schmuki P. Self-ordering electrochemistry: a review on growth and functionality of TiO<sub>2</sub> nanotubes and other self-aligned MO(x) structures. *Chem Comm (Camb)* **2009**, 2, 2791–2808.
14. Losic D, Simovic S. Self-ordered nanopore and nanotube platforms for drug delivery applications. *Expert Opin. Drug Deliv.* **2009**, 6(12), 1363–1381.
15. Losic D, Aw MS, Santos A, Gulati K, Bariana M. Titania nanotube arrays for local drug delivery: recent advances and perspectives *Expert Opin. Drug Deliv.* **2015**, 12 (1), 103–127.
16. Santos A, Aw MS, Bariana M, Kumeria T, Wang Y, Losic D. Drug-releasing implants: Current progress, challenges and perspectives. *J. Mater. Chem. B* **2014**, 2 (37), 6157–6182.
17. Gulati K, Aw MS, Losic D. Controlling drug release from titania nanotube arrays using polymer nanocarriers and biopolymer Coating. *J. Biomater. Nanobiotechnol.* **2011**, 2, 477–484.
18. Aw MS, Addai-Mensah J, Losic D. Multi-drug delivery system with sequential release using titania nanotube arrays. *Chem Comm* **2012**, 48, 3348–3350.
19. Gulati K, Ramakrishnan S, Aw MS, Atkins GJ, Findlay DM, Losic D. Biocompatible polymer coating of titania nanotube arrays for improved drug elution and osteoblast adhesion. *Acta Biomater.* **2012**, 8, 449–456.
20. Gulati K, Aw MS, Losic D. Nanoengineered drug-releasing Ti wires as an alternative for local delivery of chemotherapeutics in the brain. *Int. J. Nanomed.* **2012**, 7, 2069–2076.
21. Gulati K, Atkins GJ, Findlay DM, Losic D. Nano-engineered titanium for enhanced bone therapy. *Proc. SPIE Biosensing Nanomed. VI* **2013**, 8812, 88120C–1.

22. Aw MS, Khalid KA, Gulati K, Atkins GJ, Pivonka P, Findlay DM, Losic D. Characterization of drug-release kinetics in trabecular bone from titania nanotube implants. *Int. J. Nanomed.* **2012**, 7, 4883–4892.
23. Davies CM, Jones DB, Stoddart MJ, Koller K, Smith E, Archer CW, Richards RG. Mechanically loaded ex vivo bone culture system ‘Zetos’: systems and culture preparation. *Eur. Cell Mater.* **2006**, 11, 57–75.
24. Jones DB, Broeckmann E, Pohl T, Smith EL. Development of a mechanical testing and loading system for trabecular bone studies for long term culture. *Eur. Cell Mater.* **2003**, 5, 48–59.
25. So S, Lee K, Schmuki P. Ultrafast growth of highly ordered anodic TiO<sub>2</sub> nanotubes in lactic acid electrolytes. *J. Am. Chem. Soc.* **2012**, 134, 11316–11318.
26. Gulati K, Aw MS, Findlay D, Losic D. Local drug delivery to the bone by drug releasing implants: perspectives of nanoengineered titania nanotube arrays. *Ther. Deliv.* **2012**, 3, 857–873.
27. Gulati K, Aw MS, Losic D. Drug-eluting Ti wires with titania nanotube arrays for bone fixation and reduced bone infection. *Nanoscale Res. Lett.* **2011**, 6, 571–576.
28. Bjursten LM, Rasmusson L, Oh S, Smith GC, Brammer KS, Jin S. Titanium dioxide nanotubes enhance bone bonding in vivo. *J. Biomed. Mater. Res. A* **2010**, 92, 1218–1224.
29. Popat KC, Leoni L, Grimes CA, Desai TA. Influence of engineered titania nanotubular surfaces on bone cells. *Biomaterials* **2007**, 28, 3188–3197.
30. Tan AW, Pinguan-Murphy B, Ahmad R, Akbar SA. Review of titania nanotubes: Fabrication and cellular response. *Ceram. Int.* **2012**, 38(6), 4421–4435.
31. Anselme K, Ploux L, Ponche A. Cell/material interfaces: Influence of surface chemistry and surface topography on cell adhesion. *J. Adhes. Sci. Technol.* **2010**, 24(5), 831–852.
32. Oh S, Daraio C, Chen LH, Pisanic TR, Finones RR, Jin S. Significantly accelerated osteoblast cell growth on aligned TiO<sub>2</sub> nanotubes. *J. Biomed. Mater. Res. Part A* **2006**, 78A, 97–103.
33. Park J, Bauer S, Schlegel KA, Neukam FW, Vonder Mark K, Schmuki P. TiO<sub>2</sub> nanotube surfaces: 15 nm—an optimal length scale of surface topography for cell adhesion and differentiation. *Small* **2009**, 5(6), 666–671.
34. David V, Guignandon A, Martin A, Malaval L, Lafage-Proust MH, Rattner A, Mann V, Noble B, Jones DB, Vico L. *Ex vivo* bone formation in bovine trabecular bone cultured in a dynamic 3D bioreactor is enhanced by compressive mechanical strain. *Tissue Eng. Part A* **2008**, 14(1), 117–126.
35. Arvidsson A, Franke-Stenport V, Andersson M, Kjellin P, Sul YT, Wennerberg A. Formation of calcium phosphates on titanium implants with four different bioactive surface preparations, an *in vitro* study. *J. Mater. Sci.: Mater. Med.* **2007**, 18 (10), 1945–1954.



36. Von WC, Bauer S, Lutz R, Meisel M, Neukam FW, Toyoshima T, Schmuki P, Nkenke E, Schlegel KA. *In vivo* evaluation of anodic TiO<sub>2</sub> nanotubes: an experimental study in the pig. *J. Biomed. Mater. Res. B Appl. Biomater.* **2009**, 89B (1),165–171.
37. Xiao J, Zhou H, Zhao L, Sun Y, Guan S, Liu B, Kong L. The effect of hierarchical micro/nanosurface titanium implant on osseointegration in ovariectomized sheep. *Osteoporos Int.* **2011**, 22(6),1907–1913.
38. Park JM, Koak JY, Jang JH, Han CH, Kim SK, Heo SJ. Osseointegration of anodized titanium implants coated with fibroblast growth factor-fibronectin (FGF-FN) fusion protein. *Int. J. Oral Maxillofac. Implants* **2006**, 21(6), 859–866.

# Supporting Information

## ***Ex-Vivo* Implantation of Nano-Engineered Implants: Investigating Drug Diffusion and Integration inside the Bone Microenvironment**

Shafiur Rahman<sup>1\*</sup>, Karan Gulati<sup>1\*</sup>, Masakazu Kogawa<sup>2</sup>, Gerald J. Atkins<sup>2</sup>, Peter Pivonka<sup>3</sup>,  
David M. Findlay<sup>2</sup>, Dusan Losic<sup>1</sup>✉

<sup>1</sup>School of Chemical Engineering, University of Adelaide, SA, Australia

<sup>2</sup>Discipline of Orthopaedics & Trauma, University of Adelaide, SA, Australia

<sup>3</sup>Australian Institute for Musculoskeletal Science, University of Melbourne, VIC, Australia

\*Equal first author status

✉Corresponding Author: Prof. Dusan Losic,

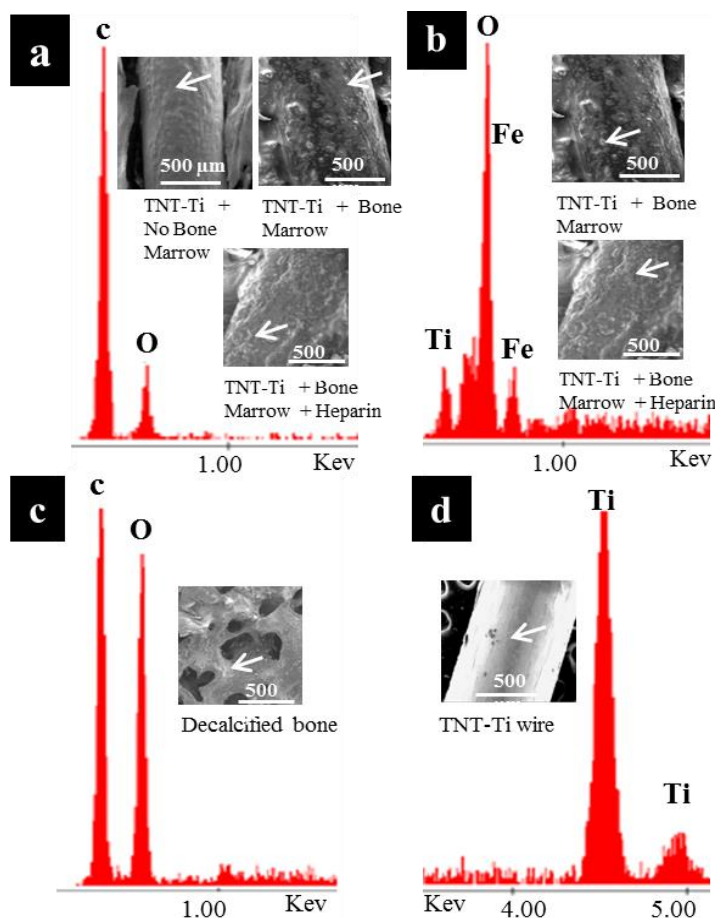
School of Chemical Engineering,

The University of Adelaide,

Adelaide, SA5005 Australia,

Phone: +61 8 8013 4648,

Email: *dusan.losic@adelaide.edu.au*



**S1.** SEM-EDS characterization of bone materials deposited on the TNT-Ti wire implants surfaces. a) The implants in all three types of bone indicating presence of majorly ‘C’ and ‘O’ which were also found in c) decalcified bone, with d) bare TNT-Ti wire surface indicating presence of ‘Ti’. b) Implants in both types of bone marrow showed the presence of ‘Fe’, in addition to other elements of c) decalcified bone. The bone core samples with inserted TNT-Ti wire were collected at the end of *ex-vivo* study, decalcified, cross sectioned, and specially coated with platinum for imaging purpose.

**Table S2.** Factors influencing diffusion of model drug (RB) inside the bone microenvironment.

<b>Factors Influencing Drug Diffusion</b>	<b>No Bone Marrow (No BM)</b>	<b>Bone Marrow (BM)</b>	<b>Bone Marrow + Heparin (BM + HEP)</b>
Blood coagulation	N.A.	Marrow coagulates and impedes media perfusion and drug diffusion	Marrow coagulation is prevented via addition of anti-coagulant (HEP)
Diffusion of drug molecules from TNTs inside the bone core	Very fast, as empty porous architecture of bone (filled with media) increases the diffusion gradient	Presence of marrow and its coagulation blocks the open pores of TNTs and reduces the diffusion gradient	Presence of marrow (which is uncoagulated) partially impedes the diffusion of dye
Perfusion of media in the bone core	Very effective and results in quick removal of drug molecules from inside the bone, thereby maintaining the diffusion gradient	Very restricted and almost negligible (in the later phase of experiment) due to coagulated marrow	Partially effective as the marrow impedes the flow of culture media, thereby the clearing rate of dye is reduced

## **APPENDIX B**

---

# **NANO-ENGINEERED TITANIUM for ENHANCED BONE THERAPY**

**Karan Gulati**

School of Chemical Engineering, University of Adelaide, South Australia 5005, Australia

**K. Gulati**, G. J. Atkins, D. M. Findlay, D. Losic “Nano-engineered titanium for enhanced bone therapy”. Proc SPIE Biosensing and Nanomedicine VI 2013: published online 11 September 2013, doi:10.1117/12.2027151

## Nano-engineered titanium for enhanced bone therapy

Karan Gulati<sup>\*a</sup>, Gerald J. Atkins<sup>b</sup>, David M. Findlay<sup>b</sup>, Dusan Losic<sup>a</sup>

<sup>a</sup> School of Chemical Engineering, The University of Adelaide, Adelaide, SA, Australia;

<sup>b</sup> Centre for Orthopaedic & Trauma Research, The University of Adelaide, Adelaide, SA, Australia

### ABSTRACT

Current treatment of a number of orthopaedic conditions, for example fractures, bone infection, joint replacement and bone cancers, could be improved if mechanical support could be combined with drug delivery. A very challenging example is that of infection following joint replacement, which is very difficult to treat, can require multiple surgeries and compromises both the implant and the patient's wellbeing. An implant capable of providing appropriate bio-mechanics and releasing drugs/proteins locally might ensure improved healing of the traumatized bone. We propose fabrication of nanoengineered titanium bone implants using bioinert titanium wires in order to achieve this goal. Titanium in the form of flat foils and wires were modified by fabrication of titania nanotubes (TNTs), which are hollow self-ordered cylindrical tubes capable of accommodating substantial drug amounts and releasing them locally. To further control the release of drug to over a period of months, a thin layer of biodegradable polymer PLGA poly(lactic-co-glycolic acid) was coated onto the drug loaded TNTs. This delayed release of drug and additionally the polymer enhanced bone cell adhesion and proliferation.

**Keywords:** Bone implants, titania nanotubes, local drug delivery, bone therapeutics, bone healing, bone infection

### INTRODUCTION

Healing of bone fracture requires mechanical support such as that provided by titanium plates and screws. There are some circumstances, such as infection of the bone, where pharmacological therapy is also required. However, currently treatment of bone with drugs, such as antibiotics or anti-cancer drugs, is performed using systemic drug delivery, which both limits the amount of drug available at the bone site and exposes all tissues to the drug [1]. A potential solution to this dilemma lies in producing implants that combine mechanical support with enhanced therapeutic action [2].

Because of their biological inertness, titanium metal and its alloys are good candidates for bone implants and hence have been well researched and utilized extensively for both orthopedic and dental applications [3]. Titanium also has established biocompatibility and osseointegration characteristics. Various therapeutic coatings have been tested on titanium implants, including antibiotics, biopolymers, to combine bone fixation with therapeutics [4,5]. However, rapid drug diffusion and unfavorable release patterns have compromised these approaches [6]. In order to achieve prolonged drug release, drugs have been mixed with various polymers, such as PMMA or poly(methyl methacrylate), but these do not offer sufficient mechanical support and release toxic degradation byproducts [7]. Nanostructuring on titanium has been suggested to incorporate greater drug amounts and enhance bone cell functions [8]. We have suggested an alternative approach to local delivery of drug to bone sites, that has the additional advantage of the ability to load substantial amounts and delayed release kinetics of drug. This approach involves the fabrication of titania nanotubes (TNTs) on titanium surfaces, such as orthopaedic implants. TNTs, which are nano-scale vacant cylinders composed of titanium dioxide (TiO<sub>2</sub>), can be self-ordered onto titanium substrates by electrochemical anodisation [3]. TNTs can easily be integrated into current titanium implant technology and offer improved bioactivity, mechanics and surface modification, as compared to conventional implants. The biomedical applications of TNTs include delayed drug release, enhanced bone cell adhesion/ proliferation, better integration into bone and improved bone healing [9,10,11].

In addition to conventional orthopaedic implants, nano-scale implant devices that can be surgically inserted into bone, and which are capable of releasing antibiotics, hormones, chemotherapeutics and growth factors in an effective concentration directly where they are required provides a potential solution to local drug delivery in bone. We hereby describe the production of titanium wires (diameter 0.75 mm and length 25 mm) with titania nanotubes fabricated onto the surface, which can be loaded with various drugs, each catering to a particular bone condition. TNTs have been loaded with anti-inflammatory drugs, antibiotics, and anti-cancer drugs in order to develop this novel technology aiming at



effective treatment of, for example, osteoporosis, osteomyelitis (bone infection) and primary (osteosarcoma) and metastatic (e.g. breast or prostate) bone cancer.

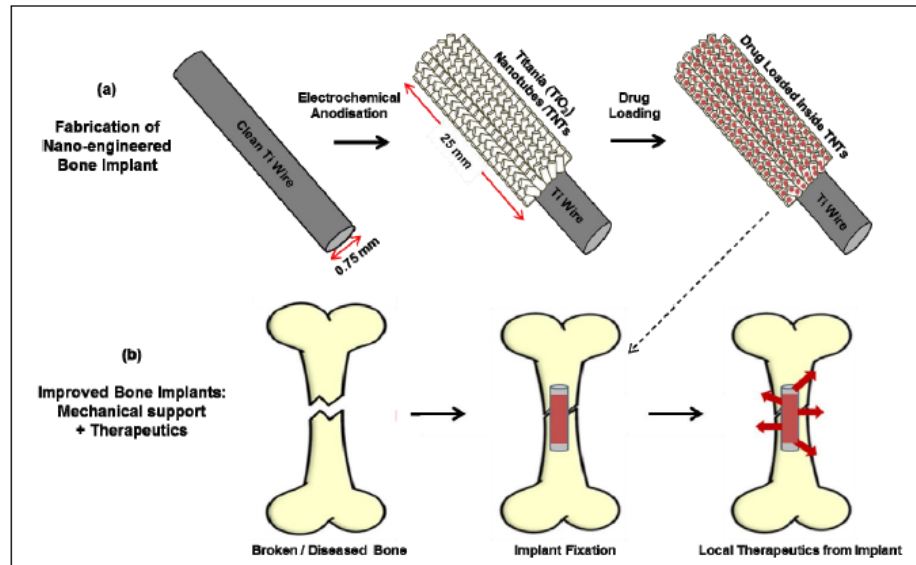


**Figure 1.** Scheme depicting (a) fabrication of titania nanotubes (TNTs) on Ti wires and drug loading into the nanotubes, and (b) adaptation of the technology to produce a bone implant that combines biomechanical support with nanotube-based drug release

## MATERIAL AND METHODS

### 1.1 Materials

Titanium wire (99.7%) (diameter 0.75 mm) and flat foil (thickness 0.25 mm) was supplied by Alfa Aesar (MA, USA). Ethylene glycol, ammonium fluoride ( $\text{NH}_4\text{F}$ ), PLGA, indomethacin, gentamicin sulfate and doxorubicin hydrochloride were purchased from Sigma-Aldrich (New South Wales, Australia). High purity Milli-Q water (Millipore Co., Billerica, MA, USA), ultra-pure grade (18.2 M $\Omega$ ) and sieved through a 0.22-  $\mu\text{m}$  filter was used.

### 1.2 Fabrication of Titania Nanotubes

Titanium wires were mechanically polished using coarse/fine sand papers and porous alumina powder, followed by extended sonication in ethanol and acetone. Anodisation of the cleaned Ti wires was performed using a specially designed electrochemical cell and computer-controlled power supply (Agilent Technologies Inc.) as described previously [12]. 25 mm of the Ti wire was exposed to the electrolyte (3% water, 0.3 %  $\text{NH}_4\text{F}$  in ethylene glycol) and anodisation was carried out at 100 V for 1 hr at 20°C. For anodisation of flat Ti foil, a similar method was adopted with only a circular area (of diameter 12 mm) exposed for anodisation. The voltage and current signals were adjusted and continuously recorded during the fabrication process by specialised software (Labview, National Instruments, Austin, TX, USA). The structural characterisation of the prepared TNT samples was performed using a field emission scanning electron microscope or SEM (Philips XL 30, SEMTech Solutions, Inc., North Billerica, MA, USA).

### 1.3 Drug loading and analysis

Drug solutions (1% w/v) of gentamicin (Genta) and doxorubicin (Doxo) were prepared in water and for indomethacin (Indo) in pure ethanol. TNT/Ti wires were cleaned with deionised water and dried in  $\text{N}_2$ . Loading for each of the model drug was achieved by immersion of TNTs in a fixed volume of respective drug solution for 24 h. Following this, the TNTs were dried and quickly flushed with a fixed volume of sterile phosphate buffer saline (PBS) in order to remove

any surface adhered drug. To determine the amount of drug loaded, thermo-gravimetric analysis (TGA) was performed with analysis of the characteristic drug decomposition peak for each model drug. TNT/Ti Flat preloaded with indomethacin was dip-coated with a thin layer of PLGA solution (1% (w/v) in chloroform) in an attempt to delay the release of the drug.

#### 1.4 *In-vitro* drug release

Drug loaded TNTs were immersed in 5ml PBS in a vial and the absorbance of the solution was measured at predetermined time intervals using UV-Vis spectroscopy. Each measurement involved removing a 3ml aliquot of PBS, measuring absorbance at a particular wavelength (characteristic for each model drug) and later replenishing the vial with fresh PBS (3 ml). The absorbance readings were converted into concentration using a calibration curve for the corresponding drug. Ultimately, the release profiles of each experimental set were expressed as burst (initial 6 h) and delayed release (every 24 h) in a plot with released weight percentage (wt. %) vs. time.

## RESULTS

#### 1.5 Structural Characterization of TNTs

The morphology of TNTs fabricated on Ti wires as characterised by SEM is depicted in figure 2. Figure 2a shows a top view of the TNTs with clearly visible open pores. TNTs were observed to have an average pore diameter of  $180 \pm 10$  nm and length of  $70 \pm 5$   $\mu$ m. The dimensions of these nanostructures could be further tailored as per the requirements; for instance, accommodating more drug or controlling its release [13]. Figure 2b shows the closed bottom of the TNTs as observed after scratching the TNT layer from the underlying substrate. The TNT layer also had few surface cracks, which is the result of radial outgrowth and mechanical stress during the fabrication of TNTs on the circular surface of the Ti wire. However, the overall structure of TNT on Ti wire was very stable, and the presence of few cracks aided in loading increased drug amounts. SEM imaging of TNTs revealed well-aligned nanotubes using this method (Fig. 2c). PLGA polymer coating resulted in effective covering of open pores, as shown in the case of indomethacin loaded TNTs fabricated on flat Ti (Fig. 2d).

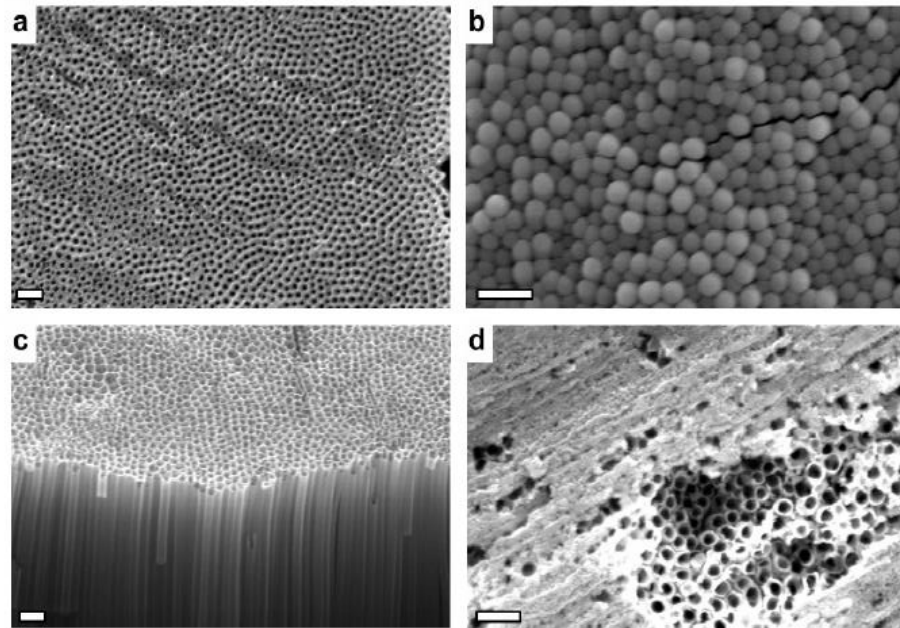


**Figure 2.** Scanning electron microscopy (SEM) images showing (a) top view of TNTs with open pores, (b) bottom of TNTs (closed pore) obtained by removal of TNT layer, (c) cross-section with well-aligned nanotubes and, (d) PLGA



coated onto drug loaded TNTs fabricated on a flat Ti substrate to delay drug release (scratched to show underlying nanotubes). All scale bars represent 1  $\mu\text{m}$ .

### 1.6 Drug loading

Three model drugs including Indo, Genta and Doxo were loaded into nanotubes, with each drug representing a varied chemistry, water solubility and structural weight, catering to specific bone conditions. TGA studies confirmed the loaded amounts of drugs in the TNTs on Ti wire as 0.16 mg, 0.2 mg and 1.2 mg for Indo, Genta and Doxo, respectively. TNTs with large pore diameters and lengths ensured substantial drug loading amounts, which can be further tailored by adjusting TNT dimensions, immersion times and drug solution concentrations. Variations in the amount of drug loaded were as a result of the relative attributes of the drugs with respect to their different chemistries and molecular weights. While more drug was retained inside of TNTs (post-washing the surfaces with PBS) in cases of the hydrophilic Genta and Doxo, less of the hydrophobic Indo could be loaded due the hydrophilic TNT interior walls. Due to its hydrophobic nature, more amount of Indo is expected to be loaded near the open pore of the TNTs as compared to deeper loading expected for hydrophilic drugs.

Drug Loaded	Loaded Amount (mg)	Initial Burst Release (Wt. %)	Total Release Time (Days)
Indomethacin	0.16	74	10
Gentamicin	0.20	36	11
Doxorubicin	1.20	25	8

Table 1. Release characteristics of model drugs from nanotubes.

### 1.7 Drug release profile

A biphasic release pattern with high initial burst release (IBR for 1<sup>st</sup> 6 hrs) followed by slow sustained release was observed for each of the model drugs, as represented in figure 3a. The drug loaded near the open pores would be eluted initially at a faster rate due to the high concentration gradient at the start of the release experiment. The slow release in the later phase is due to the diminishing concentration of drug remaining in the nanotubes. This kind of release pattern would be beneficial to treat severe conditions, such as bacterial infection, by delivering a high initial dose to reduce pathogen number, followed by a sustained release period to inhibit residual pathogen growth and thereby reduce the recurrence of bacterial adhesion [14]. For the IBR, around 74, 36 and 25 Wt. % of the Indo, Genta and Doxo were released from the TNTs, respectively. As most of the Indo is expected to be loaded near the open ends of the tubes (due to its hydrophobic nature), and hence in the initial phase of high concentration gradient, quick release is observed. The amount released of the hydrophobic Indo is very high but could be further reduced by applying a thin layer of biopolymer in order to cover the open pores, as described previously [13]. The total release of the drugs from the TNTs (~ 100% wt.) occurred over 10, 11 and 8 days for Indo, Genta and Doxo, respectively, from the surfaces of the TNT/Ti wire implants. This phenomenon again correlates with the varied water solubility, and the molecular weights of the model drugs which may have influenced not only the corresponding amounts that could be loaded but also the release behaviour. Table 1 summarises the drug loading amounts and release behaviours of the three model drugs from the TNT wire. For Indo loaded TNT/Ti flat foil, a thin layer of PLGA (2.5 $\mu\text{m}$ ), as confirmed by ellipsometry, reduced the IBR (from 77% to approximately 12%) and the total release was also delayed from 4 to 31 days, as compared with the uncoated samples (Fig. 3b). This delayed release technology could potentially be extended to TNT/Ti wires but this will require extensive further optimisation.

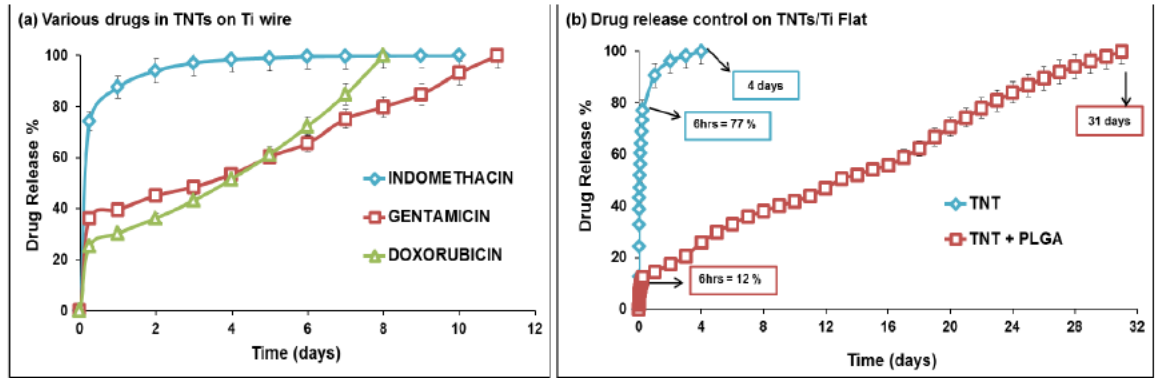


**Figure 3.** Plots showing release of loaded drug from TNTs into the surrounding PBS: (a) release of various drugs from TNT/Ti wires and, (b) controlled release of indomethacin from TNTs fabricated on Ti flat foil and coated with PLGA.

### CONCLUSION

Titania nanotubes (TNTs) were successfully fabricated on the entire cylindrical surface area of the Ti wire. The TNTs were later loaded with a variety of model drugs, each catering to a particular bone condition, such as osteoporosis, bone infection and bone cancer. The release from the TNTs was sustained for over 10 days, which could be further extended using biopolymer coatings. These proposed wire bone implants of just 25 mm length and 0.75 mm diameter could easily be inserted inside traumatised bone and hence local drug elution could be achieved directly at the required site, potentially leading to enhanced therapeutic effects and faster bone healing.

### REFERENCES

- [1] Tran, P.A., Sarin, L., Hurt, R.H. et al., "Opportunities for nanotechnology-enabled bioactive bone implants," *J. Mater. Chem.* 19(18), 2653-9 (2009)
- [2] Gulati, K., Aw, M.S., Findlay, D. et al., "Local drug delivery to the bone by drug-releasing implants: perspectives of nano-engineered titania nanotube arrays," *Ther. Deliv.* 3(7), 857-73 (2012).
- [3] Losic, D., Simovic, S., "Self-ordered nanopore and nanotube platforms for drug delivery applications," *Expert Opin. Drug Deliv.* 6(12), 1363-81(2009).
- [4] Harris, L.G., Mead, L., Muller-Oberlander, E. et al., "Bacteria and cell cytocompatibility studies on coated medical grade titanium surfaces. *J. Biomed. Mater. Res. A.* 78A(1), 50-8 (2006).
- [5] Okada, M., Yasuda, S., Kimura, T. et al., "Optimization of amino group density on surfaces of titanium dioxide nanoparticles covalently bonded to a silicone substrate for antibacterial and cell adhesion activities," *J. Biomed. Mater. Res. A.* 76A(1), 95-101 (2006).
- [6] Hetrick, E.M., Schoenfisch, M.H., "Reducing implant-related infections: active release strategies," *Chem. Soc. Rev.* 35(9), 780-9 (2006).
- [7] Harper, E.J., "Bioactive bone cements," *Proc. Inst. Mech. Eng. H.* 212(H2), 113-20 (1998).
- [8] Webster, T.J., Ejiogor, J.U., "Increased osteoblast adhesion on nanophase metals: Ti, Ti6Al4V, and CoCrMo," *Biomaterials.* 25(19), 4731-9 (2004).
- [9] Yao, C., Webster, T.J., "Prolonged Antibiotic Delivery From Anodized Nanotubular Titanium Using a Co-precipitation Drug Loading Method," *J. Biomed. Mater. Res. B Appl. Biomater.* 91B(2), 587-95 (2009).
- [10] Zhao, L., Wang, H., Huo, K. et al., "Antibacterial nano-structured titania coating incorporated with silver nanoparticles," *Biomaterials.* 32(24), 5706-16 (2011).
- [11] Popat, K.C., Leoni, L., Grimes, C.A., et al., "Influence of engineered titania nanotubular surfaces on bone cells," *Biomaterials.* 28(21), 3188-97 (2007).

[12] Gulati, K., Aw, M.S., Losic, D., “Drug-eluting Ti wires with titania nanotube arrays for bone fixation and reduced bone infection,” *Nanoscale Res. Lett.* 6(1), 571-76 (2011).

[13] Gulati, K., Ramakrishnan, S., Aw, M.S. et al., “Biocompatible polymer coating of titania nanotube arrays for improved drug elution and osteoblast adhesion,” *Acta Biomater.* 8(1), 449-56 (2012).

[14] Hickok, N.J., Shapiro, I.M., “Immobilized antibiotics to prevent orthopaedic implant infections,” *Adv. Drug Deliv. Rev.* 64(12), 1165-76 (2012).

## **APPENDIX C**

---

# **LOCAL DRUG DELIVERY in BONE by DRUG RELEASING IMPLANTS: PERSPECTIVES of NANO-ENGINEERED TITANIA NANOTUBES**

**Karan Gulati**

School of Chemical Engineering, University of Adelaide, South Australia 5005, Australia

**K. Gulati**, M. S. Aw, D. Findlay, D. Losic “Local Drug Delivery in Bone by Drug Releasing Implants: Perspectives of Nano-Engineered Titania Nanotubes” *Therapeutic Delivery*, 2012, **3**, 857.



Gulati, K., Aw, M.S., Findlay, D. & Losic, D. (2012). Local Drug Delivery in Bone by Drug Releasing Implants: Perspectives of Nano-Engineered Titania Nanotubes. *Therapeutic Delivery*, 3(7), 857-873.

NOTE:

This publication is included on pages 266 - 282 in the print copy of the thesis held in the University of Adelaide Library.

It is also available online to authorised users at:

<http://dx.doi.org/10.4155/TDE.12.66>

## **APPENDIX D**

---

# **TITANIA NANOTUBES for LOCAL DRUG DELIVERY from IMPLANT SURFACES**

**Karan Gulati**

School of Chemical Engineering, University of Adelaide, South Australia 5005, Australia

**K. Gulati**, M. Kogawa, S. Maher, G. Atkins, D. Findlay, D. Lopic “Titania Nanotubes for Local Drug Delivery from Implant Surfaces” in book *Electrochemically Engineered Nanoporous Materials: Methods, Properties and Applications 2015*, ed. by D. Lopic and A. Santos (Springer International Publishing AG - Germany). Springer Series in Materials Science 220, **DOI** 10.1007/978-3-319-20346-1\_10

Gulati, K., Kogawa, M., Maher, S., Atkins, G., Findlay, D. & Losic, D. (2015). Titania Nanotubes for Local Drug Delivery from Implant Surface. In D. Losic & A. Santos (Eds.), *Electrochemically Engineered Nanoporous Materials: Methods, Properties and Applications: Vol. 220. Springer Series in Materials Science* (pp. 307-355). Springer International Publishing AG – Germany.

NOTE:

This publication is included on pages 284 - 332 in the print copy of the thesis held in the University of Adelaide Library.

It is also available online to authorised users at:

[http://dx.doi.org/10.1007/978-3-319-20346-1\\_10](http://dx.doi.org/10.1007/978-3-319-20346-1_10)